THE UNIVERSITY *of* EDINBURGH

Metagenomic, Metabolic and Functional Characterisation of Polyextremophilic Microbial Consortia Endogenous to Acid Mine Drainage.

OILTHIGH DHÙN ÈIDEANN

Michael Anthony McDonald BSc (Hons) MSc

A thesis submitted for the award of Doctor of Philosophy (PhD) in Microbiology

Institute of Quantitative Biology, Biochemistry and Biotechnology
The School of Biological Sciences
College of Science and Engineering
The University of Edinburgh

Contents of Thesis

Declaration

In accordance with the University of Edinburgh's standards for postgraduate doctoral research theses, I declare that this thesis has been written solely by myself. The work presented is of my own, unless otherwise stated, and has not been submitted for the award of any previous degree.

Michael McDonald
March 2024

Publication Related to this Thesis

The introductory material presented in **Chapter 1** builds upon work contained within a previously published review, in which the author of this PhD was a contributor. This review article is fully referenced below and has been cited within this work where appropriate:

Free, A., **McDonald, M. A.** and Pagaling, E. (2018). Diversity-function relationships in natural, applied and host associated microbial ecosystems. In: *Advances in Applied Microbiology*. **108:** 131-189. (Available at: https://doi.org/10.1016/bs.aambs.2018.07.002).

Acknowledgments

My biggest thanks go to my primary supervisor, Dr. Andrew Free, whose guidance and generous support throughout my PhD have made it possible for me to complete my doctoral degree. Thank you for making me a better and more independent scientist and allowing me the academic freedom to explore such a unique and exciting area within our field. A huge thank you for your continual belief in my abilities over the last eight years.

I am also indebted to the supervision and support of both Prof. Rosalind Allen and Prof. Garry Blakely for their valuable insights, active interest in my work, and constant and lively encouragement throughout my PhD. I also want to extend my thanks to Dr. James Chong for his support during the early phases of this work, and for supplying the iChips used during cultivation trials.

To Fi, thank you for being a continual source of positive energy and encouragement, not just to me, but to everyone within our lab. Your commitment to my PhD was vital in getting to this point, and I could not have asked for a more enthusiastic lab technician to work alongside with. I've been fortunate to see our lab group through various iterations and I could not have asked for a better research group to have been a part of. You are all incredible scientists and even better pals. Most recently, thank you Martina, Hanna, and Joana for your support during my final experiments and writing up of my thesis. Thank you to Dr. Heather Barker, Dr. Annegret Honsbein and Holly Pantidos for their help during my PhD, particularly during my PIPS during 2018 and 2019.

A massive amount of thanks also needs to go to those outside of the lab. A huge thank you go to Jenna, Keith, and Clare. Getting to this point was a collective effort and I could not have done it without you all encouraging me both academically, and otherwise. Your massive amounts of support throughout my PhD, and everything else over the last few years, has been incredible. Also, to my friends outside the lab who have made sure I've had enough breaks from my laptop, have texted me weekly check-ins and have been invested in my PhD progress from the start who also all need a big thank you (particularly Tegan, Deedee, Kirsty, Andrew, Tylar, and Claire).

To Jackie and Alistair, thank you for fostering my scientific curiosity and instilling in me a sense of determination. An extra thank you to Catherine for being the first to show me the structure of the double helix, (unintentionally) setting me down the route to my PhD.

Lastly, an extra big thank you to Noah, Reuben and Quinn. You've always reminded me to focus on the bigger picture and helped me maintain a good life-work balance. I hope I've managed to make a small contribution that will let you all grow up on a planet with a renewed focus on achieving a more ecologically conscious future.

List of Abbreviations

Abbreviation	Full Description
AD	Anaerobic Digestion
AGE	Agarose Gel Electrophoresis
AhR	Aryl Hydrocarbon Receptor
AMD	Acid Mine Drainage
AN	Anaerobic Microplate
ANI	Average Nucleotide Identify
ANME	Anaerobic Methane Oxidising Archaea
ARD	Aqua Regia Digestion
ARMAN	Archaeal Richmond Mine Acidophilic Nanoorganism
ASV	Amplicon Sequence Variant
ATP	Adenosine Triphosphate
AWCD	Average Well Colour Development
BLAST	Basic Local Alignment Search Tool
CBB	Calvin Bassham-Benson Cycle
cChip	Cultivation Chip
CF-IRMS	Continuous Flow-Isotope Ratio Mass Spectrometry
COD	Chemical Oxygen Demand
CSTR	Continually Stirred Tank Reactor
CWS	Constructed Wetland System
DIC	Dissolved Inorganic Carbon
DIET	Direct Interspecies Electron Transfer
DNA	Deoxyribose Nucleic Acid
DOC	Dissolved Organic Carbon
DOM	Dissolved Organic Matter
DRAM	Distilled and Refined Annotation of Metabolism
DSMZ	German Collection of Microorganisms and Cell Cultures (*Deutsche Sammlung von Mikroorganismen und Zellkulturen*)
eAD	Environmental Anaerobic Digestion
EBI	European Bioinformatics Institute
ECO	EcoPlate
EDP	Entner–Doudoroff Pathway
EET	Extracellular Electron Transfer
EMP	Embden-Meyerhof-Parnas Pathway
ENA	European Nucleotide Archive
ETS	External Transcribed Spacer
FYS	Faint Young Sun
GOE	Great Oxidation Event

HGT	Horizontal Gene Transfer
HMM	Hidden Markov Model
HS-CoB	Co-enzyme B
HS-CoM	Co-enzyme M
IC	Ion Chromatography
iChip	Isolation Chip
ICP-OES	Inductively Coupled Plasma-Optical Emission Mass Spectroscopy
IS	Insertion Sequence
ITS	Internal Transcribed Spacer
JHI	The James Hutton Institute
KAAS	Kyoto Encyclopaedia of Genes and Genomes Automatic Annotation Server
KEGG	Kyoto Encyclopaedia of Genes and Genomes
KN	Kjeldahl Nitrogen
KO	Kyoto Encyclopaedia of Genes and Genomes Orthology
LB	Luria-Bertani Medium
LUCA	Last Universal Common Ancestor
MAC	Methoxylated Aromatic Compound
MAG	Metagenome Assembled Genome
Mb	Megabases
Mcr	Methyl Coenzyme Reductase Complex
MEGA	Molecular Evolutionary Genetic Analysis
MG-RAST	Metagenome-Rapid Annotation Server Tool
MWL	Municipal Waste Landfill
NCBI	National Centre for Biotechnology Information
NGS	Next Generation Sequencing
NMDS	Non-Metric Dimensional Scaling
OA	Organic Acids
OD	Optical Density
OD*i*	Corrected Optical Density
ODU	Optical Density Units
PAH	Polyaromatic Hydrocarbon
PBS	Phosphate Buffered Saline
PCR	Polymerase Chain Reaction
PDB	Protein Database Bank
pH	Power of Hydrogen
PHA	Polyhydroxyalkanoate
PHB	Polyhydroxybutyrate
pK_a	Acid Dissociation Constant
pMMO	Particulate Methane Monooxygenase
POP	Persistent Organic Pollutant
PPP	Pentose Phosphate Pathway
PPU	Protein Phosphorylation and Ubiquitylation Unit

QIIME 2	Quantitative Insights into Microbial Ecology 2
qPCR	Quantitative Polymerase Chain Reaction
R2A	Reasoner's 2-A Medium
RAS	Return Activated Sludge
RAST	Rapid Annotation Server Tool
RFU	Relative Fluorescence Units
RISC	Reduced Inorganic Sulphur Compounds
ROS	Reactive Oxygen Species
rTCA	Reductive Tricarboxylic Acid Cycle
SBH	Single Best Hit
SOC	Super Optimal Broth with Catabolite Repression
TCA	Tricarboxylic Acid Cycle
TAE	Tris-Acetate Ethylenediaminetetraacetic Acid
TC	Total Carbon
TCA	Tricarboxylic Acid Cycle
TDS	Total Dissolved Solids
TOC	Total Organic Carbon
TP	Total Phosphorus
TS	Total Solids
VFA	Volatile Fatty Acid
WAS	Waste Activated Sludge
WC	Wolfe Cycle
WLP	Wood-Ljundahl Pathway
WWTP	Wastewater Treatment Plant
X-GAL	5-Bromo-4-Chloro-3-Indolyl-β-D-Galactopyranoside
YEFS	Yeast Extract Ferrous Sulphate Medium
μ_{max}	Maximum Specific Growth Rate

List of Figures

Chapter 1 – Literature Review

Chapter 2 – Materials and Methods

Chapter 3 – Chemical Analysis, Metabolic Profiling and Cultivation

Chapter 4 – Detection and Quantification of Functional Genes Involved in the Carbon Cycle

Chapter 5 - Unassembled Metagenomic Analysis

Chapter 6 – Metagenome Assembled Genomes and Functional Characterisation

Chapter 7 – Derivation of Methanogenic Function in Bioreactors

Supplementary Data

List of Tables

Chapter 1 – Literature Review

Chapter 2 – Materials and Methods

Chapter 3 – Chemical Analysis, Metabolic Profiling and Cultivation

Chapter 4 – Detection and Quantification of Functional Genes

Chapter 5 – Unassembled Metagenomic Analysis

Chapter 6 – Metagenome Assembled Genomes and Functional Characterisation

Chapter 7 – Derivation of Methanogenic Function in Bioreactors

Supplementary Data

Table S1: Summary of taxonomic bins containing assembled reads < 100,000 bp after MAG assembly.

Lay Summary

Global demand for materials has led to excessive and unsustainable exploitation of Earth's natural resources. Mining for metals is environmentally destructive, and little thought is given to the metallic waste products following closure of mining sites. Failure to manage mining wastes correctly leads to residues being left in 'spoil heaps' or 'tailings' and then abandoned. Exposure of mining wastes to water and oxygen causes microorganisms present to rapidly alter the chemistry of the metals present. These microbially driven processes produce an acidic and iron-rich effluent termed 'acid mine drainage'.

The acidic, and characteristically orange, effluent contaminates nearby streams, surrounding soil and can leach into groundwater through geological processes. Metallic pollutants can migrate far from the mining site in waterbodies and are hazardous to human and environmental health. However, how the microorganisms present can persist in high metal concentrations, as well as how they influence the fate of the pollutants, and wider ecosystem processes, is poorly understood. This is due in part to the difficultly in growing organisms from acid mine drainage sites in the laboratory as they require chemically unusual conditions to survive, which are challenging to replicate.

The research presented here aimed to characterise and determine the function of microorganisms present in acid mine drainage sediment. Focus was given initially to the carbon cycle, and in particular methane production, due to its significance to global climate. Results reported here explore how microbial consortia breakdown or degrade carbon-containing compounds, and the detection of key functions of microorganisms through molecular approaches. This includes detecting strategies employed by microorganisms to counteract hazardous metallic pollutants and how this is linked environmental chemical cycles. The presence of methane-generating organisms ('methanogens') and methane-utilising organisms ('methanotrophs') in these harsh environmental conditions was explored. Methane generation was assessed in several bioreactor-based trials. Non-heavy metal contaminated samples were used as controls which were reflective of more conventional carbon cycling microbial ecosystems.

Several metabolic strategies previously unseen in acid mine drainage microbial species were observed, expanding our knowledge on how heavily polluted systems work and how they impact the wider environment. The reconstruction of high-quality bacterial genomes allowed insights into metal detoxification and degradation of hydrocarbons. It is hoped that these specialised capabilities will be exploited to aid ecosystem restoration in previously mined sites.

Scientific Abstract

The generation of extremely acidic and metal-contaminated effluent from mining can cause large scale environmental destruction, degradation of surrounding freshwater and soil and poses risks to both ecosystem and human health. Due to the chemistry of this synthetic 'acid mine drainage' (AMD), the diversity and function of microbial consortia native to such sites has been largely neglected.

Firstly, in order determine the chemical composition of the acidic sediment, elemental analysis was performed, and compared to two non-extreme freshwater sites not impacted by mining-derived pollution. The acid mine drainage sediment (collected from a previous mined site in Central Scotland) demonstrated an extremely low pH, carbon levels reflective of oligotrophic conditions, elevated concentrations of heavy metals, and high sulphate levels. Taken together, these chemical characteristics demonstrated the abiotic conditions and nutritional scarcity associated with microbial proliferation in heavily contaminated systems.

Subsequent metabolic profiling of sediment communities involving carbon-source degradation again demonstrated the acidophilic consortia's more restricted diversity and reduced capacity to catabolise organic compounds compared to control environments and revealed significantly different carbon source utilisation patterns compared to copiotrophic and an additional oligotrophic microbial assemblage.

Using a novel cultivation strategy, a member of the genus *Thiomonas* was successfully isolated, demonstrating the premise that extremophiles can be successfully recovered from their native conditions using non-conventional culture-based approaches. Further amplicon-based molecular analyses allowed elucidation of key taxonomic groups of microorganisms, and quantitation of their functional marker gene abundance. qPCR demonstrated the presence of methane cycling organisms via detection of the *mcrA* and *pmoA* genes, responsible for functions previously poorly, or not reported for, in members of acid mine drainage assemblages. Fungal presence was confirmed via quantification of the intergenic ITS2 region, expanding current knowledge on the biogeographical distribution of eukaryotes in low pH, synthetically derived effluents.

Thereafter, the routes to community characterisation focused on metagenomic and metataxonomic approaches; allowing the elucidation of members of the acidophilic population and functional attributes which promote microbial survival in hazardous conditions. Long read DNA sequencing using Oxford Nanopore Technology successful allowed the reconstruction of metagenomic assembled genomes (MAGs); assemblies pertaining to organisms from the Pseudomonadota and Actinomycetota phyla were selected for further genomic analysis.

Metabolic functions previously unreported for members of acid mine drainage communities were evident within the reassembled bacterial chromosomes. The highest quality assembly pertaining to a genome recovered from *Metallibacterium scheffleri* demonstrated multiple polyextremophilic adaptations, including resistance mechanisms to counteract acid influx into the cell. The *Metallibacterium* MAG sequence also demonstrated metabolic strategies employed by this taxon to survive in otherwise deleterious concentrations of pollutants, chiefly exposure to transition metals (via the presence of *zitB, copA/B, cutA*, *merA* and *ATM-1* genes) and the metalloid arsenic (via *arsB/C*). Importantly, the *Metallibacterium* assembled genome also demonstrated more diverse carbon utilisation routes than previously reported, with three complete glycolytic pathways noted. Sulphur cycling capabilities previously contested for *Metallibacterium* were also evident within the content of the assembled chromosome.

These results indicated *Metallibacterium's* importance in underpinning biogeochemical function in acidic waste streams and the array of metabolic strategies that could exploited if using *Metallibacterium* as a future candidate for bioremediation. The *Metallibacterium* MAG also demonstrated an array of sulphur cycling mechanisms unreported in the previous literature. Additional MAGs relating to *Acidiphilum* and *Mycobacterium* are also presented; these MAGs also indicate novel functions, including extreme acid tolerance, autotrophy, and hydrocarbon degradation.

Lastly, bioreactor-based experiments were employed to explore whether a specific community function (methanogenesis) could be established from sediment communities. A strong derivation of methanogenic function was achieved using copiotrophic communities. Methane output when using the acidophilic assemblage as a novel inocula was sporadic, however methane was detected in a single bioreactor. In this case, the archaeal community from Benhar Bing within the starting inocula appeared to withstand the bioreactor conditions and produced

biogas (with over 65% methane detected within the headspace gas). Based on phylogenetic analysis of both the starting sample and the end point bioreactor samples following dismantling of the reactors (by pre-amplification of the archaeal 16S rRNA gene and subsequent analysis of the V4 region), it is likely that methanogens native to the extremely acidic conditions belong to the Thermoplasmatales which like their sister lineage, the Methanoplasmatales, may utilise a methylotrophic methanogenic pathway to conserve energy.

Overall, acidophilic assemblages underpin ecological function in ecosystems degraded by anthropogenic mining activities and can promote pollutant mobility. Despite this, metagenomic results demonstrated that microbial species present can also aid in ecosystem recovery and can promote metal detoxication and the closure of metal redox cycles. Future work could continue to focus on methane cycling occurring in non-standard systems which have been overlooked regarding potential greenhouse gas emissions, which have likely been underestimated. Acidophilic assemblages hold an untapped metabolic repertoire that could be exploited in both the remediation of contaminated systems and potential low pH waste to resource biotechnologies.

CHAPTER 1 – Literature Review

1.1 Overview of Acid Mine Drainage

1.1.1 The Global Impacts of Mining Effluents

Acid mine drainage (AMD) is the highly acidic and metallic-rich effluent arising from the waste outflow from previous metal and coal mines (Aguilar-Garrido *et al.,* 2023). Despite the abiotic challenges associated with elevated metal concentrations and decreased pH in mine-generated waste streams, native microbial consortia can still proliferate. The destructive environmental consequences of mine-derived effluents can be long-lasting and detrimental to human and environmental well-being, and yet the microbial consortia native to this unique and anthropogenically influenced niche remain poorly understood.

During extraction of metals and coal, large volumes of metallic mine wastes, with little to no economic value, are produced. These wastes are stored in mine tailings, heaps (colloquially in Scotland, 'bings') or impounded and remain at the excavation site after closure of the mine. Following contamination of the surrounding catchment, acidic and metal-rich wastewater flows from the site contaminating the surrounding environment. This process decreases quality of the receiving waterbodies and has long-lasting environmental impacts including soil degradation, an increase in metal toxicity and a reduction in ecosystem productivity. Additionally, pollutants derived from mining residues can be highly mobile in solution and be carried by receiving waters distant from their point of origin. Several of the metal pollutants are considered critical contaminants to monitor, with the mutagenic, carcinogenic, and teratogenic effects of heavy metals on mammalian systems being well documented (Dutta *et al.,* 2022; Li *et al.,* 2023).

Acid mine leachate can have detrimental impacts on human health through indirect contact; predominantly through increased concentrations of metallic pollutants entering groundwater and the contamination of soils which may be used for agricultural purposes. Metallic compounds can be maintained and persist in the terrestrial environment through adherence to organic matter within soils and can demonstrate recalcitrance to degradation (Raffa *et al.,* 2021). The work of Fernandez-Caliani *et al*. (2019) observed that metal levels, specifically lead, zinc and arsenic, in agricultural soil in Spain impacted by acid mine drainage were elevated beyond statutory limits stated in environmental frameworks for agricultural soil quality and showed elevated oral bioavailability.

Similarly, the work of Tomiyama and Igarashi (2022) states that groundwater and aquifers used for drinking water and irrigation are at risk of contamination by acidic run-off in areas that have been heavily mined previously; the issue of diffuse pollution compounds the complexities in restoring and maintaining groundwater quality. Despite growing attention regarding the threats of acid mine drainage on communities, the fate of metallic toxicants and their interactions through trophic systems remains unclear. The wider biogeochemical cycling of metals, as well as potential detoxification strategies utilised by acidophilic species to survive under harsh environmental conditions remain a key open question; understanding how these microbial processes drive function under such abiotic constraints is becoming increasing important as mining of metals remains exploitative and, in some cases, is growing to meet global demand for metallic ores (Savinova *et al.,* 2023).

Acid mine drainage is generated readily from mining wastes irrespective of the metal species being excavated, and can be produced excessively, with damage to entire ecosystems resulting from large-scale mining operations. Two examples of severe acid mine contamination of freshwater systems are shown in **Figure 1.1.**

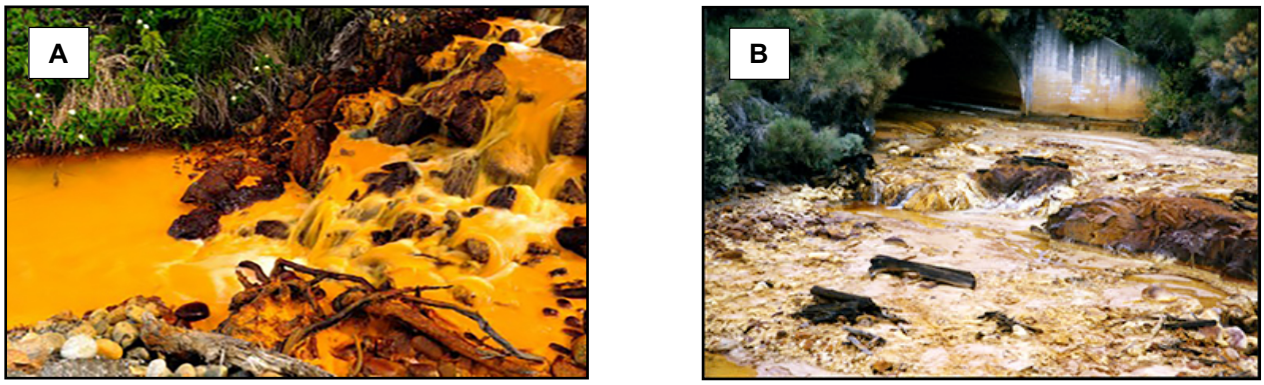

FIGURE 1.1: Acid mine drainage effluent. Contamination of the Tulsequa River (British Columbia, Canada) by AMD generated from previous copper mining operations (**A**). Iron Mountain Mine (California, USA), has been mined extensively for various metals, resulting in widespread ecological damage to surrounding freshwater systems, particularly Boulder Creek pictured (**B**). [*Images from the Columbia Environmental Research Council (2018) and the US Fish and Wildlife Service (2002)].*

Direct human contact with acid mine drainage contaminated water is limited, however one study by Garland (2012) demonstrated the detrimental risks to human health posed by mining effluents. In this case, the combination of extreme water stress resulting in drought, combined with limited drinking water supplies becoming contaminated with nearby acid mine effluent resulted in the use of mine-contaminated drinking water by populations in South Africa. It was noted that those who handled or ingested the contaminated water supplies stated an increase in incidences of skin irritation, gastrointestinal pain and in some cases, impaired kidney function indicative of metal toxicity.

It should be stressed that this work did not consider additional factors posing risks to health through reduced water quality (*e.g.*, viral load, the presence of potentially pathogenic *Bacteria,* or parasitic eukaryotes); but given the high metal contents of contaminated water, it is likely that direct use of water impacted by mining waste caused the impaired renal function and other associated illnesses. Similarly, the Witwatersrand catchment in South Africa is estimated to received mining discharges of ~ 300,000 m^3 daily since mining intensified in the region in the early 2000s (Tutu *et al*., 2008).

These data are further strengthened when the work of Talukdar *et al*. (2017) is considered which observed the pathological effects of mine-derived pollutants on freshwater fish and noted kidney toxicity, defective formation of the gills and corrosive-like abrasions on scales. Long-term ingestion of soluble pollutants and food-web accumulation of metals were noted as the expected causes of the decline in fish health and associated macroecological mortality.

Likewise, Olsvik *et al*. (2016) demonstrated that upon exposure to mine effluent containing high concentrations of copper in a contaminated fjord, that metal accumulation in gill tissue and protein misfolding following translation was noted to occur in developing Atlantic Salmon (*Salmo salmar)* populations.

The consumption of fish from the Pilcomayo River in Colombia which is heavily impacted by mining operations is thought to expose communities to lead concentrations 16 times over the maximum acceptable threshold (Smolders *et al*., 2003). Further work by Stassen *et al*. (2012) stated that exposure of indigenous communities living along the Bolivian regions of the Pilcomayo River to lead was proposed to be a factor in the elevated incidence of reproductive health disorders observed within the population. Additionally, children were noted to have delayed neurological development and mobility, possibly resulting from heavy metal exposure *in utero*.

Large areas of previously mined landscapes continue to suffer the detrimental ecological consequences arising from low-pH mine drainage; the immediate environmental impacts are more initially evident that impacts on human health. As a result of this, the economic inputs required to reclaim contaminated waterways are high, with some individual states within the USA requiring budgets of over $5 billion dollars to act on remediating past mining operations and aid ecosystem recovery (Bergerson and Lave, 2004). Meyer *et al*. (2022) had moderate success in remediating acid mine drainage impacted creeks in Colorado, a state which has been mined extensively for copper. The authors observed that their following reclamation, aquatic environments can reach a new steady state relatively quickly and some level of ecological function restored. Yet, elevated rainfall and snowmelt increasing river flow was noted to cause fluxes in contamination from the leaching of soil-bound metals. This further accelerated dissolution of metallic minerals from historic deposits leading to increased acidity.

The findings of Meyer *et al*. (2022) stress the challenges left by mining legacies and the complexities in removal of pollutants which pose a constant threat to ecosystems even following application of reclamation strategies. Most routes to environmental recovery rely on low-cost, passive approaches (*e.g*., buffering of the pH with alkalinity). However, active remediation strategies utilising microbial communities to reclaim mining sites via their native ability to detoxify metals are not well explored; microbial approaches may be more valuable in long-term to aid in removal of persistent contaminants.

Abandoning of hazardous mine waste resulting in leachate production is a global issue, with severe examples of acid mine drainage contaminated ecosystems being noted in the United States, South Africa, Spain, and Australia. An overview of major sites of AMD impacted sites are listed in **Table 1.1.** In Wales, long-term mining activity at Parys Mountain, Anglesey, caused the release of acid mine drainage effluent containing 7.5 tonnes of copper, 14.8 tonnes of zinc and approximately 3 tonnes of manganese into the Irish Sea in 2003 alone (Coupland and Johnson, 2004).

Management of the resulting effluent can be contentious particularly when it impacts aquatic systems which transverse geographical boundaries; an example of this being the contamination of Alaskan rivers by acidic run-off generated by Canadian mining operations. Poorly managed waste heaps and associated effluent also leads to complexities surrounding future land use of previously mined landscapes. Central Scotland has been mined extensively yet the potential impacts on the economically vital agricultural sector, water quality, and wider infrastructure are seldomly reported. MacGregor *et al*. (2015) did state that leaching of antimony, arsenic, and lead into streams from a previous mine in Southern Scotland could continue over extended periods, from decades to centuries if continually left untreated. Elevated concentrations of arsenic, cadmium and lead have been noted with the Clyde Basin within areas impacted by former mining activity; this is an area of particular concern as the Clyde Valley's reservoirs supply much of Scotland's population within the Central Belt (Fordyce *et al*., 2017).

TABLE 1.1 Examples of acid mine drainage impacted sites.

AMD Location	pH	Contamination	Authors
Balya and Çan Regions, Turkey	2.8-3.05	Zn/Pb/FeS_2	Aytar *et al.* (2015)
Parys Mountain, Wales	1.8-3.1	Cu	Dean *et al.* (2019)
Anhui Province, China	3.0	FeS_2	Hao *et al.* (2010)
Madhya Pradesh, India	2.0	Cu	Kumar *et al.* (2023)
Richmond Mountain Mine, California	0.83	Fe	Tyson *et al.* (2004)
Los Rueldos, Spain	2.0	Hg	Vidal *et al.* (2019)
Harz Mountains, Germany	2.05	FeS_2	Ziegler *et al.* (2013a).
Carolina, South Africa	2.5	Au	Moeng (2019)
Black Swan Mine, Western Australia	< 4.0	Ni	Lei and Watkins (2005)

1.1.2 Acid Mine Drainage: Generation and Biogeochemistry

Acid mine drainage is predominately produced by the oxidation of sulphide-containing minerals present in the mine tailings and is produced readily due to co-contamination of heavy metal waste and sulphides. The metal-rich effluent is an example of an environmental niche in which iron cycling microbial communities have a dominant role in energy conservation and are involved in simplified biogeochemistry given the abiotic constraints on microbial growth.

Iron sulphide (FeS_2), or 'pyrite', is the most common sulphide mineral found in acid mine drainage waste streams, however, chalcopyrite ($CuFeS_2$), arsenopyrite (FeAsS) and pyrrhotite ($Fe_{1-x}S$), where $x = 0$ - 0.2 are also common (Elghali *et al*., 2023). FeS_2 is chemically stable across a wide pH range, however, upon exposure to molecular oxygen and water it is readily oxidised to ferrous iron (Fe^{2+}) as shown in reaction one in **Figure 1.2**. This reaction can also be facilitated with ferric iron (Fe^{3+}) as the oxidant (see reaction three below in **Figure 1.2)**. This reaction is abiotic and occurs spontaneously upon exposure of pyrite to oxidants. This reaction can proceed under both aerobic (with oxygen as the electron acceptor) and anaerobic (with Fe^{3+} as the electron acceptor) conditions.

The ferrous iron (Fe^{2+}) produced through the oxidative dissolution of pyrite is further re-oxidised by iron-oxidising acidophilic *Bacteria* as shown in reaction two **(Figure 1.2).** The further dissolution of pyrite is accelerated by lithotrophic acidophiles regenerating the oxidant, ferric iron, (Fe^{3+}). Under extremely acidic conditions, oxidation of ferrous to ferric iron ions would be impaired, however, in AMD, it is enhanced through acidophilic microbial metabolism.

The Fe^{3+} ions produced during ferrous iron oxidation can be consumed during further pyrite dissolution or utilised in the generation of iron hydroxides [$Fe(OH)_3$]. However, as noted in the work of Tong *et al*. (2021) at acidic pHs (below 3.5) ferric iron becomes soluble and iron complexes will dissolve into the acidic effluent (see reactions three and four, **Figure 1.2).** The continual generation of acidity is enhanced through the production of additional hydrogen ions which lower the pH of the impacted catchment (Johnson and Hallberg, 2003).

The work of Johnson and Hallberg (2003) also states that acidity in AMD is generated through the oxidation of intermediate reduced inorganic sulphur compounds (RISCs) such as thiosulphate ($S_2O_3^{2-}$) which can result in the generation of sulphuric acid, which dissociates in solution to sulphate ions (SO_4^{2-}). Sulphur oxidising bacteria can produce further free protons via sulphur-mediated reactions, yet many taxa involved in this process remain poorly characterised (see reaction five in **Figure 1.2**). Sulphate-reducing *Bacteria* (SRB) can also influence proton mobility, organic acid concentrations and sulphide availability in AMD contaminated sediments (Sanchez-Andrea *et al.*, 2014).

1. $2FeS_{2(s)} + 7O_2 + 2H_2O \rightarrow 2Fe^{2+} + 4SO_4^{2-} + 4H^+$
2. $4Fe^{2+} + O_2 + 4H^+ \rightarrow 4Fe^{3+} + 2H_2O$
3. $FeS_{2(s)} + 14\ Fe^{3+} + 8H_2O \rightarrow 15\ Fe^{2+}\ 2SO_4^{2-} + 16H^+$
4. $Fe^{3+} + 3H_2O \rightarrow Fe(OH)_3 + 3H^+$
5. $S_2O_3^{2-} + 2O_2 + H_2O \rightarrow 2H^+ + 2SO_4^{2-}$

FIGURE 1.2: Reactions involved in AMD generation. Reactions one - four relate to iron cycling and the generation of hydrogen ions which contribute to the generation of acidity. Reaction five relates to the use of RISCs and the generation of sulphuric acid, which dissociates in solution. Note that reactions shown in blue are microbially catalysed. **Note that iron hydroxides (reaction three) will not remain solid at low pH and contribute to the dissolved iron within AMD waste streams.**

Through the continual oxidation of sulphide rich minerals, acid mine drainage can be self-sustaining and cause continual and excessive environmental degradation. Large scale mining sites have been the focus on previous studies, including Richmond Mine California, USA, which has been noted to be extremely acidic (**Table 1.1**). The work of Baker *et al*. (2006) elucidated the occurrence of the 'ultra-small' *Archaea* through reassembly of community genomic DNA from biofilms present in highly acidic samples with pH values in the range of pH 0.5 – 1.0. These 'ultra-small' archaeans are characterised by compact genomes, reduced cell size and possess limited metabolic capacities. Often these taxa often also require syntrophic interactions with other acidophiles within the community to overcome nutritional scarcity in heavily contaminated effluents (Gios *et al.*, 2023). Further exploration of these archaeal community members led to the discovery of the novel archaeal lineage, the 'Archaeal Richmond Mine Acidophilic Nanoorganism (ARMAN) Group' which further aided current understanding of the importance of low abundance, rare taxa in extreme environments.

1.1.3 Adaptations to Life at Extreme pH

Much of the understanding regarding the microbial contribution to acid mine drainage comes from acidophilic taxa that have been successfully cultured. However, as will be discussed in **Chapter 3** of this thesis, cultivation of extremophiles is challenging and the pool of cultivated acidophilic taxa remains small. The two iron-cycling organisms *Acidothiobacillus ferrooxidans* and *Leptospirillium ferrooxidans* are routinely cultured (Chen *et al*., 2021 Khachatryan *et al*., 2023). Many of the mechanisms involved in iron-cycling were elucidated from isolates of these species.

Wider biogeochemical cycling outside of iron-mediated reactions driven by AMD communities have often been neglected due to challenges in studying chemically extreme environmental samples recovered from mining areas. Other metals and metalloids which have been observed in the low pH effluents have been given less attention due to the elevated iron levels and the predominance of iron-driven chemolithotrophy proposed by the limited number of studies on cultivated taxa. Likewise, how acidophilic species acquire and utilise carbon containing substrates required in central metabolism remains unclear, even for cultivated acidophiles.

The limited pool of cultivated AMD species has led to a lack of understanding of how key members of the microbial consortia tolerate and cycle heavy metals (*e.g.,* other transition/D-block metals) and metalloids in hazardous concentrations Similarly, how organic material is cycled under low pH conditions with little carbon influx has not been characterised. The lack of data regarding cryptic carbon cycling pathways has resulted in evident gaps in the current understanding of how these globally distributed sites impact the wider environmental function regarding the carbon budget.

Importantly, the work of Cruz *et al*. (2021) states that hydrocarbons have been found to co-occur in mining wastes, yet the cycling of alkanes, including the potential generation and consumption of the methane under acidic pH unknown and is not well documented. Additionally, the leaching of polyaromatic hydrocarbons (PAHs) from mining waste heaps has been noted by Marques *et al*. (2021). An overview of ecosystem function and the consequences of acid mine drainage pollution in freshwater systems is shown in **Figure 1.3**. It should be noted that despite many genera listed in **Figure 1.3** having broad metabolic function, the specific taxa listed have been implicated in biogeochemical cycling in acid mine drainage impacted ecosystems; particularly pertinent is *Clostridium desulfuricans (strain Essex 6)* which has been noted to contribute to sulphate reduction (Costa *et al*., 2005).

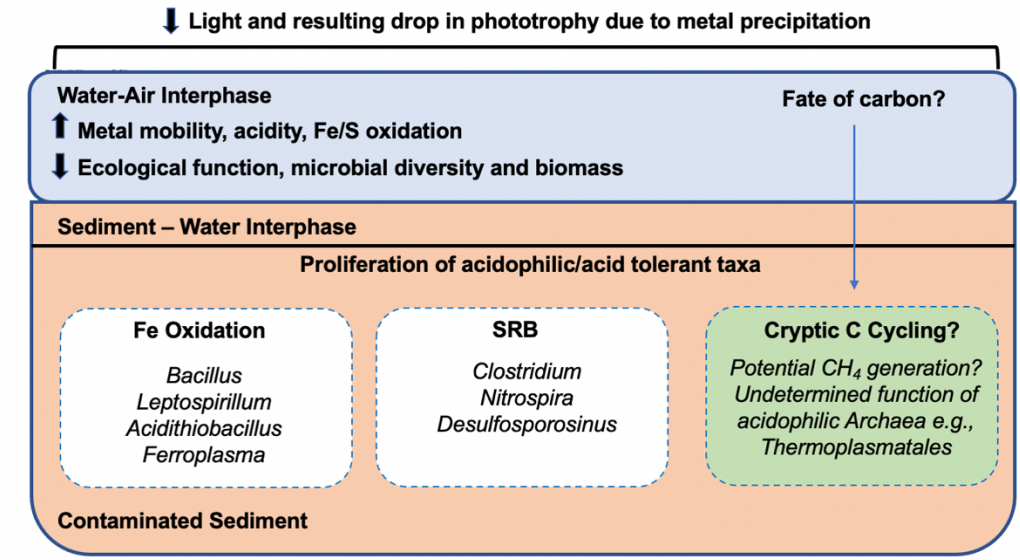

FIGURE 1.3: The impacts of acid mine drainage effluent on receiving waterbodies. The oxidation of sulphide containing minerals is driven by acidophilic iron-oxidising *Bacteria* and sulphate reducing *Bacteria* (SRB). Acidophilic *Archaea* have also been identified in AMD contaminated sediments (*e.g., Ferroplasma*). Little is known regarding the fate of carbon in acidic systems and which organisms facilitate potential carbon cycling routes. (Figure adapted from Munyai *et al.,* 2021)

Extremophiles native to acidic and heavily polluted systems display multiple adaptations to their cellular physiology to allow growth and persistence under extreme abiotic stress. It has been noted that specific modifications to the cell envelope are critical and are often the most advantageous adaptations in preventing H^+ ion entry to the cell; many of these adaptations have been determined from the limited pool of acidophiles available in culture. The ability of both archaeal and bacterial cell walls to withstand acidic conditions aids in maintaining the function of both membrane proteins and components of the intracellular proteome. Short chain fatty acids and lipid monolayers have been detected in the membranes of acidophilic taxa (Siliakus *et al*., 2017).

The ability of acidophiles to reverse the membrane potential is critical in preventing influx of damaging charged ions into the intracellular space. This is considered to occur via an increased concentration of potassium or sodium ions within the cell, localised close to the membrane, that create an electrochemical barrier to proton influx (Neira *et al*., 2022). Further to this, acidophilic consortia are prolific producers of extracellular polysaccharides (EPS), upregulation of which allows biofilm and streamer formation to occur; structures which assist in maintaining robust community attachment on environmental matrixes under harsh physiochemical constraints (Zhang *et al*., 2019).

Despite numerous strategies to overcome the challenges of persisting under extreme pH, many of the adaptations outlined above can be applied to a range of acidophilic species and are considered general mechanisms which promote cellular survival. How acid mine drainage associated taxa specifically counteract highly mobile and toxic concentrations of specific metals warrants further work. Importantly, routes to future reclamation of contaminated systems may be heavily reliant on the overlooked metabolic flexibility of acidophilic assemblages capable of degrading or otherwise immobilising toxicants.

1.1.4 Acid Mine Drainage: Can Carbon Cycling Persist?

The global carbon cycle underpins the Earth's climate. Carbon reservoirs both on land and in aquatic systems act as the key moderators of atmospheric CO_2 flux with freshwater sites acting as transitional zones for the cycling of both terrestrial and aquatic derived organic material (Regnier *et al*., 2022). The carbon cycle has been well documented in conventional freshwater systems and marine environments. Considerable work has been performed to elucidate carbon storage and how this process varies between marine and in-land aquatic ecosystems. Despite being major global carbon sinks, freshwater systems are estimated to contribute to ~ 20% of naturally occurring greenhouse gas release to the atmosphere.

Freshwater systems are considerably dense in carbon and disproportionally cycle high concentrations of organic matter; more than their modest global coverage would suggest when compared to ocean coverage. The maintenance of carbon reserves within freshwater systems allows these ecosystems to act as natural sentinels of changes in climate due to their sensitivity to environmental disruption, which impacts carbon storage and release (Woolway *et al*., 2020). Critically, climate change induced positive feedback loops, elevated nutrient loads and anthropogenic encroachment on freshwater systems have been noted to be disruptive to microbial carbon cycling leading to alterations in biogeochemical function (Woolway *et al*., 2021).

Due to the combination of high metal concentrations and low organic inputs in acid mine drainage, any attempts at elucidating how the microbial biogeochemical cycling of carbon persists under extreme abiotic constraints remain limited. Taken together, both the fate of carbon and heavy metals in contaminated effluents represent two broad metabolic cycles which underpin acidophiles' function, yet they have received little attention compared to the equivalent functions in conventional systems. Similarly, assimilation of carbon by acidophiles to drive central metabolic pathways is also poorly described in these extremophilic species.

Acid mine drainage literature has sporadically referred to potential carbon cycling routes. However, mechanistically, the cycling of carbon, particularly degradation of organic material under low pH conditions remains largely under researched. Despite their geographical distribution, acid mine drainage sites and impacted receiving waters may potentially be sources of carbon-derived greenhouse gas emissions which have been ignored. In particular, the biological generation of methane resulting from the anaerobic degradation of carbon has not been well-established under extreme conditions, or in aquatic systems contaminated by mining effluents when compared to knowledge of methanogenesis and carbon storage in lake and oceanic systems.

Only recently did the work of Brown *et al*. (2023) observe that mine water inputs into the River Clyde influenced greenhouse gas emissions, one of the first studies to link both the elevated presence of metals with the co-occurring use of organic compounds. The authors noted that anthropogenically-derived nutrients elevated greenhouse gas emissions; CO_2 output increased through contamination by agricultural run-off into the river, whereas overloading of the riverine system by wastewater and mining water led to reduced oxygen levels. Brown *et al*. (2023) established that apparent anoxia promoted the generation of methanogenic conditions and methane output linked to inflow of mining and other industrial residues.

Regarding acid mine drainage sediments specifically, FeS_2, the major contributor to acid mine drainage generation, was long considered biologically inert and a non-bioavailable sink of iron and sulphur when in the absence of oxidants (Payne *et al*., 2021). Recently this has been contested, as there is evidence that suggests that methanogens can cause an increase in the mobility of iron in metallic-rich anoxic habitats via reductively dissolving FeS_2 (Spietz *et al*., 2022a). Many of the enzymes required for extremophilic organisms require transition metals within their active sites or present in co-factors which allow holoenzymes to become fully functional (Fontecilla-Camps, 2022). Regarding carbon cycling, the critical co-factor F_{430} of the methanogenic *Archaea* is key of this, requiring nickel to facilitate the final methanogenic reaction. Additionally, iron is required in [NiFe]-hydrogenases used by several function groups of microorganisms. This includes the hydrogenotrophic methanogens, one functional group of the methane-generating organisms discuss later in **Section 1.3.2.1**.

Importantly, heterodisulphide reductase (encoded by *Hdr*), which catalyses the regeneration of the methanogenic co-enzyme M (HS-CoM) and B (HS-CoB) from the intermediate molecule heterodisulphide (CoM-S-S-CoB), requires chemically uncommon iron-containing noncubane (Fe_4S_4) clusters to allow the reduction reaction to proceed (Wu and Chen, 2022). The ability of methanogens to 'leach' iron from iron sulphide minerals may provide an advantage during biogeochemical cycling to maintain functional metalloenzymes, both currently and during methanogen evolution on ancestral Earth, thereby allowing effective catalysis of several critical methanogenic reactions.

It has been suggested that methanogens reduce FeS_2 to mobilise both the iron and sulphur components through extracellular electron transfer (EET) directly from the surface of the cell to the sulphide mineral. This contact and subsequent electron shuttling causes FeS_2 to transition through various redox states; intermediate stages involve the production of hydrogen sulphide in its ionic form, (HS^-) and Fe^{2+} ions which readily form inorganic complexes. This reductive process allows the cell to accumulate iron monosulphide clusters [$Fe\text{-}S_{(aq)}$] which can enter the cell via diffusion or active transport if electrochemically charged. The reduction of FeS_2 is thought to be mediated by electrically conductive surface appendages on the archaeal cell envelope or enhanced through extracellular polysaccharide production, however the exact mechanism has not been fully determined (Spietz *et al.,* 2022b).

Importantly, this brings new attention to the role of methanogenic species in accessing and cycling inorganic minerals through reductive pathways, which crucially do not produce the acidic by-products associated with acid mine drainage. Yet, if methanogenic species *can* survive in underexplored, metal-rich, and low pH conditions, this mechanism may allow for maintenance of intracellular metal reserves for enzyme synthesis as well as sulphur sequestration. Therefore, this novel mode of metal and sulphur acquisition by methanogens may reveal that the available routes to mineral utilisation by anaerobes are more complex than previously thought, allowing methanogenic energy conservation to persist in non-conventional systems.

Critically, methanogen persistence in metal contaminated environments would also require access to bioavailable precursor molecules for energy conservation via methanogenesis, such as those derived from fermentative bacterial reactions. Again, this is a major restriction on methanogenic growth in systems with low carbon inputs and where metal-containing inorganic nutrients may be in excess, contributing to abiotic stress. More broadly, an understanding of cryptic carbon cycling pathways would be advantageous in allowing a greater appreciation of microbial survival and community persistence in contaminated locations. Acidophilic consortia provide a unique opportunity to tackle unresolved questions in low diversity microbially driven ecosystems which function under physiochemically extreme abiotic conditions and may sources of both unrecognised greenhouse gases and metabolically diverse metal bioconversion pathways.

To understand the mechanisms and key taxa involved in carbon cycling in contaminated systems, an overview of the biological routes to methane generation under conventional systems should be considered. The following sections provide an overview of the anaerobic degradation of carbon and the functional diversity of methanogens responsible for methane evasion from microbial ecosystems.

1.2 The Methanogenic *Archaea:* Evolutionary History

Methanogenesis is the terminal stage of the carbon cycle under anaerobic conditions, resulting in the generation of biologically produced methane. Attributed to the function of the methanogenic *Archaea* ('methanogens'), methanogenesis is thought to be one of the most ancient metabolisms utilised by microorganisms and evolved approximately 4.1 - 3.8 billion years before the present (Wolfe and Fournier, 2018). Prior the methane generation in anoxic systems, organic polymers are converted to one-carbon compounds via bacterial mediated fermentative reactions (hydrolysis, acidogenesis and acetogenesis). The biochemical reactions involved in bacterial fermentation are more widely reported and are previously outlined elsewhere (Free *et al*., 2018). An overview of the anaerobic carbon cycle is shown in **Figure 1.4.**

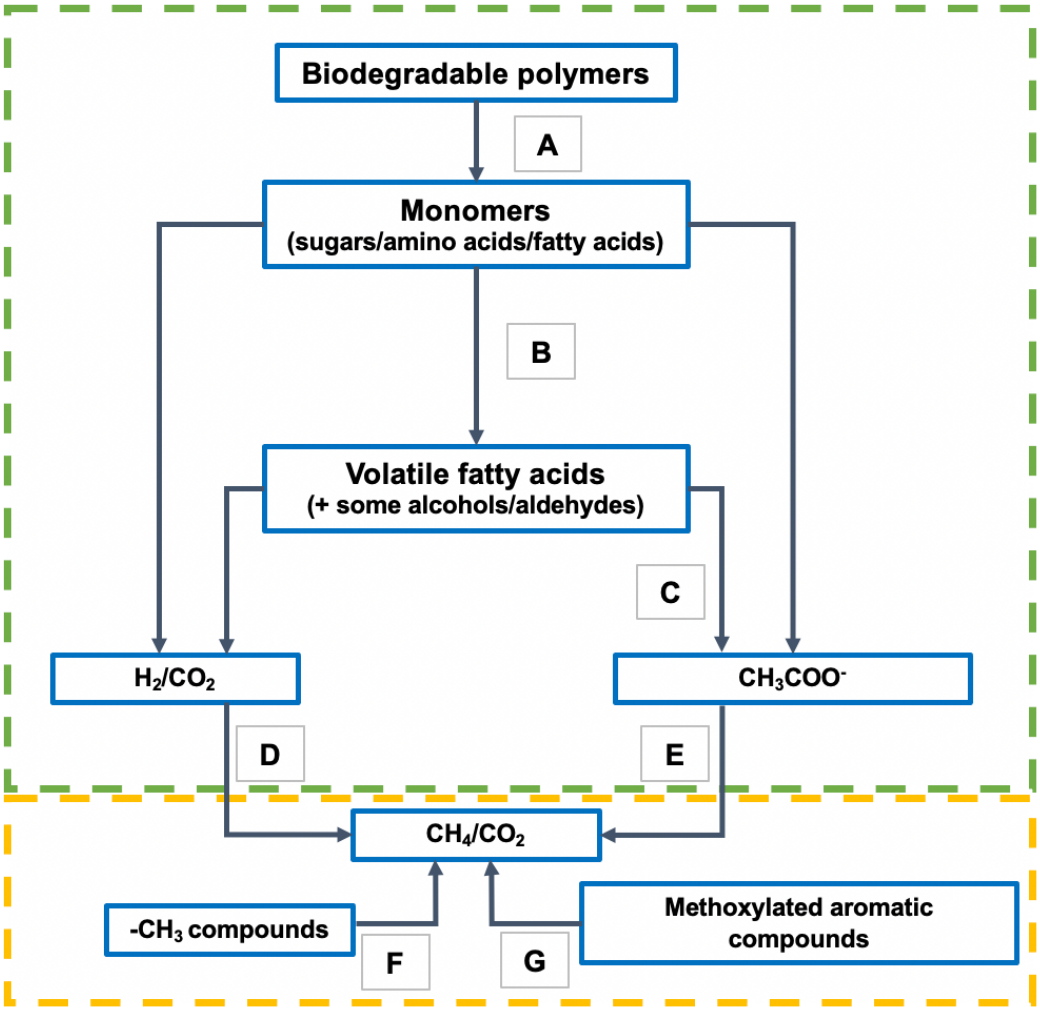

FIGURE 1.4: The anaerobic degradation of carbon. Reactions mediated by *Bacteria* are outlined in green. Reactions performed by methanogenic *Archaea* are outlined in yellow. Individually, **Reaction A** shows depolymerisation by hydrolysing *Bacteria,* producing monomeric subunits. Monomers are converted to fermentative end products, volatile fatty acids (**Reaction B**) and acetate (**Reaction C**). The resulting free H_2/CO_2 are utilised by hydrogenotrophic methanogens (**reaction D**), acetate is converted to methane by acetoclastic methanogens (**Reaction E**). Additional substrates such as methylated compounds (**Reaction F**) and aromatic compounds (**Reaction G**) can be converted to methane by specialised methanogenic taxa. Figure modified from Free *et al.* (2018).

Methanogens are likely to be the most ancient group of currently extant organisms. It is thought that methanogenesis was one of the principal metabolic pathways on Earth during the Archean Eon, prior to the Great Oxidation Event (GOE) and the resultant evolution of primitive multicellular life. Prior to the GOE, it is suggested that the vast methane outputs due to methanogens' dominance during the Archaean Era aided in maintaining a warm climate on early Earth by trapping heat within the anoxic atmosphere. This would have been advantageous when the faint young sun (FYS) only illuminated the sky weakly, as methane accumulation would have prevented drastic drops in global temperature and allowed the oceans of the Archaean Earth to remain liquid (Catling and Zahnle, 2020; Kasting and Siefert, 2002). Recent evidence suggests that the early Earth was engulfed by a high-temperature, turbulent global ocean which would have selected for the evolution of extremophilic microorganisms and allowed conditions optimal for the proliferation of ancestral prokaryotes (Dong *et al.,* 2021).

Precipitation of metals from the ancient oceans and the resultant integration into enzymatic machinery and metal-containing co-factors allowed diversification of microbial metabolic capabilities (Saito *et al.,* 2003). Incorporation of nickel (Ni) and iron (Fe) into early enzymes was fundamental in the evolution of the methanogenic *Archaea*. Additionally, methanogens also require tungsten (W) and molybdenum (Mo) for growth which were readily available on early Earth; these metals are exchangeable, and their utilisation by extant methanogens is dependent on metal bioavailability (Moore *et al.,* 2017). A timeline of methanogen evolution is shown in **Figure 1.5**.

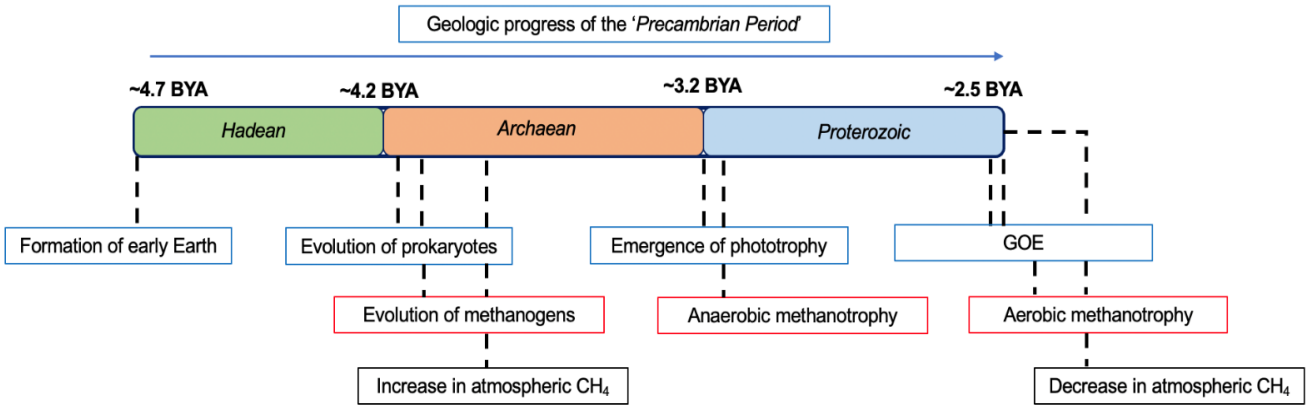

FIGURE 1.5: Evolutionary history of the methanogenic *Archaea*. Methanogenesis is thought to have evolved close to the Hadean/Archaean boundary, approximately 4.1 billion years ago (BYA) when early Earth's atmosphere remained anoxic. This was followed by rapid diversification of prokaryotic metabolic capabilities within the bacterial and archaeal domains; reactions that evolved pertaining to methane cycling are outlined in red. Figure developed from work of Battistuzzi *et al.* 2004; Moore *et al.,* 2017.

1.2.1 The Methanogenic Archaea: Discovery and Ecological Dispersal

Archaea, the third domain of life, were discovered through the pioneering work of Carl Woese in 1977 who identified, through variations in the 16S ribosomal RNA (rRNA) gene sequence, that the archaeans were phylogenetically distinct from the *Bacteria* (Woese and Fox, 1977). Woese's findings changed the fundamentals of taxonomy, disproving the previously utilised 'five kingdoms' approach due to the division now required within the prokaryotes. This resulted in the now recognised 'three domains' of life: the *Eukarya*, *Bacteria* and *Archaea*.

Archaea, often less metabolically diverse than *Bacteria* are highly adaptable and thrive in extreme habitats at the physiochemical boundaries habitable for life and show an extraordinary range in terms of their extremophilic lifestyles. Extremophilic *Archaea* inhabit ecosystems across the pH scale. Similarly, *Archaea* thrive in hypersaline conditions, under high hydrostatic pressure and at extremes of temperature.

Historically, *Archaea* were initially considered strict extremophiles. However, as knowledge of archaeal diversity and dispersal has increased, archaeans have been observed in more conventional environments whereby they function under less physiochemically stressful conditions. Importantly, archaeal taxa in conventional ecosystems also maintain essential roles in ecosystem function and can contribute to the nitrogen and sulphur cycling as well as removing excess hydrogen during organic matter decomposition. Additionally, some archaeal species form symbiotic relationships with 'higher' organisms (Sogin *et al.,* 2017).

Conventionally, most known methanogens are classified within the archaeal phylum Euryarchaeota**.** Generally confined to environmental niches in which oxygen is absent or excluded, methanogens are found in lake and marine sediments, waterlogged soils and within the gastrointestinal tract of mammals, particularly ruminants. Several studies have discussed extremophilic methanogens found in environments such as ice sheets (Tung *et al.,* 2006) and desiccated desert soils (Hernandez *et al.,* 2019) showing the environmental flexibility and adaptability to harsh environmental conditions so often attributed to members of their taxonomic domain. To date, no known methanogens (or archaeans more widely) are pathogenic, however their relative abundance has been noted to change in the GI tract of in patients with inflammatory bowel disease and diverticulitis (Hoegenauer *et al.,* 2022). Methanogens have also been implicated in oral biofilms (Robichaux *et al.,* 2003).

Regarding acidophilic methanogens, *Methanoregula boonei* is considered the most acid-tolerant methanogen detected to date and was isolated from a moderately acidic peatbog (pH 4.5). Potential methanogenic function has been observed in archaeal species classified in phyla other than Euryarchaeota (Zhou *et al.,* 2018; Berben *et al.,* 2022). Divergence in the *mcr* gene function is discussed further in **Section 1.3.3.**

Additionally, methanogens play important roles in carbon cycling in many industrial environments, such as landfill sites and wastewater treatment plants. During the landfilling process, waste compaction and degradation results in the release of biologically produced methane. Municipal waste landfills (MWLs) are the one of the largest contributors to human-related methane release; with ~ 30% of the total methane annual release from Europe being produced through landfill waste disposal routes (European Environment Agency, 2019). Preventing methane release to the atmosphere in spatially diverse landfill sites treating heterogenous and often hazardous wastes can be challenging, however gas release can be reduced through the drilling of methane collection wells, aiding in carbon capture.

Landfill sites fluctuate between methanogenic and non-methanogenic stages as the methanogenic consortia become disrupted. Loss of methanogenic activity is caused by both the accumulation of ammoniacal nitrogen (NH_3-N) during anoxic degradation of wastes, common in the acetogenic phase, and by the introduction of oxygen during waste handling (Kormi *et al.,* 2017). Despite the alkalinity, presence of persistent organic pollutants (POPs) and elevated Kjeldahl nitrogen (KN) levels, methanogens have been detected in leachates resulting from the landfilling process, despite challenging abiotic factors and growth conditions (Huang *et al.,* 2003).

The aerobic wastewater process produces vast quantities of settled sludge, a complex semi-solid or solid matrix of residual organic material and microbial consortia. The resultant sludge is subjected to anaerobic digestion (AD). During the AD process, large polymeric material within the sludge is degraded by anoxic consortia, producing methane-containing biogas and digestate. The biogas produced can be 'scrubbed' to improve methane yields and subsequently used as a source of sustainable bioenergy during wastewater treatment; this is advantageous as the water recovery process demands high energy inputs. The resultant digestate is a nutrient rich material composed of residual organic material. Digestate contains a liquid fraction termed 'reactor liquor' and a solid fraction. During optimal AD, sludge volume is reduced, with most of the organic material being degraded and converted to biogas. However, once dewatered, the solid fraction which remains high in nitrogen, phosphorus, and potassium can be applied to land as a biosolid fertiliser.

As the anaerobic digestion process is analogous to the reactions involved in the anoxic degradation of carbon (**Figure 1.4**) and is driven by microbial consortia, it can be prone to performance variability and process failure. Acidification of bioreactors through excessive acidogenesis and substrate recalcitrance can cause the function of methanogenic consortia to become impaired or cease, as methanogens are sensitive to fluxes in environmental conditions (Kong *et al*., 2016). Additionally, if sludge that has settled poorly through excessive growth of mycolic acid containing organisms during previous aerobic treatment stages enters the AD bioreactor infrastructure, the digesters can suffer poor performance (Davenport and Curtis, 2002; Jiang *et al*., 2016). In some cases, a high temperature thermal hydrolysis stage prior to anaerobic digestion can aid in the depolymerisation of complex substrates which otherwise could impede microbial hydrolysis. The ability to inoculate fully functioning reactors with digestate produced previously can aid in bioreactor recovery if community function within the bioreactor performance has been compromised.

In ecological studies, the relative abundance and diversity of *Archaea* is often low compared to their more widely studied bacterial counterparts. However, their ecological function in completing carbon breakdown and the consequent impacts of greenhouse gas emissions from natural and applied microbial ecosystems cannot be overstated.

It has been found that methanogens are globally ubiquitous in soils yet will remain physiologically dormant until conditions are optimal for growth. In the work of Angel *et al*. (2011) it was found that waterlogging of soil allowed reactivation of methanogenic communities and stimulated the subsequent generation of methane. Furthermore, the work of Grossart *et al*. (2011) successfully found evidence for the presence of methanogenic *Archaea* in well-oxygenated water columns in oligotrophic systems. It was hypothesised that in this case methanogenesis was coupled to hydrogen (H_2) production by tightly associated bacterial photoautotrophic partners. Crucially, this mechanism would allow the uncoupling of methanogenesis and methane consumption. The metabolic pathways involved in methane production and cycling are discussed in the following sections.

1.2.2 Methanogenesis and the Methyl Co-Enzyme M Reductase Complex

All methanogens use the methyl co-enzyme M reductase (Mcr) complex. This nickel-corrinoid enzyme complex contains two active sites for the binding and catalysis of substrate-bound methyl co-enzyme M (HS-CoM) and co-enzyme B (HS-CoB) to methane. Co-enzyme M and B transfer a methyl group and hydrogen to the Mcr complex, respectively. The methanogenic co-factor F_{430} assists in the final reduction to methane, completing methanogenesis (Wongnate and Ragsdale, 2015). Methane flux can vary widely due to physiochemical differences in anoxic ecosystem types, making global methane output extrapolations difficult (Dlugokencky *et al.,* 2011). Currently, estimates suggest that ~ 3% of wetlands' net annual ecosystem production is released to the atmosphere as methane, resulting in the production of approximately one billion metric tonnes of biologically produced methane per year (Ferry, 2010).

The structure of the *mcr* encoded enzyme complex is discussed in greater detail in **Chapter 4.** The activity of the Mcr complex in *Archaea* is the main contributor to biological methane release. However, some evidence suggests that organisms from both the eukaryotic and bacterial domains can also produce methane to a lesser extent using methylated compounds as precursors to methane under aerobic conditions (as reviewed by Liu *et al.,* 2022). Despite being likely minor contributors to methane release, these non-archaeal methanogenic pathways warrant further study.

It should be noted that not all biologically produced methane diffuses to the atmosphere; both archaeal and bacterial methane oxidising microorganisms evolved mechanisms to counteract the function of the Mcr complex. Methanotrophy, and the key enzyme required, particulate methane monooxygenase (pMMO), is discussed further in **Chapter 4.** Methanotrophy can function under both aerobic and anaerobic conditions, oxidising methane back to carbon dioxide (CO_2), thereby completing the global carbon cycle.

Critically, some methanogens are also capable of reverse methanogenesis during periods of excess methane production leading to trace levels of oxidation under anoxic conditions (Ferry, 2020; Moran *et al*., 2005). It is thought that the structure of the enzyme complex involved in the reverse methanogenesis pathway is a paralog of that which facilitates the production of methane, with specific modifications unseen in the methanogenic counterpart. It is assumed these modifications evolved later to allow the bidirectional reaction to occur more effectively. These changes to the enzyme's architecture include regions rich in cysteine residues, alternative post translational modifications and an adapted structure of the F_{430} co-factor required for the reverse oxidation reaction to proceed (Shima *et al*., 2012).

Despite the *mcr* encoded enzyme complex being conserved in all methanogens, there are three major metabolic routes which result in the generation of methane. A fourth more minor and less well documented pathway also is known to exist. Methanogens can be physiologically diverse but overall have a limited substrate spectrum available for their growth. The seven methanogenic orders and their metabolic capabilities are shown in **Table 1.2.** Typically, hydrogenotrophic, acetoclastic and methylotrophic pathways are utilised to yield energy, resulting in the production of methane. Several species can act facultatively and have acquired genes for more than one pathway; this is often observed in *Methanosarcina* species. It is thought that once methanogenesis evolved within the Euryarchaeota, the hydrogenotrophic pathway prevailed to become the most prevalent amongst the methanogens.

TABLE 1.2: The seven taxonomic orders of methanogenic *Archaea* and their metabolic routes to methane.

Methanogenic Order	Pathway(s) Utilised in CH_4 Production
Methanobacteriales	Hydrogenotrophic, Methylotrophic.
Methanococcales	Hydrogenotrophic.
Methanomicrobiales	Hydrogenotrophic
Methanosarcinales	**Acetoclastic*,** Hydrogenotrophic, Methylotrophic.
Methanomassiliicoccales	Methylotrophic.
Methanocellales	Hydrogenotrophic.
Methanopyrales	Hydrogenotrophic.

* *Methanosaeta* and *Methanosarcina* species **only**.

1.2.2.1 Hydrogenotrophic Methanogenesis

Hydrogenotrophic methanogenesis involves the reduction of carbon dioxide (CO_2) by electrons from hydrogen (H_2) to form methane and water. Hydrogenotrophy is widespread in the methanogens, and the work of Bapteste *et al*. (2005) suggests that hydrogenotrophic metabolism evolved once only, and that the genes involved in the hydrogenotrophic pathway have remained unchanged from those within the last evolutionary ancestor of all methanogenic hydrogenotrophs. There is no evidence of horizontal gene transfer (HGT) of hydrogenotrophic molecular machinery between methanogenic species.

The work of Wang *et al*. (2021) states that early methanogenic machinery was present in a common ancestor of the Euryarchaeota, members of the TACK superphylum and within the Asgard archaeal group, and that the individual methanogenic metabolic pathways diverged thereafter. Hydrogenotrophy is found in the order Methanopyrales (**Table 1.2**), an evolutionary ancient and deep branching methanogenic lineage showing its widespread presence across taxonomically distinct methanogenic groups within the Euryarchaeota phylum (Lever and Teske, 2015).

The hydrogenotrophic substrates, CO_2 and H_2 would have been readily available to the ancient methanogens through volcanism on Earth during the Archaean Era, allowing hydrogenotrophic methanogenesis to proceed without substrate limitation. This hydrogen-dependent metabolism would have depleted much of the free H_2 within the anoxic atmosphere following the formation of the planet. Further to this, Sauterey *et al*. (2022) suggests that the methane produced via the hydrogenotrophic pathway would have undergone photolysis prior the closure of the biological methane cycle.

During the H_2/CO_2 reductive pathway, hydrogen acts as the electron donor via the Wolfe Cycle (WC) and is coupled to the methyl-branch of the Wood-Ljundahl Pathway (WLP) (Borrel *et al*., 2016). Coupling of the WLP to methanogenesis allows transfer of electrons to CO_2, conserving energy and thereby allows hydrogenotrophic metabolism to be more energetically favourable. The terminal reaction involves the regeneration of the two methanogenic thiol co-enzymes via heterodisulphide reductase and the generation of CH_4 from the Mcr complex. The hydrogenotrophic metabolic pathway to methane is shown in **Figure 1.6.** The final reaction is shown in **Figure 1.7**.

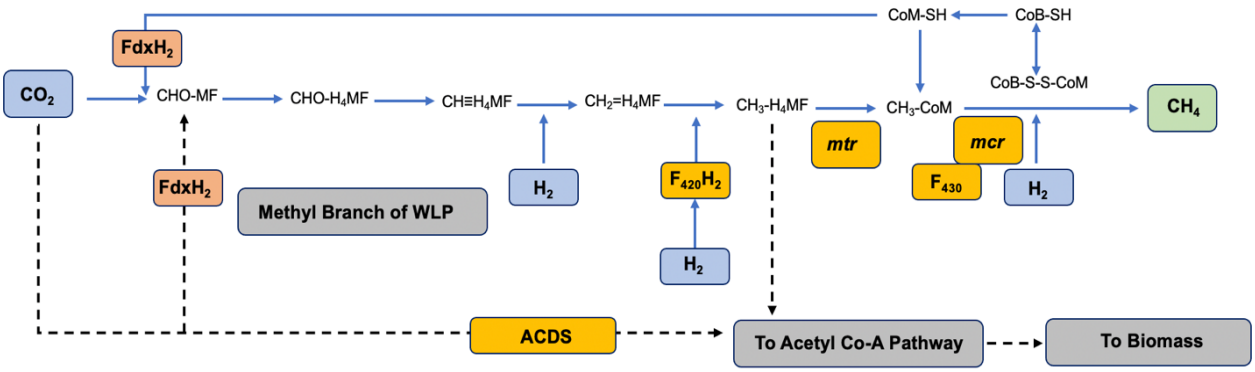

FIGURE 1.6: The biochemical pathway utilised by hydrogenotrophic methanogens. Key enzymes and co-factors involved are shown in yellow: *mtr* indicates CH_3-H_4MF methyl transferase, Mcr indicates the methyl co-enzyme M reductase complex, the H_2-carrying co-factor F_{420} and Mcr associated co-factor F_{430} are also shown at their locations in the pathway. ACDS indicates the acetyl Co-A dehydratase/synthase complex which enters the central acetyl Co-A pathway. Reduced ferredoxin ($FdxH_2$) which donate electrons are shown in orange. Hydrogenotrophic substrates (CO_2 and H_2) are shown in blue, with the final product methane (CH_4) shown in green. Coupling to the Wood-Ljundahl Pathway (WLP) is shown by dashed arrows.

$$CO_2 + 4H_2 \rightarrow CH_4 + 2H_2O \ (\Delta G^{o'} = -131 kJ/mol)$$

FIGURE 1.7: Hydrogenotrophic production of methane. The reaction is energetically favourable as demonstrated by the negative Gibbs' Free Energy (ΔG) change under standard conditions (25 ^oC and 1 atm of pressure). $\Delta G^{o'}$ value has been normalised by number of moles of available C-substrate reduced via Mcr enzyme activity, in this reaction, one mole of CO_2 (Fenchel *et al.,* 2006).

During anoxic degradation of organic material, H_2 becomes a competitive substrate, which both hydrogenotrophic methanogens and acetogens utilising the reductive H_2/CO_2 pathway both require. Methanogens can tolerate a lower critical threshold of hydrogen than acetogens can; this, coupled with the fact that the reduction of CO_2 with H_2 oxidation provides a greater energy yield for CH_4 than it does for acetate, means that hydrogenotrophic methanogens often act as the primary hydrogen-utilising organisms in anaerobic sediments (Ragsdale and Pierce, 2008). The ability of methanogens to tolerate a lower threshold of H_2 is of critical importance as an accumulation of free H_2 can lead to inhibitory growth conditions and cause an unfavourable thermodynamic equilibrium for anaerobic reactions to proceed.

In some cases, hydrogenotrophic methanogens can reduce carbon monoxide (CO) if CO_2 is not readily available. However, high CO concentrations can impede methanogenic growth if allowed to accumulate. It remains unclear if CO is a viable carbon source for all methanogens as this mechanism has only been documented to date in a limited number of *Methanosarcina* species (Ferry, 2010).

1.2.2.2 Acetoclastic Methanogenesis

The second major metabolic route to the production of methane involves the acetoclastic methanogens; those species which utilise acetate to generate methane. Acetoclastic methanogenesis has been noted to be the more significant methanogenic route in well-oxygenated soils where methanogens inhabit anoxic micro-environments, which shields their enzymes from inhibition by oxygen (Yuan *et al*., 2009). Likewise, the acetoclastic pathway is thought to be the major route of methane production in natural wetland systems, particularly across elevated latitudes within the northern hemisphere. Methane evasion resulting from acetate use is estimated to be responsible for up to two-thirds of annual biogenic emissions.

Acetoclastic metabolism is restricted to members of the Methanosaetaceae and Methanosarcinaceae taxonomic families only. Despite both methanogenic families being capable of converting acetate to methane, the pathways utilised by each taxonomic family are enzymatically distinct.

The acetolactic metabolic pathway is shown in **Figure 1.8.** The final reaction, the production of methane from acetate, is shown in **Figure 1.9.**

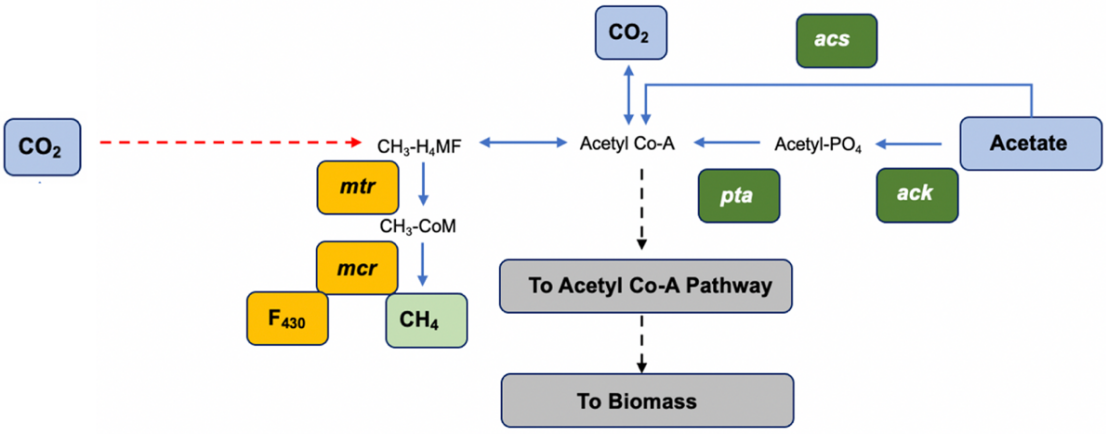

FIGURE 1.8: The biochemical pathway utilised by acetoclastic methanogens. Key enzymes and co-factors involved which are shared with the hydrogenotrophic pathway are shown in yellow: *mtr* indicates CH_3-H_4MF methyl transferase, *mcr* indicates the methyl co-enzyme M reductase complex, and the *mcr* associated co-factor F_{430} are shown at their locations in the pathway. Enzymes involved in the conversion of acetate to methane are shown in dark green. The two-stage reaction via acetate kinase (*ack)* and phosphoacetyl transferase *(pta)* expression is performed by *Methanosarcina. Methanosaeta* can bypass this route by utilising acetyl co-A synthase *(acs)*. Substrates are shown in blue. Methane is shown in pale green. Note the red dashed line indicates reactions occurring from CO_2 to CH_3-H_4MF as shown in **Figure 1.11.** Black dashed line indicates reactions which enter the acetyl Co-A pathway. Note that the regeneration of Co-M and Co-B occurs as outlined in **Figure 1.6.**

$$CH_3COO^- + H^+ \rightarrow CH_4 + CO_2 \ (\Delta G^{o'} = -36 \text{ kJ/mol})$$

FIGURE 1.9: Acetoclastic production of methane. The change in Gibbs' Free Energy (ΔG) indicates an energy yielding reaction, however this reaction can be performed in syntropy with acetogenesis. ΔG shown at 25 ^oC and 1 atm of pressure. $\Delta G^{o'}$ value has been normalised by number of moles of available C-substrate reduced via Mcr enzyme activity, in this reaction, one mole of acetate (Fenchel *et al.,* 2006).

During acetoclastic methanogenesis, acetate is converted to acetyl co-enzyme A (acetyl co-A), allowing the transfer of a methyl group to enter the central methanogenic pathway, terminating at the Mcr enzyme complex. *Methanosaeta* species use acetyl Co-A synthase to achieve this, whereas *Methanosarcina* utilise acetate kinase (AckA) and phosphoacetyl transferase (Pta). Neither *ackA* or *pta* gene homologs are found in any other *Archaea,* and it has been observed by Fournier and Gogarten (2008) that the acetoclastic machinery present in *Methanosarcina* resulted from a single HGT event.

It is likely that the archaeal forms of the *ackA* and *pta* arose via genetic transfer from an ancestral cellulytic *Clostridium* species. The genome of *Clostridium* contains both *ackA* and *pta* homologs which are expressed to allow acetate utilisation within fermentative pathways. This contrasts with the evolution of the hydrogenotrophic pathway which has not undergone any HGT events between species within in Euryarchaeota. Unlike the evolution of the hydrogenotrophic pathway, the acquisition of acetoclastic genes occurred relatively recently in evolutionary history, estimates placing this HGT event at 500 million years before the present.

After the evolution of acetoclastic methanogenesis occurred, it is likely that a methane 'burst' resulting from the combination of the methanogenic pathways' activity caused a rapid increase in global temperature and contributed to the Permian-Triassic Extinction; the most severe mass extinction event to have occurred on Earth impacting multicellular life (Rothman *et al*., 2014). The release of methane from stored oceanic methane hydrates ($8CH_4.46H_2O$) may have also accelerated the rapid rate of planetary warming.

Methanosarcina species are well documented as being the most metabolically flexible of the methanogens and it is thought that *Methanosarcina acetivorans* has the largest archaeal genome recorded (Maeder *et al*., 2006). *Methanosarcina* species can utilise acetate as a methanogenic precursor in periods of low H_2/CO_2 utilisation, or if methylated compounds are not present for conversion to methane.

Conversely, *Methanosaeta* species are strictly acetoclastic and are therefore restricted to utilising acetate as their sole carbon source. The work of Rotaru *et al*. (2014) stated that despite being considered strict acetate utilisers, *Methanosaeta* carries the full complement of genes required to perform CO_2 reduction to methane. Strikingly, it was noted that this mechanism was activated when electrons were shuttled to *Methanosaeta* by *Geobacter* through direct interspecies electron transfer (DIET) via electrically conductive pili on the cell surfaces. This mechanism may allow *Methanosaeta* species to increase their metabolic capabilities through direct coupling with neighbouring bacterial partners and overcome acetoclastic limitations (Zhao *et al*., 2015). This electron transfer between *Methonosaeta* and their electrogenic bacterial partners may benefit the methanogen when competing for acetate with syntropic acetate oxidising *Bacteria* (SAOB) (Dyksma *et al*., 2020). Additionally, and in contrast to the hydrogenotrophic methanogens, acetoclastic methanogens form syntrophic relationships with acetate producing *Bacteria* which produce their substrate for methanogenesis.

1.2.2.3 Methylotrophic Methanogenesis

Methylotrophic methanogenesis involves the use of methylated compounds (substrates containing at least a single -CH_3 functional group) to produce methane; the use of methanol (CH_3OH) and trimethylamine [$(CH_3)_3N$] are common. Methylotrophic ability is found across three methanogenic orders: the Methanosarcinales, Methanobacteriales and Methanomassiliicoccales (see **Table 1.2**). The pathways to methane vary between the methylotrophic orders; the Methanosarcinales possess cytochromes which allow them to metabolise methyl groups to CO_2 via electron transport chains within the cell membrane. However, methylotrophic methanogens which lack cytochromes are dependent on the availability of H_2 to reduce methyl groups to methane (Vanwonterghem *et al*., 2016).

The metabolic pathway involved in methylotrophic methanogenesis is shown in **Figure 1.10** An example of the methylotrophic production of methane is shown in **Figure 1.11** Two of the specific enzymes involved in the conversion of methanol and methylated compounds to methane are discussed further in **Chapter 4.**

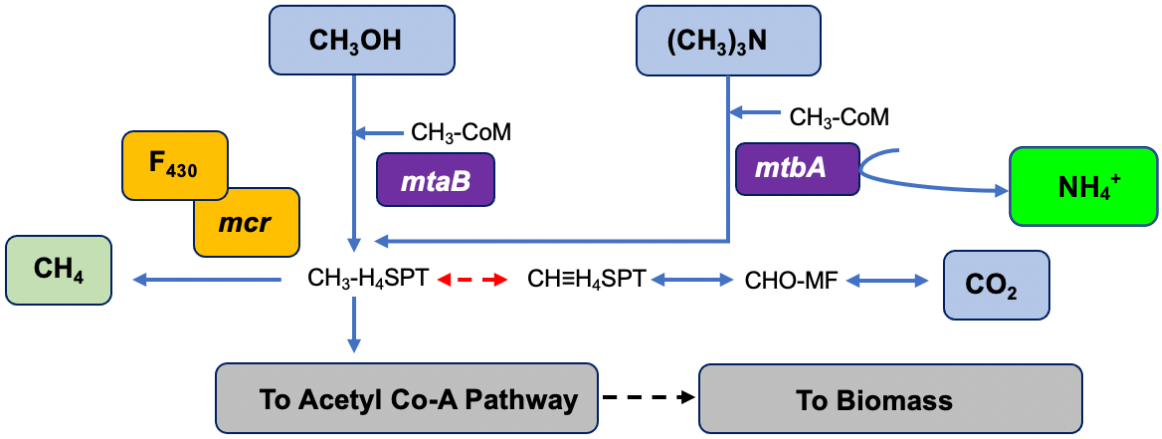

FIGURE 1.10: The biochemical pathway utilised for methanol *or* trimethylamine by methylotrophic methanogens. Key enzymes and co-factors involved which are shared with the hydrogenotrophic and acetoclastic pathway are shown in yellow: *mcr* indicates the methyl co-enzyme M reductase complex, and the *mcr* associated co-factor F_{430} are shown at their locations in the pathway. Key enzymes involved in the conversion of methanol [CH_3OH] (*mtaB*) and trimethylamine [$(CH_3)_3N$ *(mtbA)* to their metabolic intermediates prior to methane production are shown in purple. The activity of *mtbA* releases ammonium (NH_4^+), shown in green. Methane is shown in green. Note the red dashed line indicates intermediate bidirectional reactions not shown. Black dashed line indicates reactions which enter the acetyl Co-A pathway. Note that the regeneration of Co-M and Co-B occurs as outlined in **Figure 1.6.**

$$4(CH_3)_3N + 6H_2O + 4H^+ \rightarrow 4NH_4^+ + 9CH_4 + 3CO_2 \ (\Delta G^o = -31 \text{ kJ/mol})$$

FIGURE 1.11: Methylotrophic methanogenesis from trimethylamine. Gibbs' Free Energy reflects that this is the least energetically favourable of the methanogenic reactions shown in the preceding figures. The ΔG for the methylotrophic reaction shown at standard conditions. Reaction normalised for number of moles of trimethylamine converted to methane (Kurth *et al.,* 2020; Cozannet *et al.,* 2023).

1.2.2.4 Methoxytrophic Methanogenesis

Recently, a fourth methanogenic pathway has been observed. This peculiar pathway utilises methoxylated aromatic compounds (MACs) as substrates and is performed by *Methermicoccus shengliensis* which was isolated in the work of Mayumi *et al*. (2016). Expanding on this, Kurth *et al*. (2021) explored the metabolism of *M. shengliensis*. It was discovered that this novel metabolic route relies on a dual stage reaction mediated by methyltransferases; homologs to those found within the acetogenic *Bacteria*. Interestingly, based upon the inferred amino acid sequences of the *mcrA* gene, *M. shengliensis* is closely related to methanogens within the family Methanosaetaceae. However, *M. shengliensis* lacks the ability to catabolise acetate, typically a feature considered essential in the Methanosaetaceae and therefore is not considered to be capable of acetoclastic methanogenesis (Cheng *et al*., 2007).

Energy conservation and methane generation by *M. shengliensis* through MACs is thought to be an atypical form of methylotrophic methanogenesis, reliant on methyl-transfer to generate ATP opposed to electron-transfer as observed in other methyl-utilising methanogens (Kurth *et al*., 2021). Current knowledge of methanogenic metabolisms will continue to expand as novel methanogens are isolated and their physiological capabilities determined. A predicted pathway of achieving methanogenesis from MACs is shown in **Figure 1.12**.

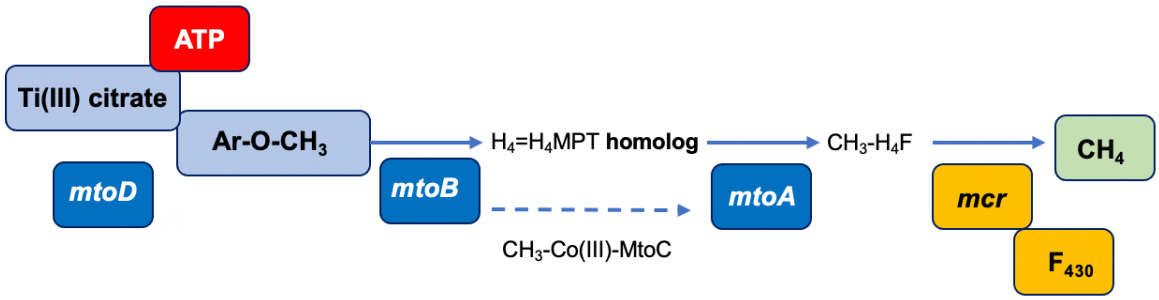

FIGURE 1.12: Predicted methanogenic pathway utilised by *Methermicoccus shengliensis* during conversion of aromatic compounds to methane. Key enzymes and co-factors involved which are shared with the other methanogenic pathways are shown in yellow: Mcr indicates the methyl co-enzyme M reductase complex, and the Mcr associated co-factor F_{430} is shown. Titanium (III) citrate ($TiC_{12}H_{28}O_{14}$) is required as an additional substrate to activate the aromatic compounds (Ar-O-CH_3), requiring ATP in the process. It is thought that the pathway is catalysed by a series of methyl transferases (expressed by *mtoD, mtoB* and *mtoA*) shown in dark blue. MtoC is predicted to be additional carrier protein for the -CH_3 group (mechanism shown as a dashed line), requiring a cobalt-containing co-factor. Figure adapted from Kurth *et al.* (2021).

1.2.3 Evolutionary Divergence in the Mcr Complex

Divergent *mcr* subunit gene sequences have been discovered in methane rich environments within the genomes of organisms classified in the archaeal phylum Verstraetearchaeota, itself classified within the TACK superphylum (discussed further in **Figure 1.13)**. It is hypothesised that members of the Verstraetearchaeota utilise a pathway homologous to the H_2-dependent pathway observed in the methylotrophic Methanomassiliicoccales (Vanwonterghem *et al*., 2016). It should be noted that *Methanomassiliicoccus* species lack several enzymes upstream of the *mcr* genes and utilise a truncated form of the pathway for conversion of methylated substrates (Sollinger and Urich, 2019). This gives rise to the theory that methanogenesis may be more widespread than originally thought and could occur in organisms classified in phyla outside of the 'traditional' methanogenic group, the Euryarchaeota. This novel methanogenic diversity should not be neglected when considering methanogens' role in maintenance of the global carbon budget and adds to the complex evolutionary history of the methanogenic *Archaea*.

Further to this, genes required for methanogenesis have also been observed within the reconstructed genomes of members of the archaeal phylum Bathyarchaeota (previously the Miscellaneous Crenarchaeotal Group). The metagenomes these were assembled from have been recovered from a range of anoxic environments, particularly marine and subsurface environments (Berben *et al*., 2022). Through metagenomic analysis, it has been implied that metabolic potential for members of the Bathyarchaeota include the ability to both anaerobically oxidise methane and produce methane via use of methylamines (CH_3NH_2), methanol (CH_3OH), and methylsulphates ($CH_3O_4S^-$). Bathyarchaeotal reconstructed genomes have been noted to possess genes involved in both the Wood-Ljundahl Pathway and methane generation via a putative *mcr* containing pathway, strengthening the evidence that these non-Euryarchaeotal organisms are capable of key alkane cycling reactions observed within Euryarchaeotal methanogens (Zhou *et al*., 2018).

Similarly, the work of Lynes *et al*. (2023) demonstrated the presence and expression of novel alkane cycling genes present within hot springs in Yellowstone National Park, USA. It was observed that *mcrA* sequences were present in both cultivated methanogenic lineages as well divergent sequences within the genomes of members of the candidate methanogenic phyla: Methanomethylicia, Hadesarchaeia and Archaeoglobi. Methanogenic pathway diversification, including function observed in non-euryarchaeal organisms is shown in **Figure 1.13.**

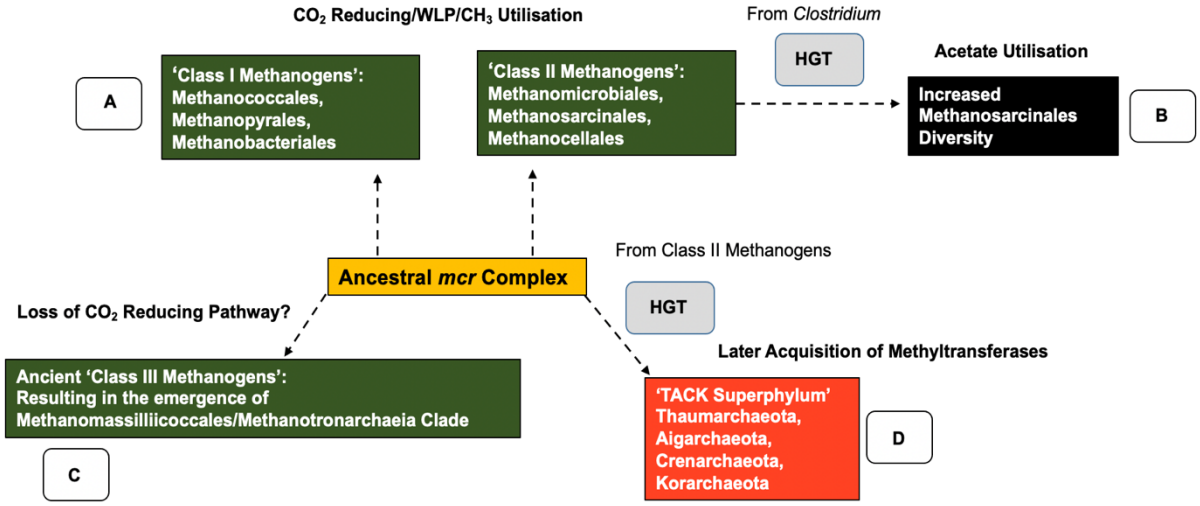

FIGURE 1.13: Predicted routes of diversification in and evolution of the major methanogenic pathways in the Euryarchaeota and the TACK superphylum. Methanogenic enzymatic mechanisms evolved on early Earth in an ancestral methanogenic archaeon and diversified thereafter within the Euryarchaeota (green boxes). **Evolutionary event A** indicates the emergence of the hydrogenotrophic-coupling and -CH_3 utilising pathways in Class I and II methanogens. Acetoclastic methanogenesis arose following ancestral *AckA* and *Pta* gene acquisition from *Clostridium,* expanding the metabolic capabilities of the Methanosarcinales; see **Event B**. Loss of the ability to perform the full H_2/CO_2 reductive pathway, as well as niche speciation likely led to the evolution of Class III methanogens (**Event C**). Methane, and further multi-carbon metabolism likely evolved in the TACK superphylum (**Event D**) via horizontal gene transfer of methyl transferases. Note some TACK taxa retain CO_2 reducing mechanisms. (Figure adapted from Berghuis *et al.* 2019; Wang *et al.* 2021).

Note: *AckA:* Acetate kinase; HGT: Horizontal Gene Transfer; Wood-Ljundahl Pathway; *mcr:* methyl co-enzyme reductase complex; -CH_3: indicates use of methanol, methylated compounds and/or methyl sulphates; *Pta:* Phosphoacetyl transferase; TACK: originally, Thaumarchaeota, Aigarchaeota*, Crenarchaeota◊ and Korarchaeota phyla. [Reclassified as: *Nitrososphaerota and ◊ Thermoproteota].

It should be noted that within the Euryarchaeota are non-methanogenic taxonomic lineages; it is hypothesised that the partial or complete loss of methanogenic machinery was relatively rare across taxa and was an ancient loss of function occurring within early methanogens' genomes. This allowed proliferation into alternative lifestyles seen in the halophilic *Archaea* within the Euryarchaeota which although related to methanogens, do not retain any enzymes reflective of their ancestral ability to produce methane (Borrel *et al*., 2016). Dissimilarly, methylotrophic methanogens retained their function, although utilise alternate means to produce methane as outlined previously.

1.3 Approaches to Studying Microbial Assemblages

Within the last decade, interest in understanding the ecological principles which govern the structure and function of microbial assemblages has increased rapidly. This is in part due to the ability to explore microbial communities to previously unprecedented depths through advancements in next generation sequencing (NGS) technologies. Historically, tackling open questions in microbial ecology has often lagged when compared to work on macroecological systems due to the limitations of conventional microbiological techniques, particularly when researching extreme microbial ecosystems.

Both cultivation based and molecular techniques utilised by microbial ecologists to explore assemblages of interest have been reviewed in more detail elsewhere (Free *et al.,* 2018). However, a brief overview of specific techniques, and how they are utilised regarding microbial consortia characterised in this work will be described below.

Despite the increasing number of studies utilising NGS techniques, cultivation of taxa remains key for determination of ecological function. Novel cultivation strategies have been developed and applied successfully to recover isolates from a range of extreme environments. Similarly, metabolic profiling of microbial consortia can provide valuable insights into the activity of the culturable community. Metabolic profiling has a more limited application than DNA based techniques which characterise prokaryotic assemblages in greater depth, yet focussing on a specific function (*e.g.,* substrate utilisation/degradation) can be advantageous and can also promote further enrichment of a specific functional characteristic of a community.

DNA-based techniques provide a powerful suite of tools which allow a greater level of community characterisation and functional attributes held within microbial genomes to be elucidated. Gene-based and both short and long-read sequencing (both utilised in metagenomics-based approaches) can be used together to determine both the composition of microbial communities, and the functional potential of members of the consortium. Further to this, the use of additional -omics techniques exploring gene expression and protein synthesis by communities is increasing, however, to date these novel approaches are more routinely applied to more conventional systems. Yet, as tools continue to develop, it is likely these techniques will become more applicable to extreme environments.

A summary of techniques applied in this thesis and the chapters were these appear is shown in **Figure 1.14**. More details regarding specific techniques are outlined at the start of each respective chapter.

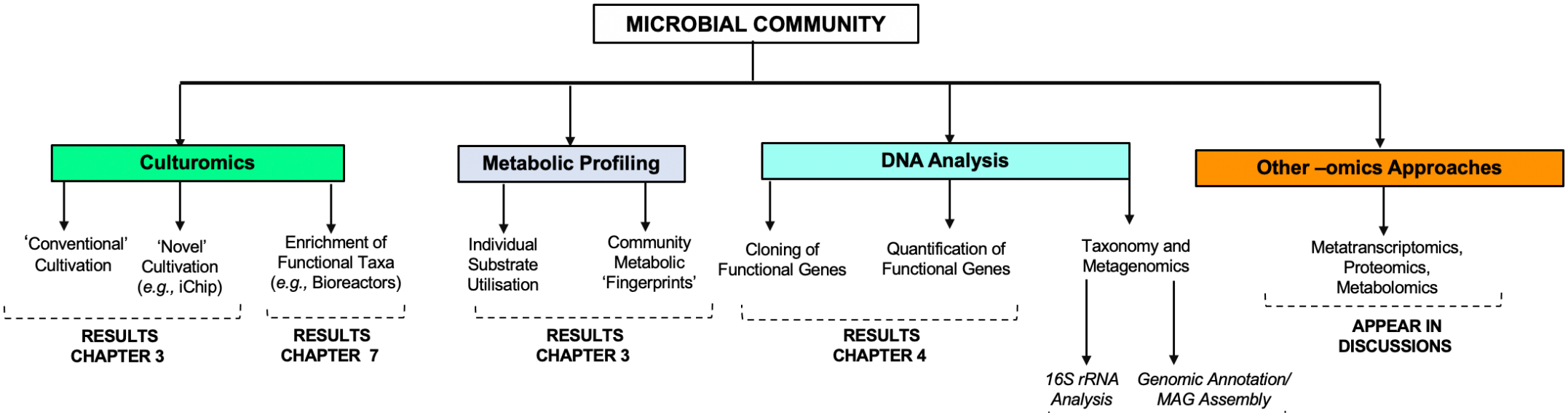

FIGURE 1.14.: Cultivation-dependent and molecular approaches that can be applied to the study of microbial assemblages. Growth of isolates and community enrichment can allow insights into ecological function in the environment, and lab-scale systems (green box). Characterisation of community members collectively performing a particular metabolic function can be explored via metabolic profiling (grey box). Genomic analysis using DNA (blue box) can involve both traditional amplicon sequencing (molecular cloning), gene quantification (qPCR), as well as metataxonomic and metagenomic community characterisation and reassembly of microbial chromosomes. Further to this, additional -omics techniques can determine the products of active community members using RNA transcripts and synthesised proteins and other metabolites (orange box). Techniques applicable to individual chapters within this thesis are shown in **bold**.

1.4 Aims and Structure of Thesis

1.4.1 Overall Aim of Thesis

Acid mine drainage microbial communities are poorly understood due to the complexities in studying consortia native to sites with an extremely low pH and high metallic content. Little is known regarding how acidophile-dominated microbial consortia drive ecosystem function and how this is linked more globally to biogeochemical cycling. Extremophilic methanogens have been detected in a range of ecosystems, yet their potential for methane release from mining impacted waterbodies has not been explored. Crucially, current understanding of the climatic implications of gas emissions from globally ubiquitous mine effluents and their impacted tributaries have lagged when compared to greenhouse gas generation in more conventional systems. Moreover, conventional microbiological strategies often have limited success when elucidating the mechanistic functioning of polyextremophilic assemblages.

To this end, the main aim of this work was to perform community characterisation of the microbial assemblage present within an acid mine drainage site (Benhar Bing, Lanarkshire, Scotland); with a particular focus of examining evidence of any carbon cycling mechanisms present as well as mechanisms utilised to withstand extreme abiotic stress (*e.g.,* metal[loid] cycling mechanisms). To demonstrate the deviation of acidophiles' physiology from more conventional microbial communities, this involved a comparison with several supplementary sites. These are more reflective of microbial ecosystems which derive energy from the decomposition of organic carbon, and the resulting production of methane via methanogenesis. Two non-extreme freshwater systems which had not been exposed to mining waste were selected for this purpose (Blackford Pond, Edinburgh, and Loch Bà, Scottish Highlands). Additionally, digestate samples from full-scale methanogenic bioreactors treating wastewater derived sludge were used as sources of highly enriched methanogenic consortia.

1.4.2 Structure of Results Chapters

Briefly, the results chapters begin at **Chapter 3** which presents a broad chemical and metabolic characterisation of the Benhar Bing acidophilic community and the two additional sediments. Additionally, this chapter also presents the results of cultivation trails to recover members of the acidophilic consortia native to acid mine drainage sediment. **Chapter 4** presents the first set of data exploring microbial assemblages using amplicon-based molecular approaches. In this case, results from the cloning and sequencing of bacterial, archaeal, and eukaryotic functional genes are presented, alongside quantification of target genes via qPCR. **Chapter 5** describes the metataxonomic composition of the Benhar Bing community, alongside taxonomic prediction from unassembled metagenomic data. Additionally, this chapters provides an overview of community-wide functional attributes determined from unassembled reads. Following this, metagenomic data was successfully assembled into annotated metagenome assembled genomes (MAGs), the results are presented in **Chapter 6.** These data present previously unreported functions in several acidophilic taxa which allow proliferation and survival in Benhar Bing's highly contaminated effluent. Lastly, **Chapter 7** explores the derivation of specific community function (methanogenesis) in bioreactors. Individual aims and objectives are listed are listed at the beginning of each results chapter.

CHAPTER 2 – Materials and Methods

2.1 Sample Collection

2.1.1. Selection of Sampling Sites

Three freshwater sites around Scotland were selected to act as sources of microbial communities within this study. This consisted of one acid mine drainage site (Benhar Bing) which was the predominant focus of the work. Blackford Pond and Loch Bà acted as two examples of more conventional sediments which were used as control sites. These sites were pre-selected and representative of non-contaminated and more conventionally methanogenic environments. Anaerobic digestate was collected from industrial scale anaerobic digesters at Seafield Wastewater Treatment Plant (WWTP) at various points during this study. The digestate acted as a source of pre-adapted methanogenic consortia and a source of previously partially hydrolysed organic substrate for microbial enrichment. Sampling locations are shown in **Figure 2.1**.

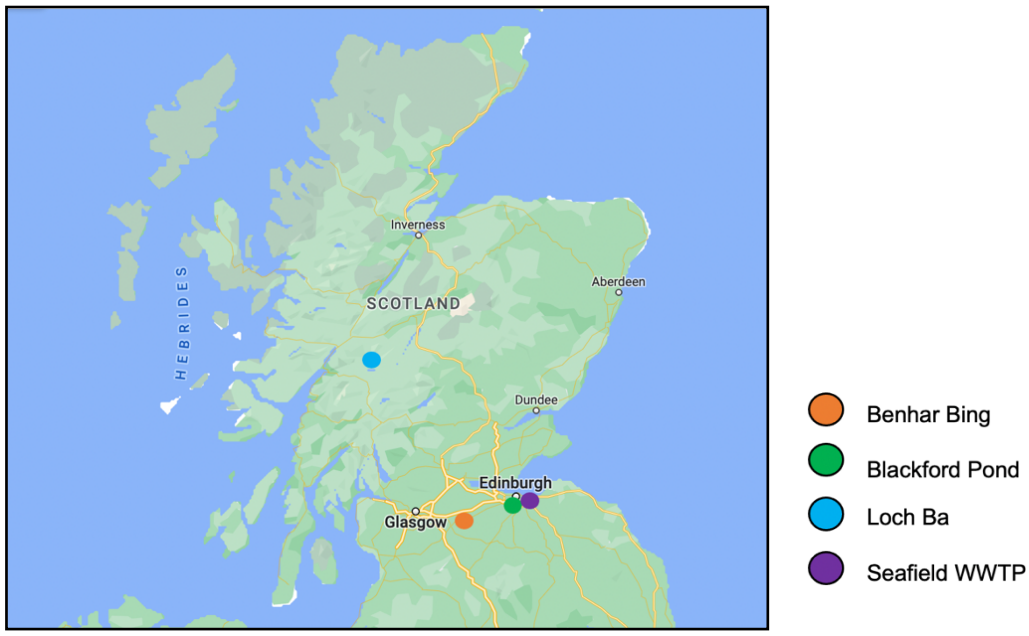

FIGURE 2.1: Locations of sampling sites. All samples were returned to the laboratory and stored at 4 ºC if not used immediately for analysis. Map of Scotland retrieved from Google Earth (v10.41.2.1).

2.1.2 Benhar Bing

Benhar Bing is a mine spoil heap resulting from past excavation of ironstone in central Scotland, approximately 45 km east of Glasgow (55.823°N 3.804°W) (Heal and Salt, 1999). Bioremediation and reclamation of the area began in 1996 through the development of a constructed wetland system (CWS). This wetland aimed to both slow and divert the flow of the acid mine drainage effluent, resulting in precipitation of metals into the sediment and therefore resulting in remedial treatment of the acidic and metal contaminated surface waters. Exact dates regarding the historical mining activities surrounding Benhar Bing are challenging to predict, however evidence of coal mining appears to have begun in the 1700s, following periods of times where mining activity appears to have ceased. Rapid expansion of iron mining appears to have occurred in the 1940s, which peak production of iron exceeding 200,000 tonnes a year (National Record of the Historic Environment, 2006).

Reclamation efforts reported in the work of Heal and Salt (1999) state that planting of alder (*Alnus sp*.) and birch (*Betula sp*.) trees was first trialled to stabilise the surrounding environment, increase biodiversity, and improve productivity of the site. Following this, the top layers of the acidic soil surrounding the area were amended with caked sewage sludge to increase the organic matter (OM) content of the soil. Development of the constructed wetland resulted in a settling pond, followed by a baffled flow system of 16 cells produced from the excavation of the downstream site as well as the layering of mushroom compost, peat, and limestone, prior to diverting effluent flow. This allowed the establishment of both surface and subsurface active flow bioremediation strategies. Cattails (*Typha sp.)* were planted into the wetland substrate to enhance phytoremediation and precipitation of metals as well as allowing the growth of microbial biofilms to occur on the sediment and adsorption of contaminants onto subsurface matrixes, the baffles and plant surfaces.

The polluted effluent exits the wetland into the River Almond, which then joins with the Firth of Forth Estuary in north-west Edinburgh. The acidity and metal contamination within the effluent into the River Almond may have factored in the decrease noted in the river's ecological status from class one (unpolluted) to between class three and four (grossly polluted). It should be noted that additional sources of diffuse pollution including agricultural runoff, proximity of heavy industry and wastewater effluent release will also contribute to the river's poor water quality (Pollard *et al*., 2001).

All sediment samples collected from Benhar Bing were taken from the settling pond. A schematic of the constructed wetland is shown in **Figure 2.2.** The surface of the settling pond and drainage ditch are shown in **Figure 2.3**

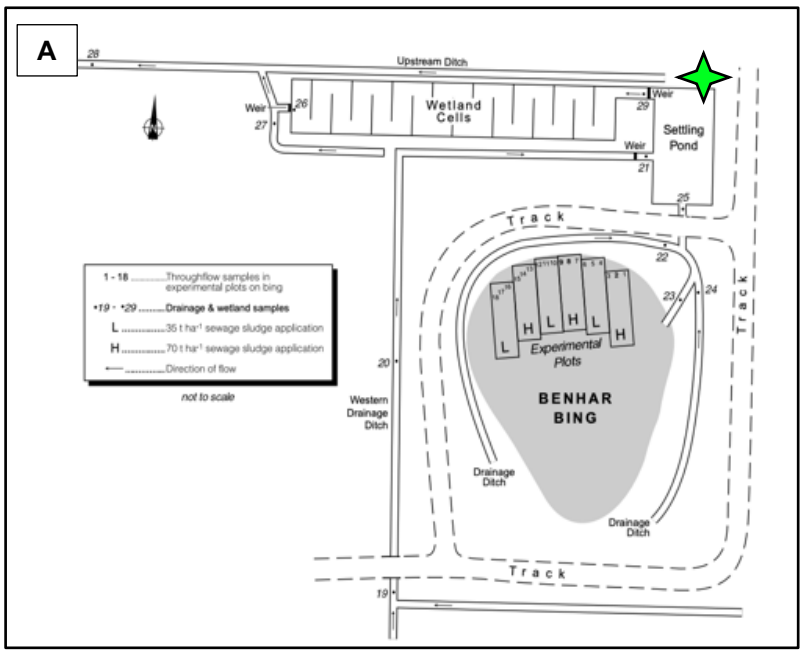

FIGURE 2.2: Schematic of Benhar Bing. The constructed wetland **(A)** contains a settling pond and a series of wetland cells ('baffles') which retain the effluent prior to joining the River Almond. The samples were collected from the settling pond, the surface of which is shown in **(B).** The weir exiting the settling towards the wetland cells is shown in (**C).** *[For source of Benhar Bing layout diagram, see Salt and Heal (2001)].* Sampling location shown by green star.

2.1.3 Blackford Pond

Blackford Pond is an artificial pond within a glacial hollow in the south of Edinburgh, Scotland (55 .5531°N, 3.114°W). There is no visible inflow, as would be expected with a natural body of water, however one outflow site exists. It is noted for becoming eutrophic through high organic inputs (City of Edinburgh Council, 2011) and the sediment is highly reduced. Blackford Pond is shown in **Figure 2.3.**

FIGURE 2.3: Blackford Pond. Samples were collected from the shore, approximately sampling location shown in (**A)** marked by green star. Sediment was covered with a layer of water from the pond **(B)** to maintain anaerobicity. Satellite image from Google Earth (v10.41.2.1).

2.1.4 Loch Bà

Loch Bà is a freshwater loch located on Rannoch Moor in the Scottish Highlands, approximately 80 meters above sea level (56.370°N, 4 .444°W). Rannoch Moor is considered as one of the remaining wildernesses in northern Europe. Due to Loch Bà's importance in maintaining the flow of freshwater ecosystem services, it is considered a Wetland of International Importance listed in the Ramsar Freshwater Convention (Flower *et al*., 1988; United Nations, 2023).

The bottom of the loch is highly irregular, with multiple basins. Loch Bà has a maximum depth of nine metres, with a mean depth of over two metres. Drainage enters from three surrounding lochs: Loch Buidhe, Lochan na Stainge and Lochan h-Aclaise. Loch Bà is shown in **Figure 2.4.**

FIGURE 2.4: Loch Bà. Loch Bà is located on an expanse of moorland **(A).** Sediment samples were collected by wading into the loch and removed with shovel or handheld corer **(B).** Satellite image from Google Earth (v10.41.2.1).

2.1.5 Seafield Wastewater Treatment Plant

Seafield Wastewater Treatment Plant (WWTP) treats municipal sewage from catchments within Edinburgh and East Lothian and is the largest water recovery plant in Scotland. During the water treatment process, which remediates 300 million litres of wastewater per day, influent sludge is settled and subjected to secondary biological treatment (Scottish Water, 2023). Subsequently, sludges are mixed and thickened to ~20% total solids (TS) and enter thermal hydrolysis reactors; treated water is discharged to the Firth of Forth Estuary. Following treatment, the effluent must comply with chemical and biological standards outlined in the Urban Wastewater Treatment Directive for water containing organic wastes.

Following this, the thermally depolymerised sludge leaves thermal hydrolysis at 100 °C and is dewatered to ~10% total solids prior to anaerobic digestion (AD) at mesophilic temperatures. At this point, the resultant waste entering AD is termed reactor 'feedstock'. This feedstock is digested by microbial consortia in the absence of oxygen for ~22-28 days in large scale anaerobic digesters, configured as continuously stirred tank reactors (CSTRs). Following the AD process, the digestate is centrifuged and dewatered, resulting in a 'caked' digestate. Feedstock, active digestate and caked digestate samples were used in this study. A schematic of the water treatment process is shown in **Figure 2.5.**

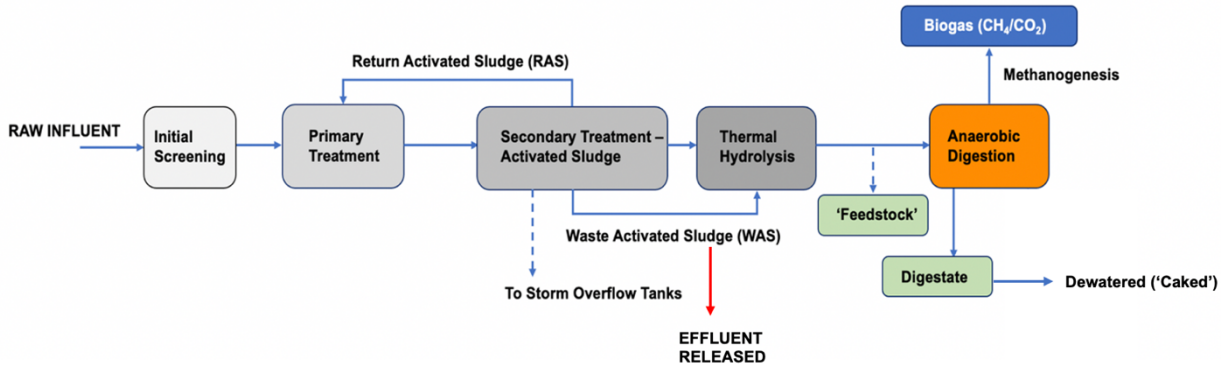

FIGURE 2.5: Schematic of the water recovery process at Seafield Wastewater Treatment Plant. Wastewater samples used in this study were collected following thermal hydrolysis, termed the anaerobic digestion 'feedstock', and digestate produced following anaerobic digestion; both sampling points during the process are shown in green. The feedstock and residual digestate (green boxes) are products of sludge settling from treatment processes prior to thermal hydrolysis; samples of both were collected during this study. Following dewatering, 'caked' digestate (stored in aerobic conditions) was also collected.

2.1.6 Sampling Techniques and Storage

Multiple sediment samples from each site were collected throughout the study, all from close to the edge of the sampling sites or shore. The initial samples were collected using a sterilised trowel and samples placed in sterilised plastic buckets with screw-top lids and stored at 4 °C until use.

Additional samples were collected on further dates during the project using a metal handheld corer with an inner plastic tube. Plastic filters were used on the corer to allow excess water to drain from the sediment during sampling. The corer allowed ~30 cm of intact sediment to be removed thus aiming to maintain anaerobic conditions within the centre of the sediment core. Sub-cores were removed from the larger ~30 cm core by embedding a sterile 50 ml Falcon tube into the centre of sediment core as an additional means of preserving anaerobicity. These sub-cores were stored alongside other sediment samples at 4 °C. Water samples were collected from Benhar Bing, Blackford Pond and Loch Ba in sterile 500 ml Duran bottles and stored at 4 °C.

Samples from Seafield WWTP were collected from the treatment works on various dates throughout this work. Digestate was collected in ~ 40 litre cannisters and kept at 4 °C. Despite methanogenesis decelerating at low temperatures, cannisters were routinely checked for biogas production, and any gas produced released. Feedstock samples were collected in sterile 500 ml Duran bottles and stored at 4 °C until use.

2.2. Chemical Methods

2.2.1 Determination of pH

The pH of all sediment samples, plus water, was measured after collection on a bench top pH probe (Thermo Scientific Fisher Orion 3 Star) calibrated with standard calibration solutions at pH 4, pH 7 and pH 10. Additional pH measurements were performed by The James Hutton Institute (JHI).

2.2.2 Determination of Elemental Contents

Elemental analysis was performed on all sediment samples and a digestate sample by JHI. Inductively Coupled Plasma-Optical Emission Mass Spectroscopy (ICP-OES) was used to determine elemental composition. Continuous Flow-Isotope Ratio Mass Spectrometry (CF-IRMS) was utilised to determine total carbon (TC) and the total organic carbon (TOC) fraction of the three sediments and digestate. Finally, Aqua Regia Digestion (ARD) was used to determine levels of trace metals across all sediments and digestate. All samples were sieved and dried at 37 ^{o}C for 5 days, followed by further heating at 105 ^{o}C in an oven prior to chemical analysis.

2.2.3 Determination of Chemical Oxygen Demand

Chemical Oxygen Demand (COD) was determined with the Hach Lange COD test vials (LCK 514). The COD test is routinely applied to wastewater samples as COD indicates the amount of oxygen consumed by reactions in solution; therefore, indicating the quantity of organic material that can undergo oxidation.

The commercially available COD test vials were used to determine COD in sediment, feedstock, digestate and bioreactor samples. The COD reaction is based upon an ion-exchange reaction between potassium dichromate ($K_2Cr_2O_7$) and sulphuric acid (H_2SO_4), with silver sulphate (Ag_2SO_4) as a catalyst. The manufacture's protocol (Hach Lange) was followed with the following modifications. Detection limitations for this assay were 100-2000 mg/L COD.

For sediment, digestate and bioreactor samples, 1 ml of each sample was centrifuged in sterile 1.5 ml tubes at 10,000 rpm for ten minutes in a bench top centrifuge (Thermo Scientific Heraeus Pico). Following this, the resulting supernatant was diluted (1:100) into the test vial with distilled water to ensure COD was within the measurable range. This was also performed for the supernatant collected from feedstock samples, however, with a 1:1000 dilution to ensure COD was within the measurable range for the test kit. Following incubation outlined by Hach Lange vials were measured at 605 nm once cool in a benchtop DR 1900 Hach Lange Spectrophotometer.

2.2.4 Determination of Organic Acids

Organic acid (OA) levels were determined in sediment, digestate, feedstock and bioreactor sample, using Hach Lange Organic Acid Testing Kit (LCK 365). Organic acids are a key metabolic intermediate to assess as elevated levels of short chain acids produced by acidogenic *Bacteria* can inhibit methanogenic activity.

Briefly, the protocol determines organic acids through the production of esters from organic acids in samples; the esters produced (R–COO–R′) were further reduced by Fe^{3+} ions, producing Fe-complexes. The resulting iron-ester complexes were measured as an indirect determinant of initial organic acid contents. This was performed as stated in the manufactures' protocol Hach Lange with the following modifications. All samples were centrifuged in sterile 1.5 ml tubes at 10,000 rpm for 10 minutes (Thermo Scientific Heraeus Pico centrifuge) prior to the supernatant being diluted (1:5) into the test vials with distilled water. The iron-ester complexes were determined photometrically at 497 nm in a benchtop DR 1900 Hach Lange Spectrophotometer. Note that the detection threshold for organic acids via the LCK 365 kit is 50-2500 mg/L.

2.2.5 Determination of Sulphate

Levels of sulphate (SO_4^{2-}) were determined in all samples using the Hach Lange Sulphate Test Kit (LCK 153) following the protocol made available by the manufacturer (Hach Lange). Briefly, the reaction involved aqueous sulphate ions in the sample aliquots react with barium chloride ($BaCl_2$), forming barium sulphate ($BaSO_4$), which was measured photometrically at 430 nm. For the quantification of sulphate via this assay, the limits of detection are 40-150 mg/L SO_4^{2-}.

2.2.6 Determination of Sulphide

Levels of sulphide (S^{2-}) were determined in all samples using the Hach Lange Sulphide Test Kit (LCK 653) following the protocol provided with the test cuvettes (Hach Lange). Detection of sulphide levels is performed through the reaction of sulphide in samples with *N, N*-dimethyl-*p*-phenylenediamide [$(CH_3)2NC_6H_4NH_2$] and Fe^{3+} ions, producing methylene blue ($C_{16}H_{18}ClN_3S$). Methylene blue was measured photometrically at 666 nm on a Hach Lange bench top DR 1900 spectrophotometer. Sulphide concentrations between 0.1-2.0mg/L can be detected via the LCK 653 methodology.

2.2.7 Determination of Ammonia

To determine levels of ammonia (NH_3) in each sample, AquaCheck Water Quality Test Strips (Hach Lange) were used following the provided protocol. In a modification to the protocol, sediment samples were centrifuged in 1.5 ml sterile tubes for 10 minutes at 10,000 rpm. The test strips were placed into the supernatant and submerged for 2 minutes; a modification to the manufacturer's instructions to ensure the reaction occurred using porewater as the test sample. The resulting colour change reaction was compared to NH_3 indicator scale provided with the test kit.

2.2.8 Determination of Ammonium

Ammonium (NH_4) was determined using the Hach Lange Ammonium Test Kit (LCK 303) following the instructions provided (Hach Lange). Ammonium in the sample aliquot acted as the substrate in the Berthelot's Reaction, reacting with both hypochlorite (ClO^-) and salicylate ions ($C_7H_5O_3^-$) at an alkaline pH. Sodium nitroprusside ($C_5FeN_6Na_2O$) acted as the catalyst. The reaction produced indophenol blue which was determined photometrically at 694 nm in a Hach Lange bench top DR 1900 spectrophotometer. The detection threshold of the NH_4 assays outlined here is 2.0-47 mg/L.

2.3 Culture Dependent Methods

2.3.1 BIOLOG EcoPlate Incubation

Metabolic profiling methodologies are outlined below. All 96-well plates utilised for community analysis, *ie*. both EcoPlates and anaerobic microplates were purchased from BIOLOG Inc, California, USA.

EcoPlate metabolic assays are reliant on a colour change reaction indicative of carbon source catabolism. A colourless tetrazolium salt [5-cyano-2,3-bis(4-methylphenyl)-2*H*-tetrazolium chloride] present within the EcoPlate wells acts as the electron acceptor, becoming reduced and producing the violet indicator salt, formazan (Benov, 2021). Formazans are artificial chromogenic agents produced via hydrogenase or reductase mediated redox reactions involving tetrazolium salts, the production of which is indicative of cellular metabolic activity (Ikeda *et al.,* 2023). The resulting production of reduced nicotinamide adenine dinucleotide (NADH) from substrate oxidation readily donates electrons to the electron transport chain (ETC). Redox dyes such as tetrazolium readily accept electrons, converting tetrazolium to a highly coloured and chemically reduced product (Pan *et al.,* 2023). The use of EcoPlates in metabolic profiling strategies is discussed further in **Chapter 3.**

The production of formazan can the quantified spectrophotometrically and the optical density (OD) taken as a measure of the microbial metabolic response to a particular carbon source (Yerulker *et al*., 2023). The development of formazan is directly correlated with the oxidation. Corrected OD values (OD*i*) are produced by reducing the original OD absorbance values detected by the OD value observed for the control well.

EcoPlates were inoculated by serially diluting sediment samples from neat to 10^{-4} dilution in sterile phosphate buffered saline (PBS). An aliquot of 150 µl of each 10^{-4} sediment dilution was inoculated into each well of the EcoPlate. EcoPlates were wrapped in parafilm to prevent dehydration of wells and incubated aerobically at 30 ^{o}C in a static incubator **(**Gallenkamp**).** Plates were checked routinely for formazan production. After no further utilisation of substrates was visible, plates were read on a Multiskan GO Spectrophotometer (Thermo Scientific) at 595 nm and optical density units (ODU) recorded. The above method was repeated from EcoPlates that were incubated under anaerobic conditions (however, incubation temperate was 37 ^{o}C). These plates remained incubated in an anaerobic chamber (Don Whitley Scientific) with standard anaerobic gas (80% N_2, 10% CO_2 and 10% H_2) until no further substrate utilisation was noted. The plates were then removed, and formazan production measured again using a Multiskan GO Spectrophotometer as outlined above. A schematic of the 96 well plate EcoPlate with substrates is available in the supplementary materials.

To enhance carbon utilisation by microbial communities, present in the acidic, metal rich Benhar Bing sample, an aerobic EcoPlate was inoculated as outlined above with diluted Benhar Bing sediment. However, the PBS used in the dilution was acidified with 1 M sulphuric acid (H_2SO_4) to pH 3.

2.3.2 BIOLOG Anaerobic Microplate Incubation

Specialised anaerobic plates were inoculated with 100 µl of 10^{-4} serially diluted sediment in anaerobic PBS. PBS was left in anaerobic conditions for 48 hours prior to being used as diluent to exclude oxygen and promote anaerobic activity of the diluted microbial consortia. The manufacturer's protocol states that if using the anaerobic microplates to characterise isolates, that cultures should be pre-incubated in the inoculating fluid provided and grown to a specific cell density prior to microplate inoculation. This step was omitted as microbial communities were being characterised, opposed to pure cultures of anaerobes and the inoculating fluid may have selected for specific culturable species within the community prior to inoculation. Similarly, to the anaerobic EcoPlate incubation, the anaerobic microplates were incubated at 37 ^{o}C under the anaerobic conditions stated above and checked routinely for formazan production. Plates were wrapped in parafilm to prevent dehydration of the wells. After no further utilisation of substrates was visible, plates were read on a Multiskan GO Spectrophotometer as stated above. A schematic of the 96 well plate AN microplate layout is available in the **Supplementary Material (Figure S1).**

2.3.3 Determining Microbial Activity in BIOLOG Assays

To assess BIOLOG plate responses, two measures of activity were determined: the average well colour development (AWCD) response and the mean functional diversity ($\%_{FD}$). These were calculated as follows:

- Average well colour development (AWCD) = $\Sigma OD_i/31$
- Functional diversity ($\%_{FD}$) = n / 31 x 100 where n = number of utilised substrates.
- Corrected OD (OD_i): OD value – OD reading of control well.

2.3.4 Growth Medium for Attempted Methanogen Cultivation: SAB and DSMZ 120

Several cultivation strategies were used to achieve growth of extremophilic isolates. Isolation approaches included media specific to methanogenic *Archaea* and aerobic acidophiles more generally, with the aim of culturing communities of bacterial anoxic degraders and archaeal methanogens.

Initially, two methanogen specific media types were prepared. SAB medium for the isolation of methanogens was prepared as outlined in the work of Khelaifia *et al*. (2013) and *Methanosarcina* 'growth media 120' was prepared as outlined by the German Collection of Microorganisms and Cell Cultures (DSMZ, 2022a).

The composition of SAB media was as follows: $NiCl_2$ x $6H_2O$, 1.5 mg/L; $FeSO_4$ x H_2O, 0.5 mg/L; $MgSO_4$ x $7H_2O$, 0.8 g/L; KH_2PO_4, 0.5 g/L; K_2HPO_4, 0.5 g/L; KCl, 0.05 g/L; $CaCl_2$ x $7H_2O$, 0.05 g/L; NaCl, 1.5 g/L; NH_4Cl, 1 g/L; $MnSO_4$ x $7H_2O$, 0.6 mg/L; $ZnSO_4$ x $7H_2O$, 0.1 mg/L; $CuSO_4$ x $5H_2O$, 0.02 mg/L; $KAl(SO_4)_2$. $12H_2O$, 0.2 μg/L; H_3BO_3, 7 μg/L; $CoSO_4$ x $7H_2O$, 4 μg/L; Na_2MoO_4 x $2H_2O$, 0.5 mg/L; Na_2SeO_3 x $5H_2O$, 3 μg/L; Na_2WO_4 x $2H_2O$, 4 μg/L; Nitrilotriacetic acid, 0.15 mg/L; sodium acetate, 1 g/L; trypticase, 2 g/L; yeast extract, 2 g/L; L-cysteine hydrochloride monohydrate, 0.5 g/L; valeric acid, 5 mM; isovaleric acid, 5 mM; 2-methylbutyric acid, 5 mM; isobutyric acid, 6 mM; 2-methyl valeric acid and distilled water to one litre.

The composition of *Methanosarcina* growth media 120 was prepared as follows: K_2HPO_4 0.35 g/L; KH_2PO_4 0.23 g/L; NH_4Cl 0.50 g/L; $MgSO_4$ x 7 H_2O 0.50 g/L; $CaCl_2$ x 2 H_2O 0.25g/L; g NaCl 2.25 g/L; $FeSO_4$ x 7 H_2O solution (0.1% w/v) 2.00 ml; trace element solution 1.00 ml*; yeast extract (OXOID) 2.00 g/L; casitone (BD BBL) 2.00 g/L; Na-acetate 2.50 g/L; $NaHCO_3$ 2.00 g/L; methanol (50% v/v) 20.00 ml; Wolin's vitamin solution (10x) 1.00 ml**; L-cysteine HCl x H_2O 0.30 g/L; Na_2S x 9 H2O 0.30 g/L and distilled water to one litre.

Trace element solution (* above) contained: HCl (25%) 10.00 ml; $FeCl_2$ x 4 H2O 1.50 g; $ZnCl_2$ 70.00 mg; $MnCl_2$ x 4 H2O 100.00 mg; H_3BO_3 6.00 mg; $CoCl_2$ x 6 H2O 190.00 mg; $CuCl_2$ x 2 H_2O 2.00 mg; $NiCl_2$ x 6 H_2O 24.00 mg; Na_2MoO_4 x 2 H_2O 36.00 mg and distilled water to one litre.

Wolin's vitamin solution (** above) contained: biotin 20.00 mg; folic acid 20.00 mg; pyridoxine hydrochloride 100.00 mg; thiamine HCl 50.00 mg; riboflavin 50.00 mg; nicotinic acid 50.00 mg; Calcium D-(+)-pantothenate 50.00 mg; vitamin B12 1.00 mg; p-aminobenzoic acid 50.00 mg; (DL)-alpha-lipoic acid 50.00 mg and distilled water to one litre.

In place of anoxic sparging of medium components with nitrogen, plates were degassed under standard anaerobic conditions outlined previously for ~ 48 hours prior to use. Additionally, 1 mg/L of the anaerobic indicator resazurin (7-hydroxy-3H-phenoxacin-3-one-10-oxide sodium salt) ($C_{12}H_6NNaO_4$) was added to each media type. Media was autoclaved as outlined previously at 121 °C for 15 minutes and plates poured once media had cooled under anaerobic conditions.

Benhar Bing sediment was serially diluted in anaerobic PBS from neat samples to 10^{-8}, and 100 µl of each dilution plated in triplicate under anaerobic conditions and incubated at 30 °C. Plates were wrapped in parafilm following ~ 4 days of incubation as signs of agar dehydration were visible.

2.3.5 Growth Medium for General Acidophiles: R2A and YEFS

For enumeration of acidophiles, two media types were selected. Reasoner's 2-A (R2A) medium was available pre-prepared for liquid cultivation (Thermo Fisher). Yeast Extract Ferrous Sulphate (YEFS) 'growth medium 1190' was prepared following the media recipe outlined by DSMZ (2022b). YEFS medium is composed of the following: yeast extract 0.20 g; 50x heterotrophic basal salts solution 20.00 ml; ferrous sulphate solution (FeSO4 x 7 H_2O) 250 ml; D-Glucose 1.00 g; distilled water 980.00 ml. To prepare 50x heterotrophic basal salts solution: Na_2SO_4 x 10 H_2O 7.50 g; $(NH_4)_2SO_4$ 22.50 g; KCl 2.50 g; $MgSO_4$ x 7 H_2O 25.00 g; KH_2PO_4 2.50 g; $Ca(NO_3)_2$ x 4 H_2O 0.70 g; distilled water to one litre.

To prepare solid R2A medium, 15 g/L of agar powder was added to 1L dH_2O. Media was sterilised as outlined above. The R2A medium contained: dextrose 0.5 g/L; magnesium sulphate 0.024 g/L; sodium pyruvate 0.3 g/L; yeast extract 0.5 g/L; casein acid hydrolysate 0.5 g/L; proteose peptone 0.5 g/L; dipotassium phosphate 0.3 g/L and starch 0.5 g/L.

For YEFS plates, 500 ml of medium was pH adjusted to pH 3 using 1 M sulphuric acid (H_2SO_4) and 500 ml which was not pH adjusted. Similarly, to SAB plates, Benhar Bing sediment was serially diluted down to 10^{-8} in PBS and dilution aliquots plated (100 µl) onto R2A plates and YEFS plates respectively. Plates were incubated aerobically at 30 °C and checked routinely for signs of visible growth.

2.3.6 iChip Inoculation and Enrichment

The iChips used for microbial cultivation during this study were provided by The Department of Biology, The University of York, UK. Following sieving, 5 ml of Benhar Bing sediment was mixed with 50 ml of molten R2A semi-solid media; 7.5 g/L of agar was added to the standard R2A medium protocol. While still molten, ~ 2 ml of semi solid agar was pipetted onto the central disc, ensuring the wells were covered. Once set, 0.6 µm filters (Millipore) were placed each side of the central disc prior to assembling the device. iChip components were sterilised before use with ethanol and are shown in **Figure 2.6.**

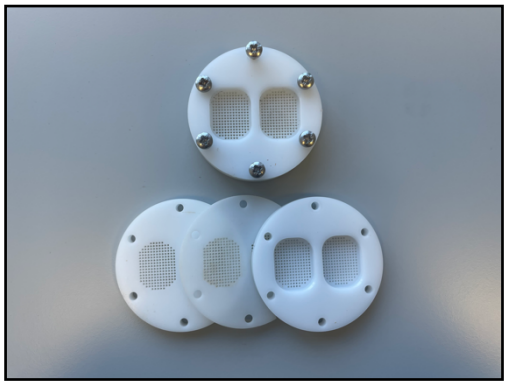

FIGURE 2.6: iChip Assembly. The top iChip shown is assembled, and below is an unassembled iChip showing the two outer plastic supports and the central disc, containing the isolation wells.

Two iChips were buried in buckets of Benhar Bing sediment and incubated at room temperature for between 7-10 days. Following incubation, plugs were removed using a sterilised thin metal rod. Plugs were re-inoculated in triplicate into 20 ml liquid R-2A broth as detailed above which was acidified to pH 3 with either 1M H_2SO_4 or sterilised water from Benhar Bing. Liquid R2A enrichments were incubated at 30 °C in a shaking incubator (New Brunswick Scientific Company Inc) at 100 rpm for 10 days. Genomic DNA (from liquid cultures was extracted using the Qiagen DNeasy PowerSoil extraction protocol as outlined below.

2.3.6 Gram Staining and Microscopy

Aliquots of liquid cultures grown from iChip plug-enrichment were Gram stained to observe cell wall characteristics and cellular morphology. 5 µl samples were loaded onto sterile microscopy slides. Gram staining was performed following the standard protocol outlined by The American Society for Microbiology (2005). Microscopy was performed on a Nikon Eclipse E200 microscope.

2.4 Molecular Methods I: DNA Extraction, PCR, qPCR, and Sanger Sequencing of Plasmids

2.4.1 Environmental DNA Extraction

Extraction of DNA from sediment, digestate and feedstock samples were initially performed using the DNeasy PowerSoil kit (Qiagen). The manufacturer's protocol was followed and DNA following elution was stored at 4 °C or -20 °C prior to use in downstream applications. Modifications to protocol involved addition of 0.25 g of sediment or digestate sample to PowerBead tubes, opposed to 250 µl of sample, due to solid consistency of samples and all 4 °C incubations were performed on ice. For extraction of genomic DNA from a liquid bacterial culture grown from the iChip enrichment, 200 µl was used in the PowerBead tube. In 2021, the standard Qiagen kit was updated, and the new Qiagen DNeasy PowerSoil Pro kit was used thereafter to extract DNA following manufacturer's protocol.

2.4.2 Determining Quality and Concentration of Extracted DNA

Following all extractions, DNA was quantified using a Nanodrop Spectrophotometer using the C6 elution buffer (provided by Qiagen) as a blank control and the concentration of 1 µl of DNA determined; concentration, 260:280 and 230:260 ratios were recorded. DNA quantification was also performed using the Quant-*iT* dsDNA High Sensitivity Assay on a Qubit using the manufacturer's protocol (Invitrogen).

2.4.3 Polymerase Chain Reaction (PCR) Methods

The Polymerase Chain Reaction (PCR) was applied numerous times during this work to amplify target genes from DNA. All PCRs were performed in a Labnet MultiGene Optimax Thermocycler, apart from methanogen-specific PCRs which were all performed in an Applied Biosystems SimpliAmp Thermal Cycler, which allowed temperature ramping stages to be programmed. All primer sequences used during this work are shown in **Table 2.1**.

All reagents and specified volumes for each PCR reaction are available in **Table 2.2.** All PCR products were stored -20 ^{o}C if not used immediately for downstream visualisation or subsequent second round PCR reactions.

TABLE 2.1: List of primer sequences used during this study. All primers were produced using Sigma's oligo synthesis platform.

Target	Forward Primer (5' – 3')	Reverse Primer(s) (5' – 3')	Reference
mcrA	GGTGGTGTMGGATTCACACARTAYGCWACAGC	TTCATTGCRTAGTTWGGRTAGTT	Luton *et al.* (2002)
mcrB	TWYCARGGHYTVAAYGC	CCDCCSCCDCCRTARAT	Dziewit *et al.* (2015)
mcrG	CAYCCSCCDYTNGADGARATGGA	TCRAACATYANWCCRTYYTCRTC	Dziewit *et al.* (2015)
mtaB	CARGCHAAYACYGCMATGTT	CYTGDGGRTCYCKGTA	Dziewit *et al.* (2015)
mtbA	TTCTCCCTTGCMATGTT	ACWGGRTCVAGRTTWCC	Dziewit *et al.* (2015)
pmoA	GGNGACTGGGACTTCTGG (A189F)	ACGTCCTTACCGAAGGT (A650R) CCGGMGCAACGTCYTTACC (mb661)	Bourne *et al.* (2001)
ITS	GCATCGATGAAGAACGCAGC (ITS3)	TCCTCCGCTTATTGATATGC (ITS4)	Op De Beeck *et al.* (2014)
PCR2.1 Vector	GTAAAACGACGGCCAGTG (M13F)	GGAAACAGCTATGACCATG (M13R)	Zhou *et al.* (2021)
16S V4 rRNA	AATGATACGGCGACCACCGAGATCTACACTAT GGTAATTGTGTGYCAGCMGCCGCGGTAA (a515F)	CAAGCAGAAGACGGCATACGAGAT******** ****AGTCAGTCAGCCGGACTACHVGGGTWTC TAAT (806R)	Modified from Caporaso *et al.* (2011)
Bacterial 16S rRNA	AGAGTTTGATCCTGGCTCAG (BactF)	AAGGAGGTGATCCAGCCGCA (BactR)	Li *et al.* (2014)
Bacterial V3 16S rRNA	CCCGCCTACGGGAGGCAGCAG (341F)	ATTACCGCGGCTGCTGG (534R)	Muyzer *et al.* (1993)
Archaeal 16S rRNA	TAAGCCATGCRAGTCGAAYG (ArchF)	YCCGGCGTTGAMTCCAATT (ArchR)	Li *et al.* (2014)

2.4.3.1 Amplification of the Bacterial 16S rRNA Gene and V3 Region

Amplification of the entire bacterial 16S rRNA gene was performed following the protocol of Li *et al*. (2014) using the BactF/BactR primer pair. Following this, the V3 region of the gene was amplified in a second-round PCR following the protocol of Muyzer *et al*. (1993) using the 341F/534R primer set. Cycling conditions for each PCR were unchanged from the published protocols. Each round of this nested PCR was prepared in a UV cabinet (LabCaire) to prevent contamination of reagents and amplification of common laboratory contaminating DNA. UV decontamination stages ran for 15 minutes. The final volume of each reaction totalled 50 µl and contained 1 x PCR buffer (NEB), 33.5 µl nuclease free water, 1 mM $MgCl_2$, 200 mM dTNPs (NEB), 0.25 mM of each primer (**Table 2.1)** and 0.025 U/µl Taq Polymerase (NEB). Note, amplification of the V3 region of 16S rRNA gene was only performed for taxonomic characterisation of the *Thiomonas* isolate (data presented in **Chapter 3**). Additionally, a V3 sequence from an *Arcobacter* species was cloned into a PCR2.1 vector and used for normalisation in qPCR (clone prepared previously and made available during this study).

2.4.3.2 Amplification of the Bacterial 16S rRNA V4 Region

The V4 region of the 16S rRNA gene was amplified following the protocol of Caporaso *et al*. (2011). The forward primer contained a modification in the fourth nucleotide position, whereby the original primer sequence contained a cytosine (C). However, in this position, the modified primer contained a pyrimidine base (a Y nucleotide) which increased amplification efficacy of the archaeal 16S V4 rRNA region (Parada *et al*., 2016). Cycling conditions were kept as stated in Caporaso *et al*. (2011), however cycle number was reduced to 25.

All bacterial 16S rRNA V4 PCRs were prepared in a UV cabinet as outlined above. In some cases, the template DNA for this PCR reaction was the PCR product produced from the ArchF/ArchR amplification of DNA. This archaeal 'pre-amplification' PCR is described below. The final volume of each reaction totalled 25 µl and contained 1 x PCR buffer (NEB), 18.5 µl nuclease free water, 1 mM $MgCl_2$, 200 mM dTNPs (NEB), 0.25 mM of each primer (**Table 2.1)** and 0.025 U/µl Taq Polymerase (NEB). Note that the barcoded reverse primer was added individually. Each DNA template (1 ml) was added to the reactions outside of the UV cabinet.

2.4.3.3 Amplification of the Archaeal 16S rRNA Gene

The protocol of Fernandez *et al*. (1999) was followed to amplify an 869 bp fragment of the archaeal 16S rRNA gene; all cycling conditions were kept as stated by the authors. The ArchF/ArchR primer pair were utilised, and reactions prepared in clean conditions in a UV cabinet as mentioned previously. The final volume of each reaction totalled 50 µl and contained 1 x PCR buffer (NEB), 33.5 µl nuclease free water, 1 mM $MgCl_2$, 200 mM dTNPs (NEB), 0.25 mM of each primer (**Table 2.1**) and 0.025 U/µl Taq Polymerase (NEB).

2.4.3.4 Amplification of the Methyl Co-Enzyme M Reductase (Mcr) *Complex Subunits: mcrA, mcrB and mcrG*

Amplification of the *mcrA*, *mcrB* and *mcrG* (the α, β and γ subunits of the *mcr* complex respectively) was performed following the work of Luton *et al*. (2013) for the *mcrA*, and Dziewit *et al*. (2015) for *mcrB* and *mcrG* PCRs. The template DNA volume was increased to 2.0 µl in some cases in attempts to amplify the *mcrB* and *mcrG* subunits. Cycling conditions were kept as stated in Luton *et al*. (2013) for all *mcr* subunits. An additional modification between the annealing and extension stages was added. This involved ramping of the temperature increments by 0.1 $^oC/s^{-1}$ for the first five cycles of the PCR reaction to allow the degenerate primers to anneal to the target strand and amplify DNA successfully. All methanogen and methanotroph specific (**Section 2.4.3.6**) PCRs reactions contained: 1 x PCR buffer (NEB), 33.5 µl nuclease free water, 1 mM $MgCl_2$, 200 mM dTNPs (NEB), 0.25 mM of each primer (**Table 2.1**) and 0.025 U/µl Taq Polymerase (NEB).

This produced the following cycling conditions: 95 ^oC for 5 minutes; followed by 40 cycles of 95 ^oC for 1 minute, 55 ^oC for 1 minute and 72 ^oC for one minute (with the outlined ramping for the initial five cycles). The final extension occurred at 72 ^oC for 10 minutes.

2.4.3.5 Amplification of the Methanol-5-hydroxybenzimidazolylcobamide Co-Methyltransferase Subunit (mtaB) and the Methylcobamide Co-Enzyme M Methyltransferase Subunit (mtbA)

Amplification of the *mtaB* and *mtbA* was performed using the primers outlined by Dziewit *et al*. (2015). Cycling conditions were modified to match those used for *mcr* encoded *subunits* as described above (**Section 2.4.3.4**); this included the additional ramping stage.

2.4.3.6 Amplification of the Particulate Methane Monooxygenase Subunit (pmoA)

The β subunit of the particulate methane monooxygenase gene (*pmoA*) was amplified following the protocol stated in Bourne *et al*. (2001). The published protocol was followed, and cycling conditions remained the same for each alternative reverse primer. An optimisation attempt was trialled increasing the template volumes to 1.5 µl and 2.0 µl in samples which were proving difficult to amplify.

2.4.3.7 Amplification of the Internal Transcribed Spacer (ITS) Region of the Eukaryotic 18S rRNA Operon

End point PCR of the ITS2 region was performed using the primers outlined in the protocol of Op De Beeck *et al*. (2014). Cycling conditions were kept as stated in the authors' work. The PCR reactions for ITS2 amplification contained: 1 x PCR buffer (NEB), 18.5 µl nuclease free water, 1 mM $MgCl_2$, 200 mM dTNPs (NEB), 0.25 mM of each primer (**Table 2.1)** and 0.025 U/µl Taq Polymerase (NEB). Final reaction volume was 25 µl.

TABLE 2.2: PCR Reaction Volumes Used for 1 x Reaction for all target genes within this study.

Reagent (x1 Reaction)	All volumes shown below are in µl										
	mcrA	*mcrB*	*mcrG*	*mtaB*	*mtbA*	*pmoA*	ITS	V4 16S rRNA	16S rRNA R1	16S rRNA R2	Arch 16S rRNA R1
Nuclease Free PCR Grade Water (Sigma)	34.75	34.75	34.75	34.75	34.75	34.75	15.25	19.0	34.75	34.75	34.75
PCR Buffer 10X (NEB)	5.0	5.0	5.0	5.0	5.0	5.0	2.75	2.5	5.0	5.0	5.0
$MgCl_2$ (25 mM)	1.0	1.0	1.0	1.0	1.0	1.0	1.0	0.5	5.0	5.0	5.0
Forward Primer (20µM) (Sigma)	3.0	3.0	3.0	3.0	3.0	3.0	2.0	0.625	1.0	1.0	1.0
Reverse Primer (20µM) (Sigma)	3.0	3.0	3.0	3.0	3.0	3.0	2.0	0.625**	1.0	1.0	1.0
dNTPs (10mM) (NEB)	1.0	1.0	1.0	1.0	1.0	1.0	1.0	0.5	1.0	1.0	1.0
Taq DNA Polymerase (5U/µl) (NEB)	0.25	0.25	0.25	0.25	0.25	0.25	0.25	0.25	0.25	0.25	0.25
Bovine Serum Albumin (BSA) (20mg/ml) (NEB)	1.0	1.0	1.0	1.0	1.0	1.0	NA	NA	NA	NA	NA
DNA	1.0	1.0	1.0	1.0	1.0	1.0	1.0	1.0	1.0	1.0*	1.0
Total Reaction Volume (µl)	50.0	50.0	50.0	50.0	50.0	50.0	25.0	25.0	50.0	50.0	50.0
Number of Cycles	35	35	35	35	35	30	40	25	25	25	35
Expected Amplicon Size (bp)	464-491	392	356	413	436	478	330	~300	1534	196	869

2.4.4 Gel Electrophoresis of Amplified PCR Products

All amplicons were visualised using agarose gel electrophoresis (AGE). The exception to this were the PCR products produced by the ArchF/ArchR and BactF/BactR primers. These products were used as template DNA for subsequent PCRs and therefore visualisation was not required.

Agarose gels at 1.5 % were produced by melting agarose powder in 1 x Tris-Acetate EDTA (TAE) buffer for ~ 10 minutes. Once cool, ethidium bromide ($C_{21}H_{20}BrN_3$) was added at a final concentration of 0.5 ug/ml to act as the DNA intercalating agent. Gels were run at between 90 volts for 60 – 120 minutes using a DC Powerpack (Biorad) dependant on expected amplicon sizes. Gels were visualised on a UV camera (UVP Equipment). Excision of any DNA bands of interest within the agarose was performed on a UV transilluminator (Fotodyne) with a sterilised scalpel and agarose slices were stored in sterile 1.5 ml tubes at 4 ^{o}C until amplicon clean-up. DNA ladders (New England Biolabs) were electrophoresed alongside amplicons and were either 100 bp or 1 kb dependant on expected product size. For DNA which was used in Illumina and Nanopore sequencing, extracted DNA was visualised on 1.5 % gels to confirm successful extraction.

2.4.5 Amplicon Clean Up

DNA within agarose gel bands was purified using the Wizard SV Gel and PCR Clean-Up System kit (Promega). Amplicon bands were excised from agarose gels using a sterilised scalpel. Gel slices were weighed (using an empty 1.5 ml tube as a blank weight) prior to commencing to the purification to determine the correct volume of membrane binding solution to be added to each gel slice. Agarose gel slices were melted in a bench top heat block (Techne Dri-Block DB2A) at 60 ^{o}C until the contents appeared liquid. Purified amplicons were stored at –20 ^{o}C. The Wizard SV Clean-Up protocol was followed without modification (Promega).

2.4.6 Determining Concentration of End Point PCR Amplicons

The concentration of PCR products was determined prior to Illumina sequencing using the Quant-*iT* PicoGreen dsDNA assay kit (Invitrogen) as outlined in the provided protocol. A Gemini XPS Microplate Reader (Molecular Devices) was used to assess DNA concentration. Excitation wavelength was set to 480 nm and emission wavelength set to 520 nm. The output in relative fluorescence units (RFU) were then converted to DNA concentration in ng/µl for quantification of DNA.

2.4.7 Molecular Cloning of PCR Products

Purified PCR products selected for cloning where ligated into the PCR 2.1 vector using the TA Cloning Kit (Invitrogen) following the protocol outline provided. To maximise PCR product ligation, the protocol was modified, and each ligation reaction contained the following: 5 µl of purified DNA, 2 µl of 5X T4 DNA Ligase Reaction Buffer, 2 µl of PCR 2.1 vector (25 ng/L) and 1 µl of ExpressLink T4 DNA Ligase (5U/µl). Reactions were incubated at room temperature for 60 – 90 minutes to allow maximum ligation to occur.

Following ligation, plasmids were transformed via the heat-shock method into component One Shot INVαF' *Escherichia coli* cells. The heat-shock was performed in a bench top water bath (Grant Instruments) at 42 °C for 30 seconds and the cells immediately returned to ice. Cell recovery occurred in Super Optimal Broth with Catabolite Repression (SOC) medium at 37 °C with agitation for one hour.

Bacterial colonies were grown on Lysogeny Broth/Luria Bertani plates with X-Gal (5-Bromo-4-Chloro-3-Indolyl-β-D-Galactopyranoside) and kanamycin as the selective marker. Kanamycin sulphate (50 mg/ml) was prepared by dissolving kanamycin powder in distilled water (dH_2O), followed by 0.22 µm filter-sterilisation (Camlab). X-Gal (80 mg/ml) was prepared by dissolving the X-Gal powder (Melford Biolabs Ltd) in dimethyl sulphoxide (DMSO). Final concentrations in plates were 50 µg/ml and 80 µg/ml for kanamycin and X-Gal, respectively. Plates were incubated in a static incubator for 24 – 36 hours at 37 °C. All media was prepared beforehand using 10 g of Bactotryptone, 5 g of yeast extract, 10 g of sodium chloride (NaCl) and 12 g/L of agar dissolved in 1 L of dH_2O. All media was autoclaved at 121 °C.

Following growth of One Shot INVαF' *E. coli* cells, white colonies were selected with a sterile loop, and complex streaks performed onto new LB/X-GAL/kanamycin plates. Following overnight growth at 37 °C, single colonies were selected again using a sterile loop and inoculated for overnight culture in 5 ml lysogeny broth containing 5 µl kanamycin, (50 µg/ml) at 37 °C with agitation (200 rpm). Following growth, turbid liquid cultures were selected for plasmid extraction.

2.4.8 Plasmid DNA Extraction from One Shot INVaF' E. coli Cultures and Restriction Digestion of Plasmid DNA by EcoRI

Extraction of PCR 2.1 plasmid DNA was performed using the QIAprep Spin Miniprep Kit (Promega) following the manufacturers' instructions. The overnight 5 ml cell cultures were pelleted prior to plasmid extraction in a benchtop 3 – 16 K centrifuge (Sigma) at 8000 rpm for 5 minutes at room temperature.

Extracted plasmid DNA was subjected to restriction digestion with the High Fidelity (HF) endonuclease *EcoRI* (NEB) for two hours at 37 °C. To maximise enzymatic digestion, each reaction contained: 12 µl of distilled water (dH_2O), 5 µl of plasmid DNA, 2 µl of 10X SmartCut Buffer and 1 µl of *EcoRI* (20,000 U/ml). Linearised plasmids and inserts were visualised on 1.5 % agarose gels following the digestion reaction, as outlined previously. Plasmid DNA was stored at -20 °C in LoBind tubes.

2.4.9 Sanger Sequencing of PCR 2.1 Plasmids

Two Sanger Sequencing services were used during this work. Initially, Edinburgh Genomics (School of Biological Sciences, The University of Edinburgh, Scotland) performed Sanger Sequencing on PCR 2.1 plasmids. This was performed using a Thermofisher ABI3730XL capillary DNA sequencer with Big-Dye 3.1 chemistry.

Subsequently, additional plasmid sequencing was performed by the Medical Research Council Protein Phosphorylation and Ubiquitylation Unit (MRC-PPU) (School of Life Sciences, The University of Dundee, Scotland) using an Applied Biosystems 3730 automated capillary DNA sequencer with Big-Dye 3.1 chemistry. All Sanger sequencing reactions utilised the M13 primer pair (see **Table 2.1** for oligonucleotide sequences). M13 primers were supplied to Edinburgh Genomics (Sigma), while MRC PPU supplied M13 oligonucleotides for sequencing runs. The resulting chromatograms were analysed using 4peaks (version 2015.1). Sequences were searched against the NCBI BLAST database for the highest homology matches using blastn or metablast options.

2.4.10 Quantitative PCR (qPCR) of Functional Genes

To determine the copy number of specific target genes within sediment DNA samples, qPCR was performed. This study utilised the *mcrA* and *pmoA* genes in qPCR, as well as the ITS2 intergenic region. Cycling conditions for each of these genetic regions was kept the same as in end point PCR, outlined in **Table 2.1** The qPCR standard curve was produced by serially diluting a PCR 2.1 plasmid containing the gene of interest in elution buffer from 10^{-1} to 10^{-10}. Copy number of each gene was determined by:

$$\textbf{Copy number of target gene} = \frac{\textbf{Amount of DNA (ng) x Avogadro's Constant } [N_A])}{\textbf{Size of DNA Molecule (bp) x 660 x Conversion Factor}}$$

→ Whereby, Avogadro's Constant = 6.022×10^{23}; 660 = average mass of a basepair; conversion factor = 1×10^{9}

Each qPCR reaction contained 2 ml of DNA (diluted to approximately 10 ng/µl), 10 mM of each primer (0.3 µM final concentration), 25 mM of $MgCl_2$ (3.5 mM final) and 10 X SYBR Green Master Mix (Roche). All qPCRs had a final reaction volume of 20 ml which was made up to the total by the addition of nuclease free water (NFW). For each qPCR run, negative controls were performed within the 96 well plate (with nuclease free water replacing template DNA). The total abundance of the *mcrA, pmoA* and ITS regions in qPCR assays was normalised to the 16S rRNA gene to allow determination of relative abundance across samples. This was performed by using a 16S rRNA V3 region containing PCR 2.1 plasmid diluted serially as a standard curve as outlined above. The qPCR conditions for this reaction are listed in **Table 2.1.**

2.5 Molecular Methods II: Next Generation Sequencing Approaches

2.5.1 Long Read Sequencing with Oxford Nanopore Technology

Prior to performing long-read DNA sequencing, several DNA samples from Benhar Bing sediment were pooled. This was performed to achieve the required concentration of starting DNA required to prepare a metagenomic library for Nanopore sequencing, as previous attempts to perform long sequencing had been impaired by poor DNA recovery.

Out of 50 replicate DNA extractions from Benhar Bing sediment, the 15 DNA samples with highest DNA concentrations and optimal 260:280 ratios were selected for addition to the metagenomic DNA pool. The pooled DNA samples were purified again using the ProNex Size-Selective Purification System (Promega) and eluted into a final volume of 100 µl. Following purification, the combined concentration of pooled samples was determined using the Quant-*iT* dsDNA High Sensitivity Assay (Invitrogen), as outlined previously, to ensure that the minimum target of 1 µg of DNA required for metagenomic sequencing had been successfully reached. Pooled DNA quality was assessed using a Nanodrop Spectrophotometer as outlined above. An aliquot of pooled DNA (1.5 ug total) was diluted in nuclease-free water to the correct starting volume for nanopore library preparation.

Metagenomic sequencing was performed using the Ligation Sequencing Kit (SQK-LSK109) commercially available from Oxford Nanopore Technologies, UK, following the protocol available for this sequencing kit (Oxford Nanopore, UK). The DNA used for metagenomic sequencing was purified at several stages of the library preparation using the ProNex Size-Selective Purification System as outlined above. The DNA end repair reaction was performed in a Biosystems SimpliAmp Thermal Cycler.

Following the DNA end-repair stage, DNA was purified using ProNex beads and eluted into 61 µl of elution buffer. Following this, DNA concentration was determined using the Quant-*iT* dsDNA High Sensitivity Assay as outlined above. After adapter ligation with Adapter Mix X (AMX), DNA was purified on magnetic beads again, and resuspended in short fragment buffer (SFB) to retain DNA fragments of all sizes. DNA fragmentation was not performed. The final purified eluate from ProNex bead purification contained 15 µl of prepared DNA for use in the metagenomic library.

Following this final purification on the magnetic ProNex beads, DNA concentration was determined again using the Qubit Assay as discussed above. The pellet drying time during DNA purification was extended to 10 minutes to allow optimal DNA adherence to the beads. Purified DNA and the prepared library were stored in 1.5 ml Lo-Bind tubes on ice, throughout the procedure.

Following this, DNA was eluted from the beads. Priming and loading of the flow cell prior to sequencing was performed as outlined in the provided protocol (Oxford Nanopore), however with modifications to allow the most efficient sequencing run. Briefly, air was removed from the flow cell device via the priming port and 800 ml of priming solution loaded into the flow cell to prepare the pores for sequencing. After 5 minutes, the remaining 100 ml of priming solution was added to the flow cell via the priming port.

Specifically, the use of the ProNex Size-Selective Purification System (Promega) to purify the initial pooled DNA was a modification from the protocol provided and was performed to increase quality of the DNA which would be used in library preparation. DNA end-repair and adapter ligation were performed using the companion modules for Oxford Nanopore Sequencing, available from New England Biolabs (NEB). The use of the supplied 3.6 kb control DNA strand (CS DNA) was omitted. Metagenomic sequencing was performed using a minION sequencer (MK1B model) and compatible DNA sequencing flow cell (R9.4.1).

To facilitate metagenomic sequencing, the MinKNOW software version 4.05 (Oxford Nanopore) was used with the following parameters: SQK-LCK 109 kit was selected, and the native base-calling option was turned off. A quality control check was performed to assess the number of pores available for sequencing. The sequencing run was set to run for 48 hours and any DNA fragments of 200 bp or less were excluded from the analysis.

The purified DNA library was added to the flow cell via the sample SpotON port immediately prior to the sequencing run; the sample was mixed continuously via gently pipetting to avoid precipitation of the loading beads. The loading procedure was modified from the published Nanopore protocol. Addition of the prepared library into the flow cell was performed by loading half of the library initially into the loading port and performing the sequencing for 20 hours. Following this, sequencing was paused, and the remainder of the library was loaded for the remainder of the sequencing run to ensure that sequencing via the nanopore channels was continually running, and loss of library did not occur following previous flow cell attempts which had not performed successfully.

2.5.2 Metagenomic Downstream Analysis

Following the nanopore sequencing run, base calling was performed using Guppy (version 4.4.0) pipeline using high accuracy mode with GPU processing. Filtering of reads was performed using the filter fastq sequence toolkit (version 1.1.5) to retain reads of 1000 bp or greater and adapter sequences were trimmed from the filtered reads using Porechop (version 0.2.4); trimmed reads plus adapter quality score of 7 was used as default. Filtered fastq files were converted to fasta format using the FASTX toolkit (version 1.0.2).

2.5.2.1 Unassembled Metagenomic Reads: Taxonomic and Gene Prediction

Functional gene prediction from unassembled metagenomic reads was performed using the KEGG Automatic Annotation Server (KAAS) (https://www.genome.jp/kegg/kaas) using the metagenomics option with the default single direction best hit (SBH) approach for matching nucleotide sequences using to the NCBI database with blastn. KAAS output files were uploaded to KEGG Mapper using the Reconstruct Tool (https://www.genome.jp/kegg/mapper) to determine gene content from each annotated read. Predicted gene names were determined via their KEGG Orthology (KO) allocation by using the KO Database Tool (https://www.genome.jp/kegg/ko.html). Gene counts were determined from the output files of the KEGG mapper tool.

Taxonomic prediction of the metagenomic communities using unassembled fasta reads was performed using two pipelines. In the first instance, Kaiju version 1.9.2 (https://kaiju.binf.ku.dk/server) was utilised as outlined in Menzel *et al*. (2016) using the NCBI non redundant protein database as the reference database for sequence matching. Greedy mode was applied to allow mismatches, with the default Greedy mode settings used (minimum match score: 75, mismatches allowed: 5, maximum E-value: 0.01).

2.5.2.1 Metagenome Assembled Genomes: Assembly, Taxonomic Binning and Functional Characterisation

Contig assembly was performed using flye (version 2.9.3) with the --meta option utilised for metagenomes, which quality scores kept as default. The -nano-hq option was used to indicate that quality filtering had been applied during base calling. Taxonomic binning of contigs assembled via (meta)flye was performed using the BugSplit (https://bugseq.com/academic) approach outlined by Chandrakumar *et al.* (2022). Briefly, refinement of MAGs involved four rounds of assembly polishing with Racon and a single round of polishing with both medaka and homopolish. Taxonomic binning of MAGs was performed using alignment with Mashmap/Minimap2 against the RefSeq database to allow binning into taxonomic folders.

Quality of assembled MAGs was determined with CheckM (version 1.1.18). Visualisation of MAGs was performed using the Proksee (version 1.1.0) interface (https://proksee.ca/) developed by Grant *et al.* (2023). Subsequent annotation of reconstructed genomes was performed using Prokka (version 1.14.6) (developed by Seeman, 2014). Average Nucleotide Identify (ANI) comparisons were performed using the FastANI tool (version.1.3.3), see Jian *et al.* (2018) for full details. The GC content of assembled MAGs was determined using the Novo Pro Lab GC calculator tool (https://www.novoprolabs.com/tools/gc-content).

Alignments to other genomes was performed using the BLAST Comparison Proksee tool (version 1.3.1). 16S rRNA genes were manually selected from assemblies and compared to full length 16S rRNA genes from phylogenetically closest organisms via multiple alignment using blastn (https://blast.ncbi.nlm.nih.gov/). 16S rRNA sequences were retrieved from DSMZ (https://bacdive.dsmz.de/).

To assess carbohydrate active enzymes within metagenomes, assemblies were scanned using the Hidden Markov Models (HMMs) from the dbCAN2 CAZy tool (v. 11.0) as developed by Chivian *et al.* (2023). Central metabolic pathway completeness and detection of electron transport chain components were assessed with the Distillation and Refinement of Annotated Metagenomes (DRAM) tool (v.0.1.2), see Shaffer *et al.* (2020) for pipeline. All tools utilised for annotation and metabolic exploration of metagenome assembled genomes had no modifications from the standard analysis routes.

2.5.3 Illumina MiSeq Sequencing of V4 16S rRNA Library

DNA extracted from sediment samples and selected sediment-inoculated bioreactors were used in taxonomic analysis to assess the composition of the microbial community present. Assessment of the microbial community structure in these environmental samples was performed using next generation sequencing of the hypervariable V4 region of the 16S rRNA gene. The full protocol for this sequencing method has been described by the original authors (Caporaso *et al.,* 2011) and is outlined briefly in **Section 2.4.3.2** with primer details given in **Table 2.1.**

Following purification of V4 16S rRNA amplicons, PCR products were quantified via the Quant-*iT* dsDNA High Sensitivity Assay (Invitrogen) and pooled in equimolar volumes. The V4 16S rRNA library was sequenced using the MiSeq Illumina platform, producing 250 bp pair ended reads. Illumina sequencing was performed by Edinburgh Genomics, The University of Edinburgh. During this study, an additional single sample (Benhar Bing sediment DNA, amplified with a515F/806R, without pre-amplification of the archaeal 16S rRNA gene) was also sequenced by Novagene using the MiSeq Illumina technology.

2.5.3.1 Processing of Illumina Data

To determine the microbial composition of DNA samples retrieved from sediments and bioreactors, the Quantitative Insights into Microbial Ecology 2 (QIIME2 2020.8) pipeline was utilised (as outlined in Bolyen *et al.,* 2019). Following sequencing, the quality distribution of the reads was deemed normal, therefore no quality trimming was performed. Demultiplexed reads were denoised and paired following the DADA2 pipeline (Callahan *et al.,* 2016) using default parameters.

To assign taxonomic prediction to the 250 bp amplicons, the Bayesian classifier built within DADA2 was utilised, using the SILVA (version 138) as the taxonomic database (Yilmaz *et al.,* 2014). Any highly abundant ASV reads present in the negative control samples were contaminating sequences and were removed from the dataset; this was performed by converting the biom taxonomy table to a text file and ranking taxonomically allocated reads by abundances within the negative control samples (DNA kit controls). Rarefaction of the number of reads was performed to control for uneven sequencing. This was performed by selecting a value

below the lowest sequencing depth of 29,486 (rarefy depth equalled 29,400). QIIME 2 view was utilised to visualise data during analysis (www.view.qiime2.org).

2.6 Additional Computational Methods

2.6.1 Additional Software

PRIMER (version 7) was used to produce Bray-Curtis dissimilarity matrixes and to perform multivariant statistical analysis on metabolic profiling datasets. Data was exported to Excel for additional analysis. R Studio (version 2021.09.1+371) was utilised with the ggplot2 (version 3.3.5) package to generate heatmaps. The heatmapper tool (http://heatmapper.ca/) was also utilised during this work.

2.6.2 Nucleotide Sequences Searches Using NCBI's Basic Local Alignment Search Tool (BLAST)

The National Centre for Biotechnology Information (NCBI) BLAST software was used routinely in querying nucleotide sequences. Most commonly, search criteria were left as the 'Default Megablast' using the standard nucleotide database. However, if queries were matching poorly, 'Discontiguous Megablast' or 'BLASTn' options were selected. The translated nucleotide option, 'tBLASTx', was also applied to sequenced PCR products to assess matches of amplicon sequences at the protein level.

2.6.3 Phylogenetic Analysis

Phylogenetic trees were produced to infer evolutionary history between DNA sequences using the Molecular Evolutionary Genetic Analysis (MEGA) software (version 11). Trees were constructed following the protocol outlined by Hall (2013). Briefly, the evolutionary history of sequences was inferred using the neighbour-joining method. The evolutionary distances were computed using the maximum composite likelihood method and are in the units of the number of base substitutions per site. Codon positions included were the first, second and third positions, as well as non-coding regions. All nucleotide positions containing gaps and missing data were eliminated from alignments. Sequences were aligned using ClustalW using the DNA sequencing parameter. Additionally, ClustalW aligned sequences were also used to make phylogenies using the European Bioinformatics Institute (EBI) phylogenetic tree tool using default parameters (https://www.ebi.ac.uk/jdispatcher/phylogeny/simple_phylogeny).

The UNITE ITS database (version 10.0) was used to access DNA sequences from acidophilic fungi for inclusion within phylogenies based on the ITS2 sequences retrieved from Sanger sequencing (https://unite.ut.ee/). This tool was developed and utilised as described in the work of Nilsson *et al*. (2018). Two ITS2 sequences were retrieved pertaining to an *Acidomyces* species (European Nucleotide Archive [ENA] identifier: AJ244237) and *Acidothrix acidophila* (ENA identifier: FJ430781) for use ITS2 sequence alignments.

2.7 Bioreactor Methods

2.7.1 General Bioreactor Design

All bioreactor trials were performed in sterile 60 ml plastic syringes with varying reactor contents. All reactors were batch scale and incubated with agitation at 37 °C. All sediment samples were sieved (1.5 – 2.0 mm mesh size) prior to being used as inocula to remove large debris and particulate matter. Sterile one-way luerlock stopcocks (Promega) were used to prevent gas loss from the headspace and allow access to reactor samples. All autoclaved samples were sterilised at 121 °C for 15 minutes to prevent microbial activity. In some cases, digestate and feedstock samples were subjected to two rounds of sterilisation.

Gas production was measured using the scale on the plastic syringe and when gas volume exceeded ~20 ml, syringes were selected for degassing. Samples were removed from syringes during bioreactor incubations under anaerobic conditions and were stored at -20 °C in sterile 1.5 ml tubes for further analysis. Bioreactor trials were performed with varying reactor contents and incubation lengths and are outlined in **Table 2.3**. A schematic of an example bioreactor is shown below in **Figure 2.7**

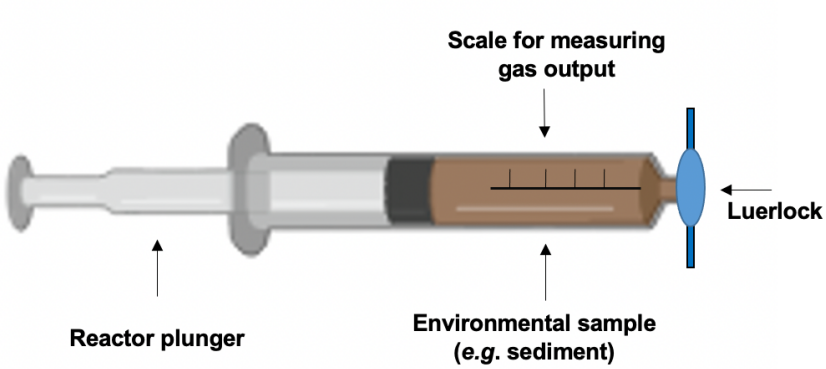

FIGURE 2.7: Bioreactor design used in environmental anaerobic digestion (eAD) trials. All bioreactor trials occurred in plastic 60 ml batch scale syringes and were closed using plastic luerlocks to prevent loss of bioreactor contents or biogas.

2.6.2 Benhar Bing Sediment and Cellulose Amended Reactors

To increase the bioavailable carbon for Benhar Bing consortia to metabolise, 3 g of cellulose (Sigma) was mixed with 30 g of Benhar Bing sediment in triplicate within sterile reactors. Active digestate (30g) amended with cellulose (3 g) was set-up in triplicate to act as positive controls. Benhar Bing sediment without cellulose was added to syringes to act as negative controls.

2.6.3 Environmental Anaerobic Digestion Trial One (eAD1)

The initial eAD1 experiment to assess methanogenic potential contained 15 bioreactors, each sediment sample in triplicate, plus positive and negative controls also in triplicate. Each environmental reactor (*ie*., non control) was inoculated with 19 ml of double autoclaved digestate to act as an environmental matrix and complex nutrient to support microbial growth. Following this, 1 ml of 'active' sediment was added to act as the microbial inoculum; this was taken from previously stored anaerobic mini-cored sediment samples.

After addition of sterilised digestate and sediment, plungers were placed back into the syringe bases and syringes inverted. Luerlocks were opened to expel any air from the syringe and the reactor contents pushed to the top of the syringe before the stopcock was locked, ensuring anaerobicity. Reactors were incubated for 100 days at 37 °C with agitation. Reactors were removed from mesophilic conditions for degassing. Sampling from eAD1 bioreactors was performed under anaerobic conditions outlined previously. Reactor samples were stored in sterile 1.5 ml tubes at -20 °C until use.

2.6.4 Environmental Anaerobic Digestion Trial Two (eAD2)

The second bioreactor trial, eAD2, contained 15 syringes as above. Each environmental reactor was inoculated 5 ml of 'active' sediment, taken from anaerobic mini-cored samples and 15 ml of double autoclaved digestate. Air was removed from reactors following methods outlined for eAD1 syringes. Prior to inoculation of syringes, both the sediment samples and sterilised digestate were preincubated for 24 hours at 37 °C to enhance microbial metabolic recovery following storage at 4 °C prior to reactor set-up. Reactors were incubated as above. Reactors were removed from mesophilic conditions for sampling, degassing and methane recordings. Sampling was performed anaerobically as outlined for eAD1 bioreactors.

2.6.5 Environmental Anaerobic Digestion Trial Three (eAD3)

Following on from the two previous trials where volume of starting inoculum was increased, eAD3 focused on the increase of bioavailable carbon for degradation to biogas. This trial contained 15 bioreactors as above, and contained 5 ml of sediment sample, 5 ml of double sterilised feedstock and 10 ml of double sterilised digestate. Sampling, degassing, and methane measurements were performed as outlined for previous reactor trials. Reactors were incubated as described above, for 120 days. Sampling was performed anaerobically as outlined for previous reactor trials.

Table 2.3: Outline of bioreactor experiments using various inocula and additional carbon sources to stimulate methanogenic activity.

Trial Name	Contents of Reactor	Duration of Trial
Benhar Bing + Cellulose	Benhar Bing sediment + cellulose (n = 3)	35 days
	Positive control digestate + cellulose (n = 3)	
	Negative control sediment only (n = 3)	
Environmental Anaerobic Digestion 1 (eAD1)	Benhar Bing sediment + sterilised digestate (n=3)	30 days
	Blackford Pond sediment + sterilised digestate (n=3)	
	Loch Ba sediment + sterilised digestate (n=3)	
	Positive control 'active' digestate + sterilised digestate (n=3)	
	Negative control sterilised digestate (n= 3)	
Environmental Anaerobic Digestion 2 (eAD2)	Benhar Bing sediment + sterilised digestate (n=3)	100 days
	Blackford Pond sediment + sterilised digestate (n=3)	
	Loch Ba sediment + sterilised digestate (n=3)	
	Positive control 'active' digestate + sterilised digestate (n=3)	
	Negative control sterilised digestate (n= 3)	
Environmental Anaerobic Digestion 3 (eAD3)	Benhar Bing sediment, sterilised feedstock + sterilised digestate (n=3)	130 days
	Blackford Pond sediment, sterilised feedstock + sterilised digestate (n=3)	
	Loch Ba sediment, sterilised feedstock + sterilised digestate (n=3)	
	Positive control 'active' digestate, sterilised feedstock + sterilised digestate (n=3)	
	Negative control sterilised digestate (n= 3)	

2.6.6 Determining Methane Content of Biogas and Bioreactor Degassing

The content of methane within the biogas produced in the bioreactor trials was assessed with a bench top infrared methane meter (The University of Hohenheim, Germany). The methane meter was calibrated using standard biogas mixture (60% CH_4, 40% CO_2) and biogas from the headspace of the 60 ml bioreactors was injected into the methane meter via in the inlet, from the reactor syringe once the luerlock was open. Gas exited the device via the outlet tube. This allowed a percentage of CH_4 to be determined from the total gas volume. Air was used to remove methane from the device following degassing of reactors.

CHAPTER 3 - Chemical Analysis, Metabolic Profiling and Cultivation of an Acidophilic *Thiomonas* Species from Acid Mine Drainage

3.1 Characterisation of Microbial Assemblages via Culture-Based Techniques

Determining microbial community function from the taxonomic composition of microbial assemblages remains challenging. One limitation is overcoming microbial community dormancy; metabolically inactive cells that are reflected in DNA-based analysis, while not being currently metabolically active within the community. It should be noted however that members of the microbial consortia fluctuate between dormant and active states. While not metabolically active, dormant microorganisms do remain a key source of metabolic potential and can aid in niche maintenance and functional redundancy if other taxa are lost from the population (Jones and Lennon, 2010; Shade *et al*., 2012).

Cultivation of taxa remains a fundamental strategy employed to determine the function of isolates that may be recovered from communities of interest. As microbial communities are critical to ensuring optimal ecosystem function through maintaining biogeochemical cycles, determining function of members of environmental consortia is key in aiding in determining relationships between community structure and function (Ren *et al*., 2017). This is of particular importance in sites such as acid mine drainage impacted wetlands which have been challenging to study and their contribution to both metal cycling and wider carbon cycling largely neglected due to their chemically hazardous nature.

In conjunction with isolation of species, specific functional capabilities of the culturable fraction of a given community can be observed via metabolic profiling to provide a more community-wide functional overview. Assessing organic matter utilisation by prokaryotic assemblages has been challenging to elucidate, despite carbon source utilisation being fundament to central metabolism (Sala *et al*., 2020). The bioavailability of carbon is known to affect prokaryotic growth, yet the influence of specific molecules is less-well defined, as is the ability to link variation in taxonomy to alternated functional states (Ruiz-Gonzalez *et al*., 2015).

3.2 Approaches to Metabolic Profiling

Historically, attempting to elucidate carbon source catabolism by microbial consortia required the use of radioisotope or fluorogenic-labelled substrates; an approach which is often limited due to being restricted to assessing only a small number of compounds at one time. Similarly, the use of dissolved organic matter (DOM) profiling often had poor success when low weight molecular compounds were been used as available catabolic substates (Arnosti, 2011).

To explore microbial function through metabolic preferences work performed by Garland and Mills (1991) first developed a 96-well plate technique to assess degradation of various (95) carbon sources by culturable aerobic heterotrophs (with water acting as a control well). This approach overcame the previously utilised and more limited methodologies. Initially, these 'BIOLOG' plates were utilised to examine the substrate utilisation of bacterial cultures in axenic states, predominantly Gram negative medically significant isolates. As the technique gained popularity, the number of substrates was reduced to 31 carbon compounds, reflecting those most prevalently used by soil and sediment communities (Rutgers *et al*., 2016). This development allowed microbial ecologists interested in the microbial diversity of soil environments to assess community function using this metabolic profiling approach as a tool, rather than rely on substrates more suited to individual isolates.

The commercially available BIOLOG EcoPlates have been routinely utilised in studies exploring the functional diversity (analogous to carbon compound degradation ability) of microbial communities since their development. They provide a rapid and easily reproducible 'metabolic fingerprint' of the active community and have been used to determine the native function of soil and sediment communities as well as monitoring changes in microbial function following changes in environmental conditions.

The work of Gryta *et al*. (2014) used EcoPlates to determine the effect of the use of digestate biosolids as a soil amendment on microbial community function, whereas the work of both Muniz *et al*. (2014) and Ding *et al*. (2017) examined the effects of heavy metal pollution of soil communities and impacts on functional diversity. Despite there being a moderate body of work on the application of the BIOLOG technique to conventional microbial ecosystems, there is little evidence of metabolic profiling being performed extremophilic consortia or in applied microbial ecosystems whereby the native population are involved in some level of remediation.

In the few examples within the literature that do exist, as in the work of Salomo *et al*. (2018), the wetland consortia treating pollutants via EcoPlate profiling is unalike to Benhar Bing and is treating organic waste as opposed to aquatic pollution with high metal contents. As changes in microbial community function can impact higher trophic levels, determining functional diversity can be an integral part in determining the role environmental microbial consortia have in ensuring the flow of ecosystem services (Bender *et al*., 2016). Metabolic profiling of highly contaminated systems is an important tool that has been underexploited regarding community characterisation of chemically unusual environments.

3.2.1 Generation of Community Level Physiological Profiles via Carbon Source Oxidation

Briefly, the generation of metabolic profiles via the BIOLOG approach is based upon redox reactions occurring within wells of the EcoPlate following inoculation of microbial consortia. If microorganisms present within the sample aliquot within the well express enzymes which degrade the carbon source present, the compound present will be oxidised. For more detailed methodology, see **Chapter 2**. A colour change reaction indicates the utilisation of the carbon source present within the inoculated well. This reduction of tetrazolium to formazan is shown in **Figure 3.1.**

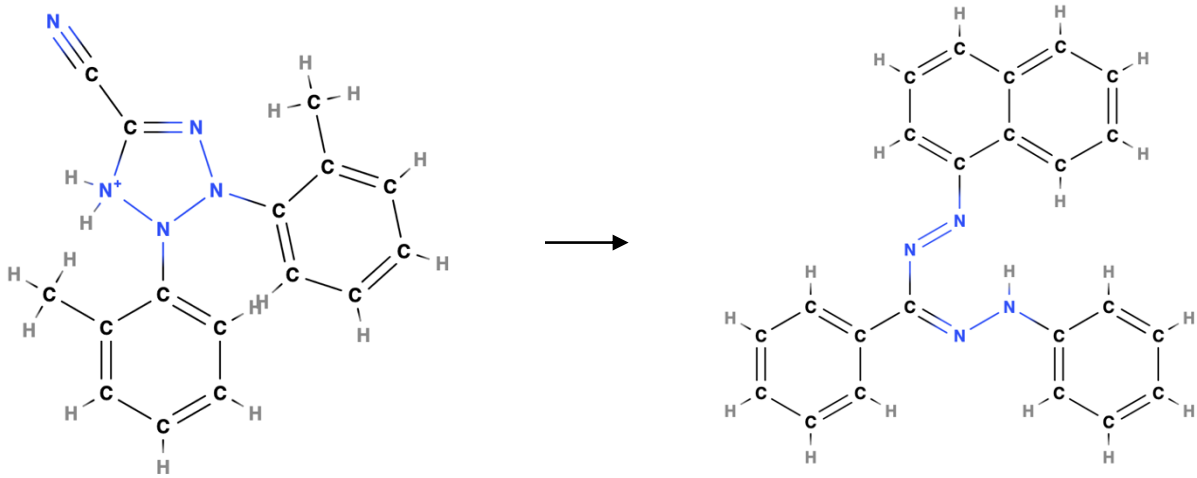

FIGURE 3.1: Reduction of tetrazolium to formazan. Note that the chlorine ion (Cl^-) in tetrazolium chloride dissociates in solution (not pictured).

It has been noted in the work of Dobranic and Zac (1999) and Classen *et al*. (2003) that fungal members of the community cannot utilise tetrazolium as an electron acceptor and therefore, do not contribute to the generation of the metabolic profile. Further to this, substrates can be divided into chemical guilds based on the structure of the compounds; with polymers, carbohydrates, carboxylic/ketonic acids and amines/amides present in the EcoPlate. **Table 3.1** details the compound groupings. Metabolic potential can therefore also be studied within these guildings, as well as individual responses to substrates (Galazka *et al*., 2018).

TABLE 3.1: Compounds present for bacterial utilisation in BIOLOG EcoPlates and their associated chemical groupings. (Table adapted from Weber and Legge, 2009).

Compound Class	**Substrates**
Amines/Amides	Phenylethylamine, Putrescine.
Amino Acids	Glycly-L-Glutamic Acid, L-Arginine, L-Asparagine, L-Phenylalanine, L-Serine, L-Threonine.
Carbohydrates	Pyruvic Acid Methyl Ester, D-Cellobiose, α-D-Lactose, β-Methyl-D-Glucoside, D-Xylose, i-Erythritol, D-Mannitol, *N*-Acetyl-D-Glucosamine, Glucose-1-Phosphate, D, L-α-Glycerol Phosphate.
Carboxylic and Ketonic Acids	D-Glucosaminic Acid, D-Galactonic Acid-γ-Lactone, D-Galacturonic Acid, **2-Hydroxybenzoic Acid*, 4-Hydroxybenzoic Acid*, γ-Aminobenzoic Acid*,** Itaconic Acid, α-Ketobutyric Acid, D-Malic Acid.
Polymers	Tween 40, Tween 80, α-Cyclodextrin, Glycogen

* Note that these substrates are classed as their own class '**phenolic compounds'** opposed to carboxylic acids in some works (Christian and Lind, 2006; Oest *et al.,* 2018).

Additionally, BIOLOG produce specialised anaerobic microplates which are optimised to evaluate the substrate utilisation of anaerobes. Unlike EcoPlates, the anaerobic equivalent contains 95 carbon sources, with a greater array of substrates including aromatic compounds and nucleotides. This assay was predominantly developed to assess the nutritional spectrum of medically significant anaerobes, and little evidence in the literature shows the use of these metabolic profiling plates for microbial communities or environmental isolates.

One study by Van Ooteghem *et al*. (2004) successfully used these specialised anaerobic microplates to determine the carbon utilisation profile of the extremophile *Thermotoga neapolitana* under microaerophilic conditions. This work involved incubating the microplates at 70 °C to reflect the extremophilic optimal temperature range for organisms from the *Thermotogales* and successfully determined metabolic potential of *T. neapolitana*. Moreover, work by Arias *et al*. (2020) utilised the specifically designed and more specialised anaerobic microplate technique to assess the substrate degradation potential of anaerobic digestate samples augmented with swine manure to improve biomethane yield. As the anaerobic microplates are based on the same redox principle as EcoPlates, they can provide insights into anaerobic community function across a greater range of carbon sources.

As the reactions which occur in anaerobic sediments and waterlogged soils (anoxic degradation) are analogous to those occurring in industrial anaerobic digestion (anaerobic depolymerisation of organic compounds), monitoring microbial functional diversity through carbon utilisation profiles is a beneficial technique to explore structure-function relationships in both natural and applied systems. Furthermore, with little known regarding the metabolic preferences of extremophilic microbial consortia, EcoPlates can provide novel insights into the catabolic potential of microorganisms with tolerance of extreme physiochemical conditions.

3.3 Microbial 'Dark Matter' and Novel Cultivation Strategies to Enhance Isolate Recovery

Cultivation of environmental microbial isolates remains key in linking taxonomy to ecological function (Prosser *et al.,* 2007). However, the concept of the 'great plate count anomaly' first described by Staley and Konopka (1985) states that only approximately one percent of total microbial species can be successfully cultivated, and their growth maintained in axenic states. Moreover, the definition of a biological species as it applies to members of the two prokaryotic domains has been historically contested (as reviewed by Rossello-Mora and Amann, 2015), and is more complex than when considering the equivalent concept at the macro-organism level. The fast rate of microbial evolution and the emergence of novel strains has hampered the ability of microbial ecologists to have a single definition of a species as it relates to prokaryotic taxa. Furthermore, prolific horizontal gene transfer between organisms, combined with potential trigger-specific speciation (*e.g.,* a gain of function mutation conferring an evolutionary advantage) compound the complexities involved in the microbial species debate (Venton, 2017; Free *et al.,* 2018). However, several working definitions can be applied to the prokaryotes, particularly when discussing cultivated isolates.

This remaining uncultivated majority of prokaryotes is often termed 'microbial dark matter' and this remarkable microbial biodiversity has been observed through predominantly metataxonomic studies or metagenome assembled genomes (MAGs). Both taxonomic based studies utilising the 16S rRNA gene as a phylogenetic marker (to determined community composition) and reconstruction of microbial genomes via metagenomics (to assess function) and high-resolution taxonomy (via phylogenomics) have proved invaluable in the characterisation of microbial communities. Through a combination of these powerful DNA based techniques, insights can be gained regarding taxa which routinely elude cultivation.

Currently, culture collections are skewed largely towards representatives which grow readily in chemically synthetic media, and due to this, the issue of re-discovery of non-fastidious microbial species can hamper novel cultivation attempts. A well-defined example of this is displayed by many aquatic taxa where an evident discrepancy exists between the elevated diversity observed from recovered 16S rRNA genes from environmental samples compared to poor cultivation of many representative species from the same sample (Cho and Giovannoni, 2004).

Many of the uncultivated clades of 'dark matter taxa' are often evolutionarily ancient and evolved to inhabit environments where physiochemical pressures are extreme. Replicating these extreme conditions in culture is challenging and often chemical components required for growth cannot be utilised in conjugation with standard microbiological media. Acidophiles are a key functional guild of prokaryotes which represent this 'bottleneck' to cultivation. As a representative of successfully cultivated acid mine drainage taxa, *Acidithiobacillus* only has a limited number of isolated species which require complex media and co-cultivation strategies. Co-culture enrichments compound the complexities in culturing novel organisms. Additionally, many environmental isolates require oligotrophic cultivation conditions not routinely described for previously captured taxa (Connon and Giovannoni, 2002).

Despite the lack of successfully cultivated 'dark matter' isolates or consortia, metagenomic analyses have revealed that these assemblages have critical roles in sustaining environmental chemistry and ecosystem function through maintenance of biogeochemical cycles and community stability (Zamkovaya *et al.,* 2021). Many of these species are considered conditionally rare organisms; low abundance taxa with critical roles in ecosystem function, which can, under specific environmental conditions, show an increase in their relative abundance. However, due to their rarity, they can be resistant to colony emergence. Additionally, these organisms can be challenging to identify in routine 16S rRNA gene based surveys.

Moreover, the genomic potential of biologically rare organisms represents an additional untapped resource with many of the metabolic pathways exploited by extremophiles remaining poorly characterised (Shade *et al.,* 2014). The apparent ecological resiliency of extremophilic taxa make them candidates for use in various biotechnologies, as they may be able to survive in 'applied' microbial ecosystems. However, functional metabolic attributes of many extremophiles remain undetermined, due to challenges in maintaining their growth in culture.

To overcome the resistance to cultivation observed by the prokaryotic majority, innovative culturing strategies have been developed in attempts to yield novel isolates. This has involved the use of co-cultivation approaches (Tanaka *et al*., 2018), selective enrichment of key community members (Lugli *et al*., 2019), and the utilisation of microfluidic devices (Ma *et al*., 2014). The work of Nichols *et al*. (2010) developed the 'isolation chip' (iChip) approach to capturing and cultivating rare taxa from environmental samples.

Formerly, it had been demonstrated that modifications to chemical components of media or incubation conditions only had limited success in allowing the growth of previously uncultivated microorganisms. Nichols *et al*. (2010) overcame the challenge of using synthetic media by allowing microbial cells trapped in a solid agar plug within the iChip to be in direct contact with naturally occurring metabolites required for growth from the organisms' native environment (**Figure 3.2**). This direct contact overrides the challenge of not having access to uncultivated species' exact nutritional requirements.

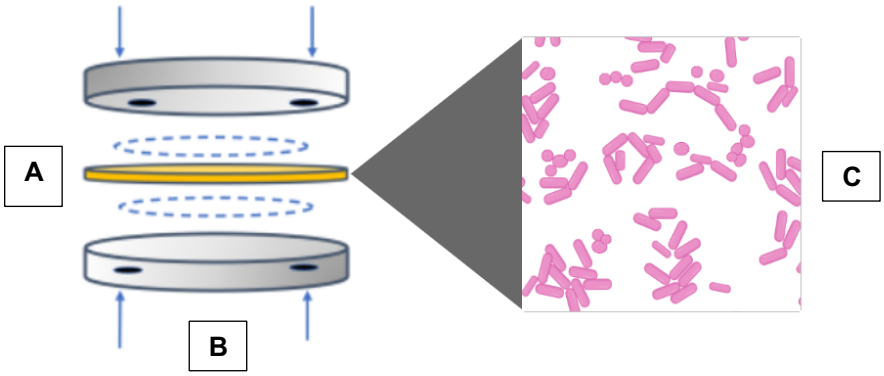

FIGURE 3.2: Microbial proliferation in iChip wells. Molten semi solid agar inoculated with a diluted environmental sample sets within the wells in the central plate (indicated in yellow) (**A**). The device is assembled entrapping the cells within the iChip. Filters across the pores (blue dashed circles) allow transfer of nutrients when iChip is returned to the sediment (**B**). Isolates proliferating within the wells can be removed for enrichment and taxonomic identification (**C**). (Image of Gram-stained cells from Biorender, 2024 version).

This work concluded that the iChip allowed the growth of taxa not observed through standard cultivation approaches. Additionally, the taxa cultivated through iChip isolation have been shown to have novel properties, including the production of significant bioactive secondary metabolites. The work of Ling *et al*. (2015) discovered the novel antibiotic, teixobactin, produced by the soil isolate *Eleftheria terrae,* grown from an iChip incubated in an agricultural field in Maine, USA. Strikingly, this metabolite also was determined to have a novel mode of action; the antibacterial effects of teixobactin against drug resistant *Staphylococcus* and members of the Enterococci was demonstrated to occur via binding to a critical precursor component of peptidoglycan, lipid II (Parmar *et al*., 2017). Recently, Shukla *et al*. (2022) demonstrated that teixobactin binds specifically to pyrophosphate-sugars in lipid II, forming a supramolecular fibrillar structure which causes incorrect integration into peptidoglycan and results in thinning of the cell wall; causing growth to cease, and subsequent rupturing of the cell.

Preventing key structural precursors from facilitating cell growth is an antibacterial route which may be challenging for pathogens to develop resistance to, compared to other antimicrobial targets, such as drugs which prevent protein synthesis (Parmar *et al*., 2017). This finding further stresses the importance of moving beyond traditional approaches towards microbial growth as novel isolates can be screened for clinically or ecologically significant functions (Piddock, 2015). More recently the work of Dos Santos *et al*. (2022) cultivated members of the Actinomycetota within an iChip and subsequently screened the isolates for bioactive secondary metabolites.

To this end, alongside chemical and metabolic profiling data, this chapter explores the use of the iChip to allow the cultivation of taxa from Benhar Bing. The BIOLOG plate approaches outlined here allow an assessment of the functional diversity of the carbon cycling potential and metabolic differences in three microbial consortia from both conventional and extreme pH freshwater sediments.

3.4 Aim of Chapter 3

The main aim of the work presented in this chapter was to perform chemical analyses of sediments, metabolically profile their native microbial consortia and attempt to cultivate taxa from acid mine drainage effluent. Additional objectives were:

- Determine **pH and key elemental contents** of sediments collected from Benhar Bing, Blackford Pond and Loch Bà.
- Assess the ability of EcoPlates to generate **metabolic profiles under both aerobic and anaerobic incubation**.
- Utilise BIOLOG's specialised **microplates for anaerobic growth** to determine any additional substrate use.
- Utilise an **iChip to cultivate extremophilic taxa** from Benhar Bing and compare the effectiveness of this novel technique to the use of conventional cultivation approaches.

3.5 Results

3.5.1 Chemical Analysis of Sediments

Chemical analysis performed at The James Hutton Institute (Craigiebuckler, Aberdeen, Scotland) successfully allowed the determination of key metallic elements (K, Ca, Fe, Al, Mg and Mn) as well as non-metals (total C [TC], organic C and total P [TP]) in each sediment sample (Blackford Pond, Benhar Bing and Loch Bà) Results are shown in **Table 3.2 and Table 3.3**.

TABLE 3.2: Elemental analysis of sediment samples. Elemental components were determined by Inductively Coupled Plasma-Optical Emission Spectroscopy (ICP-OES) and Aqua Regia Digestion (ARD).

Sample	mg/kg						
	Al	Ca	Fe	K	Mg	Mn	TP
Benhar Bing	1454	657.9	509800	2155	< 3	112.4	2632
Blackford Pond	11410	15280	45720	1282	6008	610.9	1943
Loch Bà	5323	2159	9340	775.6	2401	153.8	239.8

TABLE 3.3: **Determination of total carbon and organic carbon fraction in sediment samples.** Assessment of total carbon and organic carbon fraction was determined by Continuous Flow-Isotope Ratio Mass Spectrometry (CF-IRMS).

Sample	g/kg	
	Total Carbon (TC)	Total Organic Carbon (TOC)
Benhar Bing	41.1	40.1
Blackford Pond	82.1	79.5
Loch Bà	42.2	40.2

Chemical analysis demonstrated that Benhar Bing had elevated concentrations of iron (509.8 g/kg) compared to the other sediments assessed. The other metals assessed were generally highest in the Blackford Pond sediment (Al, Ca, Mg and Mn). An exception to this was potassium which was magnesium which was highest in the Benhar Bing sample. Blackford Pong sediment contained the highest carbon levels. (82.1 g/kg) Benhar Bing and Loch Bà both demonstrated low carbon levels within the sediment sample, with 41.1 g/kg and 42.2 g/kg, respectively.

The pH of the Benhar Bing sample was the most acidic (pH 2.41). pH values increased to near neutrality, as observed in the sediment from Blackford Pond. pH results are presented in **Table 3.4**

TABLE 3.4: pH values of sediment samples. Note that pH values indicated below were recorded as pore water samples.

Sample	pH
Benhar Bing	2.41
Blackford Pond	6.29
Loch Bà	5.56

Additional chemical analysis to determine concentrations of sulphate, sulphide, ammonia, and ammonium was performed on the three sediment samples using commercially available Hach Lange chemical assays. Unlike the elemental analysis, this data was not provided by an external laboratory, and triplicate assays were performed, unlike the chemical and pH data provided by the James Hutton Institute.

The highest sulphate level was detected in Benhar Bing (62.0 mg/L) and decreased in Blackford Pond (58.13 mg/L) and further in Loch Bà (< 40 mg/L). Sulphide concentrations were continuously below detection levels across all samples. Like the sulphate results (**Table 3.5**), Benhar Bing had the highest concentration of ammonium (16.90 mg/L) and ammonia (5.66 mg/L); both constituents demonstrated reduced concentrations in Blackford Pond and Loch Bà **(Table 3.6).**

TABLE 3.5: Mean sulphate and sulphide levels in sediment samples. [SO_4^{2-}] was determined by barium chloride ($BaCl_2$) ion exchange method and [S^{2-}] determined by H_2S-methylene blue method. *N* = 3 for each sample replicate. Standard deviations shown in parentheses.

Sample	Mean Sulphate Levels (SO_4^{2-}) (mg/L)	Mean Sulphide Levels (S^{2-}) (mg/L)
Benhar Bing	62.0 (+/- 0.81)	< 0.1 *
Blackford Pond	58.13 (+/- 0.34)	< 0. 1 *
Loch Bà	< 40.0 ◊	< 0. 1 *

* All S^{2-} replicates for each sediment sample were below the detection threshold.
◊ All SO_4^{2-} Loch Bà replicates were below the detection threshold.

TABLE 3.6: Mean ammonium and ammonia levels in sediment samples. [NH_4^+] determined by indophenol blue ion-exchange method and NH_3 by Hach Aqua-Check method. *N* = 3 for each sample replicate. Standard deviations shown in parentheses.

Sample	Mean Ammonium Levels (NH_4-N) (mg/L)	Mean Ammonia Levels ($NH3^+$) (mg/L)
Benhar Bing	16.9 (+/- 1.14)	5.66 (+/- 0.47)
Blackford Pond	6.43 (+/- 0.29)	1.66 (+/- 0.94)
Loch Bà	2.06 (+/- 0.09)	0.42 (+/- 0.12)

3.5.2 Metabolic Profiling of Sediment Communities Using the BIOLOG Approach: EcoPlates (Aerobic and Anaerobic) and Specialised Anaerobic Microplates

3.5.2.1 Overall Metabolic Responses to Catabolic Substrates: Average Well Colour Development Results

Determination of the average well colour development (AWCD), indicative of total carbon source catabolism, across each type of BIOLOG plate allowed for a comparison of the microbial responses within each metabolic assay. The average response to a carbon source within a well was determined at the end of each incubation once no further production of formazan was observed with wells. Results of AWCD as a determinate of total metabolic activity within each BIOLOG plate type is shown in **Figure 3.3.**

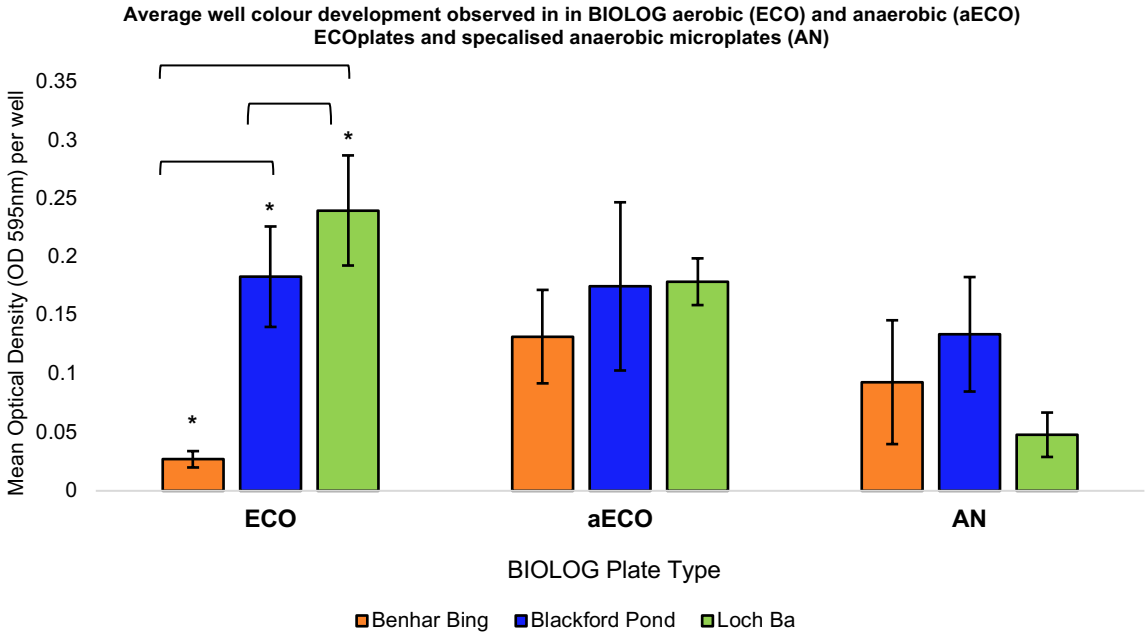

FIGURE 3.3: Average well colour development (AWCD) of each metabolic assay type as a response of overall metabolic response. Note on X axis that **ECO** = EcoPlates incubated in aerobic conditions; **aECO** = EcoPlates incubated in anaerobic conditions; **AN** = specialised BIOLOG microplates designed for anaerobic conditions. All plate types incubated at 30 °C. OD values recorded at 595 nm for AWCD calculation after no further formazan production was evident (**ECO** = 7 days of incubation; **aECO** = 10 days of incubation, **AN** = 10 days of incubation). Error bars represent the standard deviation of the mean (*n* = 3).

The acidophilic consortia from Benhar Bing responded poorly to all substrates overall and utilisation was generally impaired (AWCD = 0.027) compared to the higher observed AWCD values for both Blackford Pond (AWCD = 0.1833) and Loch Bà (AWCD = 0.24) communities when profiled aerobically in EcoPlates. This produced significant differences between the Benhar Bing response compared to the Loch Bà and Blackford Pond responses (P = < 0.001 in both cases). Additionally, the Blackford Pond and Loch Bà average responses to substrates available for catabolism were considered significantly different for each other (P = 0.038).

Incubating the EcoPlates under anoxic conditions showed a decrease in activity in both the Loch Bà community (AWCD = 0.179) and the Blackford Bond consortium (AWCD = 0.175), however the decrease in activity in Blackford Pond was less pronounced. The Benhar Bing community's response to available carbon sources in EcoPlates, on average, improved under anaerobic cultivation, with AWCD increasing to a value of 1.32 OD*i*.

Inoculating the BIOLOG plates designed for specialised anaerobic profiling specifically demonstrated the poorest response to utilisation of carbon compounds, and lower AWCD values in Blackford Pond and Loch Bà. Again, the Benhar Bing inoculated anaerobic plates demonstrated a higher AWCD (0.093) than was observed with grown aerobically the EcoPlates with a reduced number of available substrates.

3.5.2.2 *The Utilisation of Individual Substrates in Aerobically Incubated EcoPlates*

To demonstrate the metabolic activity of the three sediment communities under aerobic conditions, results of carbon source oxidation were determined at the end point of aerobic EcoPlate incubation. Substrate use by all sediment communities is presented in **Figure 3.4.**

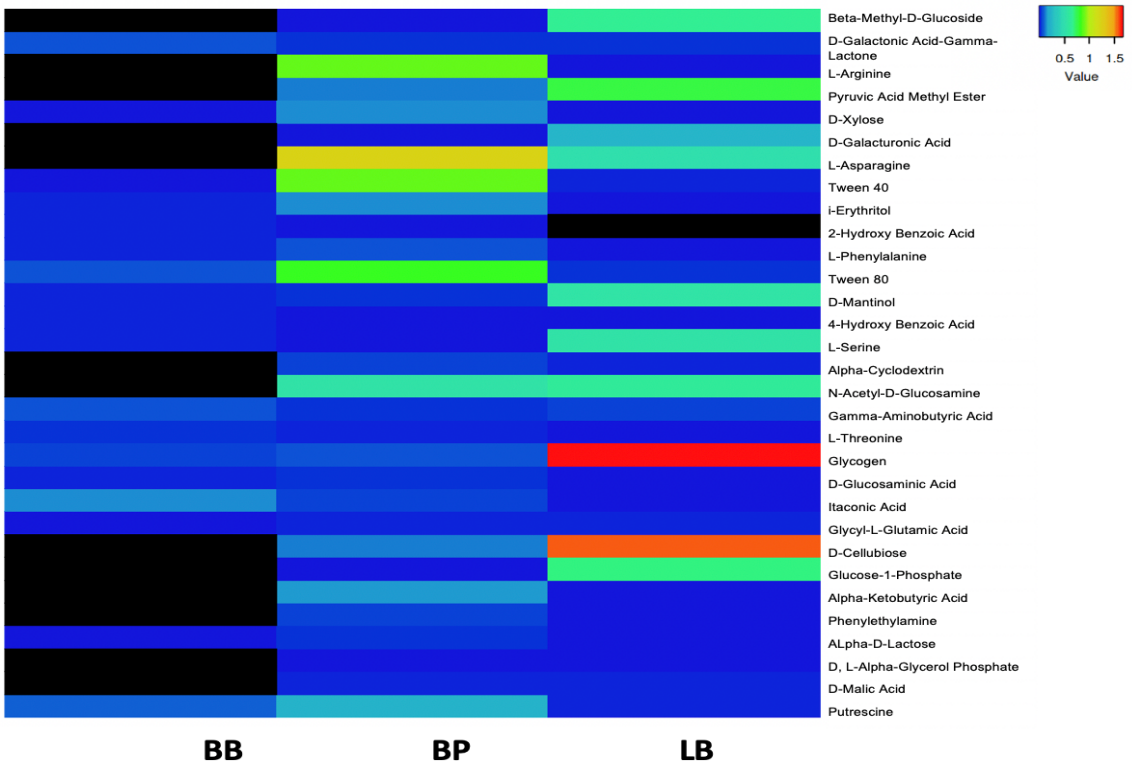

FIGURE 3.4: Heatmap displaying mean substrate utilisation in EcoPlates incubated under aerobic conditions at 37 ºC. Mean corrected optical density value shown (*n*=3). (BB = Benhar Bing; BP = Blackford Pond; LB = Loch Bà). Corrected OD value shown in key; all values retained and no 'minimum threshold' applied. Zero counts indicated in black.

The Benhar Bing sediment community had low utilisation of all carbon compounds available overall under aerobic incubation. The limited substrate use in Benhar Bing (OD*i* < 0.5) was evident compared to most readily utilised substrates in both Blackford Pond and Loch Bà which had ODi values of 0.5 – 1.6. Three compounds within the carboxylic and ketonic acid class were utilised by Benhar Bing communities. Itaconic acid ($C_5H_6O_4$), a dicarboxylic acid, was the most utilised substrate on average by Benhar Bing sediment dilutions in the EcoPlate well (OD*i* = 0.26). Following this, D-galactonic acid γ-lactone ($C_6H_80_6$) also had a weak response following Benhar Bing EcoPlate incubation (OD*i* = 0.17), as did γ-hydroxybutyric acid ($C_4H_8O_3$). Two polymers, glycogen, and Tween 80 ($C_{64}H_{124}O_{26}$) also had a visible response, albeit poorly when compared to OD*i* values observed in Loch Bà and Blackford Pond plates. Putrescine [$(CH2)_4(NH2)_2$], a derivative of arginine from the amines/amide class was utilised (OD*i* = 0.15), however utilisation of other amino acids and carbohydrates was poor or did not occur.

Both the Loch Bà and Blackford Pond communities responded more readily to the available substrates available in the EcoPlate. The Blackford Pond community demonstrated degradation of the aliphatic amino acid L-Asparagine ($C_4H_8N_2O_3$). Likewise, L-Arginine ($C_6H_{14}N_4O_2$) also showed high utilisation by Blackford Pond consortia, in contrast to the impaired amino acid use shown by the acidophilic assemblage. Tween 40 ($C_{62}H_{122}O_{26}$) and 80 were both utilised from the polymer grouping, as well as putrescine from amine/amide substrate class. Blackford Pond consortia utilised both D-xylose ($C_5H_{10}O_5$) and pyruvic acid-methyl ester ($C_4H_6O_3$) preferentially over other carbohydrates.

The Loch Bà EcoPlate had the strongest response on average to any substrates, both glycogen and the plant-derived carbohydrate, D-cellobiose ($C_{12}H_{22}O_{11}$) having corrected OD*i* values of above 1.5. Loch Bà consortia also showed the widest response across all available substrate groupings, although the carbohydrate response was most evident. Additional carbohydrates with high utilisation were in Loch Bà EcoPlates were glucose-1-phosphate ($C_6H_{13}O_9P$), D-mannitol ($C_6H_{14}O_6$), *N*-acetyl-D-glucosamine ($C_8H_{15}NO_6$), pyruvic acid methyl ester ($C_4H_6O_3$) and β-methyl-D-glucoside ($C_7H_{14}O_6$). Both L-serine and L-asparagine were used from the amino acids, while compounds from the amines/amides grouping were poorly utilised.

To demonstrate variation in substrate utilisation between the sediment communities, a multivariant statistical approach was applied. Non-metric dimensional scaling revealed that substrate utilisation was significantly different (P = 0.003) between the three samples and demonstrated close intra-replicate behaviour in the aerobic EcoPlates (**Figure 3.5).**

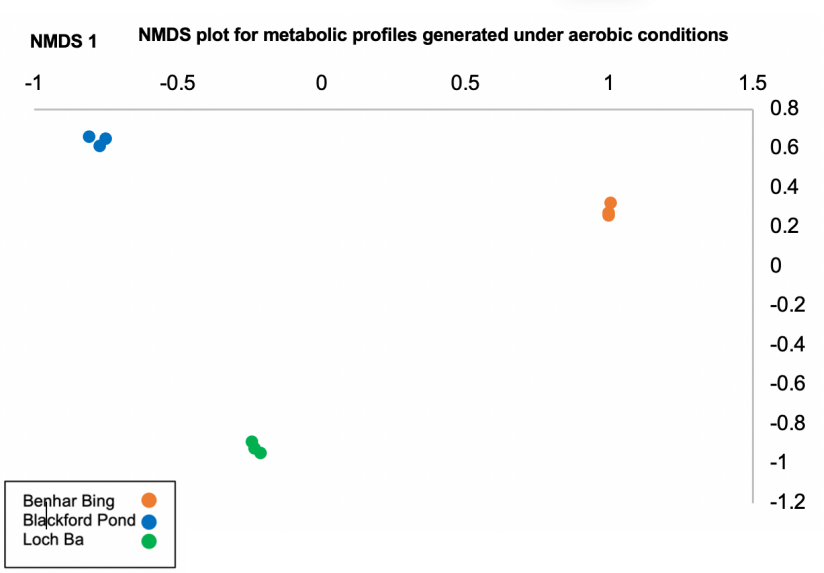

Statistic	Value
PermANOVA	7.75
PermDISP	6.89
P Value	0.003
Kruskal-Wallis 2D Stress	0.1

FIGURE 3.5: Non-metric Dimensional Scaling (NMDS) plot based on Bray-Curtis dissimilarity matrix demonstrating significantly different clustering of bacterial community responses to growth based on sole carbon sources in BIOLOG EcoPlate under aerobic conditions. PermANOVA testing for variance between factors (sampling site and substrate utilisation). P-value refers to PermDISP, indicating significance between distribution of the groups away from the centroid. Each replicate (*n*=3) is shown.

3.5.2.3 The Utilisation of Individual Substrates in Anaerobically Incubated EcoPlates

Following incubation of inoculated EcoPlates under anaerobic conditions, formazan production indicated the use carbon sources across the three sediment communities. The incubation of EcoPlates under anaerobic conditions provided some insight into carbon source preferences of the Benhar Bing, Blackford Pond and Loch Bà consortia under oxygen limitation. However, substrate responses were overall less strong compared to incubation aerobically, with highest responses at OD*i* 0.8 compared to > 1.5 observed in Loch Bà plates under aerobic conditions. The EcoPlate incubated under anoxic conditions also showed impaired substrate utilisation, and colour development was delayed; 10 days of incubation was required, which allowed substrates to be degraded.

Under anoxic incubation, D-xylose was utilised favourably by each environmental consortium (**Figure 3.6).** Two additional examples of metabolites degraded preferentially across all samples were tween 40 and pyruvic acid methyl ester. The shared use of substrates under anaerobic conditions by all communities is also reflected in the NMDS plot in **Figure 3.7** where no significant differences in utilisation profiles were observed. Benhar Bing and Loch Bà communities did not degrade tween 40 readily in the presence of oxygen, but under anaerobic incubation could express enzymes to hydrolyse the long chain tween polymer. The Blackford Pond anaerobic EcoPlate demonstrated utilisation of L-serine, L-threonine, α-cyclodextrin, α-D-lactose and 4-hydroxybuyric acid. This EcoPlate incubation showed the greatest ability to utilise compounds from across the chemical classes.

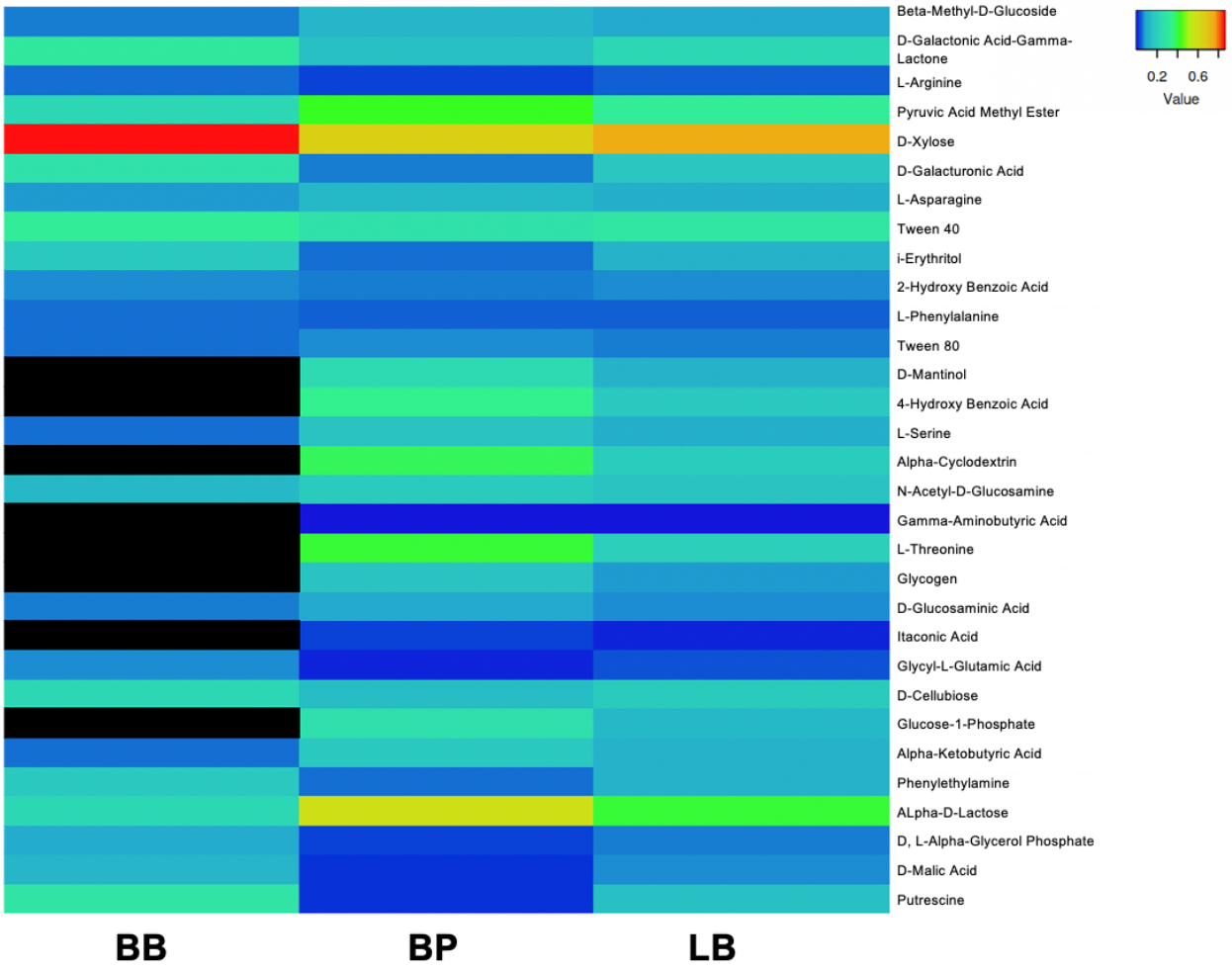

FIGURE 3.6: Heatmap displaying mean substrate utilisation in EcoPlates incubated under anaerobic conditions at 37 ºC. Mean corrected optical density value shown (n=3). (BB = Benhar Bing; BP = Blackford Pond; LB = Loch Bà). Corrected OD value shown in key; all values retained and no 'minimum threshold' applied. Zero counts indicated in black.

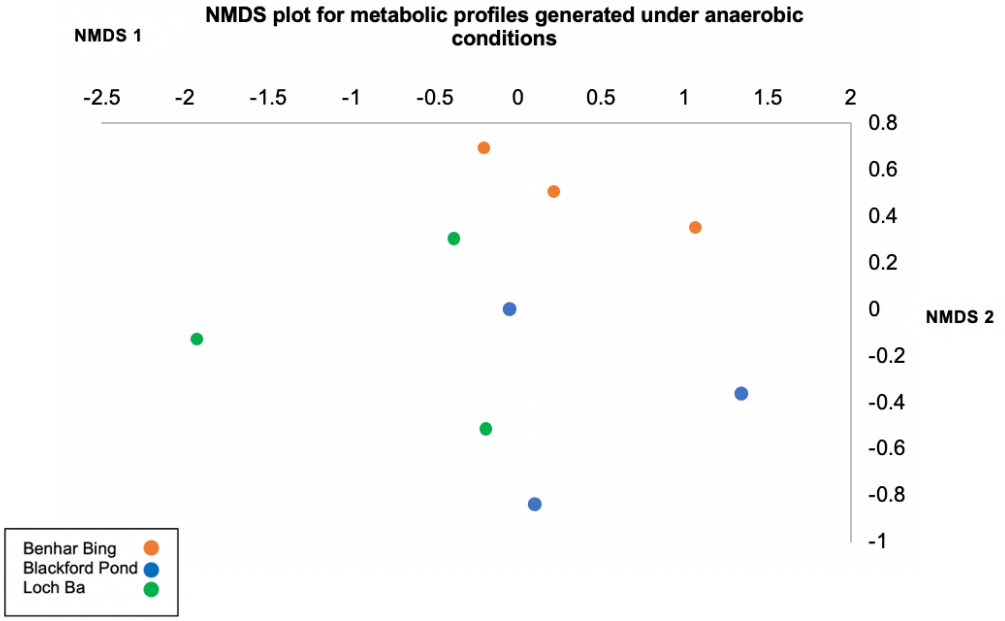

Statistic	Value
PermANOVA	1.30
PermDISP	2.13
P Value	0.261
Kruskal-Wallis 2D Stress	0.2

FIGURE 3.7: NMDS plot demonstrating non-significant clustering of bacterial community responses to growth on sole carbon sources in BIOLOG EcoPlate under anaerobic conditions. PermANOVA testing for variance between factors (sampling site and substrate utilisation). P-value refers to PermDISP, indicating no significance between distribution of the groups away from the centroid. Each replicate (*n*=3) is shown. Each replicate (*n*=3) for each sample is shown.

3.5.2.4 *The Utilisation of Individual Substrates in Anaerobe Specific BIOLOG Plates*

Overall, responses in the wells of specialised anaerobic microplate were poorer than previously demonstrated in both aerobic and anaerobically incubated EcoPlates, with the maximum mean OD*i* observed as 0.51 for β-cyclodextrin $(C_6H_{10}O_5)_7$ by the microbial consortium from Blackford Pond. Dextrin $(C_6H_{10}O_5)_n$ was also utilised more effectively on average (OD*i* mean = 0.48) in Blackford Pond plates than in Benhar Bing or Loch Bà . The Blackford Pond anaerobic microplate incubation on average showed the highest functional diversity (*ie*., utilised the highest number of available substrates) observed at the end of the incubation.

D-Fructose ($C_6H_{12}O_6$) was utilised preferentially by the Benhar Bing consortium (average OD*i* = 0.42) over other carbohydrates available. The Benhar Bing response also indicated a preference for dextrin as demonstrated in Blackford Pond responses, suggesting shared use of substrates across different anaerobic consortia as demonstrated when EcoPlates were incubated without oxygen. Also, substrates unseen in previous metabolic profiles were utilised in the anaerobic microplate assay by Benhar Bing consortia; maltotriose ($C_{18}H_{32}O_{16}$), L-rhamnose ($C_6H_{12}O_5$) and M-mannose ($C_6H_{12}O_6$). There was a moderately strong response to *i*-erythritol ($C_4H_{10}O_4$) by Benhar Bing consortia, which occurred to a greater extent and demonstrated in the anaerobic EcoPlate.

The Loch Bà incubation within the anaerobic microplates provided the lowest levels of carbon utilisation as is shown in the low OD*i* values within the heatmap in **Figure 3.8.** Loch Bà consortia struggled to reach OD*i* values above 0.1. Two substrates showed a more defined responses, dextrin and turanose ($C_{12}H_{22}O_{11}$) Many carbohydrates and organic acids were not readily degraded by Loch Bà consortia within the specialised anaerobic assay.

As was observed from the EcoPlate placed under anoxic conditions, there were no significant differences between the metabolic fingerprints of the consortia within the anaerobic microplate (**Figure 3.9**). There was wide variation observed between the three Blackford Pond replicates, which each replicate demonstrating differences in utilisation despite being inoculated with the same diluted sediment. Two of the Benhar Bing replicates cluster closely on **Figure 3.9**, indicating similarities in their utilisation of the available carbon compounds. However, the remaining Benhar Bing replicate mimics the fingerprint of two of the Loch Bà replicates.

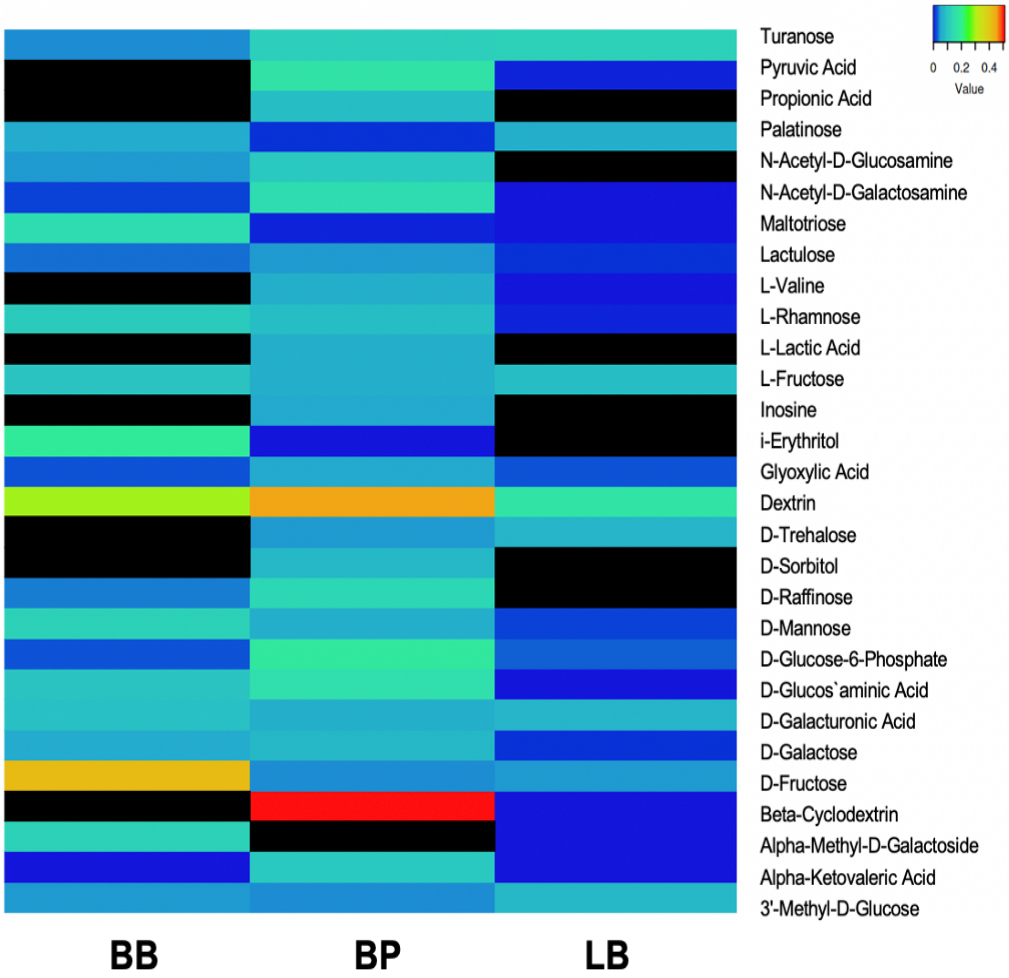

FIGURE 3.8: Heatmap displaying mean substrate utilisation in BIOLOG's specialised anaerobic microplate incubated at 37 ºC. Mean corrected optical density value shown (n=3). **Poorly utilised substrates were eliminated for clarity (threshold corrected OD <0.003).** (BB = Benhar Bing; BP = Blackford Pond; LB = Loch Bà). Corrected OD value shown in key. Zero counts indicated in black.

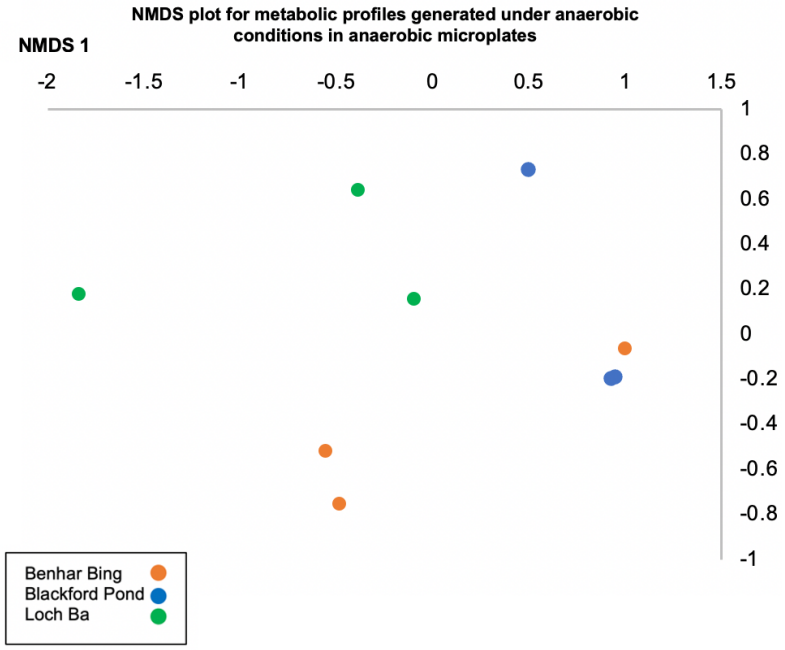

Statistic	Value
PermANOVA	1.45
PermDISP	0.431
P Value	0.811
Kruskal-Wallis 2D Stress	0.2

FIGURE 3.9: NMDS plot demonstrating non-significant clustering of bacterial community responses to growth on sole carbon sources in BIOLOG anaerobic (AN) microplate under anaerobic conditions. Each replicate (*n*=3) for each sample is shown. PermANOVA testing for variance between factors (sampling site and substrate utilisation). P-value refers to PermDISP, indicating no significance between distribution of the groups away from the centroid. Each replicate (*n*=3) is shown. Each replicate (*n*=3) for each sample is shown.

3.5.3 Cultivation Results

During cultivation trials, plating of serially diluted Benhar Bing sediment was not successful in allowing colony emergence of any acidophilic bacteria on either yeast extract ferrous sulphate (YEFS) or Reasoner's 2A (R2A) media types. However, the use of semi-solid R2A agar was successfully used as the agar-matrix to capture isolates when an iChip was used. As critical members of degradative pathway of carbon under anoxic conditions, methanogen cultivation was also attempted from Benhar Bing sediment, however no isolates were recovered despite the use of various cultivation conditions. A summary of culture-based utilised and results of each is shown in **Table 3.7.**

TABLE 3.7: Results of microbial cultivation.

Media Type		Visible Colonies	
'SAB'	'Acidified SAB'	N	N
'*Methanosarcina*' Growth Medium DSMZ 120		N	
YEFS Medium	'Modified' YEFS	N	N
R2A Plates	R2A iChip	N*	Y◊

* R2A plates at produced colonies characteristic of fungal contamination after 7 days

◊ The iChip R2A agar plugs were selected for further enrichment in acidified R2A liquid growth media (highlighted in green).

Due to the chemically unusual and highly acidic nature of the sediment collected from Benhar Bing, the standard iChip approach had to be modified. However did allow the isolation and further enrichment of a member of the Benhar Bing bacterial community. Conventionally, iChips were designed to be left in a natural environment to ensure organisms proliferating within the iChip are in constant contact with their native conditions, in an undisrupted state. Due to the acidity of Benhar Bing, incubation of the iChip was performed in a sealed bucket of sediment, to protect the iChips from corrosion or damage that may have occurred if they were buried in the constructed wetland itself.

Following 10 days of being buried in sediment (at room temperature), the device was dismantled, and agar plugs removed and used for microscopy. Inoculation of the central plate was challenging; Benhar Bing sediment was diluted in PBS and then mixed with molten semi-solid R2A agar. This sediment-agar mixture was pipetted into the central plate to 'capture' cells; due to dilution, not every well within the central plate contained cells when removed and used for microscopy.

Agar plugs that did contain bacterial cells demonstrated mixed populations based on Gram staining, but predominantly Gram-negative organisms. Following inoculation of agar plugs into acidified liquid R2A (to mimic the iChip incubation conditions), turbidity was observed after ten days; in general, between five and ten plugs were added to the acidified growth medium. However, acidification with autoclaved water collected from Benhar Bing produced no growth; turbidity was only observed when R2A media was acidified with H_2SO_4. A subsequent Gram stain using a loop of heat-fixed culture demonstrated the enrichment of a Gram-negative organism (**Figure 3.10**). Weak colony formation was observed on R2A plates using an aliquot of the turbid liquid culture; however, colonies could not be successfully reinoculated following initial colony emergence.

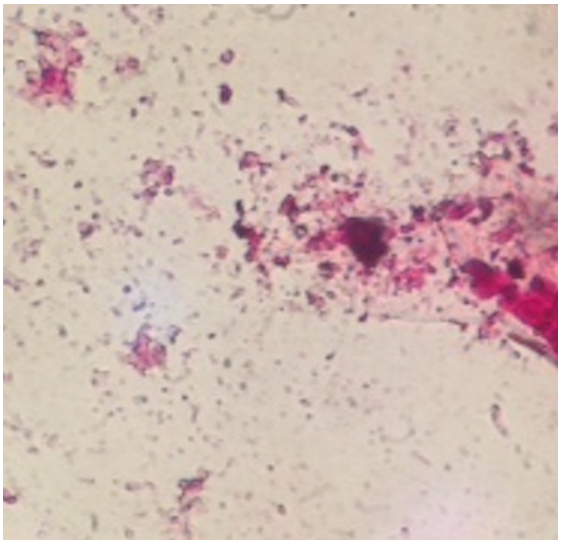

FIGURE 3.10: Microscopy and Gram staining of the enriched Benhar Bing isolate grown in acidified liquid R2A. Short Gram-negative rods were observed under 40x objective lens magnification (Nikon Eclipse E200 microscope) following Gram staining of a heat-fixed culture aliquot, retrieved using a sterile loop. Safranin crystals were noted to obscure individual colonies in some cases.

3.5.3.1 Taxonomic Identification of the Benhar Bing iChip Isolate

Following enrichment in liquid R2A of the Gram-negative isolate from the iChip, genomic DNA was successfully extracted and the V3 region of the 16S rRNA gene amplified and cloned. Sanger sequencing of the amplicon was performed. The phylogeny produced from the BLAST alignment results is shown in **Figure 3.11**.

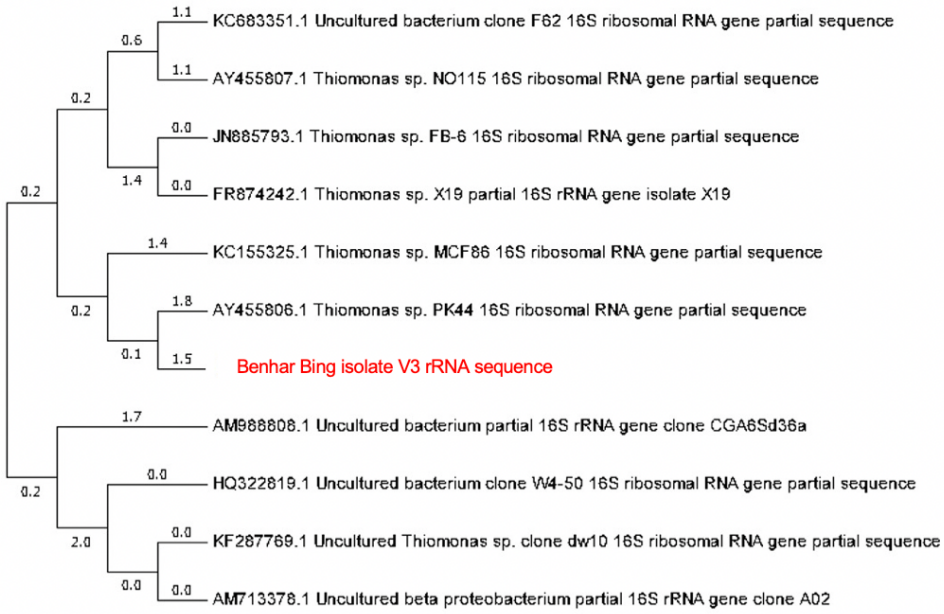

FIGURE 3.11: Phylogenetic tree demonstrating the taxonomic position of the *Thiomonas* isolate. Taxonomic position determined by alignment of partial 16S rRNA sequences from closest related sequences based on BLAST results. Sequences aligned with ClustalW and phylogenetic tree produced with MEGA (v11).

When assessing the partial V3 rRNA gene sequence recovered from Benhar Bing following nucleotide BLAST search, a 99.4% match to a *Thiomonas* species 'PK44' (AY455806.1) was observed; this species was retrieved from mine-waste contaminated water. Other partial 16S rRNA sequences with between 96.60 – 99.0% similarity to the sequence from the Benhar Bing isolate were all noted to have been retrieved from other *Thiomonas* species.

Several uncultured acidophilic bacteria also shared partial 16S rRNA sequence homology with the *Thiomonas* isolate but were not taxonomically resolved. These uncultured bacterial clones were detected in a range of acidic environments including arsenic contaminated creek sediment (AM988808.1), lake sediments polluted by waste from coal-mining excavations (AM713378.1) and an additional site impacted by acidic mining effluent (HQ322819.1).

3.6 Discussion

3.6.1 Physicochemical Analysis of Benhar Bing, Blackford Pond and Loch Bà

Chemical analysis demonstrated clear variation in elemental composition between the three sediments. The lower carbon levels in Benhar Bing and Loch Bà are one way in which the unusual environmental conditions of these sites are reflected. The low TOC/TC recorded in Loch Bà demonstrates the low bioavailable carbon present this oligotrophic highland loch, likely due to the poor vegetation and previous clearance of trees from Rannoch Moor (Walker and Lowe, 1977). There is little evidence in the literature describing carbon cycling in low-nutrient freshwater lochs, however the work of Bailey-Watts and Kirika (2009) does outline that many of the larger Scottish lochs demonstrate oligotrophy and much of the ecology is now reflective of the altered natural conditions, and much previous biodiversity and ecological interactions may have been lost. The oligotrophic status (both inorganic and organic nutrients) of Loch Bà was also noted in the work of Pagaling *et al*. (2014).

Low carbon levels are routinely reported in acid mine drainage areas since the receiving waterbodies are so greatly impacted by the metal-rich pollution and inorganic cycling dominates. Frequently, additional carbon sources must be added to sites with excessive acidic effluent production during reclamation efforts to establish greater ecosystem productivity (Heal and Salt, 1999). Often, acid mine drainage literature does not state organic carbon levels but do report on inorganic carbon, which is often considered to be in the form of dissolved carbonate (CO_3^{2-}) due to the acidity of the waste-stream. Despite this, the work of Grettenberger *et al*. (2020) states that the organic carbons levels are low and continue to decrease within their wetland system of interest contaminated by acid mine drainage. When compared to Benhar Bing (TOC = 40.1 g/kg), the study site in Grettenberger *et al*. (2020) has slightly higher TOC levels (55.48 g/kg), however this is noted to decrease in other areas of this site to 11.53 g/kg.

Benhar Bing the most acidic site of the three sediments, which is characteristic of the low pH, metal-rich synthetically derived effluents associated with mining activities. The bacterial regeneration of H^+ and dissociation of sulphuric acid in acid mine drainage leads to the observed low pH (Havig *et al*., 2017; Grettenberger *et al*., 2020). The weakly acidic pH value recorded from Loch Bà is potentially due to organic acids leaching from the surrounding moor into the loch, which has been observed occurring in other freshwater sites (Siegel *et al*., 2006). In contrast, the Blackford Pond pH value recorded was approaching neutrality, (pH 6.29). Blackford Pond was recorded as having a mean pH of 8.70 in the work of Pagaling *et al*. (2014); however repeat pH measurements during sampling from this site demonstrated the sediment was routinely recorded as having a circumneutral pH.

Sulphide (S^{2-}) proved to be an ineffective inorganic determinant to measure; the S^{2-} ion is extremely labile in solution and rapidly undergoes a substitution reaction to the hydrosulphide ion (HS^-) and additional hydroxide ions (OH^-), limiting its detection, particularly at low concentrations. It was evident that the H_2S-methylene blue ion exchange method was not capable of producing the resultant methylthioninum chloride ($C_{16}H_{18}ClN_3S$ [methylene blue]) product in high enough concentrations for detection above the assay's threshold. The generation of methylene blue is utilised as an indirect measure of initial S^{2-} concentrations via a reaction with *N, N*-dimethyl-*p*-phenylenediamine sulphate. It was apparent that all sediment samples did not contain high concentrations of bioavailable sulphide for the reaction to proceed effectively and that free S^{2-} may have undergone substitution reactions preventing the S^{2-} conversion to methylene blue.

Sulphate (SO_4^{2-}) proved to be a more reliable determinate across all sediment samples. The high SO_4^{2-} concentration observed in the Benhar Bing sediment is typical of other acid mine drainage sites, which are known to contain elevated levels of metal sulphates. When compared to the work of Grettenberger *et al*. (2020), Benhar Bing contains higher levels of sulphate than the retention pond used in the authors' study.

Compared to the initial work on Benhar Bing work by Heal and Salt (2000) following the wetland's construction, sulphate levels have decreased. In 2000, [SO_4^{2-}] was determined to be 1.7 g/L within sediment collected from the wetland. However, in the Heal and Salt (2000) report, the concentration of sulphate was resolved using ion chromatography (IC) via an anion exchange column. The current sulphate levels reported here were detected from pore water samples (recovered as supernatant) from centrifuged sediment samples and indirectly quantified via the production of sulphates via ion exchange with $BaCl_2$. The use of pore water required during this ion exchange methodology results in an underrepresentation of sulphate levels within the bulk of the sediment. Despite this, Benhar Bing contains the highest SO_4^{2-} levels across all sediment samples assessed. Furthermore, *Bacteria* capable of sulphate reduction utilise SO_4^{2-} as their terminal electron acceptor during organic matter decomposition, producing HS^-. HS^- allows the precipitation of metals and a reduction in freely bioavailable sulphate (Lewis *et al*., 2006); an important benefit when considering removal of metals from contaminated systems.

The mean levels of sulphate were lower in Blackford Pond and Loch Bà when compared to Benhar Bing. Sulphate levels were not successfully determined in Loch Bà as the ion exchange mechanism to measure SO_4^{2-} levels utilised could not detect the sulphate ion in solution below concentrations of 40 mg/ml. This is reflected in the work of Pagaling *et al*. (2014) whereby levels of sulphate were detected below 3 mg/ml using an alternative detection strategy. Again, indicative of oligotrophic status of the loch. The shallow water depth may also maintain aerobicity, limiting both the production and utilisation of sulphates. Due to the challenges in detecting sulphate, future work could utilise a more sensitive approach, such as ion chromatography.

Both ammonia and ammonium concentrations were successfully determined in each sediment sample. The work of Ramanathan *et al*. (2017) noted similar ammonium and ammonia levels to those recorded in Benhar Bing present in effluents located close to abandoned iron mines in Colorado, USA. In aqueous environments, levels of ammonium are often higher than those recorded for gaseous ammonia (as was demonstrated in Benhar Bing) as NH_3 becomes solvated by excessive free H^+ ions, resulting in the production of cationic NH_4^+ (Ishikita and Knapp, 2007). In low pH conditions, this is particularly evident as the excess of free H^+ causes the chemical equilibrium to shift away from ammonia in solution (Ramanathan *et al*., 2017). This can impede nitrification and the wider nitrogen cycle, which is challenging for prokaryotes in acidic conditions. Nitrogen cycling capabilities are poorly understood in acidophiles, yet the role of ammonium transporter proteins may enhance both environmental buffering capacity and promote energy conservation via nitrogenous compounds if bioavailable ammonia is scare (Offre *et al*., 2014).

The lower ammonium and ammonia values recorded in Blackford Pond are surprising, as other copiotrophic freshwater systems have recorded high levels of both these chemical species (Lemke *et al*., 2009). It is likely that the use of pore water from sediment centrifugation has caused an underrepresentation of the NH_3 and NH_4^+ levels, and the issue may be technical and a limitation of the methodological approach, particularly the detection of NH_3. Additionally, interference of the ion exchange mechanism utilised for ammonium detection can occur with samples which have high concentrations of Al, Ca, and Mg ions in solution (Mišić *et al*., 2021). Across the three sediment samples, Blackford Pond had the highest concentrations of these metal species, which may be caused the sodium nitroprusside catalysed reaction to be less effective, therefore impacting the generation of the product of the ammonium assay, indophenol blue (*N*-(*p*-dimethylaminophenyl)-1,4-naphthoquinoneimine [$C_{12}H_9NO_2$]).

Detection of both NH_3 and NH_4^+ is only sporadically reported in the literature regarding the environmental chemistry of oligotrophic systems. The work of Vissers (2012) could not detect ammonium or ammonia in water samples from a deep oligotrophic lake in Switzerland. The authors suggested that NH_3 and NH_4^+ levels may fluctuate seasonally and are likely dependent on nitrogen-containing compounds entering oligotrophic systems from the surrounding catchment.

3.6.2 Determining Carbon Source Catabolism by Sediment Communities

Aerobic EcoPlates proved to be a rapid and reproducible means of characterising both conventional and extremophilic microbial communities. Benhar Bing sediment communities had low utilisation of all carbon compounds available reflective of the observed low bioavailability of organic carbon in Benhar Bing sediment. An attempt to establish conditions more alike to acid mine drainage was trialled by lowering the pH of the wells of an EcoPlate using Benhar Bing sediment inocula diluted in acidified phosphate buffered saline (PBS); reduced to pH 3 with 1M sulphuric acid (H_2SO_4). However, the reduction in pH caused degradation of the redox indicator and visible peeling appeared on the base of the wells preventing quantification of any substrate use. Further to this, acidification of the wells may have degraded substrates present preventing bioavailability and subsequent oxidation.

Due to many acidophiles' metabolic ability to utilise chemolithoautotrophic pathways; predominantly sulphur and iron oxidation as outlined in the work of Emerson *et al*. (2012), it is perhaps unsurprising that Benhar Bing communities have the weakest response to growth in the EcoPlate assay. The utilisation of a compound within an EcoPlate well requires the growth of organisms which can tolerate the high concentration of the available substrate within the well and many acidophiles do not require high concentrations of organic compounds for their metabolism.

Despite this poor utilisation, the Benhar Bing aerobic metabolic profiling data was retained and not removed by applying any 'positive response thresholds' outlined by Kenarova *et al*. (2013), whereby low OD*i* values, below 0.25 are deemed low-level utilisation and removed. As little literature exists exploring the ability of acidophilic communities to degrade and assimilate carbon, it was deemed important to retain the data, despite the low OD*i* values observed. Additionally, polluted wetlands are often termed 'low biomass' and may harbour microorganisms not suited to growth within EcoPlate wells as they may elude cultivation or have reduced maximum specific growth rates (μ_{max}) in culture when *in situ* conditions cannot be replicated. Many acidophiles' growth will cease in pH conditions close to neutral (Jin and Kirk, 2018).

The literature exploring metabolic profiling of acidophilic communities through cultivation-based approaches is limited, however the work of Sutcliffe *et al*. (2019) did utilise EcoPlates to examine carbon source utilisation in a metal contaminated system. This work assessed the ability of bacterial consortia from copper (Cu) contaminated replicate artificial mesocosms to degrade available carbon sources. Sutcliffe *et al*. (2019) observed an overall decrease in carbon source use was observed in the contaminated samples, compared to the controls. Amino acid degradation was deemed significantly impacted, as was the use of 2-hydroxybenzoic acid. A reduced utilisation pattern of amino acids was reflected also by the Benhar Bing consortia.

Importantly, the inability to degrade aromatic-containing compounds such as the benzoic acids could potentially demonstrate a wider ecological issue. The combination of high metal mobility with added aromatic compound recalcitrance, which is enhanced through generally low carbon utilisation, can negatively impact bioremediation attempts in metal contaminated wetlands (Sutcliffe *et al*., 2019). Therefore, bioprospecting of acidophiles with native phenolic degradation ability remains an important and understudied metabolic function. (See **Chapter 6** for further metagenomic results exploring these, to date, previously poorly described ecological attributes of acidophiles).

Regarding the Blackford Pond community's response to specific substrates, similar amino acid degradative abilities were also demonstrated by Echavarri-Bravo *et al*. (2015). This work demonstrated degradation of amino acids by sediment microbial communities from estuary samples within EcoPlates and concluded that amino acids were the preferential energy sources the cultivable microbial community members within the EcoPlate. Two amino acids were readily degraded by Blackford Pond consortia (L-arginine and L-asparagine); a metabolic preference also observed by the work of Echavarri-Bravo *et al*. (2015).

As the EcoPlate incubated anoxically and the anaerobe-specific microplate provided less evident metabolic patterns, they are discussed here briefly. It is intriguing that such metabolic shifts occurred through alteration of oxygen availability, and that significant trends could not be observed as is reported here for aerobic metabolic profiles, despite apparent variation in substrate use during anoxic growth between differing consortia. Repeating the metabolic profiling approaches outlined here with more replicates may indicate more significant patterns and overcome the evident technical variation.

Furthermore, both the anaerobically incubated EcoPlate and the specific anaerobic microplate both required longer incubation periods to establish growth in well (indicated by formazan production). The OD values were recorded only once, at the end of the experiment when colour development ceased; the work of Echavarri-Bravo *et al*. (2015) utilised this same approach to OD quantification. In some studies, OD values are recorded at 24-hour intervals, allowing an increase of utilisation over time to be determined (Gryta *et al*., 2014). Yet, this was not deemed appropriate as it would subject the developing anaerobic assemblages to be exposed to oxygen, impeding growth. Despite not being able to determine which taxa are degrading each carbon source, it is likely that the increased incubation periods would allow co-metabolism of substrates by multiple enriched taxa which may take more time to establish as the community adjusts to growth in wells with a sole carbon source (Koner *et al*., 2022).

Potentially, this variation in metabolic response, particularly in anaerobically incubated EcoPlates and the specialised anaerobic assays could be caused by low numbers of relevant species. Each sediment sample was diluted prior to inoculation into BIOLOG plates. Dilution of the Benhar Bing community, which is already more simplistic due to chemical constraints on microbial diversity, may have caused a loss of species required for carbon source utilisation, and led to deviation in function between replicates (Nogueira *et al*., 2021).

Rare microorganisms are the most likely to be lost from a microbial population during dilution and given the predominance of lithotrophic organisms in acid mine drainage systems, the loss of less abundant carbon cyclers required to degrade the available substrates may have caused the weak and varied metabolic responses (Zhang *et al*., 2023). Additionally, the oligotrophic status of both Benhar Bing and Loch Bà demonstrate that the high concentration of substrates in BIOLOG plates may not be tolerated by community members, as this is not reflective of microbial catabolism *in situ*.

Plates were inoculated under anaerobic conditions to maintain anoxic conditions; however anaerobic function may have been impaired initial during sediment sampling or anaerobes may require alternative electron acceptors not available under standard anaerobic conditions to couple to heterotrophic reactions. Yet, there is concern surrounding the use of tetrazolium as a redox indicator under anaerobic conditions (Christian and Lind, 2006). During the experiments outlined above, the production of formazan indicated a positive response and was observed during both aerobic and anaerobic growth of inoculated sediment communities.

Christian and Lind (2006) performed an extensive review on the limitations of the BIOLOG approach and confirmed that when EcoPlates are utilised under anaerobic conditions that colour development is significantly reduced, as well as a reduction in the number of carbon compounds used by the anoxic consortia; this was also observed in the data presented here. The authors also argue that in some cases strict anaerobes can be lost during sampling and determined that metabolic responses under anaerobic incubations are due to the function of facultative anaerobes alone. However, current understanding contradicts this as oxygen can be inhibitory, but not destructive, to anaerobes which have evolved a range of tolerance mechanisms to utilise if exposed to oxygen (Lu and Imlay, 2021).

Lastly, the growth on a limited number of organic substrates may also hamper estimates of metabolic diversity through EcoPlate use, as the compounds may not be reflective of the compounds noted within acid mine drainage impacted systems (Koner *et al.,* 2021). Furthermore, competitive exclusion of some species within the wells may have occurred if fast growing heterotrophs can adapt to the cultivation conditions and proliferate while catabolising the available carbon source. As this metabolic profiling technique is reliant on bacterial growth, there is a bias towards species which can tolerate growth in culture. This will only consider a fraction of the true metabolic potential observed in communities using alternative approaches *e.g.,* metagenomic and transcriptomic approaches to community characterisation.

3.6.3 Acidophile Cultivation from Benhar Bing

Enumeration of methanogens on both SAB medium and *Methanosarcina* growth medium 120 proved unsuccessful. Several modifications were attempted to overcome the challenges in cultivating methanogens, however no alteration to growth strategies led to methanogen isolation. SAB was selected initially as it was developed to allow recovery of methanogens from the mammalian GI tract in Khelaifia *et al*. (2017), however this could not be repeated using environmental inoculum from Benhar Bing.

A major constraint on the growth of methanogens is their intolerance to molecular oxygen. Considered the strictest extant anaerobic microorganisms, oxygen is inhibitory to enzymes involved in methanogens' energy conservation. The F_{430} co-factor of the terminal methanogenic enzyme complex, methyl co-enzyme M reductase, is particularly sensitive to inhibition by aerobic conditions (Guo *et al.,* 2022). The resazurin indicator dye present within the medium demonstrated a colour change reaction during incubation of SAB plates, indicating the production of resorufin (7-hydroxy-3*H*-phenoxazin-3-one), via resazurin reduction by oxidoreductases. This demonstrated the loss of anaerobicity during the incubation, therefore negatively impacting the emergence of any methanogen colonies. To overcome these cultivation limitations, detection of methanogenic *Archaea* in environmental samples via molecular approaches is described in **Chapter 4.**

The use of '*Methanosarcina* growth medium 120' was initially attempted as a positive control with a culture of *Methanosarcina barkeri* and therefore was not acidified. Despite this, the culture could not be revived. The duration of time which the *Methanosarcina* culture was in transit prior to attempted cultivation may have also impaired the ability for the cells to be grown. Further to this, methanogens have been noted as having long incubation periods and media often became dehydrated over the duration of incubations. Several attempts were made to protect the plates in parafilm, as well as reducing the temperature within the anaerobic chamber to prevent desiccation of any emergent colonies. Neither of these optimisation approaches allowed the growth of any visible colonies. Condensation would also develop on the plates interfering with the media surface, which in some cases led to contamination by fungal colonies.

Regarding both methanogen and attempted bacterial isolation on solid plates, both SAB and YEFS medium suffered from precipitation of sulphides during incubation periods. This occurred between 5 - 7 days incubating under anoxic conditions. The work of Nancucheo *et al*. (2016) states that iron sulphide can be added to precipitate sulphides into non-bioavailable forms which can prevent microbial growth from being impeded by inhibitory sulphide concentrations. However, this approach is limited when plating environmental samples which are below pH 5. Lastly, methanogens may be not present, or rare in Benhar Bing, preventing their emergence in culture

The use of the conventional spread plate technique with acidic sample aliquots would often cause the media surface to shear as visible acid-mediated agar hydrolysis would occur. Future work could utilise substitute setting agents to prevent tearing of the agar surface and disruption of the solid growth matrix. The work of Panova *et al*. (2021) utilised the alternative solidifying agent Gelzan, a derivative of the polysaccharide gellan, to overcome agar hydrolysis during the isolation of a novel acidophilic species of *Desulfosporosinus* from a microbial mat present in gold-mine derived leachate. Alongside damaging the integrity of the agar matrix, agar hydrolysis is thought to produce small molecular weight compounds, predominantly pyruvic acid, which can impede microbial growth if produced in excess, or provide unwanted substrates to any emergent colonies (Nancucheo *et al*., 2016).

Additionally, damage to the agar matrix can prevent utilisation of the bioavailable nutrients by emerging colonies. In microbial ecosystems, methanogens are often reliant on the exchange of substrates from syntrophic bacterial partners. To achieve isolation of axenic methanogens, this requirement is replaced by the medium components which may be challenging to access following agar hydrolysis. To overcome the production of hydrolytic by-products, intricate overlay approaches have been applied to solid agar. Some success has been noted in the literature with *Acidiphilium* species when inoculated into the 'base' layer of agar. It is thought that *Acidiphilium* can metabolise organic acids produced, preventing their inhibitory effects on emerging colonies of interest (Johnson and Hallberg, 2007). The requirement for growth however becomes dependent on the activity and persistence of the 'partner' species, an additional challenge when *Acidiphilium's* own acidophilic growth is considered.

The use of the iChip proved more successful than the use of chemically defined media, and the recovery of a *Thiomonas* species was encouraging following iChip inoculation. The isolate stained Gram negative, as expected of *Thiomonas* species, however future staining could utilise basic fuchsin over safranin to provide more intense cell wall staining as safranin often left residual crystals visible under light microscopy.

First taxonomically described by Moreira and Amils (1997) *Thiomonas* are Gram negative organisms ubiquitous in acid mine drainage environments and other ecosystems with high concentrations of heavy metals. The Benhar Bing *Thiomonas* and *Thiomonas* strain PK44 share similar biogeographical biotopes which builds on the evidence of *Thiomonas* as a key taxon in contaminated ecosystems. The full metabolic capabilities of *Thiomonas* remains undetermined, and the body of literature on *Thiomonas* is limited compared to other iron oxidising acidophiles considered characteristic of acidic effluents, *e.g., Acidithiobaccillus ferrooxidans* (Chen *et al.,* 2021).

However, *Thiomonas* has been noted to proliferate in the presence heavy metals present in acid mine drainage effluents, particularly arsenic, which has been observed in mine wastes globally. However, mechanistically, how *Thiomonas* counteracts deleterious arsenic concentrations remains unclear, and may be able to both oxidise arsenic and utilise other undetermined resistance mechanisms (Ben-Fekih *et al.,* 2018). The organisation and function of arsenic detoxification genes present in members of the Benhar Bing community are resolved via metagenomic sequencing and are presented in **Chapter 6**.

Depsite the iChips's success in allowing the proliferation and subsequent enrichment of *Thiomonas*, ensuring bacterial growth within the device is complex and relies on the initial community surviving the initial molten agar-sediment mixture. Recently modifications to iChip by Lodhi *et al*. (2023) led to the development of the 'cultivation chip' (cChip) which has a modified structure (*e.g.,* larger pores and the use of a single membrane to allow nutrient and gas exchange) to encourage growth of previously uncultivated species.

Enrichment of *Thiomonas* in liquid culture following inoculation with agar plugs retrieved from the iChip was only evident when the liquid R2A was acidified with H_2SO_4 and not autoclaved Benhar Bing water. Sterilised Benhar Bing water was trialled as an acidifying agent to maintain native growth conditions and metabolites, however autoclaving of this water sample caused a chemical reaction, evident from a colour change to orange; likely due to high temperature and pressure changing the redox state of the iron ions present within the water.

This alternation of chemical species may have impacted growth, as well as potential changes occurring other Benhar Bing chemical components. Furthermore, the *Thiomonas* isolate could not be continually cultivated when grown on solid media and only grew weakly, producing small yellow colonies. This is potentially due to the R2A plates not being acidified due to issues regarding agar hydrolysis which may have prevented growth, as discussed above.

Notably, attempts to grow acidophilic members of the Benhar Bing community using standard serial dilutions onto R2A medium also resulted in no microbial growth. This suggests that the use of novel cultivation approaches holds promise in promoting recovery of extremophilic taxa, as isolation attempts on R2A without enrichment in the iChip did not allow *Thiomonas* growth. The successful use of the iChip strengthens the argument that the move away from current overreliance on chemical media components, many of which may be difficult to predict if nutritional preferences of extremophiles are not yet fully elucidated, can aid in extremophilic cultivation.

3.7 Conclusion of Chapter 3

3.7.1 The Use of Metabolic Profiling for Neutral and Acidic pH Sediment Consortia

Despite the BIOLOG approach being an easily reproducible and reliable technique to determine functional diversity, metabolic profiling has several limitations that should be considered when drawing conclusions regarding sole carbon source utilisation as a marker for broad ecosystem function. Given the limited number of substrates available, which are more reflective of microbial ecosystems with high carbon content, the results generated via BIOLOG techniques should be considered a general overview of a specific derived function.

Despite this, metabolic profiling remains a useful tool for microbial ecologists, however the issue of relating taxa to molecular level function (*i.e.,* which organisms are degrading which substrate via enzyme expression) remains challenging in natural systems such as soils and sediments with varying levels of diversity, particularly without the use of metagenome assembly and culturing of isolates.

In conclusion, it is demonstrated in the data above that aerobic consortia strongly diverge in terms of their substrate preferences and can degrade compounds to a greater degree that observed in the two anaerobic incubation strategies. Loch Bà native consortia were able to degrade the widest range of substrates, however resistance to amine/amide and aromatic compounds was noted in aerobic catabolism. Variation between replicate communities in both anaerobically incubated plate types (EcoPlates and specialised anaerobic microplates) is likely technical, potentially due to the loss of key carbon cycling species. Although chemically distinct, the low levels of bioavailable carbon in both Benhar Bing and Loch Bà may influence carbon cycling capabilities of microbial populations in these two locations, driving similar utilisation biases within these cultivation-dependant approaches, particularly under anaerobic growth.

Understanding overall community function (*ie*. which taxa are the prevalent degraders in a well understood system?) is more straightforward when the system is reliant on specific functional guilds of microorganisms performing broad functions. In contrast, determining function of an assemblage is challenging where single compound oxidation is being achieved by a mixed population selected for by the substrate.

3.7.2 Novel Growth Strategies and the Challenges of Recovering Acidophilic Isolates

More work is required to better understand acidophilic growth requirements and how best to capture this biodiversity in culture. Novel techniques such as the iChip hold promise in overcoming the challenge of growing members of the rare and fastidious microorganisms as it limits the use of chemically synthetic medium which may not match the nutritional spectrum of many extremophiles. With most microorganisms still eluding cultivation, the novel cultivation strategies, guided by metabolic profiling and potentially, more powerful metagenomics techniques may aid in improving on current cultivation methodologies.

CHAPTER 4 - Determination and Quantification of Key Functional Genes Involved in Microbial Carbon Cycling

4.1 Structure and Function of the Methyl Co-Enzyme M Reductase Complex

Microbial consortia endogenous to acid mine drainage sites are considered to facilitate reactions involved in simplified biogeochemistry given the physicochemical constraints within these extreme and anthropogenically influenced environments (Hedrich and Schippers, 2021). How the biogeochemical cycling of organic matter in acid mine drainage sites persists under multiple extreme abiotic factors is underexplored, despite the importance of the global carbon budget and its interactions with other elemental cycles. Notably, it has been observed that the bioconversions of heavy metals and metalloids are interlinked to the cycling of carbon in other contaminated systems; particularly those impacted by iron and arsenic (Yan *et al*., 2024; Zeng *et al*., 2024).

As discussed in **Chapter 3,** cultivation of anaerobic microorganisms, particularly methanogens, is challenging. Consequently, methanogenic taxa remain underrepresented in culture collections. The challenges in exploring the diversity of cultivating carbon cycling organisms from acid mine drainage sites are compounded further by complexities involved in the enumeration of acidophiles on standard media (Khelaifia *et al*., 2013). There is little literature which demonstrates the ability of the terminal stages of the anoxic carbon cycle to persist under acidic conditions and the impact that low pH conditions may have on the selection and associated function of specific methanogenic populations.

The work of Brauer *et al*. (2011) which isolated the most acid-tolerant methanogen to date, *Methanoregula boonei,* from a moderately acidic peatbog notwithstanding, most evidence of the behaviour of moderately low pH methanogenic consortia has come from applied microbial ecosystems (*ie*., methanogenic bioreactors undergoing moderate acid-induced stress) and does not represent the low pH conditions of contaminated effluents. It remains unclear to what extent methanogens have adapted to, and colonised, low pH niches and the impacts this has on potential methane release from such poorly characterised environments.

Due to current limitations in the enumeration of methanogens via cultivation-dependent techniques, much of the known methanogens' biodiversity has been observed through metataxonomic/metagenomic studies. Additionally, methanogens can be detected in DNA samples by specifically targeting unique methanogenic enzymes and eluding taxonomy from gene sequences. All methanogens share the methyl co-enzyme M reductase (Mcr*)* complex which catalyses the final reaction in the methanogenesis, facilitating the reduction of methyl-coenzyme M (HS-CoM) with coenzyme B (HS-CoB), producing methane.

Detection of the *mcrA* gene has expanded on current understanding regarding the biodiversity and dispersal of methanogens in a range of conventional anaerobic environments (*e.g.*, sediments, sewage sludge and the mammalian GI tract). However, *mcrA* sequences which imply the presence of methanogenic organisms are lacking from extreme environments. Only recently has attention been given to *mcr* gene harbouring taxa in non-conventional systems which have led to the conclusion that methanogenic consortia may be less biogeographically restricted than originally thought and methanogenesis may be energetically feasible under extreme conditions.

Recent examples of extreme environments whereby methanogenesis has been observed are described by both Buessecker *et al*. (2023) and Hou *et al*. (2023). The work of Buessecker *et al*. (2023) described *mcr* gene-dependent methanogenesis occurring in moderately acidic hot springs, whereby the taxa present were under both moderate acid and thermal stress. Additionally, Hou *et al*. (2023) demonstrated the presence of novel, non-Euryarcheotal archaeans capable of methanogenesis in deep anoxic subsurface environments whereby methanogenic precursor substrates may be scarce.

To reiterate from **Chapter 1,** the activity of the Mcr complex is responsible for the generation of approximately one billion metric tonnes of CH_4 per year. The activity of the Mcr complex underpins the importance of the link between the carbon cycle and global climate (Prakash *et al*., 2019). The structure of the multi-subunit enzyme was first elucidated from '*Methanobacterium thermoautotropicum* strain ΔH' (now reclassified as *Methanothermobacter thermoautotrophicus)* in the work of Ermler *et al*. (1997) and the genes encoding individual enzymatic subunits have used as marker genes in methanogen-targeted ecological studies (Lyautey *et al*., 2023). Sequencing of the *mcr* encoded enzymatic subunits can detect a greater level of methanogenic taxonomic richness than utilisation of the archaeal 16S rRNA gene alone (Dziewit *et al*., 2015).

The Mcr complex is a large ~ 300 kilodalton (kDa) metalloprotein synthesised as a hexamer in an $\alpha_2\beta_2\gamma_2$ arrangement (Duin, 2013; Ermler *et al*., 1997). Primarily, the *mcrA* gene (encoding the two α subunits) has been used as a specific methanogenic target gene as developed by the work of Luton *et al*. (2002). The genes which encode the remaining subunits, *mcrB* (β) and *mcrG,* (γ), have also been utilised in molecular detection of methanogens more recently, providing greater insight into methanogenic taxonomy (Dziewit *et al*., 2015).

The *mcr* encoded enzyme complex also requires a nickel containing co-factor, F_{430}, to facilitate the terminal methanogenic energy conserving reaction. Methanogens are thought to accumulate nickel via reductive dissolution of nickelian pyrite [$(NiFe)S_2$)], which has been documented in acid mine drainage, despite not being considered a major chemical form amongst the inorganic pyrite complexes. This mechanism of metal acquisition may allow methanogens to maintain their enzymes under extreme abiotic stress, whereby the leach metals for integration into co-factors (Weber *et al*., 2006; Spietz *et al*., 2023). The structure of the Mcr enzyme complex is shown in **Figure 4.1.**

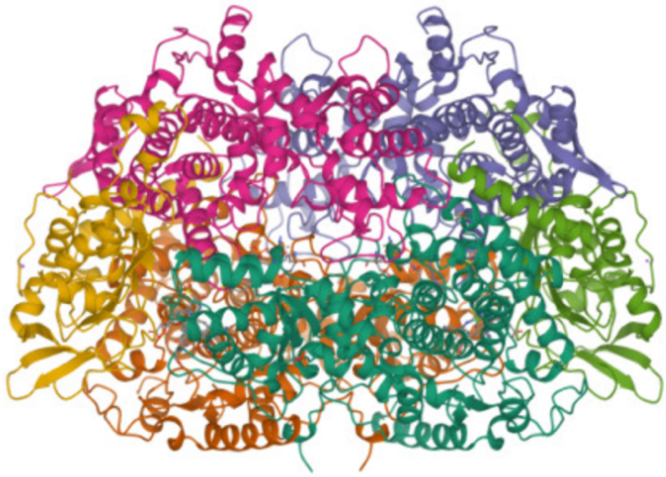

FIGURE 4.1: The secondary structure of the methyl co-enzyme M reductase (Mcr) complex. Each pair of subunits, the α, β, γ dimers, that contribute to the structure of the heterohexamer are shown. Note that this structure was determined from *Methanopyrus kandleri.* Image from Research Collaboratory for Structural Bioinformatics Protein Data Bank [PDB], (2022); deposited by Grabarse *et al.,* (2000). *PBD ID: 1E6V.*

Currently, knowledge regarding the mechanisms underpinning how the enzyme complex assembles remains incomplete, however, the operon structure remains highly conserved across methanogenic taxa (**Figure 4.2**). Most methanogenic members of the Euryarchaeota have a single copy of the *mcrBDCGA* operon (termed 'MCRI'), however some members of the Methanobacteriales possess a truncated second copy ('MCRII'), which likely evolved through a duplication event and a subsequent deletion of the *mcrC* gene. Expression of these alternative isoenzymes may allow metabolic flexibility during environmentally challenging conditions; some thermophilic methanogens, principally *Methanotorris* and closely related taxa, have a further modified operon ('MCRIII') which synthesises structurally modified *mcrG* subunits containing an additional α-helix within the secondary folds of the protein which may provide structural resilience to the enzyme under high temperature conditions (Wagner *et al*., 2017).

.

The assembled Mcr complex can account for approximately 10% of the total proteome of methanogens. High expression levels of the *mcr* operon and intracellular accumulation of the holoenzyme are thought to have evolved to counteract the often-observed low rate of catalysis and energetic constraints involved in biological methane generation (Shima and Thauer, 2005). The enzyme is thought to accumulate close to the cell membrane but is not itself membrane bound.

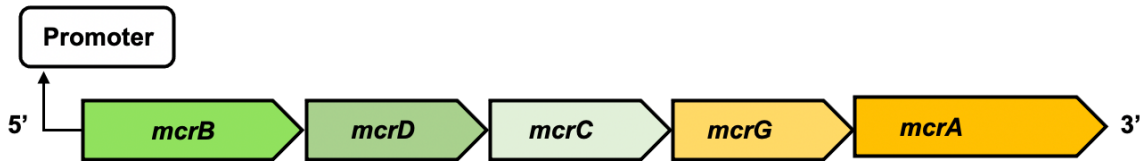

FIGURE 4.2: General structure of the methyl co-enzyme M reductase *mcrBDCGA* (MCRI) archaeal operon. Synthesis of the Mcr protein omplex requires expression of *mcrA, mcrB* and *mcrG* proteins which form a multi-subunit hexamer. Additional proteins produced through expression of *mcrC* and *mcrD* are predicted to facilitate development of optimal secondary structure and functional active sites of the reductase complex. Figure adapted from the operon structure eluded from *Methanococcus maripaludis* as described in the work of Gendron and Allen (2022).

4.2 The Function of Key Methylotrophic Methanogenic Enzymes: *mtaB* and *mtbA*

Methylotrophic methanogens which utilise methanol and additional methylated compounds to produce methane been detected through amplification of specific genes involved in the methylotrophic pathway, upstream of the Mcr complex. Two key genes involved in these processes are the *mtaB* and *mtbA*. Expression of *mtaB* produces methanol-5-hydroxybenzimidazolylcobamide co-methyltransferase which catalyses the reaction of methanol to methyl-CoM, prior to the terminal methanogenic energy conserving reaction. The *mtbA* gene encodes methylated [methylamine-specific corrinoid protein] co-enzyme M methyltransferase, which converts mono-, di- and trimethylamines to methane (Tsola *et al*., 2024).

Both *mtaB* and *mtbA*, can be used as genetic targets, specific to this methanogenic functional group. The methylotrophic methanogens have often been overlooked in their function; however, it has been revealed recently that they have a more prominent role in carbon cycling than previously thought (Sollinger and Urich, 2019), and allowing detection of these specialised enzymes encourages further work to elucidate their taxonomy and ecological preferences.

Once considered biogeographically constricted to sulphate-containing marine sediments, where other methanogenic groups have been excluded, hydrogen-dependent methylotrophic methanogens are now noted to be prominent taxa in a range of environments, whereby they remove excess H_2 via methylotrophic pathways from anoxic microbial ecosystems (Sollinger and Urich, 2019). Many of the methanogenic lineages which have been detected via metagenomic analyses have been noted to carry genes involved in the methylotrophic reactions and may the methanogenic energy strategy most widely utilised in less conventional ecosystems to close the carbon cycle (Wang *et al.,* 2023c). Despite this, the *mtaB* and *mtbA* genes remain poorly characterised; continual attempts to detect methylotrophic genes may be relevant in understanding methanogenic routes which dominate in non Euryarcheotal methanogenic taxa (Kang *et al.,* 2024).

4.3 Methane Oxidation and the Particulate Methane Monooxygenase Complex

The production of methane through methanogenesis can be counteracted through the oxidation of methane by methanotrophic microorganisms. Methanotrophs therefore act as a crucial 'biofilter', preventing the majority of biologically produced methane from being released to the atmosphere and close the methane cycle (Moore *et al.,* 2017; Mayr *et al.,* 2020). The most widely characterised methanotrophs are the aerobic methanotrophic *Bacteria*, however anaerobic methanotrophic *Archaea* (ANME) are also capable of methane oxidation in environments where oxygen has been depleted. Aerobic methanotrophy is found within the Alphaproteobacterial and Gammaproteobacterial classes, candidate phylum NC10 and within the phylum Verrucomicrobia.

Methanotrophic reactions are specialised forms of methylotrophy whereby microbial species capable of utilisation of one-carbon compounds can yield ATP from substrates more reduced than CO_2 (Fenibo *et al.,* 2023). Additionally, some methylotrophs can utilise longer chain compounds and many will only facultatively use methane. Due to their ecological role in methane oxidation in both natural and applied systems, their significance in the carbon cycle cannot be overstated due to their key role in maintenance of the global methane budget (Schmitz *et al.,* 2021; Kallistova *et al.,* 2023). Due to this, molecular detection of methanotrophs can also be used to determine taxonomy and overcome the challenges associated with culturing methanotrophs.

Methanotrophs native to low pH ecosystems have been more widely demonstrated than their methanogenic counterparts. The work of Sharp *et al*. (2014) demonstrated the presence of extremely acidophilic Verrucomicrobia in low pH hot springs (ranging from pH 1.8 – 2.6) and acidic wetlands through targeted analysis of the methanotroph specific enzyme, particulate methane monooxygenase (pMMO). Similarly, the work of Schmitz *et al*. (2021) documented the presence of the obligate methanotroph *Methyloacidiphilium infernorum* in acidic thermal soil, capable of growth at pH 1. This calls into question the ability *M. infernorum* and other methanotrophs endogenous to other low pH locations to achieve substrate acquisition as low pH biological methanogenesis remains poorly documented.

More recently, Karthikeyan *et al*. (2021) demonstrated that aerobic bacterial methanotrophs are tolerant to heavy metals and contribute to redox cycling and detoxification of transition metals, in addition to performing methane oxidation. In this work, the authors described methanotrophic activity in acid mine drainage effluent produced from gold mining activities. Importantly, this acid mine drainage was noted to have elevated concentrations of other metallic co-contaminants (*e.g.,* copper and mercury); thereby establishing that methanotrophic taxa demonstrate polyextremophilic adaptations to their cellular physiology. Due to these recent insights into methanotrophs' ecological dispersal and potential metal utilisation pathways, eluding their taxonomy and metabolic functions within acid mine drainage microbial assemblages is deserving of continual work.

The pMMO enzyme is ubiquitous within all aerobic methanotrophs. It catalyses the initial reaction in methane oxidation, facilitating the hydroxylation of the carbon-hydrogen (C-H) bonds in methane to a carbon-hydroxyl bond (C-OH), producing methanol; CO_2 is produced at the terminal reaction of methanotrophy. The pMMO complex is a ~ 200 kDa alpha-helical polytopic enzyme which requires copper within the active site to achieve catalytic oxidation of the C-H bonds within the molecular structure of methane. The structure of the pMMO complex as elucidated from the Alphaproteobacterial methanotroph, *Methylosinus trichosporiumis*, is shown in **Figure 4.3.**

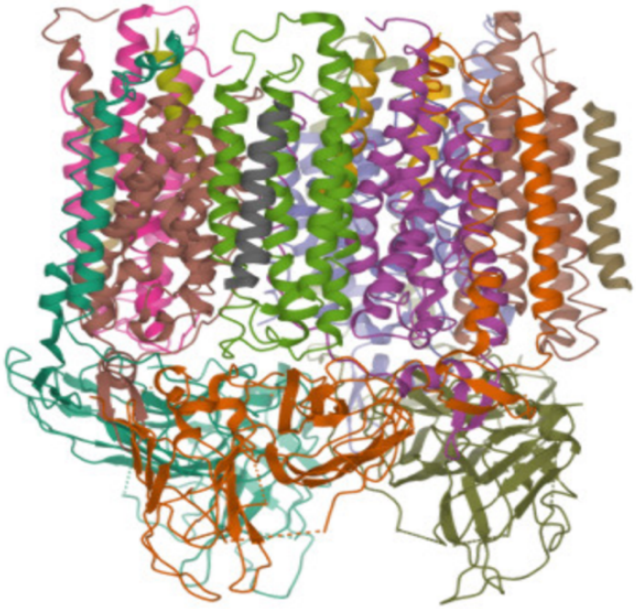

FIGURE 4.3: The secondary structure of the particulate methane monooxygenase (pMMO) complex. The membrane-bound pMMO complex is synthesised as a heterotrimer in an $\alpha_3\beta_3\gamma_3$ arrangement. The enzyme contains three copies of each subunit: *pmoA*, *pmoB* and *pmoC.* Image from the Research Collaboratory for Structural Bioinformatics Protein Data Bank [PDB], (2022); deposited by Hakemian *et al.,* (2008). *PDB ID: 3CHX.*

4.4 Taxonomic Determination of Microeukaryotic Fungi via the Internal Transcribed Spacer Regions

Lastly, the ecological role of fungi as critical members of the carbon degrading community has been well documented in conventional environments (Clemmensen *et al.,* 2013; Pickles *et al.,* 2016). Nevertheless, the fungal contribution to oligotrophic and low pH environments has been less widely studied. The role of fungi in industrial systems such as bioreactors are also received little attention.

Despite this, the work of Mosier *et al*. (2016) determined that fungi have essential roles in carbon cycling in acid mine drainage environments and are of particular importance in biofilm niches where carbon inputs can be low. However literature regarding the fungal component of acid mine drainage remains limited, despite fungi being considered key degraders of pollutants in other ecosystems. Persistent organic pollutants such as benzene (and its derivatives) have been noted to be degraded practically completely by fungal extremozymes, however only recently has this been explored (Chen *et al.,* 2023a).

Acidophilic fungi have been challenging to cultivate, requiring highly modified media and specialised equipment to maintain their growth; *Acidomyces* species isolated from Iron Mountain Mine, California, are currently recognised as the most extreme acidophilic fungi, with growth observed in culture at pH 0.1 (Rosienski *et al.,* 2018). Despite advances in the understanding of the fungal contribution to microbial ecosystem function in more conventional soil and sediment environments, acidophilic fungi still present a gap in current knowledge. To overcome these limitations, fungal taxa can be detected without the requirement for cultivation through amplification of the internal transcribed spacer (ITS) regions within the 18S rRNA eukaryotic polycistronic operon (see **Figure 4.4**).

The ITS regions provide reliable targets for fungal identification and have allowed the development of fungal taxonomic databases that do not rely on the use of cultivated species (Lucking *et al.,* 2021). The shorter intergenic ITS2 region is flanked by the 5.8S and 28S components of the eukaryotic 18S rRNA operon. The operon also contains 5' and 3' external transcribed spacer (ETS) regions. Transcription of the operon occurs through the ETS and ITS regions, however being non-coding, the ETS and ITS regions are spliced out of the mRNA strand. Subsequently, these regions are then degraded during maturation of the RNA transcript.

To this end, the ITS regions are key intergenic targets as they demonstrate less evolutionary constraint and undergo concerted evolution more readily that other genomic regions within the operon. Due to this, these regions can be utilised to assess extremophilic fungal diversity in sites where fungal populations may be pivotal in maintaining ecological function in abiotically harsh niches.

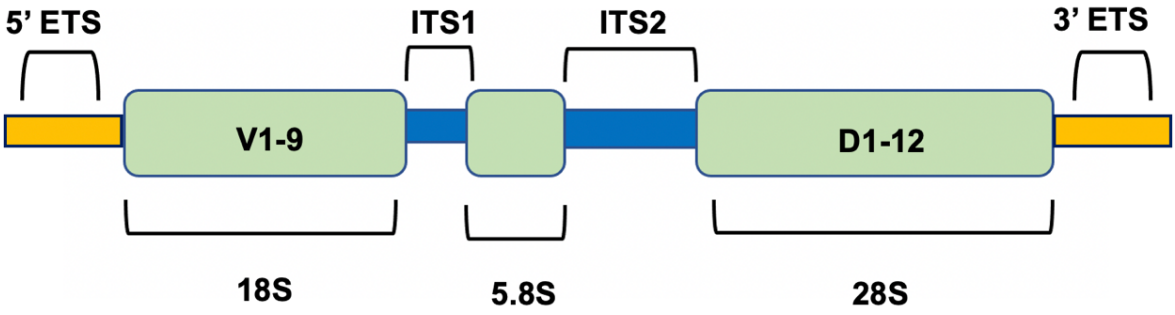

FIGURE 4.4: The structure of the eukaryotic 18S rRNA polycistronic operon. The intergenic ITS1 and ITS2 regions are shown in blue which can be used as markers for the taxonomic identification of fungi. Note that the variable (V) and divergent (D) regions are shown within the larger 18S and 28S operon components. 5' and 3' ETS regions are shown up and downstream of the ITS regions. Figure adapted from D'Andreano *et al.* (2020).

4.5 Aim of Chapter 4

Amplification and cloning of functional genes can aid in the detection of members of specific microbial populations which can be challenging to study via cultivation-based approaches. The overall aim of **Chapter 4** was to utilise the functional genes described above as genetic determinants of specific taxa and their associated metabolic function, and to quantify these target gene abundances across acidic and neutral pH sediments. Digestate collected from a full-scale anaerobic digester was used as additional control sample in this chapter. Specific objectives of this chapter were to:

- Amplify and clone genes involved in methanogenesis (*mcrA*) and methanotrophy (*pmoA*) from DNA samples and determine the taxonomy of the host organisms via phylogenetic analysis of amplicons.
- Assess the ability to utilise the ITS2 region as a taxonomic determinant for extremophilic fungi,
- Determine the relative abundance of functional genes involved in methane cycling (*mcrA* and *pmoA)* and the ITS2 intergenic and normalise these absolute abundances to relative abundance using the V3 region of the 16S rRNA gene quantified from the same sediment samples

4.6 Results

4.6.1 PCR Amplification of the mcrA and pmoA genes, and the ITS2 region

Amplification of the *mcrA* and *pmoA* genes, and the eukaryotic intronic ITS2 region, by end point PCR from DNA samples proved successful. Note that all DNA samples used in end point PCR reactions for methanogen specific genes and the *pmoA* gene were amplified from DNA extracted using the PowerSoil Pro kit only. ITS PCR reactions utilised DNA from both the PowerSoil Pro and the previously available PowerSoil kit. Subsequent qPCR reactions utilised DNA extracted using both extraction kits to allow a comparison between the recovery and quantification of target genes between samples.

The *pmoA* gene was amplified successfully in Loch Bà and Benhar Bing sediments. The ITS2 region amplified from sediment DNA collected from three sites (Benhar Bing, Blackford Pond and the control digestate sample). The key methanogenic target *mcrA* amplified from Benhar Bing, Loch Bà, Blackford Pond and the digestate DNAs. A correct sized amplicon was visualised for the *mtaB* gene from Blackford Pond but following Sanger sequencing did not match to other *mtaB* sequences when searched against the NCBI database. Note that no amplicons for *mcrB, mcrG* or *mtbA* were produced following PCR in any sample. A summary of these results in shown in **Table 4.1**.

TABLE 4.1: Summary of end point PCR results for amplification of *mcrA, mtaB, pmoA* and the ITS2 intergenic region

Sample	Gene			
	mcrA◊	*mtaB*	*pmoA*◊	ITS◊
Benhar Bing	✓	x	x	✓
Blackford Pond	✓*	✓**	✓**	✓
Loch Bà	✓*	x	✓	x
Digestate	✓	x	x	✓

* Successfully amplified but could not be cloned into PCR2.1 vector
** Cloned but erroneous sequence retrieved from Sanger sequencing
◊ Used in subsequent qPCR quantification

4.6.2 qPCR Results

4.6.2.1 mcrA gene copy number relative to 16S rRNA in sediments

As the *mcrA* gene was detected via end point PCR the most successfully across three sediments, this gene was the first to be utilised in qPCR to determine the relative abundance of this functional target relative to the 16S rRNA gene present in each sediment DNA sample. Normalisation of *mcrA* gene to the 16S rRNA gene allowed the relative abundances of *mcrA* to be compared between sediment samples (**Figure 4.5**). Relative abundance was determined by qPCR analysis of the V3 16S rRNA gene from the same representative sample.

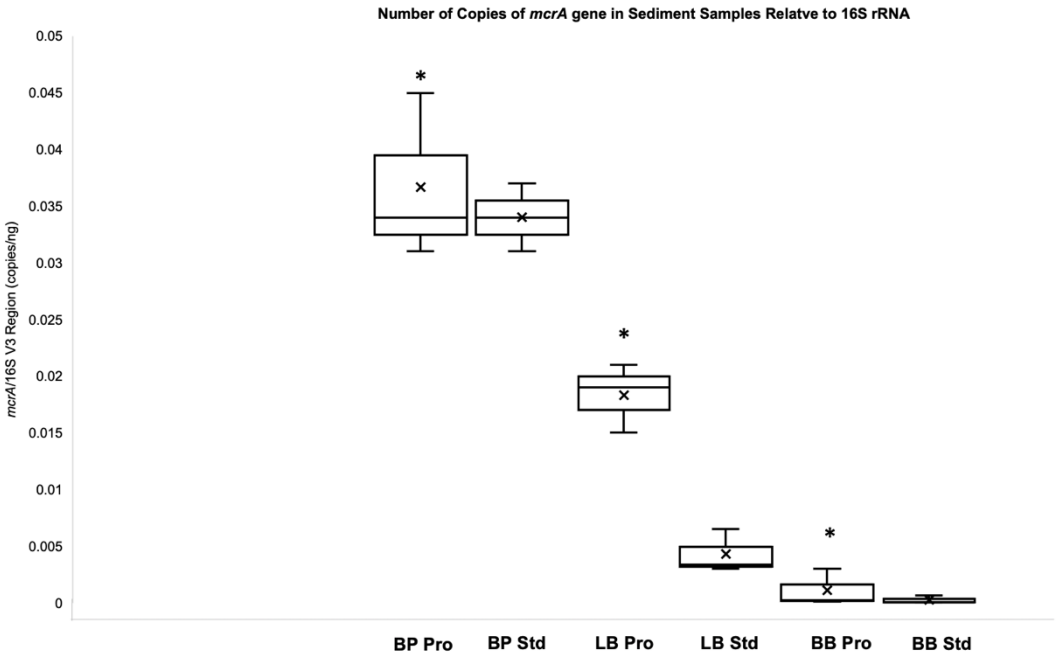

FIGURE 4.5: Gene copy number of *mcrA* normalised to the 16S rRNA gene copy number (V3 region). Box plot demonstrates each biological replicate (*n=3)* with error bar indicating standard deviation. qPCR standard curve for *mcrA* was performed in triplicate using a PCR2.1 vector and cloned *mcrA* sequence amplified from anaerobic digestate. (BP = Blackford Pond; LB = Loch Bà; BB = Benhar Bing; Pro = DNA extracted using QIAGEN PowerSoil Pro DNA extraction protocol; Std = DNA extracted using QIAGEN PowerSoil standard DNA extraction protocol). The box plots demonstrate the interquartile range of values; the mean is marked by X. Whiskers extend to the upper-most and lowest value. Quartiles and interquartile range calculated by performing equivalent linear interpolation of the three replicate values for each site.

qPCR successfully detected the *mcrA* gene in each sediment sample (Benhar Bing, Blackford Pond and Loch Bà) in DNA samples extracted with both the PowerSoil Pro and previous PowerSoil DNA extraction methodologies. The *mcrA* gene demonstrated the highest relative abundance in the Blackford Pond DNA sample extracted with the updated DNA extraction protocol (mean *mcrA*/16S; 'pro' kit = 0.036). The number of copies of *mcrA* relative to 16S rRNA copies decreased in Loch Bà and Benhar Bing. It was apparent that the *mcrA* gene was rarest in Benhar Bing compared to the other sediment communities (mean *mcrA*/16S rRNA; 'Pro' kit = 0.0011).

Overall, the previous DNA extraction kit was poorer at extracting *mcrA* genes from sediment samples than the PowerSoil Pro extraction method across all sediments. Significant differences between the *mcrA* relative abundance were apparent between samples: Blackford Pond and Loch Bà (t-test: p-value = 0.016), Blackford Pond and Benhar Bing (t-test: p-value = 0.0012)

4.6.2.2 pmoA gene copy number relative to 16S rRNA across sediments

qPCR was performed on the *pmoA* gene to determine the number of copies present in each sediment sample relative to copies of the 16S rRNA gene (**Figure 4.6)**. The *pmoA* gene was poorly detected in both the Benhar Bing and Loch Bà DNA extracted using the original DNA extraction protocol. Regarding the DNA samples extracted using the PowerSoil Pro extraction technique, significant differences were observed between the relative abundances of *pmoA* between Blackford Pond and Loch Bà (t test: p-value = 0.0003) and Loch Bà and Benhar Bing (t test: p-value = 0.01)

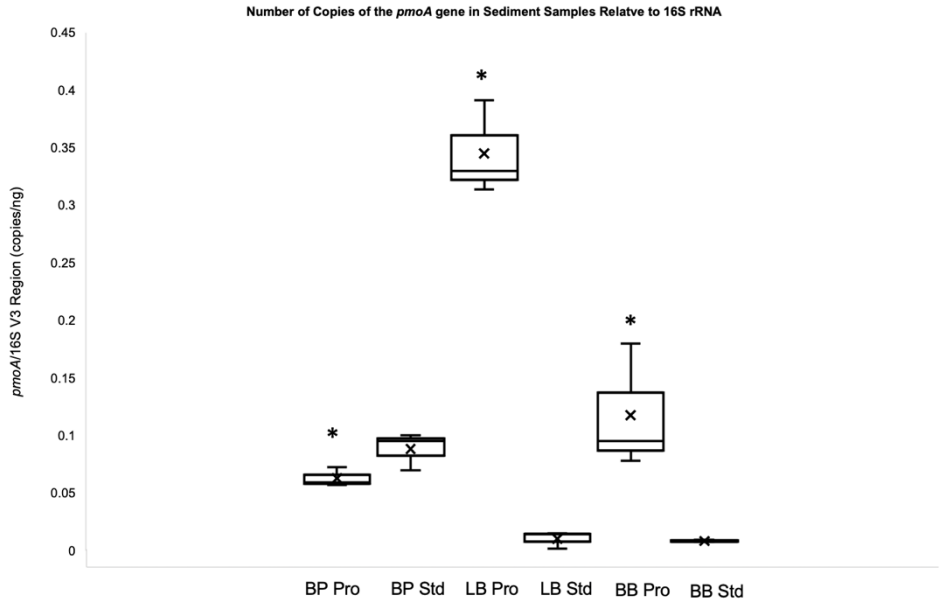

FIGURE 4.6: Copy number of the *pmoA* gene normalised to the 16S rRNA gene copy number (V3 region). Box plot demonstrates each biological replicate (*n=3)* with error bar indicating standard deviation. qPCR standard curve for the *pmoA* region was performed in triplicate using a PCR 2.1 vector and cloned *mcrA* sequence amplified from Benhar Bing. (BP = Blackford Pond; LB = Loch Bà; BB = Benhar Bing; Pro = DNA extracted using QIAGEN PowerSoil Pro DNA extraction protocol; Std = DNA extracted using QIAGEN PowerSoil standard DNA extraction protocol). The box plots demonstrate the interquartile range of values; the mean is marked by X within the interquartile range. Whiskers extend to the upper-most and lowest value. Quartiles and interquartile range calculated by performing equivalent linear interpolation of the three replicate values for each site.

4.6.2.3 *The ITS2 copy number relative to 16S rRNA across sediments*

As was observed for the *mcrA* and *pmoA* genes, qPCR successfully detected the ITS2 intergenic region most effectively when DNA extracted using the PowerSoil Pro extraction kit was used across all sediments (**Figure 4.7**). The ITS2 region was detected poorly using qPCR when the Loch Bà DNA template was used in the reaction was extracted using the original PowerSoil DNA extraction protocol.

Benhar Bing DNA extracted using the PowerSoil Pro approach demonstrated the highest relative abundance of copies of the ITS2 region to 16S rRNA (mean *mcrA*/16S; 'pro' kit = 0.038). There were statistically significant differences between the relative number of copies of the ITS2 region between the Loch Bà DNA sample and Benhar Bing sample (t test: p-value = 0.007) and Loch Bà and Blackford Pond (t test: p-value = 0.01).

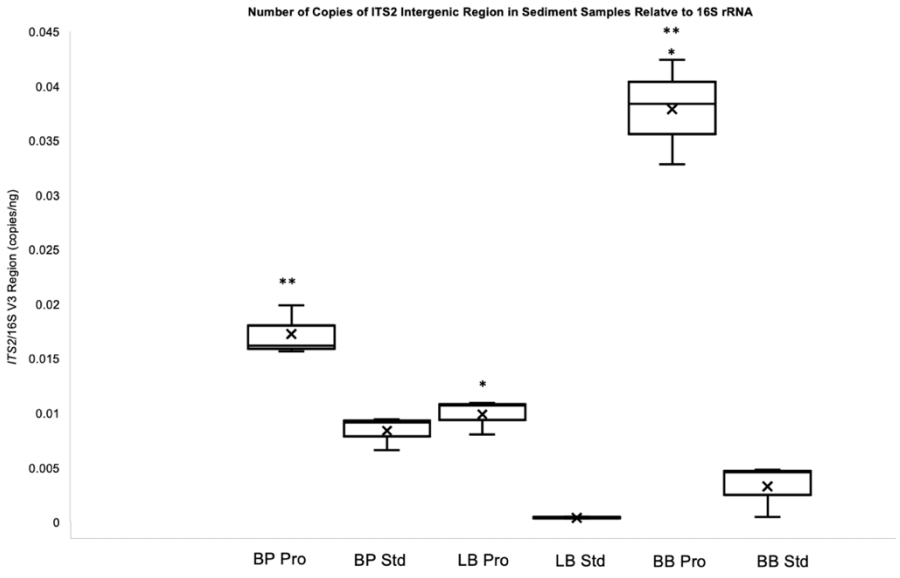

FIGURE 4.7: Copy number of intergenic ITS2 region normalised to the 16S rRNA gene copy number (V3 region). Box plot demonstrates each biological replicate (*n=3)* with error bar indicating standard deviation. qPCR standard curve for the ITS region was performed in triplicate using a PCR2.1 vector and cloned ITS sequence amplified from Benhar Bing. (BP = Blackford Pond; LB = Loch Bà; BB = Benhar Bing; Pro = DNA extracted using QIAGEN PowerSoil Pro DNA extraction protocol; Std = DNA extracted using QIAGEN PowerSoil standard DNA extraction protocol). The box plots demonstrate the interquartile range of values; the mean value is marked by X. Whiskers extend to the upper-most and lowest value. Quartiles and interquartile range calculated by performing equivalent linear interpolation of the three replicate values for each site.

4.6.3 Phylogenetic Analysis of mcrA, pmoA and ITS2 Genes

Following use in qPCR, the plasmids containing the genes of interest (*mcrA, pmoA* and ITS region) were Sanger sequenced (performed at the MRC PPU DNA Sequencing Service, University of Dundee), to assess whether taxonomy of the host organisms could be determined. In total, 12 PCR product sequences appear in the results here across the three genes of interest which demonstrated unique individual sequences.

The predicted organisms which harboured the target genes of interest were determined by closest nucleotide sequence matches on BLAST using either the megablast or blastn options. Phylogenies were then produced following sequence alignment using clustalW; several phylogenies demonstrating the taxonomic relationships were produced. A phylogeny of taxonomy based upon inferred *mcrA* gene sequences is shown in **Figure 4.8**. Similarly, phylogenetic results for the *pmoA* gene sequence are shown in **Figure 4.9** and ITS2 results in **Figure 4.10**.

4.6.3.1 Phylogenetic Results of mcrA Clones and Closest Neighbouring Taxa

The amplification of the *mcrA* gene was successful in Benhar Bing, Blackford Pond, Loch Bà and digestate DNA samples, which acted as control from an applied microbial ecosystem, known to be enriched in methanogens. However, the Blackford Pond amplicons following gel excision would not ligate successfully into the PCR 2.1 vector backbone. Cloning of the Blackford Pond *mcrA* fragment was repeated with a newly produced amplicon to prevent any loss of overhanging nucleotides required for ligation but again, no transformants grew following incubation. Therefore, no Blackford Pond *mcrA* sequences were sequenced. Similarly, the *mcrA* amplification was sporadic in Loch Bà DNA samples, and only produced a faint band following PCR amplification. Ligation of the Loch Bà *mcrA* amplicon following purification was not successful.

Three *mcrA* sequences were from clones harbouring *mcrA* genes amplified from Benhar Bing sediment. Two of these sequences were almost identical, and the third varied in nucleotide composition. However, all three sequences were photogenically similar and clustered based upon sequence homology to the *mcrA* gene retrieved from the genome of *Methanomassillicoccus lumiyensis*.

Several *mcrA* genes were amplified from the anaerobic digestate and were identical to each other. The closest sequence match (98.33%) to these sequences was to the *mcrA* sequence from the methanogen isolate, *Methanosarcina barkeri*. The majority of other *mcrA* gene sequences which shared level of homology to the digestate amplicon were recovered from other uncultivated *Methanosarcina* species (*e.g.*, KU17960.1) from bioreactor environments.

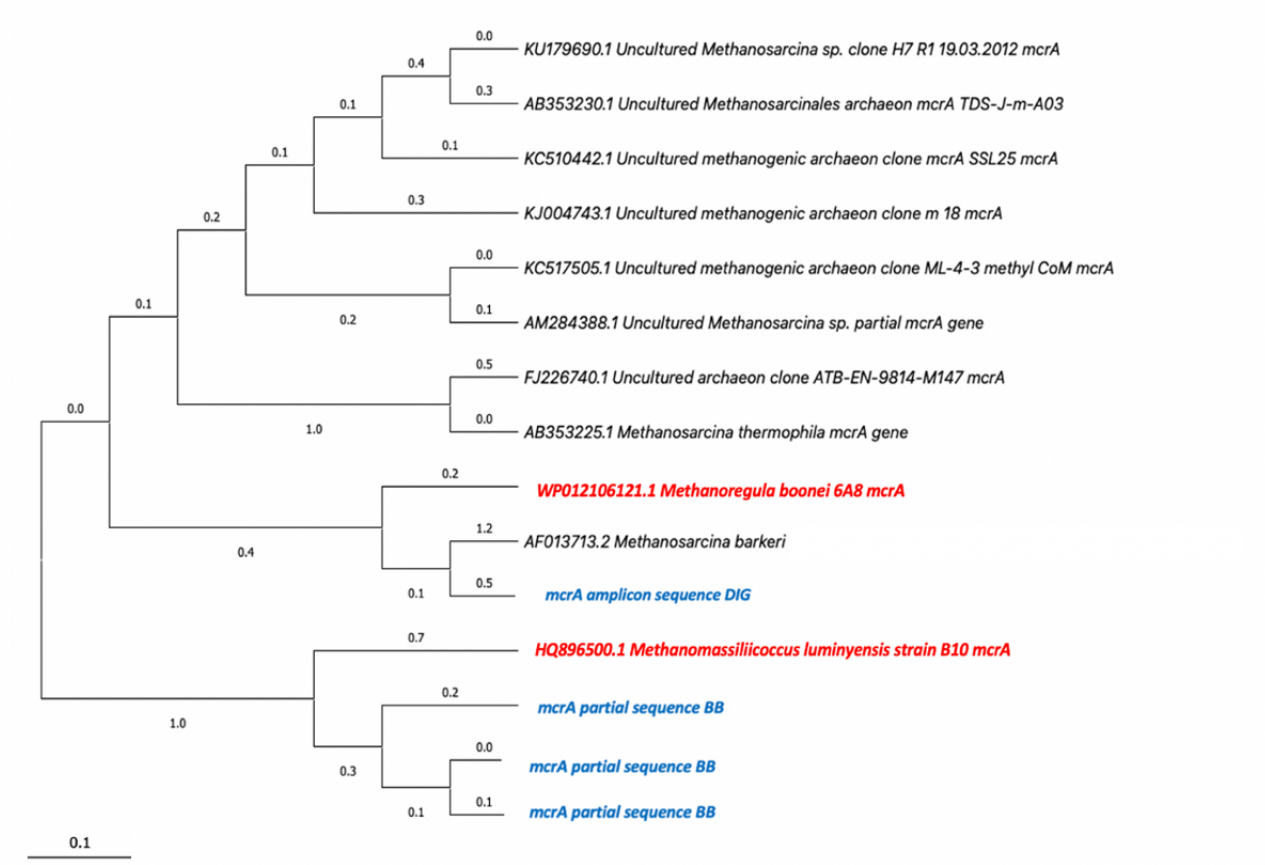

FIGURE 4.8: Evolutionary relationships of methanogens detected using *mcrA* primers (*mcrA*f/*mcrA*r) from environmental DNA samples. Successfully cloned and sequenced *mcrA* amplicons are shown in blue. BB = Benhar Bing; DIG = digestate. The value following the taxon label indicates the clone number sequenced. Where a taxon label is shown in red, *mcrA* sequences were retrieved from previously published data and used to populate the phylogeny. Figure constructed using MEGA (v11.0.10).

4.6.3.2 Phylogenetic Results of pmoA Clones and Closest Neighbouring Taxa

Initial amplification of the *pmoA* gene with the primer set A189F and A650R produced amplicons of the expected size from Loch Bà and Blackford Pond. However, following Sanger sequencing of these amplicons, the gene sequence did not match to known methanotrophic genes and matched poorly to sequences from a range of non-methanotrophic organisms, indicative of erroneous amplification. No amplicons were visualised using the A189F/A650R primer set for Benhar Bing or digestate DNA.

Altering the reverse primer to mb661 allowed amplification of the *pmoA* gene from Benhar Bing and Loch Bà. Three *pmoA* sequences recovered from clones demonstrated sequence similarity to other *pmoA* genes following searching against the NCBI database. Compared to the initial A650R primer, mb661 is a longer oligonucleotide, containing 19 nucleotides compared to 17 bases in the A650 reverse primer sequence. The mb661 primer also contains two degenerate bases in the 6th and 15th positions (a Y and M base, respectively). It is likely that the modified degenerate primer allowed amplification of the target gene more effectively than with the A650R due to the primer degeneracy capturing a greater range of methanotrophic gene diversity.

The A189F/mb661 primer pair did not allow amplification of *pmoA* from Blackford Pond sediment DNA using end point PCR. Multiple attempts to optimise this PCR reaction (including DNA extracted from newly collected sediment) failed and no *pmoA* amplicons from Blackford Pond were successfully recovered.

Two *pmoA* sequences from Benhar Bing clustered together due to the similarities in amplified sequence. The closest nucleotide matches to these sequences were a < 97% match to an uncultivated *Methylocystis* species (KF757085.1). Additionally, the Benhar Bing *pmoA* amplicons shared homology with bacterial clones carrying partial *pmoA* sequences which were not taxonomically resolved (*e.g.,* KC817764.1). Similarly, the *pmoA* sequence recovered from Loch Bà shared 100% of sequence homology with two *pmoA* sequences from uncultured methanotrophic organisms (MG545573.1 and MG545573.2).

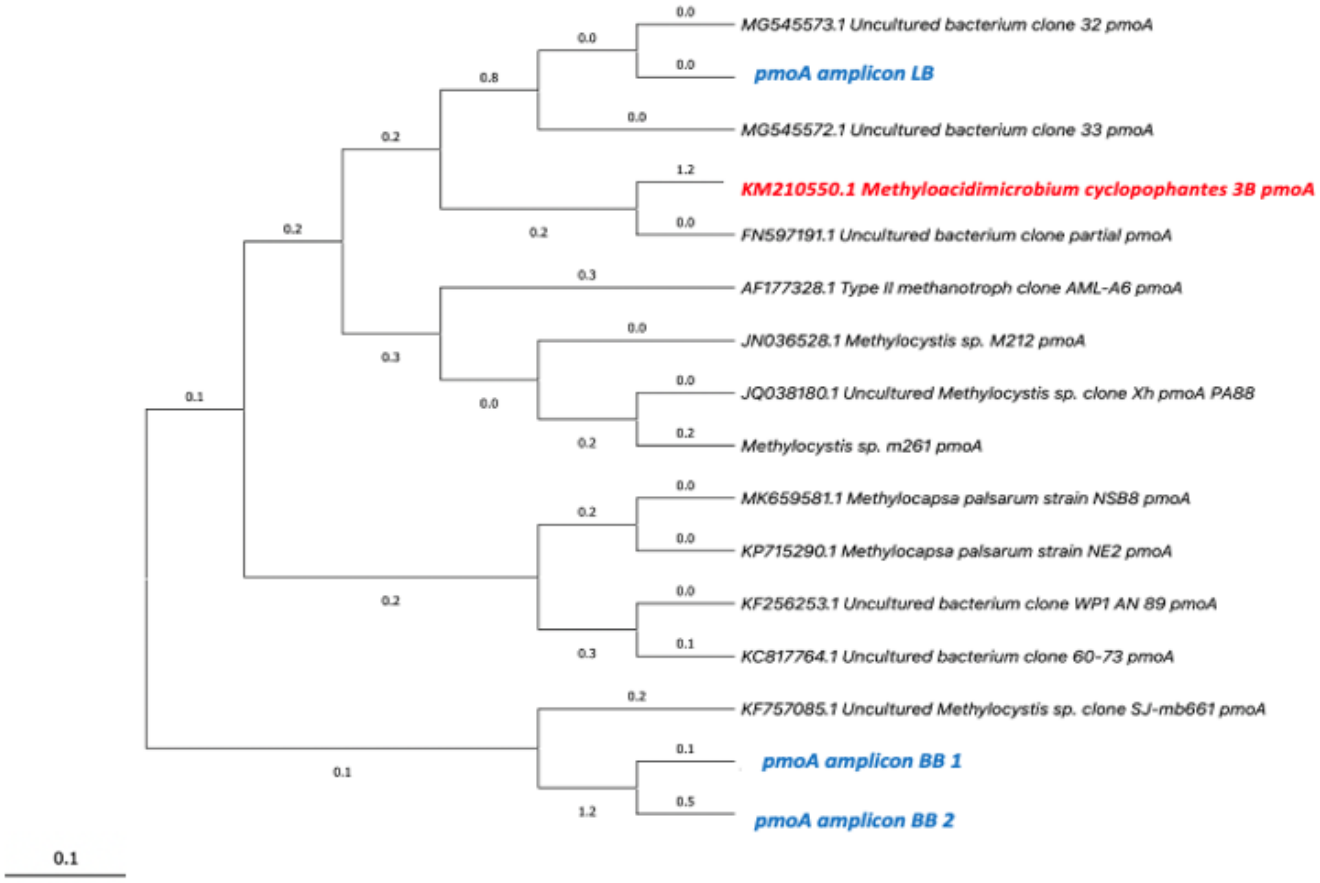

FIGURE 4.9: Evolutionary relationships of methanotrophs detected using *pmoA* primers (A189F/mb661) from environmental DNA samples. Successfully cloned and sequenced *pmoA* amplicons are shown in blue. 'BB' indicates Benhar Bing, 'LB' indicates Loch Bà. The value following the taxon label indicates the clone number sequenced. Where a taxon label is shown in red, *pmoA* sequences were retrieved from previously published data and used to populate the phylogeny. Phylogeny produced using MEGA (v11.0.10).

4.6.3.3 Phylogenetic Results of ITS2 Clones and Closest Neighbouring Taxa

Following Sanger sequencing, five ITS2 amplicons demonstrated shared nucleotide composition to other ITS2 sequences in the NCBI database. Two ITS2 sequences were retrieved from Benhar Bing; one amplicon each was successfully amplified from DNA from both the standard and pro DNA extraction methodologies. When aligned, both ITS2 sequences from Benhar Bing were most similar in their composition to ITS sequences recorded from two taxa, *Acidomyces* and *Acidothrix acidophila*. The remainder of closest nucleotide matches to the Benhar Bing sequences were distinctly related to uncultivated fungal clones harbouring the ITS2 region (*e.g.,* < 97 % similarity matches to HM131983.1 and X826893.1).

Two ITS2 sequences were retrieved and sequenced from Blackford Pond, which were not identical and varied dependant on DNA extraction approach. The ITS2 region amplified from Blackford Pond using DNA extracted from the standard approach shared homology an ITS2 sequence from the digestate DNA, extracted with the newer methodology. The majority of nucleotide matches were between 95-97% similarity to poorly revolved taxa. Yet, in some cases ITS2 sequences had been resolved to genus level as these sequences were recovered from axenic isolates (*e.g.,* the *Ramularia* isolate, MN543974.1).

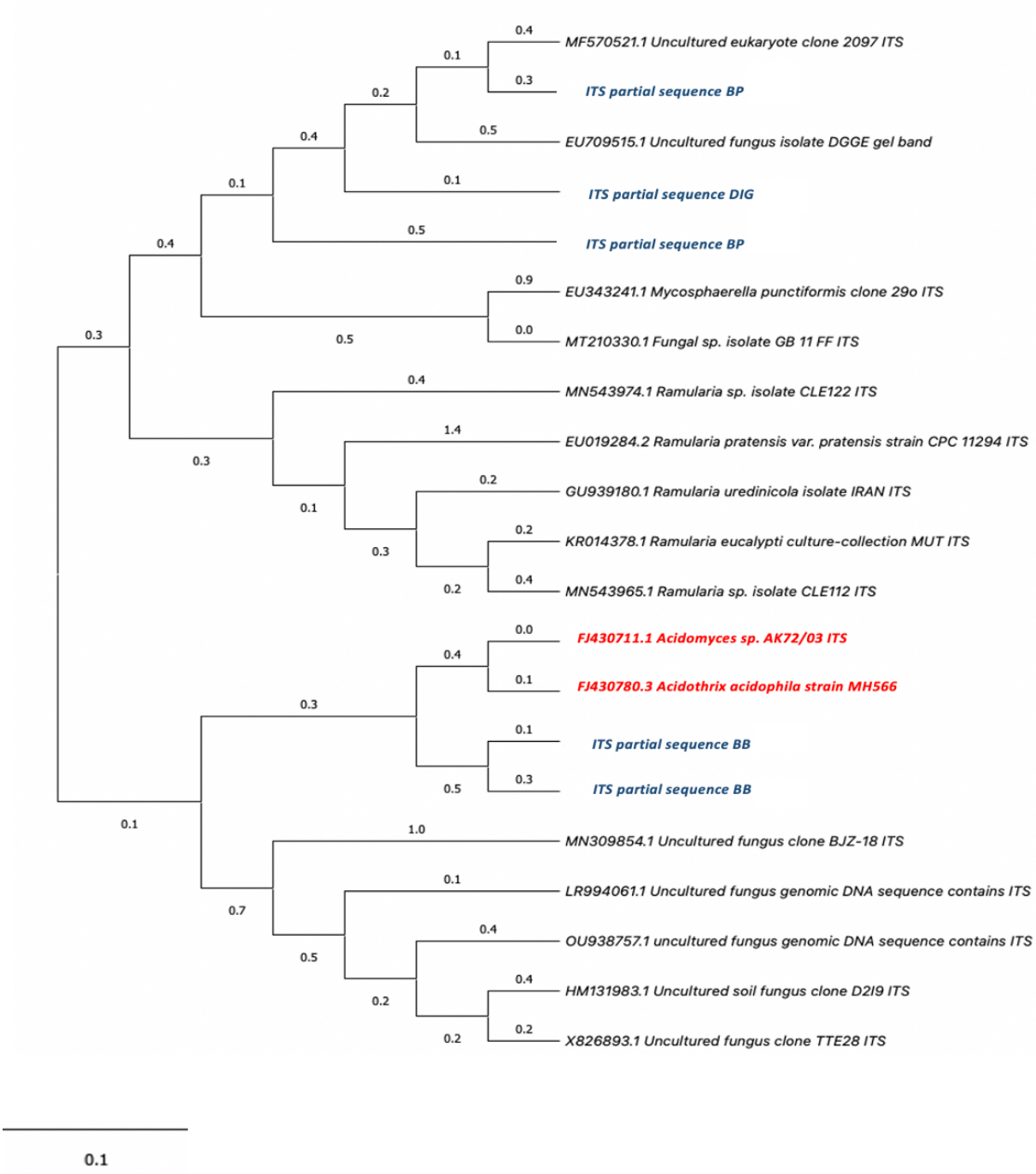

FIGURE 4.10: Evolutionary relationships of fungi detected using ITS primers (ITS3/ITS4) from environmental DNA samples. Successfully cloned and sequenced ITS amplicons are shown in blue. 'BB' indicates Benhar Bing, 'BP' indicates Blackford Pond, 'DIG' indicates digestate. Where a taxon label is shown in red, ITS sequences were retrieved from previously published data and used to populate the phylogeny. Phylogeny produced using MEGA (v11.0.10).

4.7 Discussion

4.7.1 Benhar Bing: Functional Gene Quantification and Taxonomic Identification of Clones

4.7.1.1 Evidence of mcrA Harbouring Taxa in Acid Mine Drainage

The use of qPCR confirmed the presence of the *mcrA* gene in Benhar Bing. However, the *mcrA* gene appears rare compared to the 16S rRNA gene within the Benhar Bing community. Given the low relative abundance of *mcrA* in Benhar Bing, is it likely that methanogenesis is not a widely distributed function amongst most taxa endogenous to acid mine drainage sites; this is reflected in the lack of literature documenting active methanogenesis at extremely low pH values. To date, no other literature has attempted to detect *mcrA* genes in acid mine drainage. The qPCR data supported by the cloned *mcrA* sequence recovered from Benhar Bing are the first to demonstrate taxa which have the metabolic potential to perform methanogenesis under extremely acidic conditions.

Phylogenetic analysis of the *mcrA* sequences from Benhar Bing confirmed the presence of *mcrA* harbouring *Archaea* in the extremely low pH acid mine drainage sediment, allowing insight into the rare methanogenic taxa which may be endogenous to sites contaminated by mining wastes. A single study by Van der Graaf *et al*. (2020) successfully detected 16S rRNA reads pertaining to low abundance methanogens in acidic mine pit sediment (recorded to be pH 2.9). However, the authors provided no details regarding the predicted taxonomy of these reads. Additionally, this work did not utilise the *mcrA* gene to gain further insights into any specific functional attributes of the methanogens present.

A single methanogen species, *Methanocalculus pumilus*, isolated from a waste disposal site, has been documented as exhibiting tolerance to heavy metals, particularly cadmium and copper. However, *M. pumilis* is not considered acidophilic, growing optically at pH 7.5 (Mori *et al*., 2000). Therefore, the *mcrA* sequences presented here amplified from acid mine drainage sediment at Benhar Bing are the first to demonstrate the presence of heavy metal resistant *mcr*-harbouring taxa native to pH 2.5 acidic effluents.

The *mcrA* sequences amplified from Benhar Bing DNA formed a single phylogenetic cluster, and the three amplicons shared between 96-97.7% homology to the *mcrA* sequence pertaining *Methanomassiliicoccus luminyensis*. This *mcrA* sequence was selected to populate the phylogeny and act as a representative sequence of the Methanoplasmatales, which are considered the seventh order of methanogens, known to be metabolically unusual and utilise a truncated form of the methylotrophic methanogenic pathway (Paul *et al.,* 2012). This order is considered phylogenetically distinct from all other methanogens, and contains deep branching lineages, including members of the class Thermoplasmata and the Marine Group II archaeans, which to date, have limited functional and metabolic characterisation (Mesa *et al.,* 2017; Distaso *et al.,* 2020).

The biogeographical dispersal of members of the *Methanomassillicoccus* and related taxa has been previously contested. Initially, *Methanomassillicoccus* were considered host-associated taxa, as the sole isolate of the genus (*Methanomassillicoccus luminyensis*) was recovered from a human faecal sample (Dridi *et al.,* 2012). However, genomes of members of the Methanomassiliicoccaceae family have been reassembled from DNA retrieved from sediments; the chromosomal sequence containing genes indicative of survival strategies required for growth in anoxic environmental conditions (Borrel *et al.,* 2014). These 'free-living' *Methanomassilliococcus* sequences may represent a second clade of these taxa, however, without isolates, this has been challenging to determine fully.

Despite questions remaining regarding the colonisation by *mcr*-containing organisms in low pH niches, evidence of moderately acidophilic *Methanomassillicoccus* species were reported in peat samples, by Chen *et al*. (2023b) expanding on current knowledge of these free-living taxa. Similarly, Nakonieczna *et al*. (2019) observed 16S rRNA amplicon sequence variants (ASVs) pertaining to *Methanomassillicoccus* in sediment samples recovered from a freshwater reservoir located near a previous mined area; yet the sediment was only moderately acidic at pH 5. Both Chen *et al*. (2023b) and Nakonieczna *et al*. (2019) observed these taxa via metataxonomic studies and did not target the *mcrA* gene specifically or attempted to quantify the gene's presence. Again, this stresses the importance of utilising a polyphasic approach to study microbial communities, including the use of specific target genes which are indicative of function.

Moreover, *Methanomassillicoccus* are evolutionarily closely related to members of the order of archaeal extremophiles, the Thermoplasmatales, and together they demonstrate genomic diversification away from all other known methanogens (Cozannet *et al*., 2020; Weil *et al*., 2023). This 'sister lineage' of the Methanomassiliicoccaceae have been implicated in biogeochemical cycling in extremely acidic and contaminated environments and all members are considered strict acidophiles; most Thermoplasmata have been detected via molecular approaches in sites close to pH 2 (Grettenberger and Hamilton., 2021; Sheridan *et al*., 2022).

The close evolutionary positions of the *Methanomassillicoccus* and the Thermoplasmata remains an intriguing unresolved question in the current understanding of methanogens' complex evolutionary history. The ability of members of the Thermoplasmatales to facilitate alkane cycling reactions is poorly understood and methanogenesis within this clade has not been confirmed. However, *Methanomassillicoccus* have been reported to be present within the archaeal community within hypersaline microbial mats, as well as evidence of harbouring variant forms of the *mcrA* gene (Garcia-Maldonado *et al*., 2023). Despite not being a low pH niche, these findings demonstrate the ability of *Methanomassillicoccus* to proliferate under extreme environmental conditions, outside of host-associated microbial assemblages.

4.7.1.2 Evidence of pmoA Harbouring Taxa in Acid Mine Drainage

Interestingly, DNA extracted from Benhar Bing sediment demonstrated a higher relative abundance of the *pmoA*/16S rRNA genes than was observed in Blackford Pond indicating an increased presence of organisms capable of potential methanotrophy under acidic environmental constraints. Encouragingly, methanotrophic isolates have been cultured from acidophilic environments and show physiological adaptations required for growth at low pH (Belova *et al*., 2013). To this end, the successful detection and quantification of *pmoA* in Benhar Bing expands on the literature amount of data regarding the metabolic preferences of members of acidophilic consortia. However, how acidophilic methanotrophs are capable of methane acquisition remains unclear, particularly given the observed rarity of *mcrA* carrying taxa in sediments associated with extensive mining pollution.

Furthermore, the moderately high levels of *pmoA* detected in Benhar Bing were confirmed by the successful end point PCR amplification of *pmoA* from Benhar Bing sediment. It is likely that the methanotrophic organisms detected in Benhar Bing are closely related to *Methylocystis* based upon shared sequence homology. The work of Hakobyan and Liesack (2020) discussed the metabolic potential of methanotrophs and refer to *Methylocystis* species inhabiting oligotrophic systems with low bioavailable carbon. Recently isolated *Methylocystis* species from soil have been noted to be high affinity methanotrophs, being able to oxidise methane at trace atmospheric levels through their specialised adaptations to the methane monooxygenase enzyme complexes (Tikhonova *et al*., 2021). The ability of *Methylocystis* and related taxa to synthesise high affinity methane monooxygenases to promote substrate acquisition in the presence of low concentrations of methane would allow proliferation of methanotrophs in Benhar Bing despite the apparent rarity of *mcrA* to *pmoA* harbouring organisms.

Sequences from *Methylocapsa* species (MK659581.1 and KP715290.1) matched more distantly to the Benhar Bing *pmoA* sequence (at 68.49% similarity), however are key methanotrophs to consider regarding metabolic and wider ecosystem function. *Methylocapsa,* and other uncultivated methanotrophs present in the phylogeny are annotated as 'type II' methanotrophs. Type II methanotrophs (which include *Methylocystis* species) are capable of growth in both acidic and oligotrophic systems and may demonstrate an ecological preference for niches within extreme environments. The detection of *pmoA* via qPCR combined with Sanger sequencing further expand on current understanding of the ecological role of acidophilic methanotrophs and provide valuable insights into key taxa involved in the aerobic closure of the methane cycle in contaminated effluents.

4.7.1.1 Evidence of ITS2 in Acid Mine Drainage

Benhar Bing demonstrated the highest relative abundance of ITS2 copies across all the sediment samples assessed. The high ITS2/16S rRNA relative abundance indicated that fungal species contribute substantially to the microbial community in acid mine drainage. Crucially, this expands on the current knowledge regarding fungal biogeographical distribution and abundance acidic wastes. The fungal component of microbial ecosystems has often been overlooked due to challenges in fungal cultivation, however detection via qPCR proved to be a reliable and valuable approach, particularly given the evidence of high ITS2 copies in the mine-derived acidic leachate. Limited literature exists on acidophilic fungal consortia; however, the work of Bomberg *et al*. (2019) observed fungal taxa in acid mine drainage contaminated rivers in Finland.

However, in this work, recovery of fungal DNA appeared sporadic within different sampling locations, potentially demonstrating niche specialisation within the contaminated effluent. Furthermore, the work of Crognale *et al*. (2017) demonstrated the presence of fungi in the waste stream resulting from a decommissioned gold mine, however only provided absolute abundance values following qPCR, making comparison to other works, such as this, challenging. Additionally, Crognale *et al*. (2017) utilised the 18S rRNA gene as a general eukaryotic target opposed to either of the ITS regions, which are deemed more advantageous, and the universal fungal genetic targets. Specially, the ITS2 region originated as an insertion sequence that interrupted the ancestral 23S rRNA gene and undergoes rapid concerted evolution (Jamy *et al*., 2020). This, alongside the ability to amplify the ITS2 region from heterogenous environmental samples due to its high copy number in rRNA operons, as well as this region's high variability between closely related species, makes this region advantageous as a target for fungal identification over other regions of the 18S rRNA polycistronic operon (Kauserud, 2023).

Despite the limitations of the study by Crognale *et al*. (2017), this work did document that fungal diversity present in gold mine effluent included members of the Ascomycota and Basidomycota; two fungal groups documented in other contaminated sites (Xiao *et al*., 2021). Supporting evidence of fungal diversity in low pH effluents was apparent from the taxonomic positions of the Benhar Bing ITS2 cloned sequences. The ITS2 fragments grouped together based upon sequence similarity and were phylogenetically close to the acidophilic taxa *Acidomyces sp*. and *Acidothrix acidophila*. Together *Acidomyces* and *A. acidophila* are two examples of cultured representatives of fungal species from low pH conditions. These ITS sequences were inserted into the phylogeny from the UNITE ITS database as reflective of ITS regions from acid mine drainage sites and allowed the Benhar Bing ITS fragments to form a phylogenetic cluster.

Going forward, the success of both qPCR and cloning of ITS2 fragments produced via end point PCR could lead to more targeted cultivation strategies to recover extremophilic fungal isolates from Benhar Bing, given the surprising high ITS2/16S rRNA relative abundance. Due to the limitations in cultivating members of acid mine drainage communities, acidophilic fungi and yeasts are poorly represented in culture collections. However, the work of Su *et al*. (2019) successfully determined the prevalence of *Rhodotorula* yeasts from acid mine drainage, which has the capacity to degrade recalcitrant pollutants present in the acidic waste stream, including phenolic compounds. A similar approach could be applied to the Benhar Bing fungal consortia to exploit this now observed fungal diversity.

More recently, the work of Distaso *et al*. (2022) observed that the native community recovered from a previous copper mining site at Parys Mountain, Wales, was dominated by intensive filamentous fungal growth. Strikingly, the presence of Thermoplasmatales was also detected within the same community, highlighting the co-occurrence of extremophilic archaeal and eukaryotic community members. Any syntrophic interactions occurring between fungi and archaeans where not alluded to in this study, however if interspecies metabolic interactions involved in the carbon cycle could persist under multiple abiotic stressors, this may aid in consortia in overcoming nutritional scarcity (Drake *et al*., 2021).

4.7.2 Blackford Pond: Functional Gene Quantification and Taxonomic Identification of Clones

4.7.2.1 Detection of the mcrA Gene in Blackford Pond

The highest relative abundance of *mcrA*/16S rRNA was observed in Blackford Pond, indicating a high proportion of methanogenic taxa in this site compared to both Loch Bà and Benhar Bing. Importantly, the high relative *mcrA* abundance in this copiotrophic site reflects what was been documented in other urban freshwater sites, whereby high levels of organic material result in prolific methanogenesis.

With a renewed focus on methane emissions from freshwater sites given the carbon cycle underpinning global climate, several works have documented *mcrA* abundance in systems analogous to Blackford Pond. The work of Herrero-Otega *et al*. (2019) demonstrated that methane production in a small urban pond became elevated with high-nutrient load and methane flux became unbalanced, with a net release of greenhouse gases. Building on this, Yang *et al*. (2020) utilised qPCR using *mcrA* and documented that the abundance of methanogens shifted as oxygen became depleted in a small lake due to rapid eutrophication, leading to anoxic conditions in which methanogenetic populations proliferated. Again, this work only provided absolute *mcrA* abundances. However, assessing any seasonal shifts in methanogenic populations via *mcrA* qPCR could a future route for further understanding methanogenic function over time in conventionally methanogenic systems and impacts of greenhouse release.

4.7.2.2 Detection of pmoA in Blackford Pond

Initial amplification of *pmoA* from Blackford Pond using the A189F/A650R primers did produce an amplicon of the expected size but did not match to any *pmoA* gene sequences in the NCBI database. Attempts to optimise the pmoA with the alternative mb661 reverse primer were not successful using Blackford Pond DNA as the template. Despite this, qPCR did detect *pmoA* in Blackford Pond. However, the relative abundance of *pmoA*/16S rRNA in Blackford Pond was significantly lower than in Benhar Bing and Loch Bà. Given the lack of *pmoA* end point PCR amplicon and the low detection via qPCR, potentially methanotrophy is not a major energy conserving strategy amongst the Blackford Pond community and that *pmoA* harbouring taxa are rare.

Several studies have demonstrated that despite elevated methanogenesis in sediments with high organic load, often methanotrophic reactions cannot be maintained at the same rate. This dynamic results in a lower abundance of methanotrophs and a net release of methane. To elucidate this fully in Blackford Pond would require more work, with a particular focus on metatranscriptomic analysis of carbon cycling gene expression, however this could be one reason of the observed high *mcrA* relative abundance, but low levels of *pmoA*.

The work of Zhu *et al*. (2020) demonstrated that in artificially warmed freshwater and sediment mesocosms that methanogenesis accelerated leading to changes in the methanogenic community's composition. Despite elevated methane availability, methanotrophic activity did not reflect the behaviour observed in the methanogenic counterparts. As methanotrophy is constrained to a thin oxic-anoxic sediment layer, encroaching anoxia, depletion of H_2 by hydrogenotrophic methanogens, and oversaturation of the active sites of methane monooxygenases by excessive methane have all been proposed as potential reasons for the impairment of *pmoA* carrying taxa in high carbon laden sediments. Furthermore, Nijman *et al*. (2021) demonstrated that increasing rates of methanogenesis (caused by eutrophication) lead to slower growing type II methanotrophs, potentially impacting methane oxidation rates.

4.7.2.2 Detection of ITS2 in Blackford Pond

qPCR analysis detected a moderate abundance of ITS2 in Blackford Pond; higher than was observed in Loch Bà, but not as higher as the elevated ITS2/16S rRNA relative abundance observed in Benhar Bing. As stated previously fungi are generally more poorly characterised than the bacterial members of sediment communities. The work of Tian *et al*. (2018) characterised the fungal community of lake sediments using a next generation sequencing approach and concluded that fungal taxa are dynamic and are significantly impacted by the carbon/nitrogen ratio and the availability of dissolved organic carbon within the sediment environment. This work also concluded that fungal prevalence within high carbon sediments is more heavily influenced by environmental factors than previously thought, particularly at a local scale and in isolated environments, leading to compositional changes in the fungal population more readily than observed for other taxa.

The taxonomic prediction using the ITS2 amplicons from Blackford Pond was limited. amplicons varied in their sequence depending on which extraction kit was utilised. One sequence clustered closely with an uncultivated fungal member of a biofilm community from stream sediment (Hoellein *et al*., 2010). The second ITS2 amplicon from Blackford Pond provided some more detail regarding potential taxonomy, matching to various *Ramularia* (*e.g*., and *Mycosphaerella* species. Both genera are classified within the fungal family Ascomycota and have may have roles in organic matter breakdown in niches with high carbon bioavailability (Challacombe *et al*., 2019). This provides some level of detail regarding similar biogeographical patterns of these organisms' dispersal, and it is encouraging that they have been documented in other carbon-dense sediments. Again, it may be valuable to repeat the ITS2 qPCR on Blackford Pond seasonally given other works have expressed that fungal populations may be prone to abundance fluctuation, impacting their detection via molecular approaches.

4.7.3 Loch Bà: Functional Gene Quantification and Taxonomic Identification of Clones

4.7.3.1 Detection of mcrA in Loch Bà

Despite being an oligotrophic site with little organic matter to drive the carbon cycle to completion, the weak *mcrA* presence detected by end point PCR in Loch Bà DNA was more apparent following quantification with qPCR. How methanogenic conditions are established in freshwater locations were oligotropy dominates in well oxygenated systems is not fully elucidated. Yet, methanogens have been detected in other low carbon systems and are deserving of further work, particularly as freshwater lakes are considered natural sentinels of climate change and may release stored carbon if the carbon cycling consortia becomes disrupted (Wang *et al*., 2021a). The ability of methanogenic organisms to adhere to freshwater particulates may promote the establishment of zones of anaerobic activity, overcoming the apparent methane generation paradox in oxygenated lakes (Bartosiewicz *et al*., 2023).

4.7.3.2 Detection of pmoA in Loch Bà

The high relative abundance of *pmoA* detected in Loch Bà confirms the positive *pmoA* end point PCR result from the same DNA sample, which produced the cloned sequence pertaining to *Methylocystis*. The high abundance of *pmoA* harbouring organisms in Loch Bà may reflect the shallow, well-oxygenated water column which would promote aerobic methanotrophy. Additionally, the qPCR detection of *mcrA* indicates some metabolic potential for methanogenesis present to produce preferred substrate for growth.

The single Loch Bà *pmoA* amplicon supplements the high relative abundance of *pmoA* in Loch Bà, however did not provided well resolved taxonomic information. The sequence formed a phylogenetic branch with *pmoA* sequences from unpublished data from an undefined environmental sample. Despite inferring little ecological or metabolic function from this shared sequence homology, methanotrophy has been demonstrated in oligotrophic environments (Hakobyan and Liesack, 2020). The *pmoA* gene sequence from Loch Bà is distantly related to that retrieved from the genome of *Methyloacidimicrobium*. These taxa have been observed in a range of both extremophilic and more conventional environments, including sediments whereby they may be able to yield energy from H_2 oxidation or other short chain alkanes if methane oxidation cannot proceed (Schmitz, 2001; Awala *et al.,* 2021).

Lastly, it is important to note that given the ecological importance of microbially mediated conversions of one-carbon compounds; with single-carbon molecules integral to several biogeochemical cycles, further investigations into methanotrophy and methylotrophy could focus on alternative target genes. Although not present in all methanotrophs, the soluble form of methane monooxygenase can be detected through amplification of *mmoX* gene (Guggenheim *et al.,* 2019). Organisms which facultatively utilise methane which are also capable of alternative methylotrophic substrates have been successfully identified through utilisation of primers amplifying the large subunit of the *mxaF* complex, encoding methanol dehydrogenase (Wegner *et al.,* 2019).

4.7.3.3 Detection of ITS2 in Loch Bà

ITS2 end point PCR was not successful on Loch Bà DNA samples. Despite this, a low relative abundance of ITS2/16S rRNA was detectable in Loch Bà via qPCR, however this site did demonstrate the lowest relative abundance of the fungal target. Due to the oligotrophic status on Loch Bà, fungal species may not be able to readily colonise within the sediments given the noted sensitivity of fungi to dissolved organic concentrations (Tain *et al*., 2018). Moreover, Khomich *et al*. (2017) did observe fungi via ITS2 clone libraries in oligotrophic lakes in Norway and Sweden. However, the authors did query whether all fungal ITS2 sequences detected were of true aquatic origin, and deemed that fungal species may be transiently present, entering the lakes from terrestrial routes. Additionally, Khomich *et al*. (2017) also suggested that fungal members of freshwater ecosystems may be more closely associated with the surfaces of other aquatic organisms (*ie*., host-associated) rather than localised within the sediment.

4.7.4 Limitations of the Methylotrophic Methanogenesis Marker Genes

Following Sanger sequencing, the *mtaB* amplicon retrieved from Blackford Pond matched to that of no known methylotrophic methanogens when searched against NCBI BLAST database with all stringency parameter options. It is likely that despite being an amplicon of the expected size, the PCR reaction could have produced erroneous sequences through the nucleotide degeneracies present in the primers, allowing no successful matches to highly similar *mtaB* sequences. Therefore, detecting methylotrophic methanogens in Blackford Pond from the presumptive *mtaB* sequence was not feasible. Additionally, following translation of the *mtaB* sequence to infer potential function from the amplicon, no homology or evident shared domains were detected when aligned to the consensus amino acid sequence of the *mtaB* gene from genome of *Methanosarcina barkeri*.

Despite the lack of successful *mtaB* amplicons, the *mtaB* gene was detected in the work of Pyzik *et al*. (2018). The authors found *mtaB* sequences matching to both *Methanosarcina* and the candidate genus *'Methanomethylophilus'* species in lab-scale reactors treating wastewater and agricultural biogas reactor samples. However, in natural sediment samples *mtaB* proved difficult to detect. There is some recent evidence that methylotrophic methanogenesis may dominate in sulphate-rich sediments, such as marine sediments, where alternative methanogenic pathways cannot proliferate due to the dominance of sulphate reducing bacterial species, however this is less well documented in freshwater systems (Tsola *et al*., 2024). Additionally, niche differentiation has been noted to occur strongly with methylotrophic methanogenesis and conversation of methylated compounds to methane may be a predominant energy conserving route in more extreme microbial ecosystems such as hypersaline microbial mats and gas hydrate sites on the seafloor (Katayama *et al*., 2022).

To this end, greater optimisation may be required to ensure specificity to methylotrophic methanogens using this degenerate primer pair or detect methylotrophic methanogenic taxa. One way to achieve this could be to spike biogas reactors with methanol following on from the work of Kim *et al*. (2020) to establish a methanogenic methanol-dependent consortia. Additionally, the work of Saha *et al*. (2015) states that the use of methanol can enhance methanogen resiliency and species interdependency during low to moderate temperature biogas generation. Methanobacteriales mediated proliferation by methanol subsequently promoted activity of members of the Methanosetaceae; this approach could be applied to promote expression of *mtbA* and *mtaB*, and therefore aid amplification of methylotrophic subunits from bioreactor samples in future amplicon-based studies. Despite this, anaerobic digestate proved a reliable control sample for *mcrA* and allowed detection of ITS2 region via end point PCR.

4.8 Conclusion of Chapter 4

The detection and quantification of functional genes from environmental samples by qPCR is a reliable technique which can aid characterisation of key functional groups within microbial populations. Additionally, analysis of functional gene sequences can provide some level of insight into the metabolic roles of taxa when cultivated isolates are not available. To achieve a wider assessment of biodiversity, similar work could be repeated with various alternative primers to successfully recover more and potentially divergent gene sequences. However, targeting of the *mcrA, pmoA* and ITS2 genes has acted as a starting point for further community characterisation in this study.

The results of this chapter present the first documented evidence of the persistence of *mcrA* harbouring taxa native to acidic mine drainage microbial ecosystems, detected by both end point PCR and qPCR. Despite the rarity of the *mcrA* gene compared to the total microbial community, *mcrA* carrying *Archaea* from Benhar Bing likely belong to the metabolically unusual Methanoplasmatales order and evolved within this divergent lineage.

Methane oxidation appears to be more widely distributed within the Loch Bà community. The shallow depths of the loch may promote oxygenation and not restrict the growth of aerobic bacterial methanotrophs, which appear to be less abundant in Blackford Pond. The reduced nature of Blackford Pond's sediment, combined with higher *mcrA* relative abundance may impact aerobic methanotrophy. However, how methanotrophs achieve energy conservation in oligotrophic conditions remains unclear; high affinity methane monooxygenases may favour the proliferation of the observed type II methanotrophs.

Despite the multiple abiotic stressors (high metal content, low bioavailability of organic substrates, and low pH) fungal taxa appear to be able to withstand the synthetically derived chemical constituents of acid mine drainage. Determination of functional attributes of these fungi were not resolved in this study, but this work goes some way in expanding current understanding of fungal dispersal in contaminated systems. The predominant fungal community endogenous to Benhar Bing could be a valuable focus of future work to exploit the enzymatic functions of extreme fungal species.

The success of gene detection by these techniques appears to be dependent on DNA extraction route, and encouragingly the more novel and recently redesigned methodology utilised demonstrated greater recovery of gene sequences linked to carbon cycling organisms. Going forward, a deeper level of functional characterisation of Benhar Bing's community was performed using a metagenomic approach and is reported in the following chapters.

CHAPTER 5 –Determining Taxonomy and Key Ecological Attributes in Benhar Bing's Microbial Community from Unassembled Metagenomic Reads

5.1 The Use of Unassembled Long Read Sequence Data

The development of next generation sequencing (NGS) technology has allowed microbial consortia to be explored to previously unprecedented depths through the analysis of microbial genetic material. DNA based profiling of complex assemblages of microorganisms can follow two major routes: sequencing of specific target genes, or metagenomic sequencing. Sequencing amplicons (PCR products)) can provide a taxonomic and phylogenetic overview of microbial communities via use of the 16S rRNA gene and has been fundamental in allowing exploration of the structure of microbial assemblages (Bech *et al.,* 2024).

The structure of the 16S rRNA gene is shown in **Figure 5.1.** Sequencing of specific functional genes involved in a particular pathway *e.g.,* the *mcrA* subunit of the methyl co-enzyme M reductase complex of methanogens, as outlined in this work, can provide some ability to link function to taxonomy, however this approach is limited. Targeting regions of the prokaryotic 16S rRNA gene are often more advantageous as the gene is highly conserved and the hypervariable regions (V1-V9) present demonstrate considerable sequence diversity between prokaryotic species.

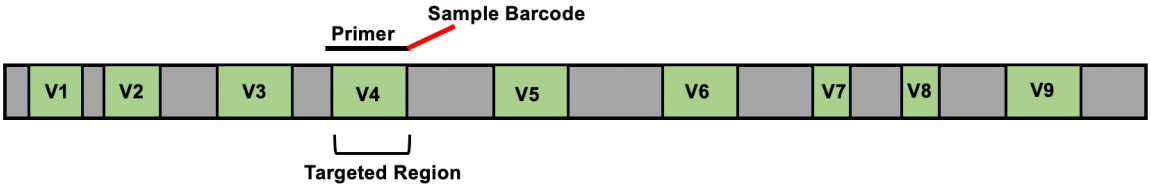

FIGURE 5.1: The structure of the 16S rRNA gene. Conversed regions are shown in grey, hypervariable regions are labelled (V1-V9) and are shown in green. In this example, the V4 region is being targeted by PCR to produce amplicon sequences pertaining to this hypervariable region which facilitates taxonomic identify of microbial community members.

The use of short amplicon sequences limit the amount of genomic information available for downstream analysis, and the use of functional genes can provide variable results particularly if the target gene being investigated is not well studied or has undergone evolutionary divergence. Tools have been developed to link metataxonomic data gained from sequencing of regions of the 16S rRNA gene to proposed function (Douglas *et al.,* 2020). Yet, this can be challenging when utilising short reads, particularly if taxa have few cultivated phylogenetically close relatives. Linking poorly studied organisms to function based purely on taxonomy can lead to ambiguous and unclear metabolic or ecological function (Grossart *et al.,* 2020).

Critically, closely related taxa may not share functional attributes, and the ability to determine function solely based on evolutionary relationships is limited. This is of particular importance in extreme environments whereby the significance of biogeochemical cycling and impacts on climate remains understudied. Variants of genes present in extreme environments may not reflect their canonical function in more conventional ecosystems; *mcr* variants involved in alkane oxidation, rather than methane production, in subsurface systems are example of niche specific functional attributes in poorly resolved taxa (Lynes *et al.,* 2023). This strengthens the argument that larger scale community characterisation of consortia requires chromosomal sequencing, in conjunction with phylogenetic based approaches, which can lead to more reliable prediction of microbial ecological function (Meziti *et al.,* 2021).

In contrast to amplicon-based analysis, metagenomic sequencing can access the genetic material of all community members, without the prior use of gene amplification via PCR. These two techniques when taken together can provide insights into both which taxa are present and indicate metabolic and ecological functions which members of the consortia are capable of facilitating. Sequencing of larger regions of prokaryotic genomes allows access to increased genomic information and therefore, greater sequencing depth.

Metagenomic analysis is a powerful approach to aid in disentangling the structure-function relationships in complex consortia, which cannot be explored solely using target genes, or with single isolates. Again, metagenomic based studies can aid in determining function of key taxa in communities which have eluded cultivation yet maintain pivotal roles in the maintenance of ecologically relevant microbial assemblages (Martínez-Pérez *et al.,* 2022; Ji *et al.,* 2023). Determination of wider environmental function and ecosystem stability arising from the combined metabolic repertoire of microbial consortia remains a key area for exploration in metagenomic studies.

Routinely, metagenomic reads are assembled into metagenome assembled genomes (MAGs); single reconstructed chromosomes of microbial taxa which allow genes and their functions to be attributed to particularly organisms. This will be discussed in greater detail next in **Chapter 6.** Due to the refinement of tools used for assembly of genomes allowing reconstruction of high-quality assemblies, often unassembled data (*ie.,* the genomic information within quality filtered long reads) is not widely reported, with annotation of MAGs favoured. Despite this, attributing function to genes contained within long reads can provide valuable insights into overall metabolic potential and allows retention of information relating the gene abundance.

Often, the assembly of MAGs is biased towards the most abundant organisms present, as larger quantities of available genomic reads from a dominant taxon can facilitate efficient reconstruction of the host species' genome (Jaarsma *et al.* 2023). To this end, not all reads are assembled into chromosomes, resulting in data which otherwise would be excluded from functional analysis. By assessing unassembled reads, a more 'community driven' approach to ecosystem function may be explored, which considers sequences pertaining to rarer taxa, or genomic material that cannot be assembled due to potential fragmentation of sequences, truncated contigs and incomplete assemblies.

Similarly, MAGs are associated with a single taxon, whereas unassembled data can be utilised to elucidate taxonomy of the wider consortia, rather than single organisms; various tools have been developed to allow taxonomic prediction from unassembled metagenomic reads *e.g.,* Kraken and Kaiju (Wood and Salzberg, 2014; Menzel *et al.,* 2016). It is evident that when combined, unassembled long read DNA sequences as well as MAGs may provide a greater insight into microbial community structure and function than when explored in isolation.

Tools to predict taxonomy from unassembled reads are in their infancy and are less well utilised than specialised curated databases based upon the use of the phylogeny of the prokaryotic 16S rRNA gene. Recently, taxa within microbial ecosystems have been documented via unassembled long reads using Kaiju in mock, simplified and complex bacterial communities. The work of Maric *et al.* (2024) explored this by using various microbial communities, with differing complexities. It was found that a higher accuracy of taxonomic prediction was achieved when the communities were composed of well-studied organisms, and reduced performance was noted in complex communities, which contained poorly studied species, impeding taxonomic prediction. Due to this, it remains valuable to confirm taxonomic identity of key species using alternative and complimentary approaches (such as metataxonomic analysis).

Unassembled metagenomic analysis is less widely reported than MAG recovery and subsequent genomic annotation, as analyses involving unassembled long reads can be computationally challenging. However, genes involved in sulphur cycling present in unassembled metagenomic reads were assessed by Yu *et al.* (2020). This work argued that accurate metagenomic functional annotation of sulphur cycling genes remains underexplored, even in more conventional microbial ecosystems. Yet, the authors did demonstrate sulphur reduction pathways in marine sediment, and sulphur oxidation routes prevalent in soil.

Similarly, detection of genes involved in the cobalamin pathway were detected by Zhou *et al.* (2021) in both data retrieved from the TARA Global Oceans Initiative and the Human Microbiome Project. In both cases, the authors utilised tailored databases for their specific gene families of interest. Yet, in most cases, dedicated databases have been slow to emerge and are often applied to reduced-size datasets; this use of tailored databases also can lead to oversight in other pathways which may be key to explore which lack specialised curation. However, several other databases are also routinely utilised to provided broader and comprehensive metabolic coverage contained within large scale sequence data, *e.g.,* the metagenomes function in KAAS and eggNOG are routinely applied to unassembled metagenomic data (Jensen *et al.,* 2007; Moriya *et al.,* 2007).

Regarding contaminated systems, Ross *et al.* (2022) explored the presence of genes involved in hydrocarbon degradation in the effluent produced from coalbed excavation. Likewise, Liu *et al.* (2023) assessed the presence of genes involved in antimony resistance and phosphorus cycling in soils contaminated by metallic pollution; both works subsequently assembled MAGs pertaining to key taxa involved. There is no evidence in the literature of assessing microbial metabolic function in acid mine drainage effluent through unassembled long read data. Specific databases consisting of heavy metal resistance pathways are also lacking which has left gaps in current knowledge regarding the cycling and potential wider impacts of microbial detoxification of metals.

A single database, FeGenie, has been developed and employed to predict genes involved in iron-based metabolism; however, this can only be applied to genomes from cultivated isolates or unbinned contigs and cannot be applied to unassembled long DNA reads (Garber *et al.,* 2020). Additionally, the genes within the database are heavily weighted towards those involved in siderophore synthesis, which limits its use in systems such as acid mine drainage where iron is in excess and siderophore use may be of limited use. Again, this is indicative of both the limited use of unassembled data and the lack of studies attempting to develop routes to characterise the wider consortia native to highly polluted systems. Despite this, unassembled reads have the potential to harbour counteracting metabolic pathways to both enhance pollutant mobility and promote amelioration.

5.2 Aim of Chapter 5

The primary aim of this chapter was to both resolve the taxonomy and gain an overview of genomic functional potential contained within unassembled long-read sequences retrieved from Benhar Bing. To understand Benhar Bing's extreme characteristics, comparative analyses to samples from a more conventional system was performed (two forms of anaerobic digestate: active and caked [dewatered]). Additional objectives were:

- Assess the **success of long read sequencing** using Oxford Nanopore Technology of metagenomic sequencing on DNA extracted from Benhar Bing's polyextremophilic microbial consortia
- **Predict taxonomy** from unassembled Nanopore sequenced DNA from Benhar Bing, and compare this to the metataxonomic community structure determined by 16S rRNA genes with Illumina sequencing
- Resolve the **most abundant genes present** in the metagenomes of Benhar Bing and compare to anaerobic digestates
- Explore key functions within the unassembled metagenomic data with particular focus on broad function: genes involved in **carbohydrate metabolism and energy conservation**
- Determine genes involved in functions known to be prolific in acid mine drainage: utilisation of sulphide compounds (and **wider sulphur cycling**) and genes involved in **metal tolerance**

5.3 Results

5.3.1 Summary of Oxford Nanopore Sequencing Run on Benhar Bing DNA

Oxford Nanopore Technology was successfully employed to sequence a pooled and purified DNA sample from acid mine drainage collected from Benhar Bing's constructed wetland. Nanopore sequencing run was performed using a flow cell (version 9 chemistry) and associated minKNOW software. A summary of sequencing output statistics is shown in **Table 5.1.**

Table 5.1 Summary of data produced from a minION flow cell sequencing metagenomic sample from Benhar Bing

Nanopore Output	Value
Estimated bases	7.76 Gb
Data produced	74.36 GB
Number of reads generated	1.93 M
Number of reads after filtering	1.64 M
Estimated N50	7.42 kb

Following base calling of reads using Guppy, and size filtering (to remove reads shorter than 1000 bp) gene annotation of unassembled reads was performed via the KAAS Server on the Benhar Bing sequence data, which allowed KEGG Orthology (KO) values to be attributed to reads. KOs were then converted to genes names with defined enzyme classifications (EC) using the KEGG database (reconstruct option).

Following allocation of gene function to reads, annotated genes were then ranked manually based on number of copies present. This was repeated for previously sequenced 'active' digestate and 'caked' digestate. Both samples were selected as representative microbial ecosystems to contrast with Benhar Bing. The digestates were collected from full-scale anaerobic digesters at Seafield Wastewater Treatment Plant, Edinburgh. The active digestate was sampled from a full-scale reactor treating previously produced sludge to generate biogas. The caked sample is a dewatered form of the active digestate, which is stored in aerobic conditions. Digestate communities are designed to promote anoxic carbon degradation and methanogenesis and contain high levels of organic carbon and digestate is chemically dissimilar to acid mine drainage sediment.

Note that these samples were sequenced using Oxford Nanopore Technology outside of this study and the filtered fasta sequences made available for a comparison to Benhar Bing's functional potential as representative metagenomes of microbial ecosystems involved in organic matter decomposition. Number of filtered reads for active digestate = 183,800; number of filtered reads for caked digestate = 60,800). The total number of reads from each unassembled metagenome which were annotated by KAAS are presented in **Table 5.2.**

Table 5.2: Summary of gene annotation from unassembled metagenomes. KAAS was utilised to predict genes within unassembled and quality filter Nanopore generated reads. Genes predicted using the single best hit (SBH) approach with default parameters for metagenomic sequences.

Unassembled Metagenomic Sample	Number of Total Reads (After Quality Filtering)	% Reads with Attributed Function
Benhar Bing	1.64 M	40.18%
Active Digestate	183,800	55.50%
Caked Digestate	60,800	63.44%

5.3.2 Determination of the Most Abundant Genes in Three Unassembled Metagenomes

The top 20 genes observed in Benhar Bing and both digestates were ranked and allocated additional information regarding the genes' wider functional role in cellular metabolism (*e.g.,* DNA replication and repair). The relative abundance of the top 20 genes across three unassembled metagenomes are presented in **Figure 5.2.**

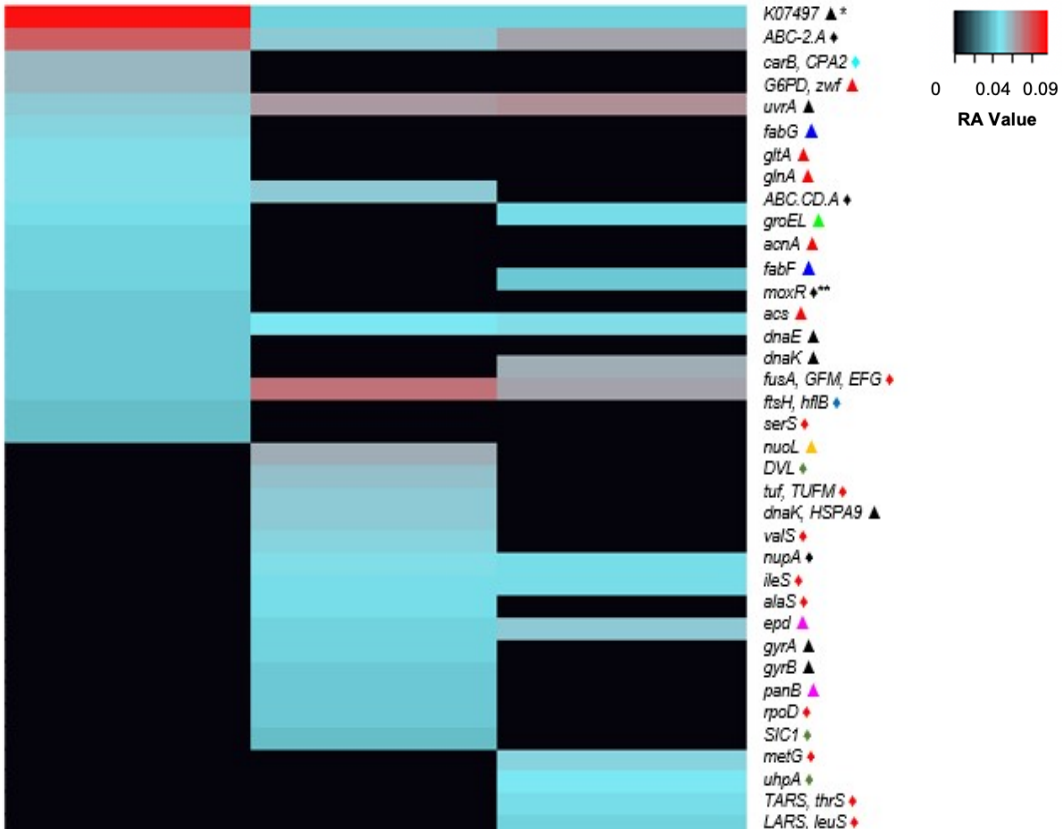

Key for mapping gene to KEGG functional category: DNA Replication and Repair (▲); Protein Function: Signalling and Transporters (♦); Nucleotide Metabolism (♦); Carbohydrate Metabolism (▲); Lipid Metabolism (▲); Protein Function: Folding and Degradation (▲); Transcription and Translation Factors (♦); Protein Function: Cell Division Catalysis (♦); Energy Metabolism: Oxidative Phosphorylation (▲); Environmental Processing: Signal Transduction (♦); Cofactor Metabolism (▲).

FIGURE 5.2: The most abundant 20 genes observed across three unassembled metagenomes KO assignment was performed via KAAS and gene prediction followed using KEGG Mapper. Note: some gene functional categories have been collapsed into a single group, *e.g.,* carbohydrate metabolism contains genes involved in various carbohydrate derived pathways. Genes with (*) = putative function; genes with (**) = limited characterisation available. The % above columns indicates the % of the total annotated reads which were allocated to the top 20 genes within each sample. Note that the black bars indicate the gene is not present in the top 20 genes, not that the gene is absent in the entire dataset.

Across the top twenty genes in the unassembled metagenomes, five genes were shared across all the samples; three of which represent genes involved in DNA replication and repair of the chromosome. A gene encoding a putative transposase enzyme (*K07947*) was identified in all samples, with this being the gene with the highest abundance in Benhar Bing. Additionally, both *dnaE* and *uvrA* were prevalent across all metagenomes.

Similarly, *ftsH/hlfB* and *ABC-2A,* a protease involved in cell division and a cell membrane transport protein, respectively, were also present across each environmental metagenome. The digestates shared five of the most abundant genes, however differed in their most abundant gene. The *ftsH* was the most abundant in active digestate, while *uvrA* was the most numerous in caked digestate. The caked and active digestates shared *ileS*, *alaS* and *gyrA*, genes not observed in Benhar Bing's most abundant genes. Benhar Bing contained *moxR;* unseen in the most abundant digestate genes, and as well as *fabG* and *fabF*.

5.3.3 Determining the Taxonomic Composition of the Microbial Community at Benhar Bing

5.3.3.1 Taxonomic Prediction of Dominant Community Members Using Nanopore Generated Long Reads with Kaiju

Taxonomic prediction of unassembled reads was successfully performed using the taxonomic prediction tool Kaiju. Kaiju performed taxonomic analysis on unassembled filtered metagenomic reads from Benhar Bing using exact matches at protein level via the Burrows-Wheeler transform algorithm against the NCBI non redundant protein database, which allows alignments to be performed between unassembled metagenomic reads and protein sequences within the NCBI database. The top genera predicted to be present within the Benhar Bing community are shown in **Figure 5.3.**

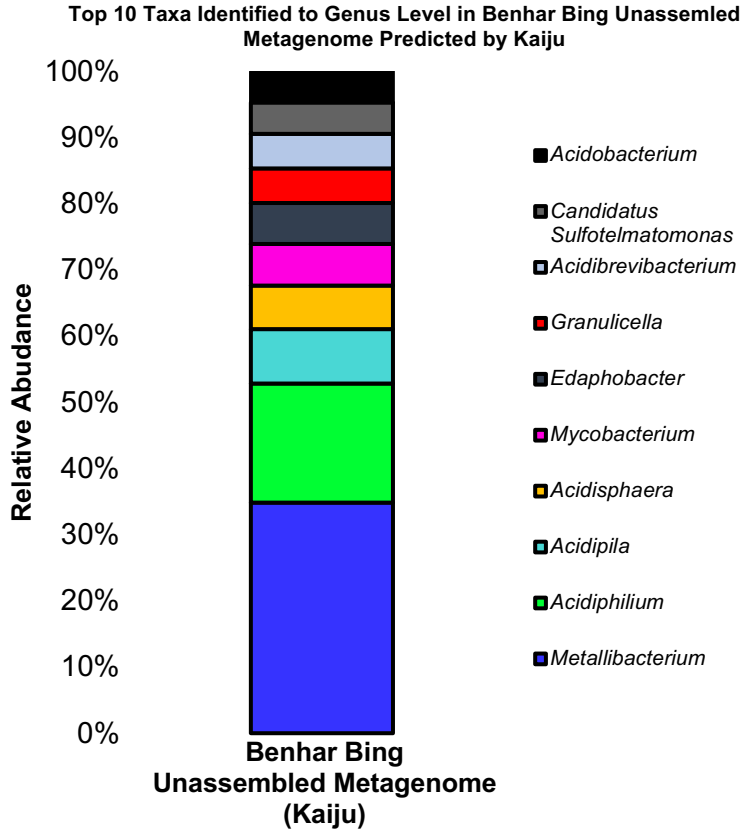

FIGURE 5.3: Top ten taxa identified to genus level using Kaiju from unassembled metagenomic reads sequences from acid mine drainage sediment at Benhar Bing. The relative abundance of each taxon was determined relative to the other top genera identified. This represents 22.3% of total reads, with the remainder of reads not classified to genus level. (Note: Kaiju version 1.9.2 was utilised using the NCBI non redundant protein database as the reference database for sequence matching via web server tool).

The most abundant genus predicted from the unassembled reads using Kaiju was determined to be *Metallibacterium* (34.83% of the most abundant reads predicted at genus level). Following this, *Acidiphilum* (17.98%) was predicted to be the next most abundant organism present. The remaining taxa all contributed > 10% of the total reads within the top ten taxa presented. Other organisms which were detected using exact protein matches via the Kaiju classifier were *Mycobacterium* (6.22%), *Acidobacterium* (4.60%), *Acidipila* (8.10%) and *Acidisphaera* (6.44%). Note that one candidate genus, *Sulfotelmatomonas* was detected within the unassembled reads (4.7%). Note that *Sulfotelmatomonas* was first proposed as a candidate phylum within the Acidobacteriota by Hausmann *et al*. (2018).

5.3.3.1 Taxonomic Prediction of Dominant Community Members Using 16S rRNA V4 Illumina Sequencing

To confirm the taxonomic composition of the acid mine drainage microbial community native to Benhar Bing sediment, metataxonomic analysis was performed targeting the hypervariable V4 region of the 16S rRNA gene. This approach revealed a greater degree of taxonomic resolution of members of the acidophilic consortium. Results showing the community structure at both phylum and genus level are shown in **Figure 5.4.**

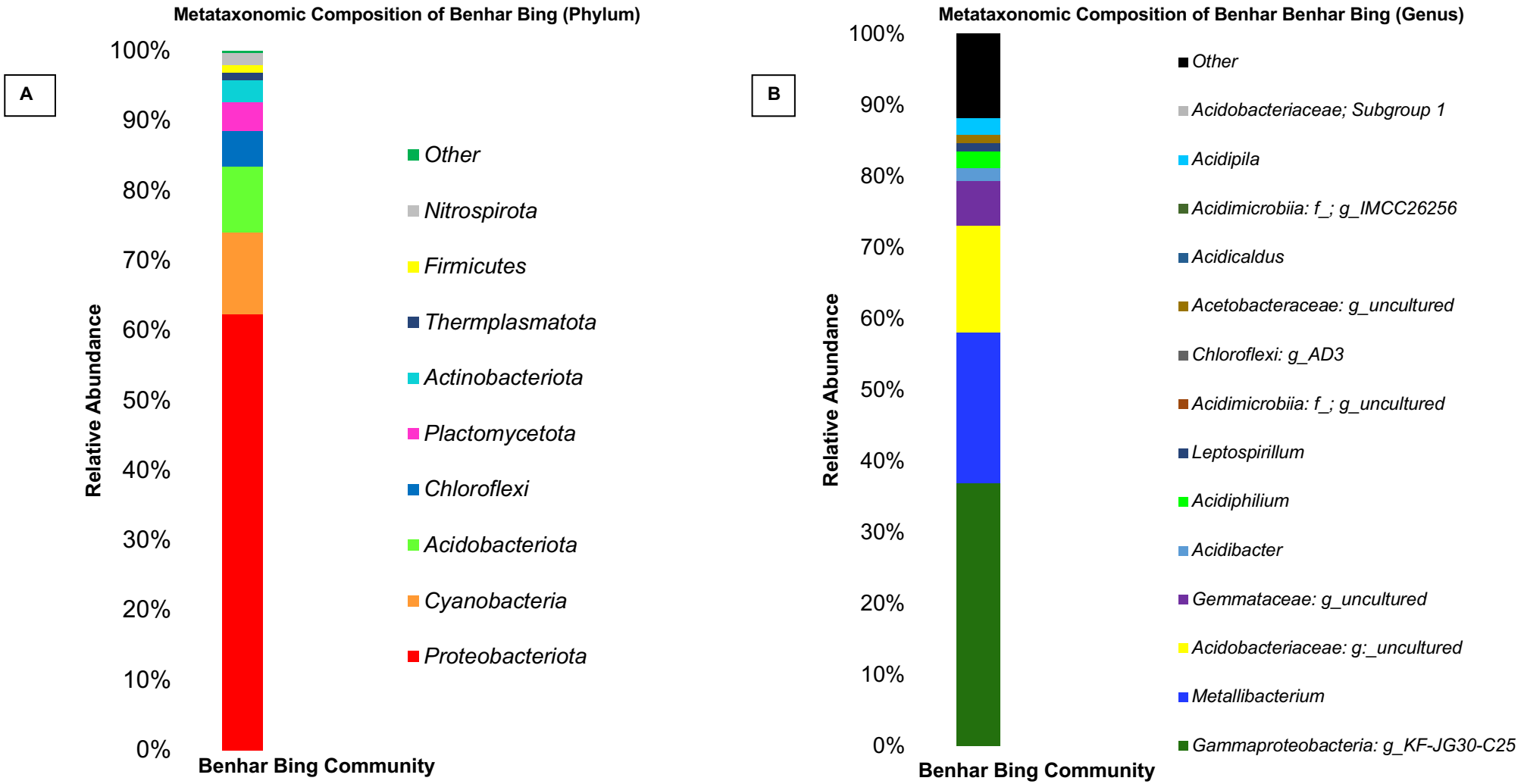

FIGURE 5.4: Taxonomic composition of the Benhar Bing microbial community at phylum (A) and genus (B) level. Taxonomic prediction of the V4 16S rRNA 250 bp reads was performed using the SILVA 138 database. Illumina reads were matched at 100% to representative sequences in SILVA 138 database as amplicon sequence variants.

Eight dominant phyla were detected within the Benhar Bing community. Proteobacteriota (synonymous with Pseudomonadota) was the most abundant phylum present in Benhar Bing, with 62.38% of the community composition being attributed to this taxonomic group. Following this, Cyanobacteria and Acidobacteriota were moderately abundant, with 11.67 and 9.5% of the relative abundance of the total community at phylum level. One archaeal phylum, Thermoplasmatota was detected in the Benhar Bing sediment, however this phylum was rare, with just over 1% of the community affiliated with this group of extremophilic archaeans.

Analysis of the 16S rRNA gene demonstrated nine organisms which contribute community at genus level, many of which are noted to be uncultivated. The most abundant community member at genus level was predicted to be a poorly characterised Gammaproteobacterial species allocated as 'KF-JG30-C25'. Following this, *Metallibacterium* was observed with a high relative abundance (21.12% of the total community at genus level). Additionally, uncultured Acidobacteriaceae and Gemmataceae species were moderately abundant. Organisms which were more taxonomically resolved included *Acidiphilium, Acidibacter, Leptospirillium, Acidicaldus* and *Acidipila*.

5.3.5 Detecting Ecologically Relevant Genes in Unassembled Metagenomes

The relative abundance of genes involved involving carbohydrate metabolism and energy conserving pathways were manually selected and explored to assess whether Benhar Bing demonstrated differences from more conventional systems when these functions were considered. However, the relative abundance of carbohydrate metabolism genes selected was generally consistent across each of the three samples. The relative abundance of genes predicted to be involved in energy generation also not did reflect Benhar Bing's unusual abiotic conditions. Due to this, more specific functions known to be representative of acidophilic conditions were considered to. As acid mine drainage sites are known to be high in sulphates (derived from dissolution of FeS_2) and metallic pollutants, genes involved in sulphur metabolism and metal transport were selected as the two functional groups of genes to assess further.

5.3.5.1 Detection of Sulphur Cycling Genes

Genes determined by KASS in be involved in sulphur cycling reactions were manually selected from gene outputs and their respective gene counts converted to relative abundance for Benhar Bing and the active and caked digestate sample. In the Benhar Bing unassembled data, 18 genes involved in reactions of sulphur-containing compounds were detected. In active and caked digestate 17 and 31 genes involved in sulphur cycling reactions were detected, respectively. Sulphur cycling genes across each of the three unassembled datasets are shown in **Figure 5.5**.

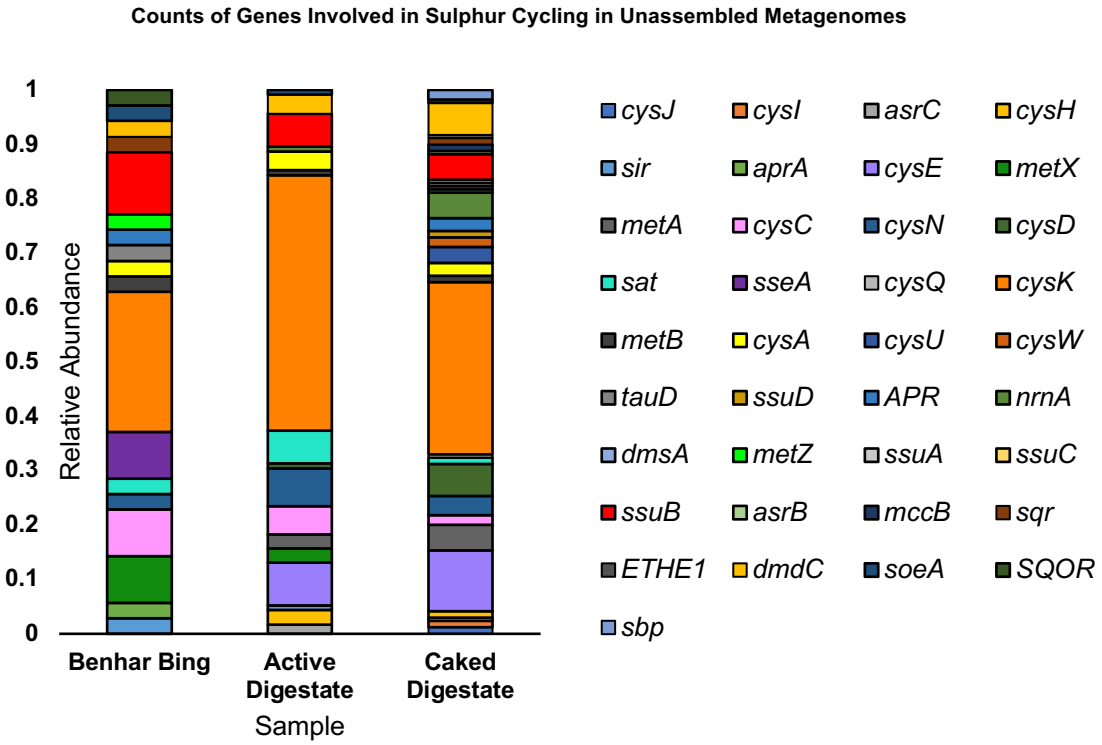

FIGURE 5.5: Counts of gene homologs extracted from individual unassembled metagenomes involved in sulphur cycling present in unassembled metagenomic data. Genes were selected from KEGG prediction and gene counts across each sample converted to relative abundance. Note the relative abundance is based upon total number of sulphur cycling genes observed within each sample (Benhar Bing: n = 18; Active Digestate = 17; Caked Digestate = 32).

Differential counts became more evident between Benhar Bing and the digestate samples when sulphur cycling genes were examined compared to when assessing the most abundant genes across the three datasets. Cysteine synthase, encoded by *cysK*, was the most abundant gene in each of the samples involved in sulphur-mediated reactions. Benhar Bing had a higher relative abundance of the *ssuB* gene (11.42%), involved in sulphonate transport and utilisation, compared to the two digestates, and a sulphur-transferase, coded by *sseA*, which was not observed in either digestate metagenome.

Additionally, *SQOR* and *aprA* were present in Benhar Bing and not present in the digestates. The two digestate samples were generally reflective of each other, however the caked digestate did contain several genes with low relative abundance not predicted to be present in either Benhar Bing or the active digestate (*e.g., cysW* and *sbp)*.

5.3.5.2 Genes Involved in Metal Transport

Differences between the three metagenomes were more pronounced when genes involved in metal transport and detoxification were explored (**Figure 5.6).** In Benhar Bing, 24 genes related to metal transport were detected. More metal transport genes were observed in the active digestate (40) and caked digestate (39), likely due to the paucity of annotated genes within the unassembled Benhar Bing reads. The most abundant genes involved in metal transport and tolerance in Benhar Bing observed were: *arsB, ddpF and ddpD*. The *ddpD* gene was the most abundant gene present in the active digestate sample yet was not observed in the caked digestate sample. The *arsB* gene was the most abundant gene in Benhar Bing; the gene is rare in active digestate, while abundance increased slightly again in the caked sample.

The genes *cusC/silC* and *cusA/silA* were moderately abundant in Benhar Bing but not present in the bioreactor derived samples. Notably, highly abundant genes appear in the digestate sample that were not detected in the acid mine drainage metagenome (*TC.FEV, feoB, mgtE, tlyC and trkH/trkG)*. As was observed for sulphur cycling genes (**Figure 5.4**), the caked digestate sample contained several genes not observed in the active digestate counterpart at low abundances.

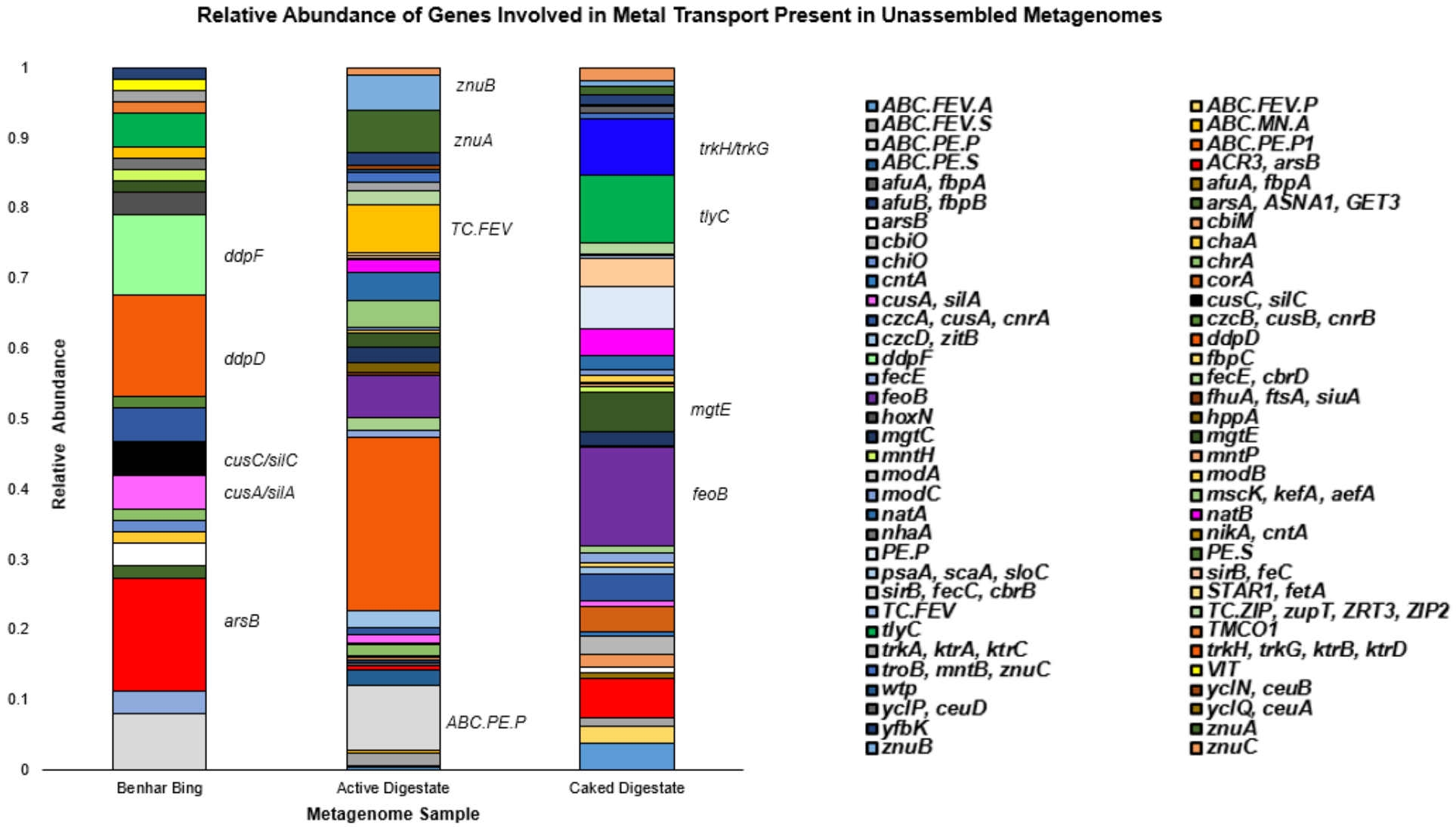

FIGURE 5.6: Relative abundance of metal transport genes manually retrieved from KEGG Mapper output for three unassembled metagenomes. Genes were selected manually from the ABC-transporter group allocated by KEGG EC prediction.

5.4 Discussion

5.4.1 Routes to Functional Analysis Using Unassembled Long DNA Reads

The use of long read DNA sequences prior to assembly into complete MAGs, or partially complete chromosomal regions, holds value in determining both the presence of functional genes which can be attributed to wider ecosystem function, and gene abundance. However, analyses involving the use of unassembled reads are limited by both the infrequently reported use of unassembled genomic data available for comparison in the literature, as well as the limited pool of robust tools that can be utilised for annotation of genes within long contiguous DNA sequences. Despite this, detection of genes involved in several key metabolic strategies employed by acidophilic consortia were observed in the unassembled metagenomic data.

The use of the metagenome-specific annotation tool within KAAS proved to be a suitable route for unassembled read gene annotation, however, KAAS is limited by data set size, causing this approach to analysis to be time consuming and requiring manual manipulation of data. The KAAS tool was initially developed by Moriya *et al* (2007) and a later update was added to allow annotation of unassembled reads. Despite this, it is suggested that unassembled reads are first translated to amino acid sequences, and then gene function detected which can provide more coverage of gene function and overcomes the stringency of the nucleotide matches employed by KAAS gene prediction. This was attempted, but due to the high number of reads requiring translation, this was not computationally feasible and is designed for a smaller data set. Additionally, translation of long DNA reads generated by Nanopore Sequencing is likely unreliable due to potential frameshifts occurring within the reads and the stop presence of stop codons.

5.4.2 Taxonomic Composition of the Microbial Community Endogenous to Acid Mine Drainage from Benhar Bing

Taxonomic prediction of reads was successful when Kaiju was applied to the unassembled metagenomic data from Benhar Bing. However, most reads could not be allocated to genus level based on exact protein homology matches. In contrast, when taxonomic prediction using Kaiju was applied to both active and caked digestate reads, more taxa were detected, presumably due to the dominant species being better characterised. Despite many taxa not being resolved to genus level within Benhar Bing using Kaiju, the most abundant taxa determined provided insights into key community members which may be driving function in low pH conditions. Importantly, amplification of the V4 region of the 16S rRNA gene from the same Benhar Bing DNA sample and subsequent metataxonomic analysis from Illumina reads allowed a greater diversity of taxa to be determined. Individual metagenomic (*ie*., non-amplified) long reads may contain full or partial 16S rRNA gene sequences, leading to a more limited taxonomic resolution, particularly from rarer species, especially if long reads are fragmented (Nelson *et al*., 2020). Therefore, the use of the 16S rRNA metataxonomic approach aided in an achieving a deeper level and more comprehensive overview of taxonomic composition.

The use of differing databases (SILVA and the NCBI non redundant protein database) may have led to the apparent variations in the most abundant genera observed. The SILVA database is highly curated and updated to reflect the most current phylogenetic annotations of prokaryotic ribosomal 16S RNA sequences (first developed by Quast *et al*., 2013). However, use of the non-redundant NCBI protein database is limited and appears to not successfully detect rarer or poorly studied organisms, which may not have close protein matches contained with this database. However, the NCBI database and SILVA had largely complemented each other, and confirmed the presence of the major genera (*e.g., Metallibacterium* and *Acidiphilium)*.

The major phyla detected by sequencing of the V4 16S rRNA are representative of the major bacterial lineages observed in acid mine drainage in the work of Baker and Banfield (2003). However, in the data presented here the Firmicutes appear rare, whereby they have been documented as being abundant in other low pH effluents The work of Sun *et al*. (2019) observed Firmicutes in acid mine drainage below pH 3 but indicated that members of this phylum may be more closely associated with mining waste heaps, rather than present in sediments.

Encouragingly, the most abundant species present, *Metallibacterium*, was detected by both the 16S rRNA gene-based approach and protein matches performed by Kaiju. A poorly characterised acidophile, the sole isolate of this genus, *Metallibacterium scheffleri*, was first isolated from an acid mine drainage impacted site in Germany (Ziegler *et al.,* 2013b). There is conflict within the extremely limited literature regarding the metabolic attributes of *Metallibacterium* and how this taxon can tolerate the multiple stressors present in acidic leachates has not been previously resolved.

Importantly, the physiology of *Metallibacterium* is discussed in greater detail in the following chapter (**Chapter 6**), as encouragingly, the high number of reads pertaining to *Metallibacterium* allowed the successful assembly of a high-quality metagenome assembled genome (MAG) pertaining to *Metallibacterium* to be recovered from the metagenomic data.

Similarly, *Acidiphilium, Acidipila* and members of the Acidobactericeae family were all detected in both the unassembled data and within the Illumina generated reads. *Acidiphilium*, *Acidipila* and *Acidobacteria* have are all considered endogenous to in heavily contaminated sites. Taken together, these three genera are indicative of taxa routinely described in metataxonomic studies on acid mine drainage sites and appear to share biogeographical dispersal patterns (Falagan *et al.,* 2017). *Granulicella,* predicted to be present via Kaiju, is less well documented in acidic leachates, however, has been known to demonstrate adaptations to both low temperature and elevated metal concentrations in soils (Falagan *et al.,* 2017; Oshkin *et al.,* 2019).

Interestingly, the proportion of reads pertaining to *Mycobacterium* within the unassembled data was not observed within the dominant taxa at genus level. The work of Radomski *et al*. (2013) states that mycobacterial species have been challenging to detect from environmental samples, even when multiple hypervariable regions of the 16S rRNA gene are utilised as phylogenetic targets. Indeed, some of the methods utilised by Radomski *et al*. (2013) failed to detect several mycobacterial species by PCR, while other primers lead to detection of closely related genera (*e.g., Corynebacterium, Nocardia* and *Rhodococcus*).

Acidisphaera has been noted most predominantly in extremely acid niches (below pH 3) and is considered to co-occur in these niches with commonly with *Acidiphilium* and acidophilic archaeans; *Acidisphaera* has been noted to exploit the niche via poorly understood heterotrophic pathways and shows enhanced abilities to tolerate high zinc and copper concentrations (Korzhenkov *et al*., 2019; Huang *et al*., 2021).

A single archaeal taxon was observed in the Illumina data belonging to the Thermomplasmatales, however this organism appeared to be rare (below 1% of the relative abundance of genera present). Based upon the ASV feature sequence, it is likely that this organism belongs to the E-plasma group. Members of the E-plasma group are documented in a limited number of metataxonomic studies, where they appear rare within the communities being analysed. Recently, members of the E-plasma have been detected in the extremely acidic effluents of Parys Mountain, Wales, which have been previously heavily mined (Bargiela *et al*., 2023). Additionally, copper contaminated effluents were noted to contain members of E-plasma and other poorly characterised Thermoplasmatales organisms in the work of Gupta *et al*. (2021).

5.4.3 Inferring Microbial Community Function from Prevalent Genes Within the Unassembled Data

Given the chemically extreme conditions in Benhar Bing, it was initially hypothesised that the most abundant genes present in the metagenome may have been reflective of metabolic adaptations which allow acidophiles to persist in low pH conditions. However, when compared to both control digestate metagenomes, several of the most abundant genes in Benhar Bing's unassembled data were also prevalent in the digestate samples.

The top twenty genes across all three samples were representative of genes involved in maintaining basal cellular integrity and function, rather that indicative of more specialised metabolism. This is likely due to the number of genes being involved in bacterial cellular maintenance and central metabolism being more abundant in the collective genomes of members of microbial populations than genes involved metabolic strategies which may not be utilised to the same extent as housekeeping genes. Determination of genes involved in maintaining a basal level of essential metabolism have not routinely been documented from metagenomic data, however, have been discussed regarding single bacterial species grown axenically. As abundant genes were often shared across all metagenomes, and not unique to Benhar Bing's community and reflective of acidophilic organismal function, the most prevalent genes are discussed here only briefly, particularly genes relating to DNA repair and carbohydrate metabolism.

5.4.3.1 Genes Involved in DNA Replication and Repair Dominated in Unassembled Metagenomes

A gene encoding a putative DNA transposase (K07947) was the most abundant annotated gene in Benhar Bing, however is this gene is poorly characterised and lacks detailed annotation. The putative transposase present shares homology other transposase enzymes, yet not further specific function can be inferred from this protein. Generally, transposases are involved in DNA rearrangement within the genome, and are often associated with mobile genetic elements. However, in the case of the putative transposase K07947, the sequence was first documented within the genome of a *Providencia* species, and potentially has undergone integration into the chromosome as an insertion sequence (IS) (Dong *et al.,* 2023). Although involved across prokaryotic species, genomic rearrangement and expansion genome have been demonstrated in a range of taxa and may promote evolution of genetically stable extremophiles following diversification of genomic function (Mao and Grogan, 2017).

Importantly, other genes involved in DNA repair and replication were found to be prevalent in the most abundant annotated genes from the Benhar Bing community. The *uvrA* gene was observed in all unassembled genomes and is a key component of the UvrABC DNA repair system, which is involved in recognition and removal of incorrect nucleotides within the genome. Specifically, *uvrA* is involved in DNA binding to regions which have been detected as damaged. Despite being a critical functional across all organisms, damage to the nucleoid can occur to taxa native to low pH conditions via excessive exposure to H^+ and metal ions; specialised DNA repair mechanisms have been noted in acidophiles which can promote their survival under hazardous environmental conditions. The generation of free radicals, generated as a response to heavy metal exposure can also damage the chromosome of acidophiles (Cortez *et al.,* 2022). Similarly, *dnaE* and *dnaK* are well documented enzymes involved in replicative synthesis of DNA in bacteria, with *dnaK* acting a key initiator of replication. Additionally, *dnaK* has implicated in stress response to protecting DNA during osmotic stress.

6.4.3.2 Genes Involved in Carbohydrate Metabolism

Carbohydrate metabolism has been challenging to elucidate in many extremophiles and often acidophiles are considered to have a narrow metabolic substrate spectrum, reflective of their evolution in niches with extreme nutritional scarcity.

The abundant genes involved in carbohydrate metabolism within the Benhar Bing were often also shared within the two unassembled digestate metagenomes. Examples of prevalent genes involved in reactions pertaining to carbohydrate metabolism were: *gltA, glnA, acnA* and *acs*. Both the GltA and GlnA proteins are oxidoreductases which facilitate trafficking of carbon-containing intermediate metabolites to amino acid biosynthesis. Additionally, other genes present (*e.g., acnA* and *acs*) are involved in reactions within central metabolism, leading to ATP generation. Literature regarding central metabolism is lacking, however, the highly conserved nature of genes involved in carbohydrate catabolism has led to the function of the genes presented here being elucidated in non-extremophilic organisms (Cunningham *et al.*, 1997*)*.

5.4.4 Determining Ecological Function via Unassembled Reads

By targeting specific functional categories apparent in the KEGG annotation outputs, more specialised ecological functional attributes were observed in Benhar Bing reads and allowed comparison to both control metagenomes. The focus of the following discussion sections will emphasise genes and their functions pertaining to the Benhar Bing community, with comparison to the digestate metagenomes were appropriate.

5.4.4.1 Sulphur Metabolism

Despite acid mine drainage sites being noted to contain high concentration of inorganic sulphates, the digestate metagenomes collectively harboured more genes involved in sulphur metabolism. This was likely since the Benhar Bing assemblage has a more simplified community structure and often acidophilic metabolic routes are restricted by the selective pressures of the chemically extreme niche.

The most abundant gene involved in sulphur-mediated reactions, *cysK*, in Benhar Bing was also abundant in caked and active digestates. The CysK protein is known to be a sulphide-utilising synthase enzyme involved in the production of the sulphur-containing amino acid cysteine, therefore is required across taxa regardless of their niche's extremity. However, some evidence suggests a dual role in the function of *cysK*, particularly critical to prokaryotic survival in low pH conditions with high metal contamination.

Evidence of the upregulated expression of *cysK* has been demonstrated by Yan *et al*. (2021) in *Klebsiella michiganesis* when growth under acidic conditions and exposed to elevated copper concentrations. Similarly, *cysK* was noted to be utilised by the metal resistant species, *Cupriavidus gilardii* when challenged with high copper toxicity (Huang *et al*., 2019). Both these works, when taken together, suggest that c*ysK* expression may facilitate a key metal tolerance mechanism in acidophiles, as the cystine produced via translation of *cysK* transcripts can form stable complexes with free copper ions, preventing intracellular copper toxicity and metal induced cellular damage.

No literature has explored the use of unassembled long reads recovered from acid mine drainage to elucidate overall community functions, yet it is encouraging that *cysK* is abundant in Benhar Bing and may confer copper resistance to community members and has been observed in acid and metal tolerant taxa from similar biotopes. Similarly, *cysC* was moderately abundant in Benhar Bing, which is also involved in the synthesis of cysteine via cyanoalanine synthase, which involves the co-production of acetate. It has been predicted that this route to cysteine production from sulphide and serine precursors is a more rapid reaction that that driven by *cysK,* and *cysC* may have a higher affinity for sulphides.

The gene *metZ* was present in low abundance compared to other sulphur-utilising genes in Benhar Bing but did not appear in the digestates. Functionally similar to both the *cysC* and *cysK* genes, the MetZ protein is also considered to be involved in the formation of sulphur-containing amino acids and may be able to prevent copper toxicity via copper-complex formation. However, mechanistically, the function of the MetZ protein has been described only rarely in the literature; expression of *metZ* been noted in pseudomonads when grown in culture spiked with elevated concentrations of inorganic sulphur sources (Foglino *et al.,* 1995). The *metX* gene was also abundant in Benhar Bing and is responsible of the putative synthesis of cysteine but may also catalyse the generation of ammonium from amino acid precursors which may provide some level of pH buffering capacity to counteract acid induced cellular stress (Lund *et al.,* 2020). The use of ammonium as a pH alkalising agent is described in more detail in the following chapter, whereby data presented demonstrates novel adaptations to acid tolerance.

Evidence of sulphur oxidation was apparent in the unassembled reads from Benhar Bing, particularly through the presence of *sqr,* not apparent in the digestate samples. The *sqr* gene product can catalyse the oxidation of sulphides via assistance with a quinone; consecutive reactions mediated by *sqr* expression can lead to the accumulation of polysulphides, which may take the form of cyclic sulphur molecules and add to the bioavailable pool of sulphur compounds for subsequent reactions (Brito *et al.,* 2009).

The acid mine drainage species *Acidiphilum* has been noted to carry *sqr* on its genome (Li *et al*., 2020); this is discussed further in **Chapter 6** where an assembled and annotated MAG pertaining to *Acidiphilium* is presented. Additionally, *Acidothiobacillus*, one of the limited numbers of acidophiles available in culture, is known to harbour *sqr* genes utilised to conserve energy via oxidation of sulphides. This metabolic strategy has been noted in *Acidithiobacillus* isolated from extremely acidic cave biofilms by the work of Jones *et al*. (2013) and appears to be a key enzyme which allows sulphur oxidation to proceed in low pH, high sulphide conditions.

The *sir* gene was also present in the unassembled reads, the gene product of which is involved in catalysing the reduction of sulphite to sulphide. Sulphur reduction has been less documented than sulphur oxidation in acidic effluents, however a study by Niu e*t al*. (2016) stated that the *sir* gene was detected in a bioleaching system recovering copper from low grade metallic ores. This work explored functional shifts in taxa during the bioleaching process at low pH, however utilised a commercially available functional gene array device (a GeoChip) opposed to detecting the gene utilising metagenomic sequencing. Again, the function of the *sir* gene will be considered further as it appears within an assembled MAG in **Chapter 6** and provides further novel insight into overlooked potential sulphur reduction pathway in a particular taxon in these non-conventional microbial ecosystems.

The *sseA* gene was present in Benhar Bing and not observed in the digestate metagenomes. The SseA protein is responsible for transferring sulphur to thiol-containing acceptor molecules and is likely a sulphur-transferase based on inferred sequence homology. This putative sulphur-transferase gene has also been observed in *Acidothiobacillus,* as well as chemolithotrophic organisms which are poorly characterised symbionts of deep-sea bivalves (Harada et al., 2009). The SseA protein may also have an additional role in serine metabolism, potentially aiding in amino acid accumulation under abiotic stress (Hama *et al*., 1994), however the full extent of the function of the SseA remains unclear and has not been explored recently.

Lastly, despite being rare in the unassembled Benhar Bing metagenomic reads, the *aprA* gene was detected. The *aprA* gene encodes a catalytic subunit of adenylylsulphate reductase, a key functional gene involved dissimilatory sulphate reduction. Due to the elevated concentrations of metal sulphides and other sulphur-containing compounds within mine leachates, *aprA* has

also been documented in several from acid mine drainage sites actoss the United States (Ly *et al.,* 2019; Grettenberger and Hamilton, 2021). The detection of the *arpA* gene within the Benhar Bing community expands on current knowledge regarding sulphate reduction in heavily contaminated ecosystems.

5.4.4.2 Metal Utilisation and Efflux Mechanisms

Assessing the comparative relative abundances of metal utilisation and transport/efflux genes between metagenome samples proved to be a valuable comparison which allowed key functions reflective of extremophilic genomic strategies employed by the consortia within acid mine drainage to be detected.

Acid mine drainage sites are heavily contaminated by metallic pollutants derived from mined ores, which must be tolerated or utilised by prokaryotes to allow continued cellular proliferation and survival. The unassembled reads from Benhar Bing which had genomic annotations relating to metal-related metabolism were dominated by sequences pertaining to the presence of *arsB* and *ddpD*/*ddpF* genes. Several genes from the *cut* and *sil* families were also evident and showed elevated abundance in Benhar Bing compared to the more conventional digestate controls.

The *asrB* gene is involved in arsenic detoxification; the metalloid arsenic is a potent toxicant and has been detected in acid mine drainage waste streams (Andreas and Bertin, 2016). Arsenic detoxification, and the importance of arsenic removal from the environment, will be discussed further in the following chapter, as the high relative abundance observed in the unassembled data presented here is reflected in assembled chromosomal sequences pertaining to acid mine drainage community members. This includes previously poorly described taxa in which arsenic detoxification and tolerance has not been reported before.

The biogeochemical conversions of arsenic are complex, and the fate of arsenic in the environment can be influenced by both microbial and abiotic factors, including adsorption to organic substrates. Additionally, the complexities of decontamination of acidic and iron rich leachates is compounded by arsenic-bearing iron compounds which require multiple microbially driven reactions to facilitate the interlinked iron and arsenic cycles (Xiu *et al.,* 2022). Briefly, the *arsB* gene noted in the unassembled reads represents the predominant

presence of the arsenical transmembrane carrier pump protein, involved in extrusion of the toxic metalloid from the intracellular space by arsenic tolerant bacteria. The arsenic detoxification strategies employed by prokaryotes are evolutionary conserved and have been demonstrated to be prevalent across distantly related taxa within various operon configurations (Andres and Bertin, 2016).

The high relative abundance of *ddpD*/*ddpF* observed in the Benhar Bing unassembled DNA represented the community's potential ability to tolerate nickel, as *ddp* genes are considered to function as peptide/nickel transport systems, allowing the bidirectional translocation of this transition metal. Both *ddpD* and *ddpF* have been detecting within the assembled bacterial genomes of assembled from metal contaminated soil (Munoz-Garcia *et al.,* 2022) and archaeal and bacterial genomes from high temperature geothermal steam vents which are known to contain elevated levels of soluble metals (Marin-Paredes *et al.,* 2023). Furthermore, the work of Munoz-Garcia *et al*. (2022) also detected the presence of *cusA*/*silA*, *cutS* and *PEP.ABC* genes involved in the efflux of various transition metals, also evident in the Benhar Bing annotated reads.

Acidic mine drainage has been noted to contain elevated concentrations of nickel, which is high concentrations can be deleterious to cellular physiology. Again, assembled genomes presented in the following chapter indicate the chromosomal organisation and functions of nickel transporting genes present within key acidophiles' genomes.

An important consideration is the apparent diversity of metal transport genes in the digestate metagenomes, despite not being considered a sample with high metal contents. Previous work on the same caked digestate sample demonstrated a high relative abundance of antimicrobial resistance genes, which have been noted in the literature to be co-selected with genes involved in heavy metal tolerance (Mazhar *et al.,* 2021; Knight, 2023).

The digestates appear to have higher relative abundance of genes involved in metal import and scavenging, unseen in the DNA recovered from Benhar Bing as it is unlikely the taxa present here must scavenge under metal excess. Two iron transporting genes, *TC.FEV* and *feoB* were evident in the active and caked digestates. The FeoB protein is involved in the uptake of iron from the environment, while the TC.FEV protein contributes to the outer membrane receptor proteins which bind of iron complexes (Chen *et al.,* 2019). Critically, *feoB* expression has a critical role in the formation of iron scavenging siderophores, particularly from ferric citrate (Josts *et al.,* 2021). Routes exploited by acidophiles in Benhar Bing to yield energy from the oxidation of iron is further documented in the following chapter regarding MAG assembly.

Reads including gene sequences involved in both zinc and magnesium uptake (*znu* and *trk* genes, respectively) were more abundant in the digestates compared to annotated metal tolerance genes observed within the unassembled reads from the acid mine drainage sample. Benhar Bing appeared to have more genes involved in the efflux of metals, reflective of metal detoxification and tolerance (*e.g., czc* genes, involved in the removal of metal species from the cell) opposed to uptake of metals requiring specialised import channels as was observed in the digestates. This is a clear distinction between the extreme nature of Benhar Bing, whereby the acidic sediment contains high concentrations of metals which consortia must counteract, rather than scare metals required for growth and must be imported into the cell. However, acidophiles do require metals for growth (for example, in enzymatic co-factors), therefore maintaining metal homeostasis via metal efflux can often be energetically challenging and requires specialised metal transport mechanisms, apparent in the genomic material recovered from Benhar Bing.

Despite the success in observing key functionally specific traits (*e.g.*, genes involved metal transport and sulphur cycling), the use of unassembled metagenomic material cannot assist in the determination of the structure of ecologically relevant operons or other genomic elements. The work of Van der Walt *et al*. (2017) states that unassembled reads can produce metagenomic data that is challenging to infer function from, as reads can be fragmented or contain uneven sequencing depth. To overcome this, analysis of unassembled reads is the carries the most value when comparisons can be performed to other metagenomic datasets, however this approach can be still poses limitations in predicting ecological function, particularly. To this end, assembly of long reads into metagenome assembled genomes may carry greater benefit in allowing specific microbial taxa-function relationships to be determined.

5.5 Conclusion of Chapter 5

Overall, Benhar Bing has a simplified community microbial structure, and the use of unassembled long reads is a valuable, but complex route to functional analysis. The use of unassembled reads to infer ecological function is challenging, as the data presented here demonstrate that the majority of DNA reads recovered from microbial communities are often reflective of genes which drive essential cellular functions, not ecological functional traits. To assess specific genes involved in more ecosystem-wide processes (*e.g.,* metal tolerance), individual genes had to be manually detected within metagenomic annotations, making this analysis route time-consuming and limited in its scope. The use of a single, non-redundant database has also led to an underrepresentation of functional attributes, given the noted divergence that occurs within the genomic content of many extremophilic species.

Additionally, determining function from reads not assembled into microbial chromosomes is the most beneficial when unassembled data sets can be compared, allowing for some level of comparative analyses, as has been performed here. The previously sequenced metagenomes from both the active and the caked anaerobic digestate samples acted as representative non-extreme systems to which Benhar Bing long read data could be compared to. This was particularly advantageous when assessing sulphur and metal cycling genes, allowing the high relative abundance of metal(loid) detoxification mechanisms present in the acid mine drainage DNA to become apparent.

Despite the constraints of working with unassembled long-read data, taxonomic prediction using long reads determined that *Metallibacterium* and *Acidiphilium* were two key genera which contribute to the microbial community structure within Benhar Bing. This was confirmed by analysis of ASVs. Going forward, assembly of genomes from unassembled data can provide greater insights into taxon-specific functional attributes.

CHAPTER 6 - Characterisation of Acid Mine Drainage Consortia Through Reconstruction and Functional Analysis of Metagenome Assembled Genomes

6.1 The Prokaryotic Chromosome and Microbial Metabolic Potential

Microorganisms native to acid mine drainage sites are responsible for facilitating reactions involved in acid generation and metal solubilisation through inorganic energy conservation, leading to elevated environmental toxicity. Acidophilic consortia, however, also hold potential to act as reservoirs of enzymes, and their associated pathways, involved in remediation of contaminated systems (Daraz *et al*., 2023). Sulphate and iron reduction can reduce acidity, elevate pH, and decrease the bioavailability of soluble heavy metals, aiding in ecosystem recovery. However, current knowledge on native microbial species and the functional potential in this unique anthropogenically-derived ecological niche is lacking, both regarding acidophilic survival mechanisms and the metabolic potential for restoring ecological conditions (Myers, 2016).

The diversity of genes within a given prokaryotic chromosome can be considered the 'trait-encoding' features which provide the host organism with the majority of its functional characteristics, alongside additional metabolic capabilities carried on extrachromosomal genetic elements (Kuzimonov, 2014). As stated previously, the metabolic potential harboured by acidophilic consortia is poorly characterised and the limited available published genomes may not reflect the structural and functional divergence observed in acidophiles' genomic content, reflective of their complex evolutionary history (Bargiela *et al*., 2023).

Furthermore, when extremophiles are considered, an understanding of metabolic routes involved in central metabolism (*e.g*., carbon utilisation and energy generation) which are well documented for members of conventional consortia is lacking. As lithotrophic metabolism has been documented routinely in the limited number of cultivated acidophiles from low pH habitats, the use of other metabolic strategies involving organic compounds remains poorly determined. Evidence is building that the metabolic functions of the scarce cultivated acid mine drainage members may be more diverse than previously thought, yet the collective metabolic roles of the wider consortia have not been fully elucidated (Chen *et al*., 2021).

The successful cultivation of a species in an axenic state has often been considered to be the most informative route to determining metabolic function of the isolate, as well as elucidating biogeochemical reactions that the specific species can perform (Grettenberger and Hamilton, 2021). However, conventional cultivation approaches often fail or result in re-cultivation of already acquired taxa, as discussed in **Chapter 3.** Therefore, recovery and assembly of partially or practically complete metagenome assembled genomes (MAGs) via metagenomic approaches can yield valuable functional and metabolic data regarding the physiology of taxa, overriding the initial requirement for cultivation.

MAGs can be taxonomically classified and functionally annotated, facilitating elucidation of the metabolic roles performed by challenging-to-cultivate species. Determination of metabolic function can also guide more targeted cultivation strategies associated with taxa from extreme environments. By targeting specific nutritional requirements observed within metagenomes, growth of novel isolates can be encouraged; this could aid in bringing members of the uncultured prokaryotic majority into cultivated states (Liu *et al.,* 2022). Thereby, expanding knowledge on microbial inhabitants in abiotically challenging ecosystems.

As previously described in **Chapter 5,** long-read sequencing allows a greater proportion of the genomic content contained within microbial chromosomes to be to be evaluated. Nanopore sequencing relies on the sequencing of a single strand of DNA through a protein nanopore, disrupting an electrical current, which can be later converted to nucleotide sequence using various tools and assembled into microbial genomes (Pugh, 2023). The methodology and rationale of this sequencing technology has been discussed in greater detail elsewhere; it is likely that this approach to MAG recovery will continue to be optimised as sequencing chemistry continues to develop (Wang *et al*., 2021b).

Briefly, *de novo* assembly of microbial genomes involves the reconstruction of genomes using individual DNA sequences. Reads are initially pieced together depending on sequence overlap. Following this, assembly tools *(e.g.,* metaflye) produce longer contiguous sequences (contigs) which allow greater chromosomal coverage. Contigs can act as scaffolds to reassemble chromosomes, depending on sequencing quality. Long-read assembly using Nanopore is advantageous as the length of initial reads aids in resolving the sequences of repetitive and complex genomic regions not accessible with short-reads. High-quality assemblies can overcome gaps in the chromosome, providing practically complete chromosomes assembled from metagenomic DNA. An overview of MAG reconstruction is shown in **Figure 6.1.**

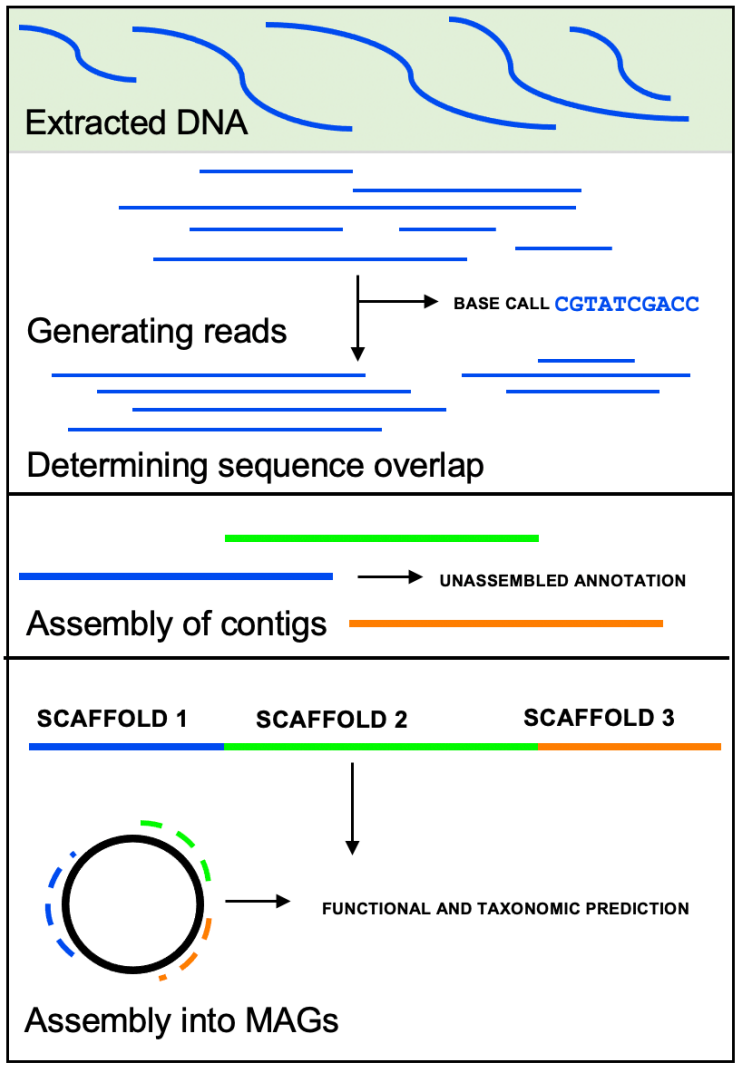

FIGURE 6.1: Assembly of metagenome assembled genomes from extracted DNA. The use of various tools allows *de novo* reassembly of genomes following DNA sequencing (*e.g.,* using Nanopore generated long reads). The assembly of MAGs allows determination of metabolic function and prediction of the host organism of the genome.

Long read sequencing using Oxford Nanopore Technology has enabled the successful reconstruction of genomes from a range of environments including freshwater aquifers (Overholt *et al*., 2020) and riverine ecosystems (Reddington *et al*., 2020). Due to their compact size, assembly of viral genomes has been performed from Nanopore generated reads from mammalian-associated samples, an example of a vital use of the technology directly regarding human health. Recently assembly of novel adenoviral genomes from primates was successful in the work of Veitch *et al*. (2023). Likewise, a single study has explored the use of Nanopore sequencing to assess bacteriophage diversity in a biogas reactor-based study by Wullenbucher *et al*. (2022), allowing novel insights into bacterial predation.

To date, there is limited literature demonstrating the use of Nanopore sequencing and reconstruction of chromosomes from microbial communities from highly polluted sites. However, this is likely to grow as the use of microbial consortia to counteract the impacts of environmental degradation in the Anthropocene becomes increasingly relevant. Nanopore sequencing has allowed recovery of metagenomes and determination of their associated functional potential from hydrocarbon degrading communities in two studies (Sandhu *et al*., 2022; Sarfo *et al*., 2023). These limited studies notwithstanding, there is little evidence of the use of genophore reconstruction via Nanopore sequencing of taxa inhabiting ecosystems which underpin biogeochemical cycling under environmentally restrained conditions, leaving evident gaps in the literature.

However, Nanopore sequencing has been used to recover and assess the metabolic function of a single acid mine drainage species, *Acidithiobacillus ferrivorans,* which was isolated from a copper mine. This work focused primarily on expanding current understanding of environmental adaptation strategies (*e.g*., acid tolerance mechanisms) within this species (Zhao *et al*., 2021). Yet, the use of nanopore sequencing technology specifically to recover and assemble multiple MAGs from members of an acid mine waste-associated community has not been reported.

It should be stressed that several MAGs have been recovered from acid mine drainage sites using alternative sequencing strategies, which have provided insight the ecological dispersal of previously unseen acidophiles. Pioneering work by Grettenberger and Hamilton (2021) demonstrated metabolic strategies by acidophilic consortia in an acid mine drainage contaminated freshwater system in Daniel Boone National Forest, Kentucky, yet only this single study exists to guide similar characterisation approaches. This approach utilised the Illumina HiSeq-2500 platform, which utilises a short read approach, rather that generating long-reads *de novo*. However, this approach is time-consuming and more costly than Nanopore sequencing (Akacin *et al*., 2022).

In some cases, taxonomic prediction of the microbial host of the MAG is provided by authors, yet any further determination of functional potential is lacking. For example, in Williams *et al*. (2023), the authors did not assess the metabolic diversity in their seven assembled bacterial and archaeal genomes recovered from acidophiles. Recently, Huang *et al*. (2023) reconstructed MAGs from water samples retrieved from pools passively treating coal mining effluent, again annotation was limited to genes involved in antimicrobial resistance. The ability to determine key community structure-function relationships can be achieved via chromosome annotation, yet previous work is limited, and many metabolic pathways which underpin ecological function and routes to environmental restoration remain underexplored.

6.2 Aim of Chapter 6

The main aim of this chapter was to utilise Oxford Nanopore Technology to facilitate long read DNA sequencing with the intention to recover, assemble metagenome assembled genomes and assess the metabolic function of members of the Benhar Bing microbial consortia. Additional objectives were:

- Determine the **quality** of assembled genomes based upon genomic content and assess **completion** and **contamination** of assembled MAGs.
- Determine the host organism/taxonomy of assembled MAGs using taxonomic binning.
- Predict the metabolic potential contained within the reconstructed genomes, with particularly focus on how key functional attributes contribute to **wider ecosystem function** and **organismal persistence** in otherwise deleterious and extreme conditions.
- Establish the **phylogenetic relationships of taxa** pertaining to the assembled MAGs through comparison of 16S rRNA sequences and evaluate homology between MAG sequences and consensus genome sequences of closest related taxa.

6.3 Results

6.3.1 Overview of MAG Recovery and Assembly

Metagenomes were assembled following Oxford Nanopore sequencing of DNA extracted from acid mine drainage sediment collected from the settling pond at Benhar Bing. Briefly, initial assembly using metaflye alone resulted in a high number (> 300) of lower-quality MAGs, which were poorly taxonomically resolved using the Rapid Annotation Subsystem Technology (RAST) Server, when the largest MAG sequences were selected manually.

To rectify this, MAGs were then assembled using metaflye, refined using Homopolish and Racon and taxonomically binned via the BUGSPLIT pipeline. Taxonomy of MAGs were predicted with the use of Minimap2 against the NCBI/RefSeq database using closest matches to available genomes (see **Chapter 2** for full details). This approach reduced the number of assemblies yet produced higher quality genomes which were then functionally annotated using Prokka in place of RAST. In total, 1.93 million reads were generated (7.76 Gb); following quality filtering, 1.64 million reads (6.52 Gb) were utilised for assembly of MAGs.

In total, 145 bins were produced from taxonomic allocation of assemblies. Six binned MAGs were constructed with > 70% completeness, across two phyla: Pseudomonadota and Actinomycetota (**Table 6.1**), with two high quality (> 90% complete) reconstructed genomes recovered. An additional seven taxonomic bins were produced from assembles below 60% complete (**Table 6.2**), however a notable reduction in completeness and assembly length occurred outside of the highest quality genomic assemblies presented in **Table 6.1** The data presented here demonstrates the functional genomic potential of three selected MAGs, pertaining to *Acidiphilum* (MAG 2), *Metallibacterium* (MAG 6) and *Mycobacterium* (MAG 3). Some further taxonomic resolution of the moderate quality, yet poorly taxonomically resolved MAG 5 was attempted and is discussed briefly.

Genomic assemblies relating to Pseudomonadota, Acidobacteriota and Actinomycetota with < 60% completeness are presented in **Table 6.2**. Reads assembled into shorter chromosomal fragments (100,000 – 700,000 bp) which were taxonomically resolved to 16 bins across three phyla (Pseudomonadota, Actinomycetota and Acidobacteriota) are presented in **Table 6.3.**

Details on the remaining contigs (below 100,000 bp) which could not be assembled into genomes but were allocated to the remaining 127 taxonomic bins are available in the **Supplementary Data (Table S1).**

TABLE 6.1: Summary of metagenome assembled genomes with **> 70 % completeness**. Completeness and contamination assessed via CheckM. MAG features (size, GC content, number of contigs, tRNAs, rRNAs) determined via Prokka. Taxonomy predicted using BUGSPLIT binning pipeline.

* Annotation not performed due to high % contamination; ** Indicates a high-quality assembly (> 90% complete); ◊ one 23S rRNA partially complete

Phylum	Predicted Taxonomy	Completeness (%)	Contamination (%)	Size (Mb)	No. of Contigs	GC Content (%)	No. of rRNAs	No. of tRNAs	Number of tRNAs for different amino acids
Pseudomonadota (MAG 1)	*Alphaproteobacteria; Rhodospirillales; Acetobacteraceae;*	77.78	**54.9***	7.93	132	68.3	9: 16S (4) 23S (4) ◊ 5S (1)	87	19
Pseudomonadota (**MAG 2**)	*Alphaproteobacteria; Rhodospirillales; Acetobacteraceae; Acidiphilium;*	75.98	7.89	2.07	19	62.6	3: 16S (1) 23S (1) 5S (1)	28	18
Actinomycetota (**MAG 3**)	*Actinomycetia; Mycobacteriales; Mycobacteriaceae; Mycobacterium;*	77.82	5.23	6.04	92	68.9	3: 16S (1) 23S (1) 5S (1)	55	19
Pseudomonadota (MAG 4)	*Gammaproteobacteria; Lysobacterales; Lysobacteraceae; Metallibacterium;*	**92.30****	6.79	4.69	91	66.6	6: 16S (2) 23S (2) 5S (2)	49	20
Actinomyceotota (MAG 5)	*Actinomycetia;*	70.69	6.33	4.38	99	66.9	11: 16S (4) 23S (4) ◊ 5S (3)	63	17
Pseudomonadota (**MAG 6**)	*Gammaproteobacteria; Lysobacterales; Lysobacteraceae; Metallibacterium; M. scheffleri*	**97.73****	5.21	3.23	50	66.7	6: 16S (2) 23S (2) 5S (2)	49	20

MAGs 2, 3 and 6 (highlighted in green) were selected for full functional annotation. Further taxonomic resolution of MAG 5 (highlighted in blue was performed).

TABLE 6.2: Summary of metagenome assembled genomes with **< 60% completeness**. Completeness and contamination assessed via CheckM. MAG features (size, GC content, number of contigs, tRNAs, rRNAs) determined via Prokka. Taxonomy predicted using BUGSPLIT binning pipeline.

Phylum	Predicted Taxonomy	Completeness (%)	Contamination (%)	Assembly Size (Mb)	Number of Contigs	GC Content (%)
Pseudomonadota (MAG 7)	*Alphaproteobacteria;*	55.28	12.90*	6.58	137	68.73
Actinomycetota (MAG 8)	*Acidmicrobiia; Acidimicrobiales; Acidimicrobiaceae; Aciditerrimonas;*	50.00	10.77	1.22	33	64.96
Pseudomonadota (MAG 9)	*Alphaproteobacterium; Rhodospirillales; Acetobacteraceae; Acidiphilium;*	40.00	0.00	3.46	125	60.11
Pseudomonadota (MAG 10)	**Unresolved below phylum**	36.06	4.39	4.74	97	68.90
Pseudomonadota (MAG 11)	*Alphaproteobacterium; Rhodospirrales;*	28.69	4.23	3.81	43	69.03
Acidobacteriota (MAG 12)	*Acidobacteriia; Acidobacteriales; Acidobacteriaceae*	38.81	5.00	3.46	125	60.11
Pseudomonadota (MAG 13)	*Betaproteobacteria; Nitrosomadales; Gallionellaceae; Gallionella;*	11.93	0.00	1.47	64	61.68

* Annotation not performed due to high % contamination

TABLE 6.3: Partially assembled contiguous sequences of **100-700 kb** binned after MAG assembly. Contig size and number determined via Proksee. Taxonomy predicted via BUGSPLIT binning route.

Phylum	Predicted Taxonomy	Contig Size (bp)	Number of Contigs
Actinomycetota	*Actinomycetota; Acidimicrobiia; Acidimicrobiales;*	677504	25
Pseudomonadota	*Gammaproteobacteria;*	642514	18
Acidobacteriota	*Acidobacteriia; Acidobacteriales; Acidobacteriaceae Edaphobacter;*	287603	33
Actinomycetota	*Actinomycetia; Streptosporangiales;*	175531	14
Pseudomonadota	*Alphaproteobacterium; Rhodospirillales; Acetobacteraceae; Rhodovastum;*	175531	14
Actinomycetota	*Acidimicrobiia; Acidimicrobiales; Iamiaceae;*	166058	9
Pseudomonadota	*Alphaproteobacteria; Hyphomicrobiales;*	162009	9
Pseudomonadota	*Gammaproteobacteria; Xanthomonadales; Rhodanobacteraceae;*	154523	5
Pseudomonadota	*Alphaproteobacteria; Rhodospirillales; Acetobacteraceae; Acidibrevibacterium*	154257	9
Pseudomonadota	*Alphaproteobacterium; Rhodospirillales; Acetobacteraceae; Acidiphilium; Acidiphilium angustum*	145847	1
Acidobacteriota	*Terriglobia; Terriglobales; Acidobacteriaceae; Paracidobacterium;*	132175	14
Acidobacteriota	*Terriglobia; Terriglobales; Acidobacteriaceae; Acidipila;*	124865	13
Pseudomonadota	*Alphaproteobacteria; Sphingomonadales; Sphingomonadaceae; Sphingomonas*	120865	5
Acidobacteriota	*Terriglobia; Terriglobales; Acidobacteriaceae; Acidicapsa;*	108300	11
Acidobacteriota	*Terriglobia; Terriglobales; Acidobacteriaceae; Allloacidobacterium;*	102654	5
Actinomycetota	*Actinomycetes; Streptosporangiales; Treboniaceae; Trebonia*	100615	6

6.3.2 MAGs Classified in the Phylum Pseudomonadota (Overview of MAG2, MAG 4 and MAG 6)

Four MAGS with > 70% completeness were taxonomically binned to the phylum Pseudomonadota; one was taxonomically positioned within *Acidiphilium* (MAG 2), and two MAGs (MAGs 4 and 6) were determined to be reconstructed genomes of *Metallibacterium*, with MAG 6 resolved to species level, predicted to be from *Metallibacterium scheffleri.* MAG 1 could not have taxonomy predicted below the family level (*Acetobacteraceae*), however due to high levels of contamination determined via CheckM, this MAG had no further functional analysis performed.

Regarding the two *Metallibacterium* assemblies, MAG 6 was selected for further analysis (see **Section 6.3.2.2)** as the genome size more closely reflected that of the assemblies' closest cultivated isolate and had higher completion and less evidence of contaminating sequences. Despite also having high completeness, MAG 4 had an inflated genome size compared to MAG 6, and when annotated had a high proportion of genes that could not be attributed to metabolic function (60.42% of the total genomic content could not be characterised), as well as more predicted repetitive regions.

Further to this, when the MAG 4 was aligned to the genome of the *Metallibacterium* isolate, despite carrying two 16S rRNAs identical to that of the isolate, the complete genome alignment demonstrated < 85 % similarity, likely due to the excess contigs within the assembly. As CheckM utilises a series of marker genes to identify contaminating sequences, it is likely that the observed overinflation in MAG size was due to extra DNA reads being assembled into the genome, but not containing genes detected by CheckM. This would have allowed the predicted contamination value to remain low, despite the MAG exceeding the expected size. To this end, MAG 4 was excluded from analysis, as were other MAGs which were not of high to moderate completion, with low contamination. From the Pseudomonadota assemblies, MAG 2, and MAG 6 (**Table 6.1**) were annotated and presented here.

6.3.2.1 The Acidiphilium Assembly (MAG 2)

MAG 2 was taxonomically determined to be a reconstruction of a genome attributed to the genus *Acidiphilium*. The assembly was 75.98% complete with 1.60% contamination, indicative of a medium-quality draft MAG. The GC content of the reconstructed genome was 62.6% (**Table 6.1**). Annotation of the *Acidiphilium* MAG indicated 2707 coding sequences with 1222 genes considered to have known or putative function (45.14% of the total annotation). The remaining 1485 exons were deemed to encode hypothetical proteins with no clearly defined function. The MAG contained 28 tRNAs associated with 15 amino acids. One non-coding tmRNA was present and three rRNA genes detected; one copy of the 16S, 5S and 23S rRNA genes were arranged in a single operon. The 1495 bp 16S rRNA gene was identical to that of *Acidiphilium rubrum*.

The Average Nucleotide Identity (ANI) demonstrated 97.44% identity between homologous genomic regions present in both the assembly and the genome of *A. rubrum* (**Figure 6.2**), although gaps were evident given the incomplete assembly. The taxonomic position of the MAG within the *Acidiphilium* is demonstrated in the phylogeny in **Figure 6.3.** The assembled chromosome contained a single highly repetitive region, containing elevated cytosine and guanine residues, determined to be 2299 bp in length. The structure of the assembled genome of *Acidiphilium* is shown in **Figure 6.4**

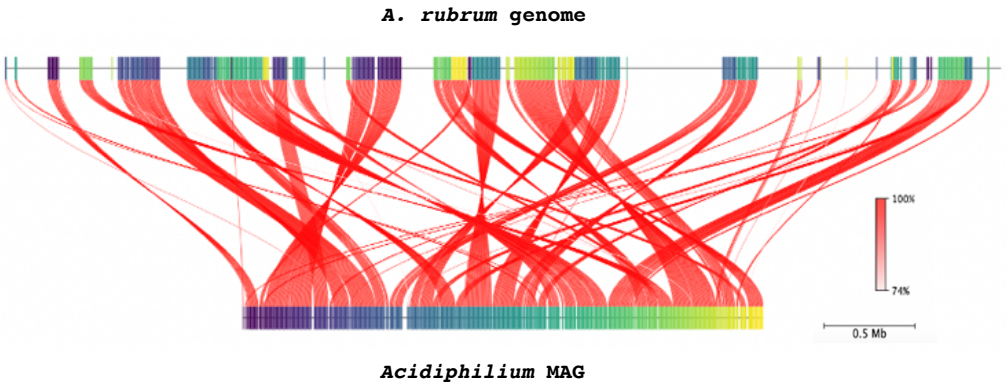

FIGURE 6.2 *Acidiphilium* assembly and *Acidiphilium rubrum* whole genome ANI alignments. Average Nucleotide Identity (ANI) comparison between the assembly and consensus genome sequence. Plot produced via *FAST-ANI* on *Proksee.*

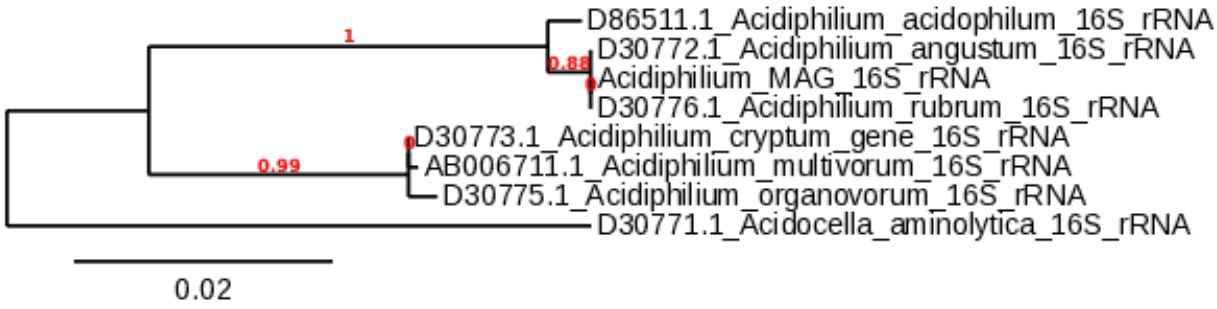

FIGURE 6.3: Phylogenetic position of assembled MAG within the *Acidiphilium* clade based on full length 16S rRNA sequences. Multiple sequence alignment indicates that the rRNA gene sequence of *A. rubrum* is an identical match to that of the MAG. The phylogeny rooted with the 16S rRNA sequence of *Acidocella aminolytica*. Phylogeny produced using the EBI ClustalW phylogenetic tool.

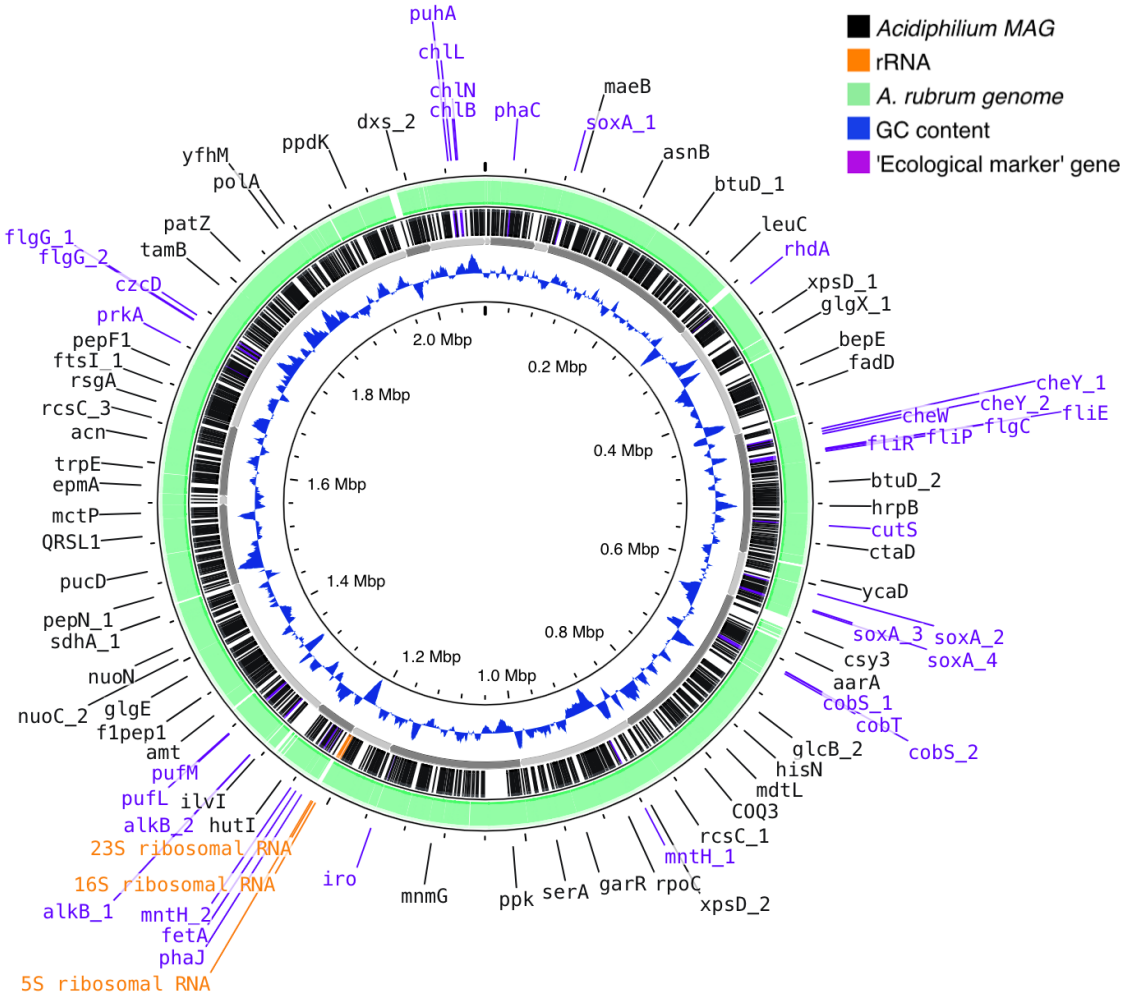

FIGURE 6.4: Structure and predicted genomic content of the assembled *Acidiphilium* chromosome (MAG 2). The 2.07 Mb *Acidiphilium* assembly (black) is shown aligned to the 3.97 Mb consensus genome sequence of *Acidiphilium rubrum* (green) [*RefSeq Genome Accession: GCF_900156265.1*]. Key functional genes involved in specific processes (*e.g., iro* involved in iron oxidation) have been highlighted in purple. Non-coding rRNA genes are shown in orange. Non-coding tRNAs, the single tmRNA and repetitive region have been removed for clarity. GC content is shown in blue. Genomic annotations determined via *Prokka.* Chromosome map prepared using *Proksee.*

Regarding the functional potential of *Acidiphilium*, genomic annotation demonstrated genes involved in performing carbon fixation through assimilation of CO_2. These functions are conferred to *Acidiphilium* principally through *cbbX*, which encodes an ATPase involved in activation of ribulose-1,5-bisphosphate carboxylase/oxygenase (RubisCo), allowing the first reaction of carbon fixation to occur. Additionally, expression of the *prk* gene synthesises phosoribulokinase, involved in the ATP-dependent irreversible conversion of ribulose-5-phosphate during the Calvin Cycle. Light-independent synthesis of associated photosynthetic pigments was observed via the potential to express genes involved in protochlorophyllide and bacteriochlorophyll (BChl): *chlL, chlB* and *chlN*. Importantly, photosystem II-type photosynthetic reaction centers (PufBALMC and PuhA) have found in all clades of *Acidiphilium*, however were not detected within the MAG pertaining to *A. rubrum* presented here. Despite this, other carbon fixation pathways are likely involved in Acidiphilium's energy conservation strategies (Liu *et al.,* 2020).

Utilisation of carbon monoxide as an alternative source of carbon was also indicated via presence of *cutS,* encoding CO-dehydrogenase, within the assembled genome. Genes involved in glycolysis and oxidative phosphorylation were evident (*e.g., ccmA, ccmE, ccmF, ctaD*). The assembled chromosome indicated the potential to utilise hydrocarbons as additional sources of carbon through expression of *alkB,* encoding alkane hydrolase. Assimilation of intracellular carbon in poly-β-hydroxybutyrate (PHB) granules was evident with both *phaJ* and *phaC* present, key enzymes involved in the synthesis of polyhydroxyalkanoic acid (PHA).

The metabolic potential to perform iron oxidation was observed via the presence of *iro,* encoding iron oxidase; cellular motility and response to nutritional gradients was evident through several genes involved in the assembly of flagella (*e.g., flgC, flgG, flgH*) as well as the ability to express the chemotaxis response proteins, CheY and CheW. The *soxA* gene suggests the metabolic potential to perform of sulphur oxidation, as well as wider sulphur utilising/trafficking capabilities encoded by several *cys* genes.

Tolerance to other heavy metals was also observed in the *Acidiphilium* assembly, with cobalt chelatase production providing cobalt resistance (encoded by *cobS* and *cobT)*. The ability to synthesise additional efflux pump proteins preventing intracellular accumulation of transition metals was apparent via *mntH;* the gene encoding the membrane bound divalent cation transporter protein. Similarly, the presence of *czc* genes indicates the potential of *Acidiphilium* to use additional mechanisms for the extrusion of metals, with *czcD* capable of co-transporting zinc, cobalt, and cadmium.

A summary of key genomic annotation results and links to physiological function in *Acidiphilium* is shown in **Figure 6.5.**

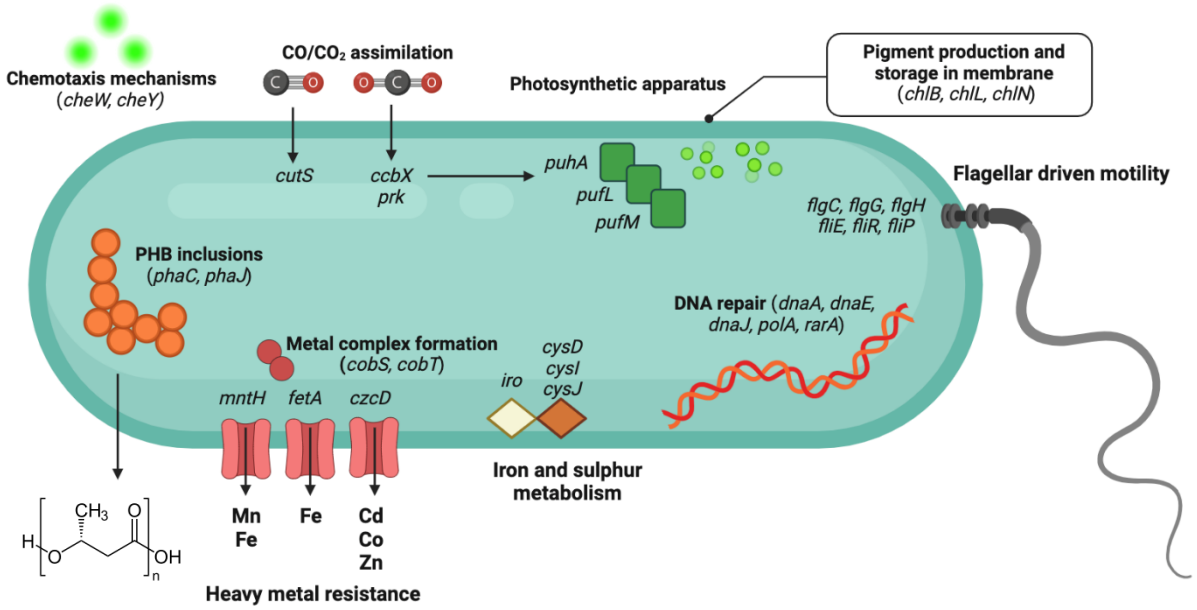

FIGURE 6.5: Summary of the metabolic features of *Acidiphilium* identified from the genomic content of the assembled MAG. Expulsion of metals from the cell proceeds via membrane channels (shown in pink). The ability of *Acidiphilium* to perform carbon fixation and photosynthesis (green squares/circles) provides metabolic flexibility despite having heterotrophic potential. During nutritional scarcity, caron-rich PHB inclusions (orange) can be degraded to yield energy. The use of iron and sulphur oxidation (diamonds) further expand metabolic routes available to *Acidiphilum.*

6.3.2.2 The Metallibacterium Assembly (MAG 6)

The *Metallibacterium* MAG selected for functional analysis (MAG 6) was determined to be a high-quality draft assembled genome, with over 90% genomic completeness. In total, 49 tRNA genes were detected, including the presence of a single transfer-messenger RNA (tmRNA). Six rRNA encoding genes (two copies of each of the 16S, 5S and 23S genes) were detected in the assembled MAG and were arranged across two rRNA operons within the genome.

Both of the 1478 bp 16S rRNA genes present in the *Metallibacterium* assembly were identical in sequence and shared 99.93% sequence homology to the 16S rRNA gene sequence of *Metallibacterium scheffleri*. The Average Nucleotide Identity (ANI) demonstrated 98.87% identity between homologous regions present in both the assembly and the genome of the *M. scheffleri* (**Figure 6.6**).

A total of 3324 protein coding regions were detected within the *Metallibacterium* MAG 6 (**Figure 6.7**), with 1682 regions attributed with a known or putative function (49.39% of the total predicted genes). The remaining 1642 coding regions were only determined to possess hypothetical function (50.06% of the total coding regions). The chromosome was considered to contain three highly repetitive regions which were 1661, 1165 and 318 bp long, respectively. These regions were deemed to have a high proportion of GC nucleotides.

FIGURE 6.6: *Metallibacterium* assembly and *Metallibacterium scheffleri* ANI whole genome alignments. Average Nucleotide Identity (ANI) comparison between the assembly and consensus genome sequence. Plot produced via *FAST-ANI* on *Proksee.*

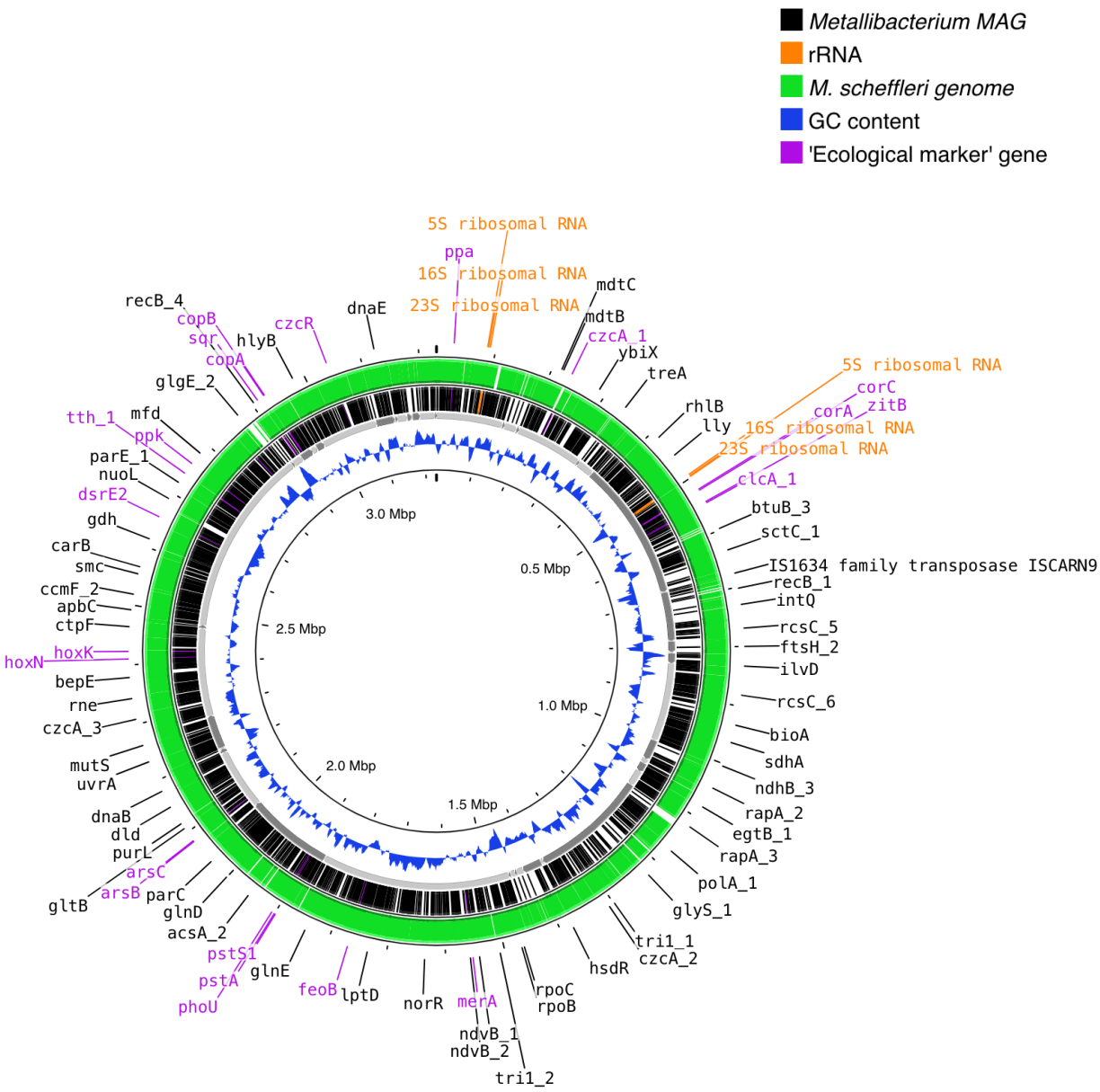

FIGURE 6.7: Structure and predicted genomic content of the assembled *Metallibacterium* chromosome (MAG 6). The 3.07 Mb *Metallibacterium* assembly (black) is shown aligned to the 3.97 Mb consensus genome sequence of *Metallibacterium scheffleri* (green) [*RefSeq Genome Accession: GCA_002077135*]. Key functional genes involved in specific processes (*e.g., merA* involved in mercury detoxification) have been highlighted in purple. Non-coding rRNA are shown in orange. Non-coding tRNAs, the single tmRNA and repetitive region have been removed for clarity. GC skew is shown in blue. Genomic annotations determined via *Prokka.* Chromosome map prepared using *Proksee.*

Due to the near-complete assembly of the chromosome, genes involved in three glycolytic pathways were identified, as well as components of the canonical electron transport chain, *e.g., cydA, ctcC, ctaE, fbcH* (**Figure 6.8 A).** Glycoside hydrolases were the most common carbohydrate active enzyme detected within the assembly. The pathway for the TCA cycle demonstrated 87.5 % completeness (**Figure 6.8 B)**. The ability to potentially use the glyoxylate shunt modification of the TCA was also partially complete.

The ability to perform autotrophy was observed within the genomic content. The MAG contained a near-complete pathway for performing the Calvin-Benson-Bassham (CBB) Cycle (with key genes detected including: *cbbA, cbbX, ccbY*). Additionally, the *Metallibacterium* MAG contained 70.0% of the genes required for the autotrophic reductive tricarboxylic acid (rTCA) cycle (**Figure 6.8 B)**.

The *Metallibacterium* MAG contained numerous genes involved in tolerance to heavy metals within the chromosome. The use of chromosomally encoded efflux systems to counteract the effects of a broad range of transition metals were indicated by *hox* genes, which allows bi-directional transport of Ni^{2+} and Co^{2+} ions. Additionally, *zitB, czcA* and *corA* all present and confer resistance to multiple ion species (Zn, Co, Cd) More specifically, mercury, arsenic and copper resistance mechanisms were evident via the *merB, arsB*/*arsC* and *copA*/*copB* genes, respectively. The general heavy metal transport gene *atm1* was also present.

Evidence of iron cycling was limited within *Metallibacterium;* the MAG indicates the potential to produce the iron-uptake protein, FeoB, yet no other iron cycling mechanisms were evident. However, genes involved in sulphur metabolism proved more numerous within the assembled genome including genes involved in sulphur trafficking and oxidation of sulphur-containing substrates (*e.g., sqr, tth, tsdA, dsrE, tusA)*.

Acquisition of phosphorus by *Metallibacterium* was observed via numerous genes in the *pho* and *pst* families involved in phosphorus uptake. Acid tolerance was indicated by the ability to produce *clc*-encoded channels and *amtB* facilitated transport mechanisms.

The 16S rRNA sequence retrieved from the *Metallibacterium* MAG was determined to be taxonomically related to that of *M. scheffleri* (**Figure 6.9**). However, phylogenetic alignment of the full length 16S rRNA sequence to other taxa indicates that the *Metallibacterium* MAG is only distantly related to closest cultivated species with < 94% rRNA sequence similarity. **Figure 6.10** demonstrates an overview of the metabolic features of *Metallibacterium*.

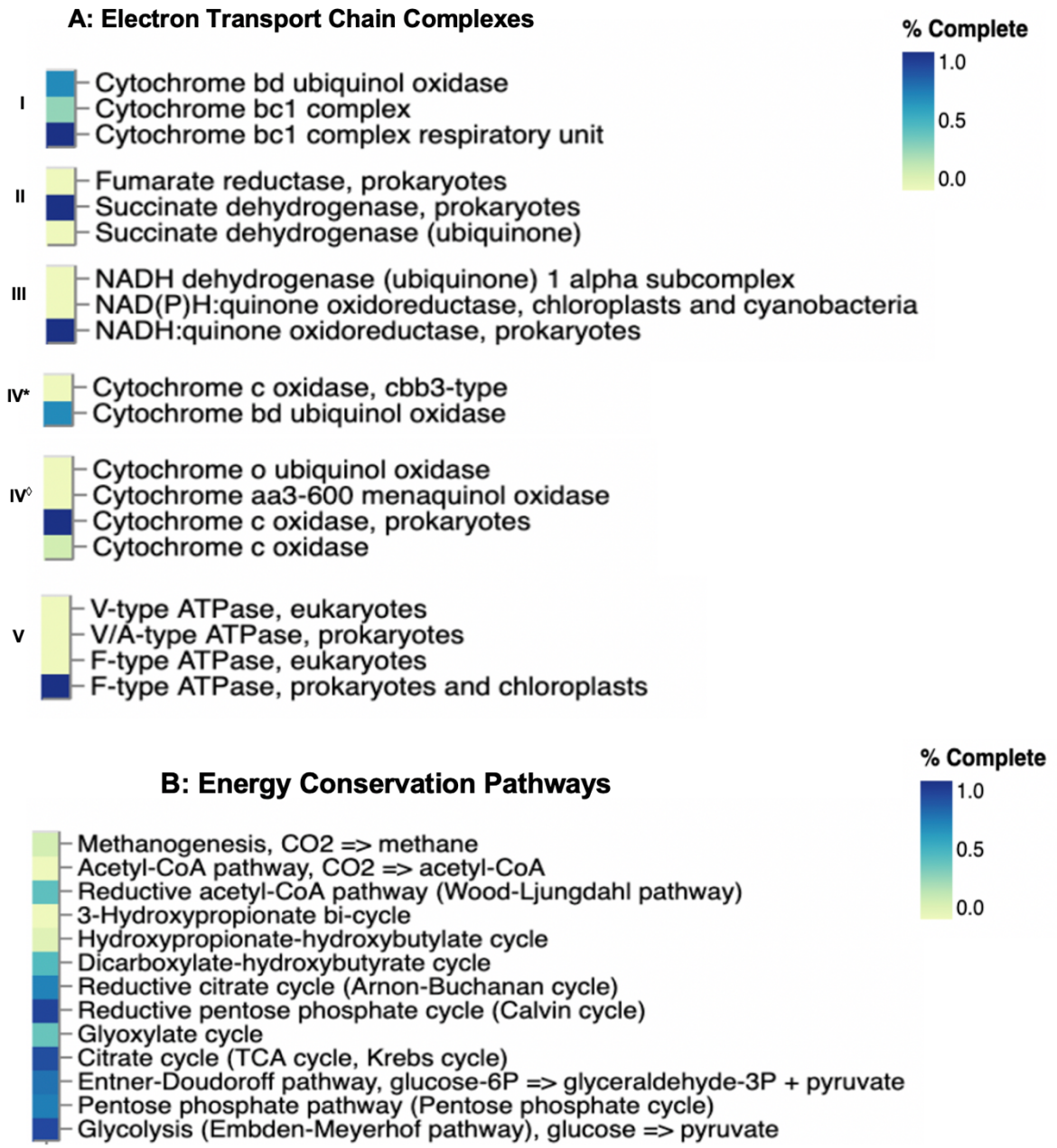

FIGURE 6.8 Central metabolic pathways and energy conservation mechanisms present in the *Metallibacterium* MAG as predicted via Distilled and Refined Annotation of Metabolism (DRAM) tool (A): Completeness of metabolic pathways involved the synthesis of electron transport chain complexes in *Metallibacterium.* **(B):** Respective completeness of individual of energy conserving pathways in *Metallibacterium.*

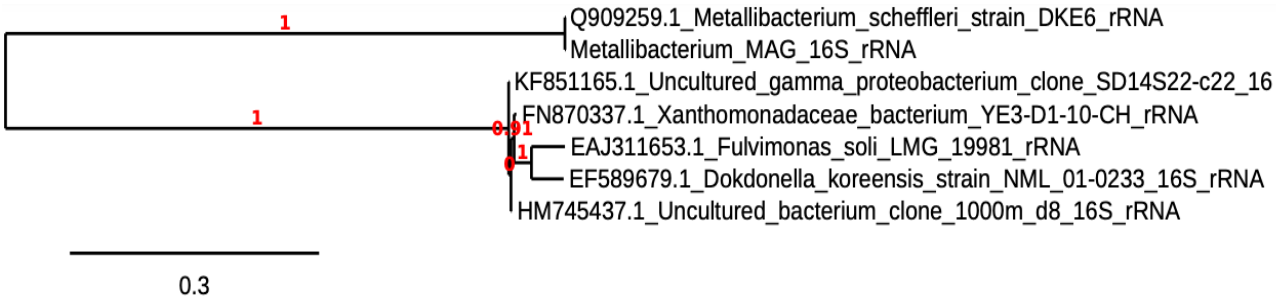

Figure 6.9: Phylogenetic position of *Metallibacterium* MAG based on full length 16S rRNA gene sequence. Multiple sequence alignment indicates that the rRNA gene sequence of *M. scheffleri* is close to that of the Benhar Bing *Metallibacterium.* Evolutionary distance to cultivated *Fulvimonas* and *Dokdonella* is evident through branch lengths. Phylogeny produced using the EBI ClustalW phylogenetic tool.

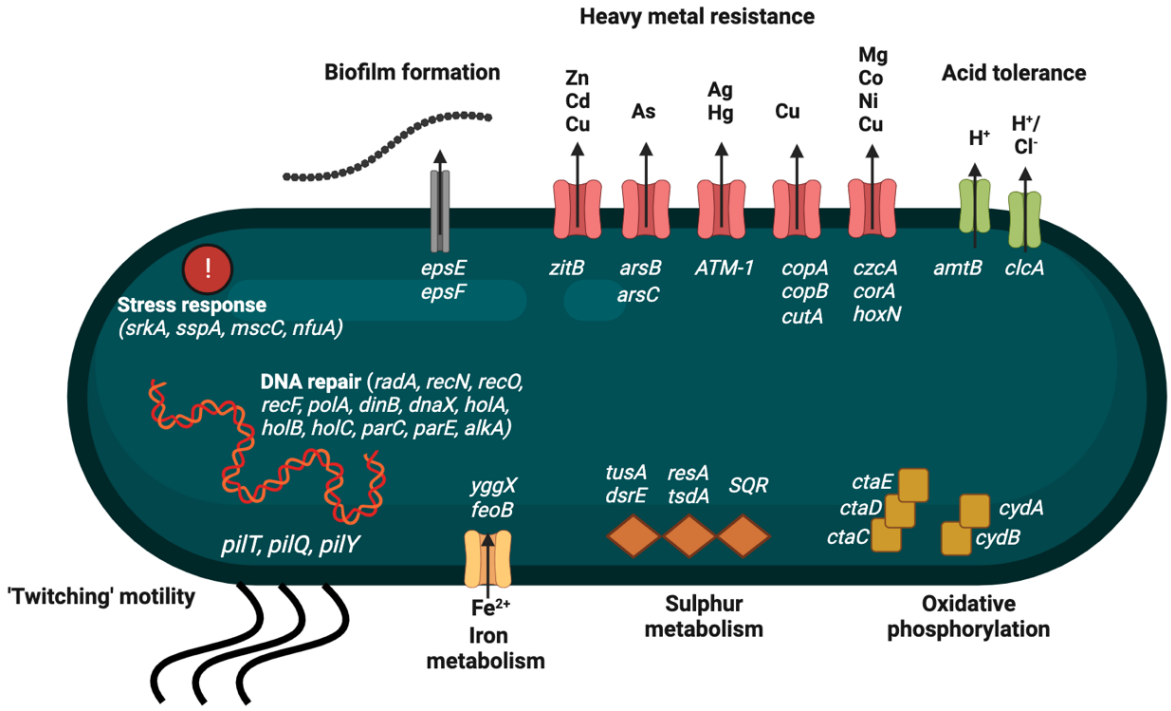

FIGURE 6.10: Summary of the metabolic features of *Metallibacterium* Identified from the genomic content of the assembled MAG. Heavy metal resistance mechanisms (pink channels) and acid tolerance mechanisms (green channels) enable *Metallibacterium* to withstand elevated metal concentrations and invasive H^+ ions. Numerous genes involved in DNA repair and stress response were detected. The use of sulphur oxidation (brown diamonds) to generate ATP was evidence. *Metallibacterium* can perform oxidative phosphorylation and multiple glycolytic pathways (brown squares).

6.3.3 MAGs Classified in the Phylum Actinomycetota (MAG 3 and MAG 5)

Two genomic assemblies with > 70% completeness were determined to be partially reconstructed chromosomes pertaining to taxa within the Actinomycetota. MAG 3 was taxonomically determined to belong to a member of the *Mycobacterium* (77.82% complete, with 5.23% contamination detected). The assembly was larger than those for the annotated Pseudomonadota MAGs (6.03 Mb), with 68.9% GC content (**Table 6.1**). The *Mycobacterium* assembly contained 55 tRNAs, one repetitive region, a single tmRNA gene and three rRNA genes (one copy of 16S, 5S and 23S rRNA genes located together within a single operon). The MAG contained 8257 protein coding regions; 5113 (61.9% of the assembly) had undetermined annotation. The remaining 3144 exons (38.1% of annotated coding sequences) were attributed with specific functions. The structure of the *Mycobacterium* MAG is shown in **Figure 6.11**

The single 1483 bp 16S rRNA gene of the MAG shared 96.47% sequence identity to that of *Mycobacterium bohemicum*. The ANI of homologous regions between the MAG and the genome of *Mycobacterium bohemicum* was 79.71%. (See **Figure 6.12).** The taxonomic position of the *Mycobacterium* MAG relative to other related mycobacteria is shown in **Figure 6.13.**

Despite being MAG 5 being classified as a medium-quality MAG (> 70% complete with < 10 % contamination), the assembled chromosome could not be taxonomically resolved below class level. From taxonomic binning, MAG 5 was predicted to be a reconstruction of a genome from a member of the Actinomycetia (**Table 6.1**). Based on 16S rRNA sequence retrieved from the assembly, the MAG host may be a '*Aciditerrimonas* related' taxon (16S rRNA similarity < 96 %). Results of the annotation of the 4.38 Mp assembly demonstrated that only 24.6% of the genome could be affiliated with known function. Most proteins were deemed to have hypothetical or putative function, and annotated proteins related to processes involved in central metabolism and carbohydrate utilisation. Therefore, MAG 5 results are not presented due to limited functional resolution. Only MAG 3 pertaining to *Mycobacterium* (**Table 6.1**) from the Actinomycetota was selected for further annotation and is presented below.

6.3.3.1 The Mycobacterium Assembly (MAG 3)

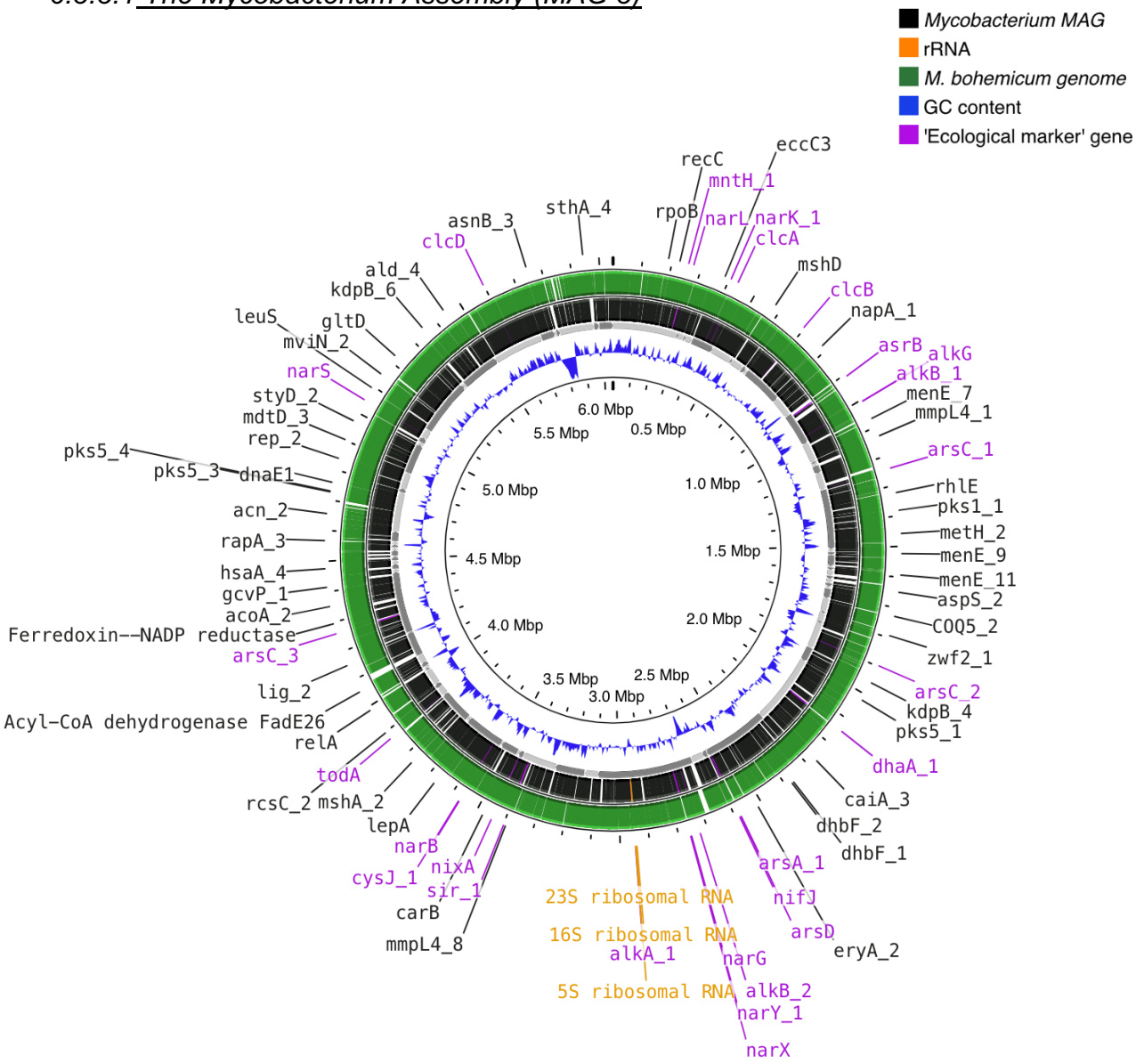

FIGURE 6.11: Structure and predicted genomic content of the assembled *Mycobacterium* chromosome. The 6.03 Mb *Mycobacterium* assembly (black) is shown aligned to the 6.45 Mb consensus genome sequence of *Mycobacterium bohemicum* (green) [*RefSeq Genome Accession: GCA_001053185*]. Key functional genes involved in ecological processes (*e.g., alkB* involved in hydrocarbon degradation) have been highlighted in purple. Non-coding rRNA are shown in orange. Non-coding tRNAs, the single tmRNA and repetitive region have been removed for clarity. GC content is shown in blue. Genomic annotations determined via *Prokka.* Chromosome map prepared using *Proksee.*

The *Mycobacterium* reconstructed genome demonstrated genes involved in arsenic detoxification (*arsA, arsB, arsC, arsD*), as well as the divalent cation transport mechanism encoded by *mntH*. The ability of *Mycobacterium* to both tolerate and acquire nickel was indicated though *nix* genes.

The genome also encoded several genes involved in alkane degradation and cycling (*alkB, alkG*) and phenolic compound oxidation; the toluene monooxygenases *tsaB* and *todA* were present. The ability to express *dhaA* also encoded on the chromosome would allow degradation ability towards haloalkanes by *Mycobacterium*. Further to these functional attributes, acid buffering mechanisms were evident via *clcA*/*clcD*-encoded proteins.

Nitrogen cycling capabilities were observed within the *Mycobacterium* MAG. Nitrate reductase subunits (*narB, narX and narY and narG)* were present, as was the functional potential to produce NarK, the nitrate/nitrite transporter protein. The metabolic ability to cycle sulphur was apparent, with the sulphite reductase encoding genes *sir and cysJ* both present.

More broadly, components of the cytochrome system were detected for oxidative phosphorylation (*e.g., bo3* and *c*-type cytochromes) as well as genes involved in carbohydrate degradation (*baeB, nylA,* and other putative hydrolases), the β-oxidation pathway and protein utilisation mechanisms (*e.g., clpP, ansP, ngcG* and additional proteases).

A summary of key physiological results indicated by metagenomic functional potential in *Mycobacterium* is shown in **Figure 6.14**

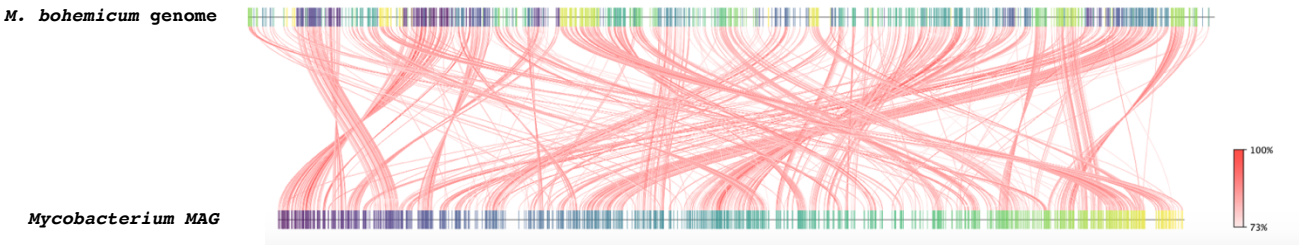

FIGURE 6.12: *Mycobacterium* assembly and *Mycobacterium bohemicum* ANI whole genome alignments. Average Nucleotide Identity (ANI) comparison between the assembly and consensus genome sequence. Plot produced via *FAST-ANI* on *Proksee.*

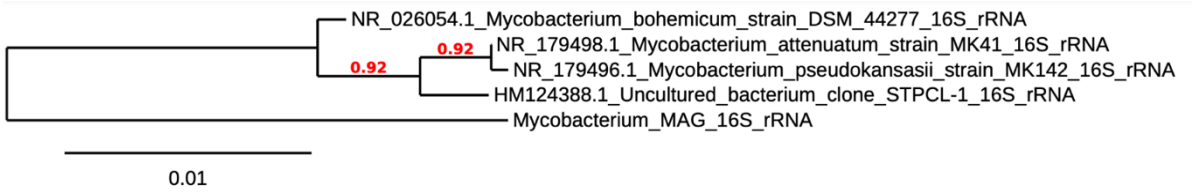

FIGURE 6.13: Taxonomic position of the *Mycobacterium* MAG based on full length 16S rRNA sequence. The Benhar Bing *Mycobacterium* does not have an exact 16S rRNA sequence match and is most closely related to *Mycobacterium bohemicum,* however evolutionary distance is evident. Phylogeny produced using the EBI ClustalW phylogenetic tool.

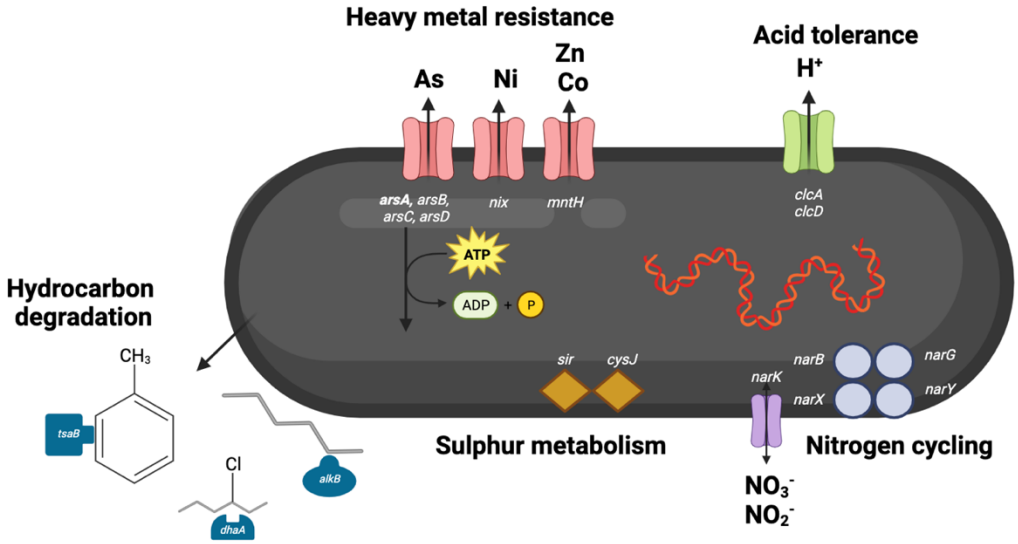

FIGURE 6.14: Summary of the metabolic features of *Mycobacterium* identified from the genomic content of the assembled MAG. Pink and green membrane bound channels indicate responses to acid and metals; the expression of *arsA* (shown in bold) and couple to ATPase activity. Brown diamonds indicate genes involved in oxidation of sulphur compounds and nitrogen cycling capabilities shown in purple. Secretion of enzymes capable of degrading structurally diverse hydrocarbons shown in blue.

6.4 Discussion

The assembly of several high-quality assembled genomes from Benhar Bing and subsequent genomic annotation provides both valuable insights into ecosystem function in highly contaminated systems and adds to the limited pool of genomic resources from heavily contaminated and metal-polluted sites. Several functional capabilities detected within the MAGs presented in this chapter have not yet been observed for the species outlined: *Metallibacterium, Acidiphilum* and *Mycobacterium*. Additionally, the genomic annotations bring further attention to overlooked metabolic routes and demonstrate diverse metabolic capabilities involved in heavy metal detoxification, acid tolerance and the ability to proliferate under nutritional scarcity utilised by polyextremophilic taxa. Taken together, the metabolic attributes outlined here present a considerable overview of microbially-mediated ecosystem function in heavily polluted sites. The functional attributes and metabolic potential of the MAG with the highest completeness, *Metallibacterium,* will be discussed first, followed by the *Acidiphilum* assembly. Following this, the genomic annotation results from the *Mycobacterium* MAG will be discussed.

6.4.1 The Genome Structure and Metabolic Potential of MAG 6 – Metallibacterium

The *Metallibacterium* assembly provides novel insights into the biogeographical dispersal, metabolism, and ecological attributes of this poorly studied and underrepresented organism. To date, *Metallibacterium scheffleri* is the sole isolate of its genus, and literature regarding the physiology of the taxon is scarce, and often conflicting. The Gram negative, non-motile isolate was initially cultivated in the work of Ziegler *et al*. (2013b) from a biofilm sample collected from a pH 2.5 acid mine drainage site in Germany. The site is known to have elevated levels of iron sulphides, indicative of mining contamination, however the prevalence and composition of other metals has not been reported (Ziegler *et al*., 2009).

The Benhar Bing *Metallibacterium* shares a similar biogeographical niche and is likely *M. scheffleri* based upon the observed similarity between 16S rRNA sequences. It is evident from the phylogenetic position of the *Metallibacterium* from Benhar Bing that it is chemotaxonomically dissimilar from *M. scheffleri's* closest cultivated relatives, which do not show adaptations to acidic environments. Due to the challenges associated with cultivating acidophiles, it is likely the closer, yet uncultivated matches, are other *Metallibacterium*-related species which have been challenging to grow axenically. The MAG annotation provides valuable insights into the metabolic strategies available to *Metallibacterium,* which may be key to target in more tailored cultivation strategies in future work.

The high ANI between the assembly sequence and the isolate's genome corroborate the MAG being reflective of a *M. scheffleri* genome. Resolving the apparent genomic rearrangement present between the *Metallibacterium* MAG and the genome of the *M. scheffleri* isolate would require further work, and may be artefactual, resulting from incorrect contigs overlapping during genome assembly. It has been noted that contigs generated from Nanopore long-reads can misassemble when numerous respective overlapping regions may share homologous DNA sequences (homopolymer regions), or if the assembled contiguous regions of the genome contain integrated transposable or other mobile genetic elements with repetitive sequences (Meng *et al*., 2022). This was noted to have led to several misassembled loci in the reconstructed genome of the pathogenic anaerobe, *Porphyromonas gingivalis,* in the work of Amador *et al*. (2018). However, to correctly resolve the genome structure, the authors required the cultivation and analysis of genomes reassembled from three *P. gingivalis* strains to improve

the initial chromosomal assembly. In this case, the incorrect placement of several loci was noted when reconstructing a genome from a single isolate, and issues regarding apparent and artificial translocations of genomic material can be more challenging to resolve in mixed metagenomic reads.

It should be noted that repetitive genomic regions between 1 – 2 kb, as was observed in the single repetitive region present within the *Metallibacterium* MAG, are unlikely to cause erroneous assembly alone and have little impact on functional prediction due to their truncated length (Nelson *et al*., 2020). To rectify any potential artefacts caused by MAG assembly would require cultivation of a *Metallibacterium* species from Benhar Bing to determine the composition of the genome from an isolate, rather a reconstructed chromosome. The work of Meng *et al*. (2022) states that approaches to identify and correct misassembled regions within MAGs is one of the key foci within the continual development and refinement of genome assemblers.

Importantly, Tripathi *et al*. (2017) state that extremophiles can demonstrate elevated levels of genome dynamism and members of the same genus may have highly variable genomic structure; maintaining a dynamic pan genome can promote metabolic flexibility and survival under harsh abiotic conditions. In part, extremophiles may be capable of species-specific inversions and other genomic rearrangements due to being naturally competent, and this has been noted to occur widely within thermophilic genera (*e.g., Thermus* species). Yet, current knowledge of genomic flexibility is less-well documented in acidophiles. Additionally, as *Metallibacterium* is poorly studied, and is currently represented by a single isolated species, performing similar genomic analysis at this point is not feasible until the genus becomes better characterised and the number of isolates increases. However, genes present within the assembly which may be mobile, or derived from previously integrated sequences were predicted using the mobileOG-db tool as developed by Brown *et al*. (2022). The location of these genes within the *Metallibacterium* MAG and the predicted classes of mobile genetic elements are available in the **Supplementary Data (Figure S2)**.

Initial *M. scheffleri* cultivation concluded the organism had a narrow metabolic repertoire. Ziegler *et al*. (2013b) determined that the isolate could only utilise a single carbon source. Yet, further metabolic work by Bartsch *et al*. (2017) stated that the isolate had a more diverse carbon-based metabolism than originally thought, and concluded the use of three major glycolytic routes, which the MAG presented here also confirms, particularly the pentose phosphate pathway (PPP), the Embder-Meyerhof-Parnas Pathway (EMPP) and the Enter-Doudoroff Pathway (EDP); the EDP has been reported as the most common alternative glycolytic route in Gram negative *Bacteria* (Venturini *et al*., 2022). Importantly, analysis of carbohydrate activity enzymes involved in central metabolism indicated that glycoside hydrolases were the most common enzyme class within the *Metallibacterium* MAG sequence. Recently, Ashcroft and Munoz (2024) have suggested that glycoside hydrolases are promising enzymes to exploit in various bioprocesses, due to their stability and reactivity. This is particulate pertinent to extremozymes from this protein family, capable of functioning under extrme abiotic conditions.

Protein degradation may be essential to *Metallibacterium* to survive in low pH conditions. Bartsch *et al*. (2017) suggested that *Metallibacterium* could produce ammonium to buffer the surrounding microenvironment, elevating the pH. Little evidence was provided regarding a mechanistic approach to this; however, the MAG assembled here suggests that putative amino acid permeases (*e.g*., YdhG) could produce NH_4^+ from amino acid precursors, which could exit the cell via *amtB* encoded ammonium transporters also evident in the assembly. This would be an advantageous and previously only a tenuously suggested adaptation to low pH conditions, preventing acid-induced damage to the genome, and other cellular structures.

To date, the YdhG protein is poorly characterised, however shares to homology to other permeases involved in amino acid import and translocation within the cell; expression of *ydhG* has been demonstrated in soil-dwelling species of *Burkholderia* and the candidate genus *Udaeobacter* (Knapp *et al*., 2016; Willms *et al*., 2020). Following uptake of amino acids via the YdhG channels, potential cleavage, and remobilisation of the nitrogen-containing amide (-NH_3) functional group could lead to the production of NH_4^+ following bacterial deamination (Yu *et al*., 2020). Additionally, the use of *clc* encoded proteins present in the genome assembly are proposed to have roles in H^+ extrusion and buffering of the intracellular environment. Clc-proteins may also influence the use of compatible solutes to overcome acid stress in low pH environments (Boase *et al*., 2022).

Initial metabolic work reported that the *M. scheffleri* isolate was capable of both sulphur oxidation and reduction, however sulphur reduction resulted in weaker colony formation. Conversely, the work of Bartsch *et al*. (2017), did not suggest any ability to perform sulphur reduction, and the discrepancies between findings regarding anaerobic growth by *Metallibacterium* warrants further work. However, the successful reconstruction of the *Metallibacterium* MAG does expand on the functional potential of the taxon to oxidise sulphur. The sulphur redox reactions which underpin much of the dominant energy conservation and ecosystem function in AMD were originally elucidated in *Acidothiobacillus* species and are less widely documented in other acidophilic and acid-tolerant taxa. Bartsch *et al*. (2017) suggested that a homolog of the sulphur oxidising gene from *Acidothiobacillus, tetH*, was involved sulphur-mediated oxidative processes in *M. scheffleri*. The *Metallibacterium* MAG confirms this ability, as *tth* present in the assembly could allow the oxidation of tetrathionate ($S_4O_6^{2-}$) resulting in the production of thiosulphate (S_2O^{3-}), sulphate (SO_4^{2-}) and elemental sulphur (S^0).

Further utilisation of S_2O^{3-} is achievable through use of the *tsdA* gene, encoding thiosulphate dehydrogenase/tetrathionate reductase, also present in the *Metallibacterium* MAG. Expression of *tsdA* is responsible for the conversion of thiosulphate back to tetrathionate via iron redox carriers localised within *c*-type cytochromes (Denkmann *et al.,* 2012). The use of the TsdA protein has also been elucidated in other acidophilic and metal tolerance taxa such as *Thiomonas intermedia* and *Sideroxydans lithotrophicus* (Kurth *et al.,* 2016). Due to the noted bifunctional properties of thiosulphate dehydrogenase/tetrathionate reductase, expression of *tsdA* may indicate some ability of sulphur reduction in *Metallibacterium*.

Furthermore, the use of sulphides via expression of *sqr*, encoding sulphide:quinone oxidoreductase present in the chromosomal assembly may be an additional potential sulphur oxidising route for *Metallibacterium*. This *sqr* encoded mechanism for sulphur utilisation has also been noted in other taxa such as *Sulfurovum indicium* capable of sulphur redox reactions (Wang *et al.,* 2023a). The exact enzymatic kinetics of sulphide:quinone oxidoreductase have been challenging to elucidate due to the limited success in isolating *sqr*-encoded enzymes in an active state from their native hosts (Duzs *et al.,* 2021). However, the expression of *sqr* is considered to lead to the generation of cyclic forms of elemental sulphur following consecutive reactions mediated by the Sqr protein. Taken together, the presence of both *sqr* and *tsdA* expands somewhat on the previously disputed potential sulphur cycling capabilities of *Metallibacterium*.

The expression of *tusA* involved in sulphur trafficking and dissimilatory sulphur oxidation is another predicted metabolic route for *Metallibacterium* to exploit. Importantly, the TusA protein may exhibit broad pleiotropic function and TusA variants can facilitate the routing of intracellular sulphur into specific pathways, for example, redox reactions involving Fe-S clusters or facilitating the intracellular sulphur relay system involved in protein synthesis and degradation (Dahl, 2015; Tanabe *et al.,* 2019). The sulphur carrier protein, encoded by *dsrE,* is also considered to be involved in sulphur trafficking during oxidative sulphur metabolism. Neither the use of TusA or DsrE proteins have been discussed previously for *Metallibacterium*.

A summary of the novel insights into sulphur cycling capabilities evident in the assembled *Metallibacterium* chromosome are demonstrated in the reactions below (**Figure 6.15**).

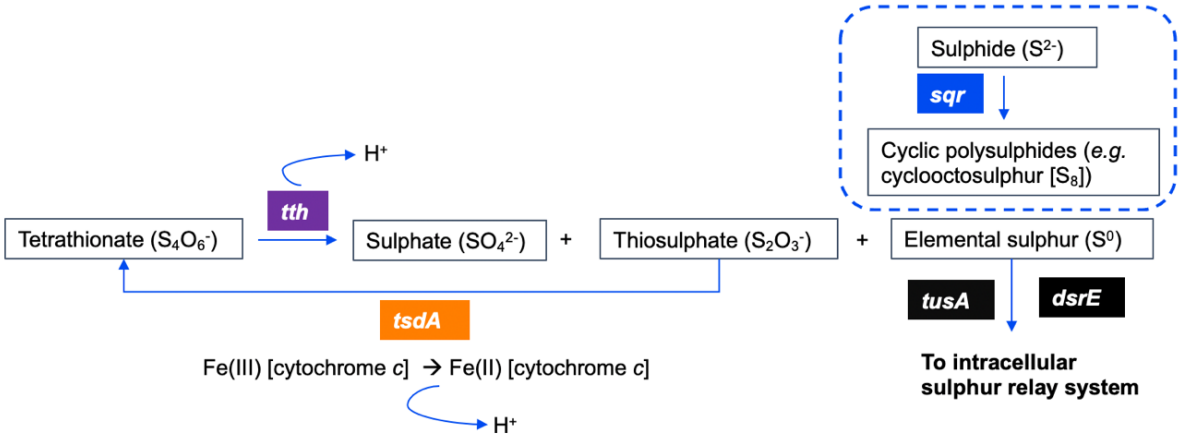

FIGURE 6.15: Proposed sulphur cycling capabilities in *Metallibacterium* (MAG 6). Oxidation of tetrathionate to produce sulphate, thiosulphate, and elemental sulphur proceeds via *tth* expression (shown in purple). Reduction of thiosulphate is proposed to occur via *tsdA* expression (orange). Oxidation of sulphides (blue dashed box) can occur via use of the *sqr* gene (shown in blue), before elemental sulphur produced is trafficked into central metabolism via the protein products of *tusA* and *dsrE* expression (black boxes).

The putative ability to perform carbon fixation in *Metallibacterium* was first discussed by Bartsch *et al*. (2017) and was not determined in the work of Ziegler *et al*. (2013b). Again, the genomic content of the MAG assembled here indicates genes involved in carbon fixation, particularly a near-complete set of genes involved in the Calvin Bassham Benson cycle, and some indication of the reductive tricarboxylic acid cycle (rTCA). The use of the rTCA is not widely reported and has not been discussed for *Metallibacterium* previously. The use of the rTCA in conjugation with the more dominant form of autotrophy, the CBB cycle, has been reported in other sulphur oxidisers, principally *Thioflavicoccus mobilis*. However, this appears to be an infrequently exploited energy conservation strategy amongst autotrophic taxa (Markert *et al*., 2007; Rubin-Blum *et al*., 2019). However, this may provide an additional autotrophic route for *Metallibacterium*.

Yet, strict autotrophy may not be possible by *Metallibacterium* due to proposed metabolic auxotrophies within the species. Auxotrophic limitations are still not fully elucidated; Ziegler *et al*. (2013b) did not discuss this physiological characteristic, while Bartsch *et al*. (2017) suggested potential amino acid auxotrophies, but not in detail. As the *Metallibacterium* MAG sequence was practically complete, a gap-fill metabolic model was performed using the ModelSEED pipeline on the annotated genome to determine whether the host *Metallibacterium* could be cultivated on growth medium constraining glucose, all amino acids, and vitamins. The model did indicate the absence of genes involved in polyamine synthesis, potentially required for growth in culture but did not suggest amino acid limitation and suggested cultivation would be feasible.

Previous work on *Metallibacterium* referred to the cellular exposure to heavy meals through habitat dispersal in mining waste, yet neither work provided insights in mechanisms for survival and tolerance in otherwise deleterious concentrations of mine-derived pollutants. Arsenic has been detected in AMD waste and can exist as various ion species in the environment. Arsenic resistance mechanisms were evident in the *Metallibacterium* genome: *arsB and arsC*, which encode the arsenical pump membrane protein and arsenate reductase, respectively (Uddin *et al*., 2022). The *ars* operon structure has been determined in several metal resistance taxa, however never in *Metallibacterium*. The operon has been shown to be structurally variable, with components being carried on plasmids in some species (Kabiraj *et al*., 2022).

In acidic conditions, the arsenate ion (AsO_4^{3-}) is the predominant form of arsenic; *arsC* facilitates the reduction of AsO_4^{3-} to arsenite (AsO_3^{3-}), conferring resistance to *ars* carrying organisms, including the *Metallibacterium* species described here. The extrusion of arsenite from the cell prevents the toxic effects of the metalloid interfering with proteins and avoids the arsenic-induced uncoupling of the TCA cycle from ATP generation (Hughes, 2002). The AsO_3^{3-} ion remains mobile in solution (Koechler *et al*., 2015); yet no further oxidative capabilities involved in arsenic conversions to the more stable As^{5+} state were apparent in the *Metallibacterium* MAG. Resistance to the hazardous metalloid antimony (Sb), also noted to be in elevated concentrations acid mine drainage waters, may also be conferred to metal(loid) resistant taxa through expression of *ars* genes due to the arsenic and antimony sharing similar atomic configurations and electronegativity (Laroche *et al*., 2023).

Regarding environmental removal of arsenic, only *Corynebacterium glutamicum* has been suggested as a potential candidate for bioremediation of arsenic to date (Mateos *et al.,* 2006). However, not being an acidophile, *C. glutamicum* may struggle with the abiotic challenges of AMD remediation if required for use *in situ,* potentially preventing environmental amelioration of contaminating metalloids. Further work could focus on the ability of *Metallibacterium* and other native community members to co-metabolise arsenic-containing compounds, reducing their toxicity and mobility. There is a need to develop sustainable bioremediation technologies to counteract the levels of toxic metalloids caused by excessive exploitation of metals. Arsenic contamination in water supplies has been reported in over 100 countries and is considered the most significant drinking water contaminant globally (World Health Organisation, 2022). The designation of arsenic as a class I human carcinogen stresses the requirement for urgent remediation of contaminated effluents (Martinez *et al.,* 2011; Shaji *et al.,* 2021).

Contaminated leachates produced from mine wastes have also been noted to contain elevated concentrations of mercury (Hg) which is toxic to multiple physiological systems; damage to neurons, cells of the immune system and the kidneys is widespread following exposure to mercury (Yang *et al.,* 2020; Martins *et al.,* 2021). Due to this, mercury is classed as one of the World Health Organisation's priority chemicals for environmental monitoring and removal (Vincenten *et al.,* 2020). Iron sulphides present in mine wastes, particularity cubic pyrite, act as the main host mineral and carrier of toxic mercury; inorganic sulphide minerals show high adsorption capacity for mercury sulphide (HgS) (Manceau *et al.,* 2018). This co-occurrence of Fe- and Hg-containing minerals compounds the challenges associated with regeneratively produced pollutants, particularly the subsequent release of mercuric compounds resulting from the microbial dissolution of pyrite. The fate of mercury is dependent on its chemical configuration, with $Hg^{2+}_{(aq)}$ being commonly released from ores via concomitant oxidation of iron. In some cases, isomorphous replacement of Fe(II) for Hg(II) in pyrite's structure has been noted (Wu *et al.,* 2023). Tolerance to mercury (Hg) via *merA* expression was detected in the *Metallibacterium* MAG, a function not discussed previously for this organism.

The ability to utilise *merA* by *Metallibacterium* results in Hg^{2+} conversion to elemental Hg^0. Ionic forms of mercury are highly thiophilic and prolifically bond to sulphur containing ligands; the metal also has no known biological function and therefore poses a risk to the intracellular environment (Wagner-Dobner, 2003). The removal of mercury is thought to occur as a vapour due to the high vapour pressure and low solubility of mercury when in the monoatomic state. Microbial oxidation of elemental mercury has been assumed to be largely insignificant, and the reduction route to Hg^0 may promote closure of the mercury redox cycle (Yu and Barkay, 2022). The *atm1* gene, involved in heavy metal export, present in the *Metallibacterium* MAG may also confer some resistance to mine-derived mercury-containing compounds.

Importantly, reduction to Hg^0 can prevent the production of methylmercury (MeHg), a potent and mobile organic form of the toxicant, as elemental mercury is deemed chemically inert and less able to bond to $-CH_3$ side chains. Elevated concentrations of MeHg have been observed in mine effluents, particularly in the western United States where local geology can influence MeHg generation (Eckley *et al*., 2021). The work of Priyadarshanee *et al*. (2022) suggests that *merA* may also partially facilitate demethylation of MeHg complexes, promoting detoxification back to the Hg^{2+} cation, before final reduction to elemental mercury. Due to this, *mer*-expressing extremophiles are sought after candidates of mercury remediation due to the well documented negative effects of mercury on human and environmental health (Buck *et al*., 2019; Basu *et al*., 2022).

Barkay *et al*. (2003) observed that *mer* containing operons are highly variable, with resistance genes being located on chromosomes, plasmids, or other transposable elements, even across differing genomic cassettes within the same bacterium. Further genomic analysis of cultivated *Metallibacterium* would be required to elucidate the organisation and transcriptional response of the *merA* gene. The use of *mer* encoding genes is considered unique across the prokaryotic metal detoxification strategies, due to the major atomic reconfiguration of the target ion species, as opposed to other mechanisms dependent on the production of metal complexes or the use of efflux pumps.

Resistance to elevated metal concentrations via efflux proteins which transport multiple metals was also detected in *Metallibacterium* including *hoxN, zitB and czcA* which can prevent the deleterious influx of nickel, cobalt, and zinc ions into the intracellular environment. The *Metallibacterium* MAG did not indicate utilisation of iron, only the presence of an iron-uptake protein, FeoB. Again, incongruities exist regarding iron metabolism of *Metallibacterium* in the literature. Ziegler *et al*. (2013b) suggested some weak iron reducing capabilities. However, Bartsch *et al*. (2017) and this work did not find evidence of iron cycling, or any other anaerobic respiratory pathways in *Metallibacterium*. Lastly, acquisition of phosphorus has been documented to be impaired in heavily contaminated soils (Liu *et al*., 2023). Both *pho* and *pst* genes involved in phosphorus uptake, previously not documented for *Metallibacterium,* could be potentially expressed to ensure phosphorus homeostasis is maintained in in the presence of pollutants.

6.4.2 The Genome Structure and Metabolic Potential of MAG 2 – Acidiphilium

To date, the genus *Acidiphilium* consists of six cultivated species. *Acidiphilium* species are considered the dominant members of the Acetobacteriaceae which are capable of colonising extremely low pH niches, where other members of their taxonomic family may be excluded or less prevalent (Li *et al*., 2020a). Despite being considered core members of acid mine drainage consortia, only limited metabolic profiling has been performed on the genus, principally the use of iron sulphides common in AMD effluents (Jones and Santini, 2023).

The *Acidiphilum* assembly indicated the ability to perform carbon fixation and photosynthesis. Photosynthesis has not been widely reported in acid mine drainage sites, whereby much of the metabolism is dominated by sulphur and iron cycling. Freshwater systems which are impacted by high levels of AMD contamination can be detrimental to photosynthesis as discoloration of the receiving waterbody by metal precipitates can prevent light penetration (Geller *et al*., 2012). Despite this, the *Acidiphilum* MAG demonstrated the functional potential to synthesise photosynthetic apparatus. This expands on the role of carbon cycling in oligotrophic systems and how primary production is facilitated under extreme environmental conditions. How photosynthesis persists under extreme abiotic stress is largely unexplored; bacteriochlorophyll can be inactivated by competing metals which can replace the zinc required for function. The metal chelatase mechanism (via expression of *cob* genes) present in *Acidiphilum* could have a protective role here, however this would require further work to elucidate fully. Photosynthetic algae have been observed in streams impacted by acid mine runoff, however bacterial species capable of performing photosynthesis have received comparatively less attention (Gomes *et al*., 2020).

The work of Li *et al*. (2020a) suggests that the speciation of *Acidiphilum* occurred ~ 60 million years before the present. After which it is thought that prolific gene acquisition occurred, providing *Acidiphilum* with a broader metabolic repertoire, including photosynthetic ability. It is predicted that the increasing solar intensity combined with a decrease in atmospheric oxygen concentration could have promoted the uptake of carbon fixation genes to overcome the challenges of aerobic growth when oxygen availability was in flux. The ability to utilise high-affinity cytochromes which overcome low oxygen concentrations are also evident in the MAG. Additionally, if environmental conditions do not favour carbon fixation, intracellular reserves of carbon in PHB granules provide routes to ATP via organotrophy. Regarding co-contaminants present in AMD, the *Acidiphilium* assembly indicated some ability to utilise hydrocarbons as additional carbon sources via *alkB,* encoding a monooxygenase capable of cleaving the backbone of hydrocarbons. However, no wider hydrocarbon degradative abilities were evident in the MAG.

Acidiphilium rubrum, first isolated from mine drainage water, is the closest phylogenetic match to the *Acidiphilium* MAG presented here (Matsuzawa *et al*., 2000). The *Acidiphilium* assembly suggests the ability to utilise carbon monoxide as a carbon source for carbon fixation via *cutS*, a mechanism unreported for *A. rubrum* to date. The use of alternative carbon monoxide dehydrogenases has observed in other *Acidiphilium* species. Intragenus metabolic variation of acidophilic taxa has been noted as a strategy to exploit multiple metabolic routes; this discrepancy between closely related species complicates attributing broad function to wider taxonomic levels (Grettenberger and Hamilton, 2021).

Sulphur cycling has been reported for *Acidiphilium* species by several authors (Li *et al*., 2020a; Panyushkina *et al*., 2021), and expression of *soxA* within the MAG is responsible for producing a sulphur-oxidising protein. Further to this, the ability to utilise sulphites was apparent through the presence of *cys* genes; Cys proteins are considered mediators of sulphite-utilising reactions and may have wider sulphur transport and electron carrying capabilities in *Acidiphilium* (Panyushkina *et al*., 2021).

Tolerance of heavy metals by *Acidiphilum* is conferred by potential expression of transporter *mtnH* and *czcD,* involved in the synthesis of efflux pumps which can remove multiple transition metal ion species. Translocation of cadmium, cobalt, copper, and zinc can be exported from the same MtnH and CzcD protein channels, preventing metal toxicity to taxa native to AMD ecosystems (Bosma *et al*., 2021; Courville *et al*., 2008). The *Acidiphilium* MAG also contains both *cobS* and *cobT* involved in the formation of cobalt complexes which facilitate detoxification and sequestration of metals from the environment. Additional chelation pathways have been determined as advantageous adaptation strategies in other organisms, including metal tolerant *Pseudomonas* species (Ducret *et al*., 2023).

Iron cycling is a well-documented form of energy conservation in AMD leachates due to the high concentrations of iron sulphide minerals available for oxidation. The *Acidiphilium* MAG harbours the *iro* gene, reflective of its ability to oxidise iron. It is likely that ancestral *Acidiphilium* underwent emigration into a low pH niche, or the original niche, which was near neutrality, became contaminated with metals and consequently acidified. The ability to utilise metals, such as iron species, by *Acidiphilium* may have been the result of genetic of transfer of mobile iron-utilising genes from the acidophile, *Acidocella* (Li *et al*., 2020a).

The emergence of flagellar proteins in *Acidiphilum* are also thought to have contributed to the organisms' success in acidic niches by allowing avoidance of hazardous conditions (*e.g., fliP, fliE, fliR)*. The use of Fe^{2+} ions is preferential to *Acidiphilium,* however if conditions are unfavourable, iron oxides can be accessed to leach soluble iron ions. *Acidiphilium* is thought to perform this via an energetically costly electron attack directed at oxide surface, potentially mediated by cell surface appendages, providing a dual function to the flagella. It has been proposed that coupling to glycolysis is thought to aid in overcoming the energetic challenge involved in accessing iron-complexes (Leang *et al*., 2003). Despite iron cycling receiving much of the attention regarding AMD biogeochemistry, the metabolic versatility of native consortia members continues to expand, particularly those involved in alternative substrate acquiring strategies.

Despite Li *et al*. (2020a) determining that all cultivated *Acidiphilium* species carry an *ars* encoding operon, the *Acidiphilium* assembly (MAG 2) did not indicate this function. However, early work on *Acidiphilium* isolates suggested that the cell retains the arsenic detoxication ability on a plasmid, which would explain the lack of apparent *ars* operon within the *Acidiphilium* assembly (Ghosh *et al*., 1997; Suzuki *et al*., 1998).

6.4.3 The Genome Structure and Metabolic Potential of MAG 3 – Mycobacterium

Despite the lowest proportion of functionally annotated genes across the three MAGs presented, the *Mycobacterium* assembled genome (MAG 3) contained metabolic capabilities with implications for wider ecosystem function unseen in the other chromosomal assemblies. For comparison, genomic annotation of the complete consensus genome of the MAG's closest cultivated species, *Mycobacterium bohemicum,* revealed 42.70% of the genes present could not be attributed to function. A large proportion of hypothetical genes within a genome is a trend also applicable to more well-studied organisms and not necessarily a reflection of issues with long-read genome assemblies.

Acid tolerance is poorly characterised within the *Mycobacterium*. Members of the genus: *M. avium, M. scrofulaceum* and *M. intercellulare* have been observed in the moderately acidic brown-water swamps of the south-eastern United States by Kirschner *et al*. (1992). Huang *et al*. (2023) assembled a MAG pertaining to *Mycobacterium numidiamssiliense* from a study exploring contaminated water sampled from coal mine treatment ponds, yet as mentioned previously, their genomic characterisation was restrictive and did not assess genes involved in wider ecosystem function. The presence of the *Mycobacterium* native to Benhar Bing expands on current understanding of mycobacterial species biogeographical dispersal in extreme environments.

The *Mycobacterium* assembly is the sole MAG to harbour genes with the ability to degrade a broad range of hydrocarbons, as well as evidence of nitrogen cycling mechanisms. Co-contamination of both hydrocarbons and heavy metals has been observed in a range of low pH ecosystems, including mining impacted soils (Khudur *et al*., 2018); the presence of which can contribute to the challenges both associated with microbial survival and environmental reclamation (Schreiber and Cozzarelli, 2021).

Contamination by hydrocarbons has been noted to pose serious risks to public health, with both aliphatic and cyclic structures exerting toxic effects on mammalian systems though contact with contaminated soils and groundwater. Barbosa *et al*. (2023) states that hydrocarbon activation via binding to the aryl hydrocarbon receptor (AhR)/cytochrome P450 *in vivo* leads to elevated production of reactive oxygen species (ROS), resulting in cellular necrosis as an indirect result of hydrocarbon exposure. Furthermore, polyaromatic hydrocarbons (PAHs) are of increased concern due to their noted haemotoxicity, renal toxicity and carcinogenic properties, as well as the ability of cyclic motilities to persist in the environment for increased durations due to their chemical and structural recalcitrance (Vogel *et al*., 2020).

The presence of *alkB* and *alkG* in the *Mycobacterium* MAG indicate the metabolic potential to degrade *n*-alkanes, which are resistant to other degradative pathways. Alkane 1-monooxygenase, encoded by *alkB*, is capable of hydroxylating alkanes at the terminal methyl group, predominantly converting aliphatic and alicyclic alkanes to alcohols (Rojo, 2005; Groves *et al*., 2023). However, as the enzyme has broad chain length specificity, other resultant organic compounds have been noted including carboxylic acids, aldehydes, and reactive polyepoxies (Chai *et al*., 2023). Production of the AlkG protein aids in hydrocarbon degradation and subsequent energy conservation by transferring electrons via a rubredoxin intermediate to alkane 1-monooxygenase.

Further to *n*-alkane oxidation, the *Mycobacterium* MAG suggests the ability to degrade haloalkanes. Alkanes consisting of halogen functional groups been noted to be components of mixed petroleum hydrocarbons present in ecosystems contaminated with mine-derived and municipal waste effluents (Uno *et al*., 2012). The work of Li *et al*. (2020b) states that haloalkanes are more challenging to degrade than alkanes and alkenes due to the covalent bond strength between the carbon and halogen atom, due to the halogens' well documented high electronegativity. The high affinity for electrons within the halogen-carbon bond can enhance the environmental persistence of haloalkanes.

The presence of *dhaA* within the assembled *Mycobacterium* chromosome indicates the potential to synthesise haloalkane dehalogenase. The expression of the functional DhaA protein would allow hydrolytic cleavage of the carbon-halogen bonds of halogenated aliphatic compounds, producing the resultant alcohol, halide ion and H^+ ions. The ability to express *dhaA* has been observed in other *Mycobacterium* species and importantly, the enzyme has broad substrate specificity for chain lengths ($\geq C_4$) allowing *Mycobacterium* to utilise various haloalkanes as carbon sources (Newman *et al*., 1999; Jesenska *et al*., 2005). Recalcitrant cyclic haloalkanes can also be enzymatically cleaved by DhaA proteins, promoting their removal from the environment, and further expanding knowledge of *Mycobacterium's* substrate flexibility (Novak *et al*., 2014).

Additional phenolic hydrocarbons could be degraded by *Mycobacterium's* ability to produce toluene monooxygenase via *tsaB* expression. Similarly, the MAG encodes *todA*, involved in the electron transport component of the toluene (methylbenzene/C_7H_8) degradation system. Only recently has toluene biodegradation been reported in *Mycobacterium* in a single study by Du *et al*. (2023), whereby a biofilm retrieved from a bio-trickling filter treating toluene waste gas demonstrated an elevated relative abundance of a *Mycobacterium* species. However, due to growth of other taxa within the biofilm, the authors suggested co-metabolism of hydrocarbons was likely occurring with *Pseudomonas* species; specific tolerance or detoxification mechanisms employed by *Mycobacterium* were unexplored.

Degradation of both toluene and other phenolic compounds has been more widely explored in pseudomonads as well as within the rhodococci. Notably, the mycolic acid containing actinomycetes, to which *Mycobacterium* belongs, are often dominant members of microbial ecosystems impacted by anthropogenic pollution (Matsubara and Hurtado, 2013; Sims *et al*., 2022). Given the degradative abilities towards a range of hydrocarbons observed within the *Mycobacterium* MAG, members of the *Mycobacterium* should not be discounted when considering bioremediation strategies for the removal of hydrocarbons from contaminated systems. Importantly, many mycobacterial species are noted opportunistic pathogens and can readily colonise and persist in hosts through prolific biofilm production and rapid alternations in gene expression, ensuring their survival despite the slower growth rates observed in mycobacterial species (Bachmann *et al*., 2020). This should be specially considered if *Mycobacterium* native to Benhar Bing were to be subsequently isolated to confirm their genomic structure and proposed metabolic activities involved in alkane removal.

The *Mycobacterium* genomic assembly also contains the arsenic resistance genes: *arsA, arsB, arsC* and *arsD*. The expanded *ars* operon gene *arsA* encodes an ATPase, which forms dimers with the ArsB efflux protein. The ArsA-ArsB association allows conventional arsenic expulsion via the efflux pump protein to be energised by ATP hydrolysis, rather than being reliant on use of the cellular electrochemical proton gradient alone, which occurs when ArsB is not within the dimer complex (Garbinski *et al*., 2019). Pseudomonads and certain *Acidothiobacillus* species have been observed to carry an expanded *ars* operon, with the capabilities to synthesise additional proteins (Páez-Espino *et al*., 2020).

Arsenic resistant prokaryotes have been noted to maintain *arsA* more conventionally on plasmids, and expression is less documented from chromosomally harboured operons (Ben-Fekih *et al.,* 2018). Despite this, the *Mycobacterium* assembly suggests chromosomal persistence of *arsA*. The work of Mateos *et al*. (2017) demonstrated that arsenic resistance in the close relative of *Mycobacterium, Mycolicibacterium smegmatis* was mediated by *arsB* and *arsC* expression but did not indicate the ability to encode the additional *ars* genes presented in MAG 3. Furthermore, use of the *AsrD* gene present in the assembly is considered to provide additional protection against arsenic ions by acting as an arsenic chaperone to minimise intracellular toxicity as the toxic ions are trafficked to efflux systems. The ArsD protein also promotes affinity of ArsA for arsenite, which elevates the ATPase activity at low metalloid concentrations (Lin *et al.,* 2006). Additional resistance to D-block metals is conferred to *Mycobacterium* via potential expression of the general metal transporters encoded by *nix, mntH* and *czcD*.

Strikingly, despite the energetic challenges of nitrogen cycling in low pH conditions, the *Mycobacterium* MAG contains multiple genes involved in the production of the multi-subunit enzyme, nitrate reductase. The nitrite/nitrate transporter encoded by *narK* is also evident. The ability to utilise nitrate reductase for anaerobic growth has been reported in other *Mycobacterium* species, particularly host associated species such as *Mycobacterium bovis* (Reis and Cunha, 2021). Mycobacterial dispersal in the wider environment (*ie.,* outside of mammalian hosts) is less well documented, and their metabolic roles in biogeochemical cycling are becoming more apparent as metataxonic and metagenomic approaches reveal their presence in soils, sediments, and aquatic environments (Falkinham, 2021).

The occurrence of other sediment dwelling *Mycobacterium* capable of tolerating low oxygen gradients and anaerobiosis reflects both the MAGs environmental niche and the ability to utilise anaerobic energy conserving pathways through nitrate reduction; the only MAG to suggest anaerobic metabolic capabilities. Khan and Sarkar (2012) state that the mycobacteria are considered strong reducers of nitrate; the use of the membrane-bound transporter, NarK, would allow transport of nitrate produced to leave the cell. Further use of nitrite was not apparent within the MAG. Moreover, several sulphur cycling genes (*e.g., sir* and *cysJ*) were observed in the MAG pertaining to *Mycobacterium*. Sulphur cycling has been documented for medically significant members of the *Mycobacterium,* but less often regarding non-host associated taxa (Hatizos and Bertozzi, 2011). Therefore, the presence of sulphur cycling genes within the reassembled *Mycobacterium* MAG brings added insight into low pH inorganic biogeochemistry in AMD sites by members of the Actinobacteria.

Overall, when assessed together, the combined metabolic functions of the three proposed hosts of the MAGs described contribute to much of the overlooked ecosystem function in low pH systems. The functional annotation of their genomes has expanded on the limited understanding of extremophiles' metabolism. Importantly, the MAGs produced which demonstrated lower completeness and therefore were not functionally annotated represent other acidophilic taxa critical to maintenance of the acidophilic consortium, many of which remain poorly characterised. Future work to repeat long-read sequencing with greater depth may aid in resolving both taxonomy and function in these less abundant, but crucial community members.

6.5 Conclusion of Chapter 6

The use of genome reconstruction and annotation is an emerging and powerful approach for mining metagenomes to determine metabolic and ecological function. As databases continually improve, wider metabolic diversity may become evident, particularly from taxa which contribute to the ecosystem function in underexplored extreme environmental niches. During MAG assembly, the use of refinement tools proved beneficial in preventing insertion/deletions (indels) which allowed the recovery of several large and practically complete reconstructed chromosomes when compared to initially assembly without the use of chromosomal refinement. Additionally, Prokka proved to be a robust tool regarding genomic annotation across the three MAGs selected for further analysis.

Taxonomic binning of MAGs was advantageous in allowing the host organisms of the MAGs to be determined. Yet, this approach is the most beneficial when the MAG is practically complete; extracting the 16S rRNA gene sequences from MAGs can aid in taxonomic identification and confirmed the correct binning of each taxon allocated to the highest quality assemblies. With a renewed focus on applying molecular strategies to extremely polluted systems, the development of function-specific databases [*e.g.,* metal(loid) redox pathways] could be a future route in metagenomic tool-development to assist in the elucidation of genomic content in extremophile MAGs following taxonomic resolution. Additionally, recovered gene sequences involved in key enzyme synthesis (*e.g.,* arsenic detoxification) could be utilised in synthetic ecology approaches as novel tools to achieve catalysis of pollutants by engineered DNA constructs.

To aid in the recovery and assembly of MAGs, DNA reads generated from alternate sequencing platforms (*e.g.,* Illumina Hi-Seq and Nanopore) could be utilised in hybrid assembly approaches to assist in promoting high-quality genome completion. A combined approach may also aid in resolving issues with erroneous bases or misassembled contigs resulting from a single sequencing platform.

Hybrid assembly routes have been used in both complete genome and plasmid recovery from clinical isolates more widely than with environmentally recovered MAGs (Craddock *et al*., 2022; Lascols *et al*., 2023). Yet this approach could yield a greater number of high-quality reconstructed chromosomes if applied to ecologically significant microbial assemblages. Furthermore, this approach could be applied to environments more complex than acidic effluents; the restrictive chemical constraints of which can aid in assembly of genomes from assorted DNA reads using a single approach. Notably, the recovery of members of the rare biosphere remains challenging and would require multiple sequencing runs, each with a high level of depth to recover less abundant genetic material.

Finally, the portability of the Nanopore device allows the technology to be applied as a promising approach for monitoring of critical members of microbial communities which directly impact both prokaryotic assemblages and 'higher' organisms *in situ*. Although in its infancy, this method has been applied to assess the population control of toxin-producing cyanobacteria by cyanophages in a freshwater lake with elevated toxin production over a two-week period (Jiang *et al*., 2019). A similar approach could be applied to acid mine drainage populations driving future bioremediation strategies to determine persistence of key taxa involved in heavy metal bioconversions in conjunction with other -omics techniques.

CHAPTER 7 - Exploring Methanogenic Activity from Sediment Microbial Communities in Batch Scale Bioreactors

7.1 Overview of Applied Microbial Ecosystems

The vast metabolic repertoire harboured by microbial assemblages has been exploited in various biotechnologies to drive desired functions relevant to human and environmental health. Historically, microbial populations have been responsible for facilitating various processes beneficial for human development for centuries. Evidence suggests that early human populations exploited microbial consortia in multiple processes including primitive landfilling processes, waste degradation and water purification, despite both the role and composition of these microbial assemblages being unknown prior to the field of microbiology developing (Lofrano and Brown, 2010; Kumar *et al*., 2011).

More recently, several works have attempted to utilise the metabolic capabilities of various assemblages in novel ways, including to degrade micropollutants as well as more complex pollutants such as hydrocarbons (Varjani, 2017). Microbial assemblages that are routinely utilised in more well-established biotechnologies, such as wastewater treatment, can be prone to bioprocess failure and microbial performance has been noted to fluctuate, which can lead to detrimental impacts on the bioprocesses. In extreme cases, microbially driven processes can cease if environmental conditions cannot be tolerated; characterising most key taxa and their associated functions is key to understanding how microbial ecosystems can be maintained and function optimally.

To this end, achieving reliable and robust community function is a major goal for both industrial biotechnologies, as well as increasing current understanding of how microbial taxa maintain function in global biogeochemical cycling. As reported in **Chapter 4,** methanogenic taxa were detected in Benhar Bing sediment via amplification of the *mcrA* gene, not previously reported as being detected in low pH effluents. Due to this, assessing if this function could be established in bioreactor conditions was deemed a valuable additional approach, which would also further expand on knowledge of methanogen populations which can perform active methane generation and continue to proliferate under acid stress.

Methanogenic *Archaea* are responsible for both the generation of biologically produced methane in natural environments, completing the carbon cycle and facilitating the transfer and conservation of energy through the Earth's biogeochemical cycles. Determination of methane outputs, and how this may be impacted by changes in climate have been studied in more conventional ecosystems and a net release of methane has been observed from freshwater mesocosms under warming conditions. However, this has been largely neglected in low pH sites and the ability for any *mcr*-harbouring taxa to become metabolically active remains poorly documented, with many studies only exploring communities at the metataxonomic level.

Equivalent reactions are also responsible for biogas production in industrial bioreactor environments during anaerobic digestion whereby the methane-rich gas is produced under controlled conditions. Moving beyond simpler metataxonomic studies is critical in progressing the ability to harnessing the metabolic potential of microbial communities to drive various bioprocesses and to understand the roles of specific populations in the wider environment (*e.g.*, methane emissions by methanogenic communities).

7.1.1 Enhancing Specific Functional Attributes in Microbial Consortia

Much of the previous literature on the exploitation of biotechnologically relevant microbial functions have focussed on the use of single species bioaugmentation; the process in which a sole isolate is added to an established community to enhance a desired outcome via the organism's preferential catalytic activity. The work of Mawang *et al*. (2021) provided an overview of several examples of single species of members of the actinomycetes, particularly *Rhodococcoccus* and *Streptomyces* to become established within a population and achieve the desired degradation of pollutants; an approach that is increasingly important as the impact of persistent pollutants on human and environmental health becomes ever more apparent. Often this route to exploiting an isolate's function is the most successful when the organism is well-studied, is metabolically flexible (and attribute often observed within the Actinobacteria) and the native community has a low diversity, potentially facilitating establishment of enhanced function within the niche. Dominant autochthonous microorganisms (*i.e.*, organisms native to the site being studied) often have the most success in these approaches as they maintained endogenously within the population and may not be impeded by competitive exclusion by other taxa.

Achieving the same approach using organisms which facilitate key functions within communities, despite being ecologically rare within microbial ecosystems, is more challenging. There has been some success reported regarding enhancing methane production in anaerobic digesters to achieve higher methane yields via bioaugmentation with *Methanoculleus* in mesophilic reactors, however the addition of *Methanothermobacter* failed in thermophilic bioreactors (Palù *et al*., 2022).

Prior to the advent of powerful long read metagenomic methodologies, Steinberg and Regan (2008) demonstrated that the methanogen biodiversity was higher in a methanogenic fen compared to an anaerobic digester through analysis of clone libraries. Additionally, Steinberg and Regan (2008) argued that environmental methanogenic consortia are considered more environmentally resilient than their bioreactor-derived counterparts. Potentially methanogenic consortia from environmental samples may harbour untapped metabolic potential, may be key populations to target for bioprospecting for novel isolates and could have their function exploited in biotechnology, stressing the overlap between environmental communities and their analogous used in more applied microbial ecosystems.

7.1.2 Global Methane Budgets and Greenhouse Release from Anoxic Environments

Despite being potentially important communities in biotechnological applications. naturally occurring methanogenic populations and their ability to generate methane natively require further attention. Wetlands have long been considered major carbon sinks; however climatic shifts have the potential to drive the release of stored carbon due to dysregulation of the microbial carbon cycle. Excessive carbon release under warming conditions has been documented in mesocosm systems using conventional wetland sediment, yet this has not been explored in extreme conditions to a great extent (Zhu *et al*., 2020).

A single study exists which attempted to combine the methanogenic function of environmental consortia with anaerobic digestion, by utilising various methanogenic communities as alternative microbial inocula in bioreactors. Routinely, if a bioreactor producing methane is failing, reestablishment of function is performed by 'seeding' the reactor with digestate from a functional reactor. To this end, this single work by Witarsa *et al*. (2016) both allowed a means of assessing methane output from natural occurring consortia and explored their use as potential inoculating communities for enhancing methane output when treating complex organic wastes.

This enhancement of biogas production through sediment communities was developed from the work of Witarsa *et al*. (2016). This work demonstrated the use of wetland sediment and landfill leachate communities to drive the carbon cycle in digesters treating dairy farm waste. It has been observed that environmental methanogens and their associated bacterial partners can perform effective anoxic degradation reactions and subsequent methane production as these functions are analogous to those underpinning the AD bioprocess, as shown in the comparison between reactor and fen communities in the work of Steinberg and Regan (2008).

Importantly, inoculum has been noted as a key factor in ensuring AD success and several works have studied how inoculum can be optimised (Kong *et al*., 2016). There is debate in the literature regarding the benefits of environmental inoculum. It is thought that natural inoculum from a variety of environments may act as a successful source of methanogens as they may show increased ecological resilience to environmental change. To this end, through the use of environmental communities, there is greater potential to introduce novel consortia which may be better adapted to proliferate under extreme reactor conditions and tolerate reactor conditions.

The work of Witasra *et al*. (2016) explored the ability of sediment communities to function at psychrophilic temperatures and allow low temperature AD to occur as wetland microbial communities can express cold active enzymes which can be exploited in AD. Likewise, the work of Braun *et al*. (2015) reported that consortia derived from polluted soils were capable of degrading similarly polluted wastes in AD through pre-adaptation to such recalcitrant pollutants. The ability of environmental communities to tolerate shifts in physiochemical conditions to a greater degree than consortia from reactor systems was also discussed by Steinberg and Regan (2008) where digesters supplemented with acidic bog sediment could withstand organic loading shocks due to metabolic flexibility exhibited by the acidophilic community.

7.2 Aim of Chapter 7

To stimulate methanogenesis and assess the methane producing potential of sediment communities from Benhar Bing, Blackford Pond and Loch Bà, a series of batch-scale syringe-based bioreactor trials were performed. Using environmental inoculum to act as the anaerobic consortia in bioreactors, it was hypothesised that each sediment consortium would adapt to the anoxic conditions and produce methane if methanogenic populations were present and enriched. Additional objectives of **Chapter 7** were to:

- Determine the **chemical composition of anaerobic digestate** being used as a substrate for microbial growth and proliferation within bioreactors
- Evaluate the use of sediment communities reflective of acidophilic, oligotrophic and copiotrophic conditions as alternative inocula in small scale batch bioreactors and **assess biogas generation** by the anaerobic assemblages
- Determine the **composition of methane** in biogas produced in bioreactors as a marker of active methanogenesis
- Assess **bioreactor performance** through appropriate physicochemical parameters (changes in chemical oxygen demand, pH, and organic acid concentrations)
- **Determine key methanogenic species present** and the main bacterial taxa which contribute to function through the use of a 16S rRNA based metataxonomic approach

7. 3 Results

7.3.1 Initial Bioreactor Tests

Three bioreactor trials were performed to assess derivation of methanogenic populations using sediment communities. The set-up of each of these three bioreactors trials are outlined in **Chapter 2**. However, only the third trial is reported here which proved to be functionally relevant and allowed the establishment of active methanogenic consortia. The work reported here is based on anaerobic digestion. Each bioreactor contained 10 ml of double autoclaved digestate, 5 ml of double autoclaved 'feedstock' (material which enters digesters and had not been previously degraded) and 5 ml of 'active' consortia (either Loch Bà, Blackford Pond or Benhar Bing sediment). Positive control reactors were inoculated with 5 ml of non-sterilised (*i.e.*, 'active' digestate) and negative controls contained an additional 5 ml of double autoclaved digestate to act as a sterilised control community.

7.3.2 Elemental Analysis of Anaerobic Digestate

Elemental analysis of anaerobic digestate which was used as sterilised substrate (and active source of methanogens in positive control reactors was performed by the James Hutton Institute, Craigiebuckler, Aberdeen. The results are shown in **Table 7.1 and 7.2.**

TABLE 7.1: Elemental analysis of anaerobic digestate collected from Seafield wastewater treatment plant which acted as a substrate for microbial growth in batch bioreactors and pre-adapted methanogenic consortia. Elemental components were determined by Inductively Coupled Plasma-Optical Emission Spectroscopy (ICP-OES) and Aqua Regia Digestion (ARD).

Sample	mg/kg						
	Al	Ca	Fe	K	Mg	Mn	TP
Digestate	14910	26980	30770	2556	5479	899.1	28320

TABLE 7.2: Determination of total carbon and organic carbon fraction in digestate. Assessment of TC and TOC was determined by Continuous Flow-Isotope Ratio Mass Spectrometry (CF-IRMS).

Sample	g/kg	
Digestate	Total Carbon (TC)	Total Organic Carbon (TOC)
	324.0	302.0

7.3.3 Biogas Generation in Sediment Mesophilic Bioreactors

7.3.3.1 Positive Control Reactors Inoculated with Active Digestate

The reactor trial outlined here, which proved the most successful in allowing the establishment of methanogenic populations, ran for 120 days at 37 °C, before final disassembly of reactors. Starting samples of the reactor contents were sampled during reactor set up. During incubation of bioreactors, production of biogas was assessed regularly by visually examining individual 60 ml syringes. Double autoclaved digestate with a sterilised digestate community acted as three negative control reactors. No biogas was detected in any negative controls which consisted of digestate and feedstock (both double-sterilised), with an additional double sterilised digestate community (5 ml) to act as an inoculum.

Following reactor incubation, positive control reactors (containing active digestate communities) produced biogas rapidly, and this trend of biogas output continued into day 21 of the reactor run (**Figure 7.1**). On day 27 one replicate of the positive controls (PC1) began to decelerate, with biogas output plateauing at day 60. Despite the remaining positive controls (PC2 and PC3) slowing their activity at day 33, they demonstrated a more rapid ceasing of biogas generation (around day 36).

7.3.3.2 Blackford Pond Sediment Inoculated Bioreactors

In contrast, the reactors inoculated with sediment communities all demonstrated a slower rate of activity and no biogas generation was noted until day 29 when all Blackford Pond reactors began to demonstrate an acceleration in biogas output (demonstrated in **Figure 7.1**). Blackford Pond reactors slowed around day 39. However, replicate BP1 and BP2 had a second, more minor, period of activity. By the end of the trial, variation was noted in the total biogas generated from each Blackford Pond inoculated reactor, with BP2 producing the most gas out of all the environmentally derived reactors (74 ml of biogas total).

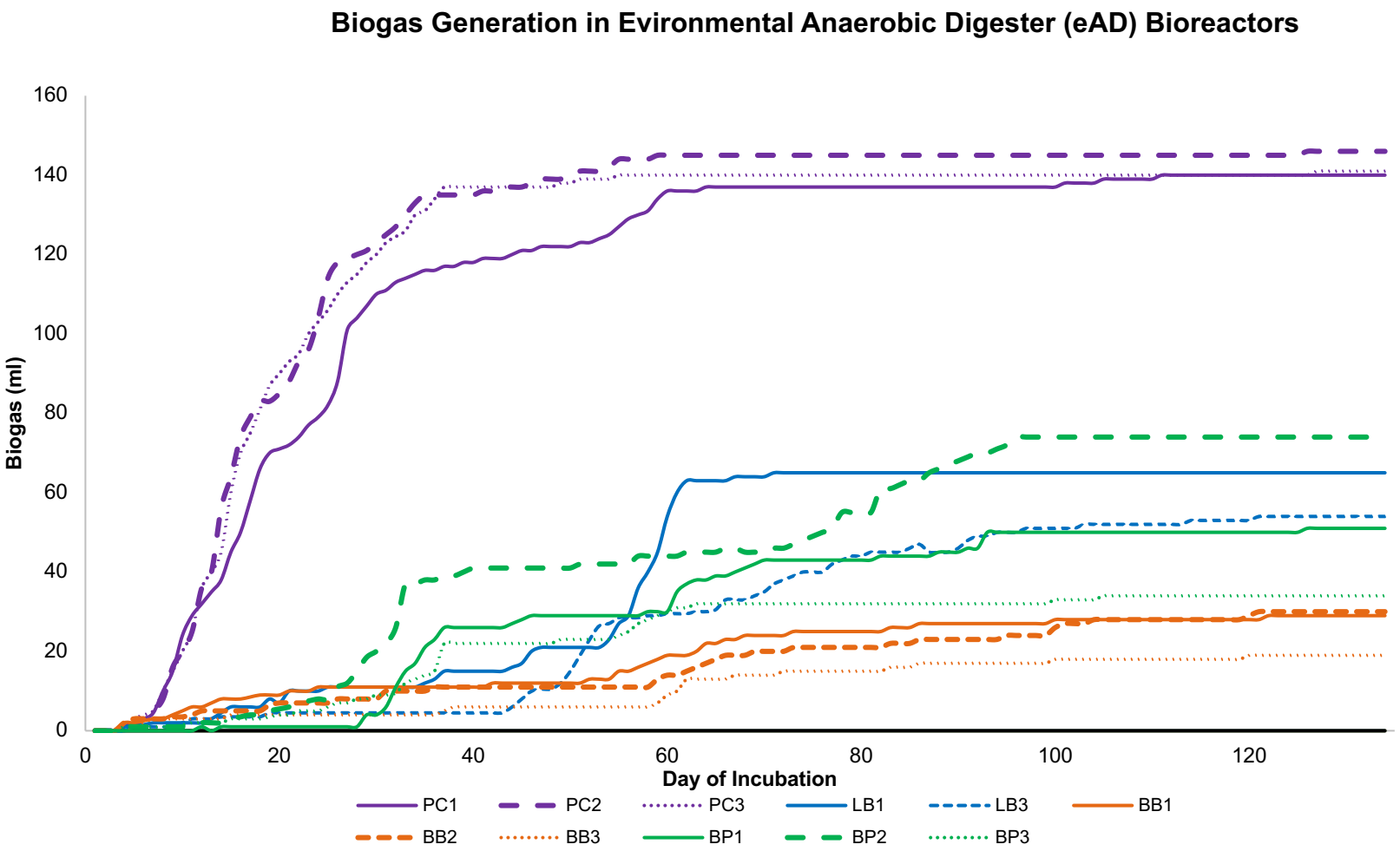

FIGURE 7.1: Biogas generation in mesophilic, batch scale anaerobic digesters containing sediment communities as the source of methanogenic consortia. Sediment samples used in bioreactor set-up were preincubated at 37 ºC for 24 hours prior to inoculation into syringe reactors. 60 ml reactors were incubated with agitation throughout and sampling performed anaerobically. Note that due to the variation between replicates, each reactor is shown individually. Negative controls and LB2 produced no biogas and are not shown in the biogas output graphs.

7.3.3.3 Loch Bà Sediment Inoculated Bioreactors

Only two of the Loch Bà reactors successfully produced biogas; the second replicate, LB2 did produce any gas and is therefore not shown in **Figure 7.1.** Loch Bà communities within LB1 and LB3 reactors demonstrated a longer lag time than was observed for all Blackford Pond reactors. By day 34, LB1 had a short period of activity, but biogas generation was erratic, and the reactor often ceased activity for periods of days at a time (particularly notable at days 37-43). Following this, a rapid phase of gas production occurred in the LB1 reactor between days 50-63, after which LB1 did not produce any further biogas. Bioreactor LB1 reached a maximum gas output of 63 ml. Interestingly, the LB3 reactor did not follow this trend; biogas generation was generally slow, and this reactor did not experience any rapid changes in performance over time. Biogas production stopped in LB3 on day 90, with a total volume of 50 ml of biogas being generated.

7.3.3.4 Benhar Bing Sediment Inoculated Bioreactors

The bioreactors inoculated with acid mine drainage sediment communities had the longest lag time. A minimal output of gas was apparent, but the volume was too low to be used for an assessment of methane content. The three Benhar Bing reactor replicates demonstrated an increase in productivity around day 60 (see **Figure 7.1**)

All Benhar Bing reactors had plateaued around day 80. The biogas output patterns were similar between BB1 and BB2, with ~30 ml of biogas generated by each replicate. BB3, however, produced less biogas, with only 19 ml total being generated after 120 days

7.3.4 The Methane Content of Microbially Produced Biogas

When biogas production had passed 20 ml of volume generated within an individual reactor's headspace, the reactor was selected for degassing. Reactors were opened via luerlocks, and biogas injected into a methane meter to determine the CH_4 content, via the reactor plunger. The mean methane output from each active bioreactor is shown in **Figure 7.2.** All positive control, Blackford Pond, and the two active Loch Bà reactors were degassed multiple times. At the end of the trial, the Benhar Bing reactors had only produced enough gas to be assessed once. Only one Benhar Bing reactor (BB2) demonstrated methanogenesis. The remaining proportion of the biogas is considered to be principally CO_2 produced during anaerobic fermentation of organic material.

The positive control reactors all consistently produced high yields of methane (> 70 % of biogas composition) with PC2 producing the highest mean value of 68.28%. Out of the Blackford Pond reactors, BP1 produced the highest content of methane (mean: 56.55%). The two active Loch Bà bioreactors were variable regarding methane composition of the biogas. Despite the variation in the performance of the Loch Bà communities, the mean value was the 64.55%, comparable to methane production in positive controls and the more reliably active Blackford Pond amended reactors. Lastly, a Benhar Bing reactor (BB2) demonstrated a methane reading of 65.5%.

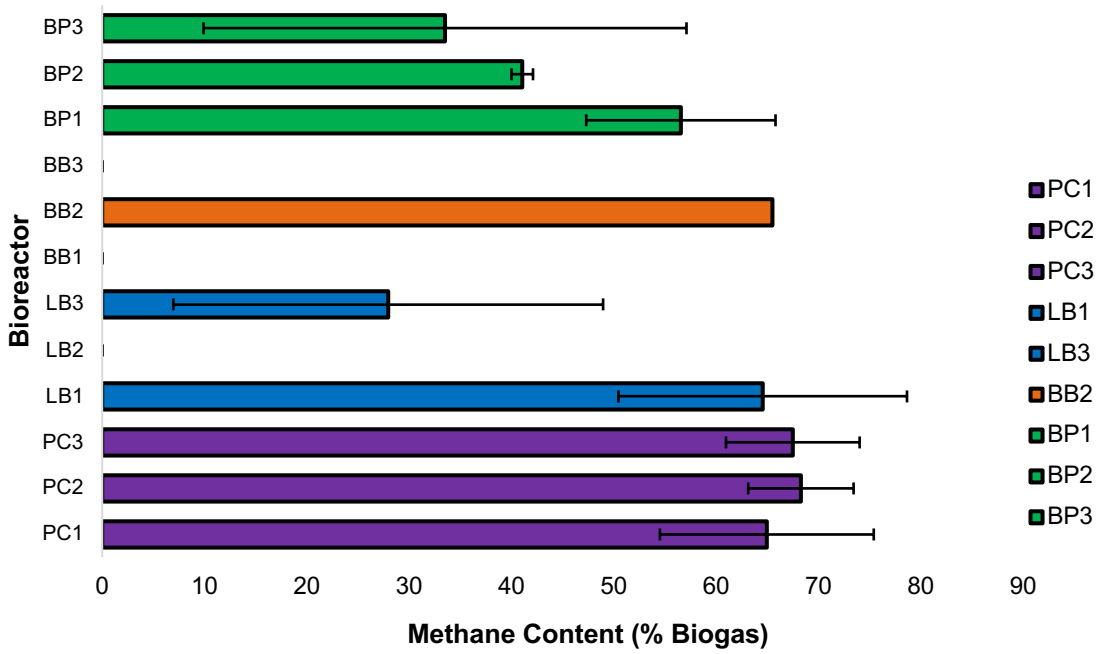

FIGURE 7.2: Average methane measurements recorded from bioreactors containing active sediment communities. Note that no negative control reactors or LB2 produced any gas. Biogas from all Benhar Bing reactors were assessed at day 120. Each positive control reactor (PC1-3) was degassed 8 times. LB1 and LB3 were degassed three times. BP1 and BP3 = 3 CH_4 measurements and BP2 = 5 CH_4 measurements. Error bars indicate standard deviation of the mean.

7.3.5 Determination of Chemical Oxygen Demand in Bioreactors

Performance of bioreactors was assessed via chemical oxygen demand (COD), representative of the amount of oxygen required to degrade biodegradable organic material. The most statistically significant change between the starting chemical composition and the final COD was observed in the positive control reactors (t test: p-value = 0.010). No significant differences were observed in the negative control reactors, indicative of no microbial activity. A decrease in COD was observed in Loch Bà reactors, however, was not deemed significant (t test; p-value = 0.08). P-values indicated a significant decrease in COD within the Benhar Bing and Blackford Pond inoculated reactors (t test; p-values = 0.031 and 0.022, respectively).

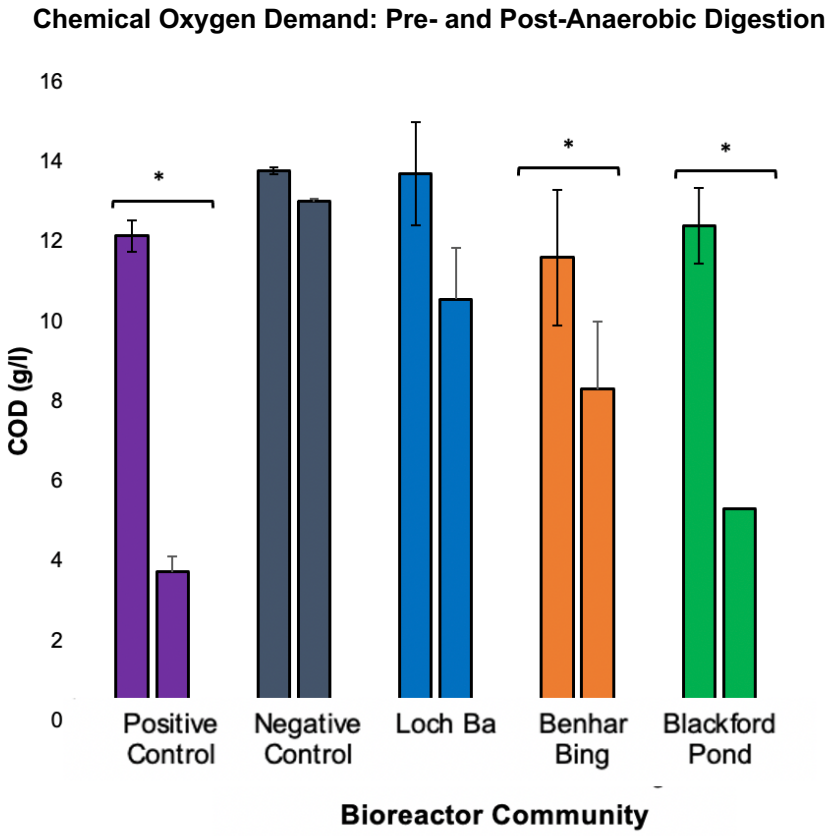

FIGURE 7.3: Changes in chemical oxygen demand within bioreactors. Soluble COD was determined via the Hach Lange COD test kit. Samples taken in triplicate for reach replicate reactor (*n* = 9). Error bars represent standard deviation of the mean.

7.3.6 Determination of Organic Acid Levels and pH in Bioreactors

Organic acid concentrations were assessed from centrifuged samples taken from the starting reactor mixtures, as well final bioreactor samples. Determination of organic acid concentrations are an important consideration in the monitoring of intermediates, which can provide valuable data regarding the phases of anaerobic decomposition. Results of the organic acids assay are presented in **Figure 7.4.**

A significant difference in organic acid contents of reactors was observed pre- and post-digestion in all reactors, apart from the negative, sterilised controls. The positive control, Loch Bà and Blackford Pond reactors all demonstrated a significant decrease: all t-tests: p-values = < 0.001. Conversely, the Benhar Bing reactors demonstrated a significant increase in organic acid contents (t test: p-value = 0.002)

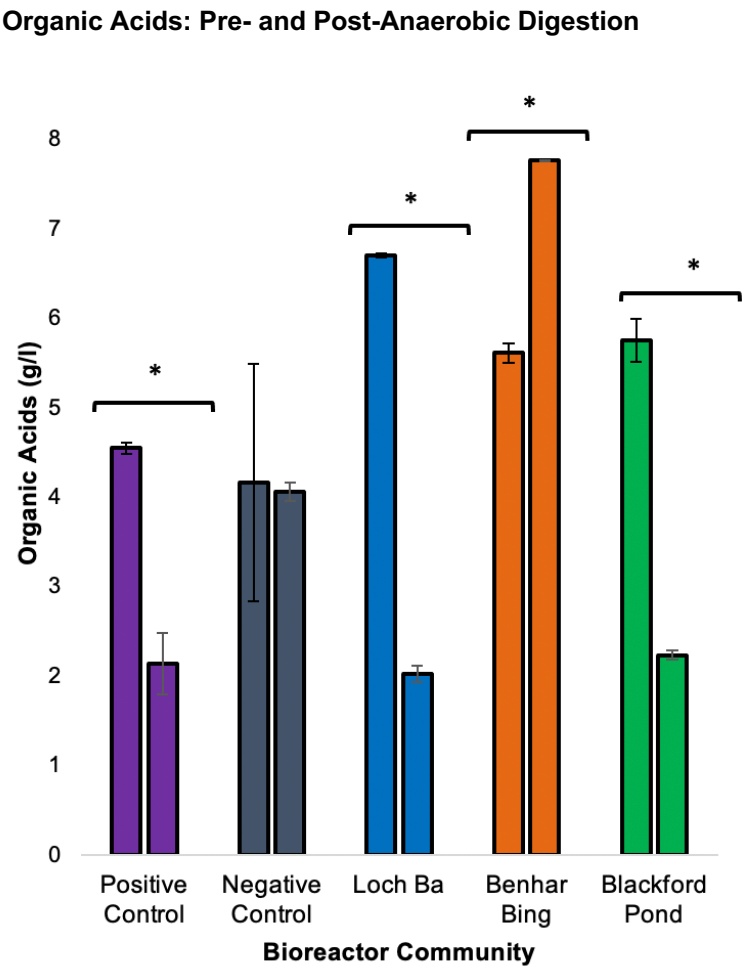

FIGURE 7.4: Changes in organic acid concentrations within bioreactors. Soluble organic acids (OA) were determined via the Hach Lange organic acid test kit. Samples taken in triplicate for each replicate reactor (*n* = 9). Error bars represent standard deviation of the mean.

To corroborate the organic acid data (**Figure 7.4**), the pH of the starting reactor contents and samples retrieved from reactors during disassembly were recorded and are presented in **Table 7.3.** The most drastic pH change was noted in Benhar Bing reactors, whereby the initial pH of 8.51 had reduced to pH 5.53

TABLE 7.3: Changes in mean pH in bioreactor samples taken from starting reactor mixtures and end-point samples (day 120). Sample pHs taken in triplicate for reach replicate reactor (*n* = 9). Note the starting pH of the digestate sample was 8.80 and the feedstock pH was recorded as 5.95.

	Positive Controls	Negative Controls	Loch Bà	Blackford Pond	Benhar Bing
Mean pH (Pre-AD)	8.80	8.35	8.46	8.54	8.51
Mean pH (Post-AD)	7.70	8.23	8.23	7.82	5.53

7.3.7 Taxonomic Composition of Bioreactors

7.3.7.1 Starting Microbial Composition of Bioreactor Inoculum (Sediment and Digestate)

The microbial composition of the four samples which acted as the sources of methanogenic consortia in each set of batch bioreactors (active digestate and three sediments) were assessed via Illumina sequencing of the V4 hypervariable of the 16S rRNA gene. Key members contributing to the microbial composition of each sample are presented in **Figure 7.5.**

At genus level, the digestate sample was dominated by *Defluviiotga* (23.17% total relative abundance), *Lentimicrobium* (23.11%) and *Pseudomonas* (17.60%). More minor genera observed were *Methanobacterium* (8.9%) and a poorly taxonomically resolved member of the Firmicutes, 'D8A-2'.

Both Blackford Pond and Loch Bà communities were more diverse. Key organisms in Blackford Pond were an ASV pertaining to Acidobacteriales (16.9%). *Tissierella* (10.27%) and *Sulfuricurivum* (10.45%) were also amongst the more dominant taxa observed in the Blackford Pond starting community. Loch Bà demonstrated an abundant ASV pertaining to an uncultured Acidobacteriales (16.9%) and dominant ASV belonging to *Occalltibacter* species (7.30%).

Benhar Bing was more simplistic in its community composition. A poorly resolved gammaproteobacterial ASV was noted in abundance, as was *Metallibacterium*.

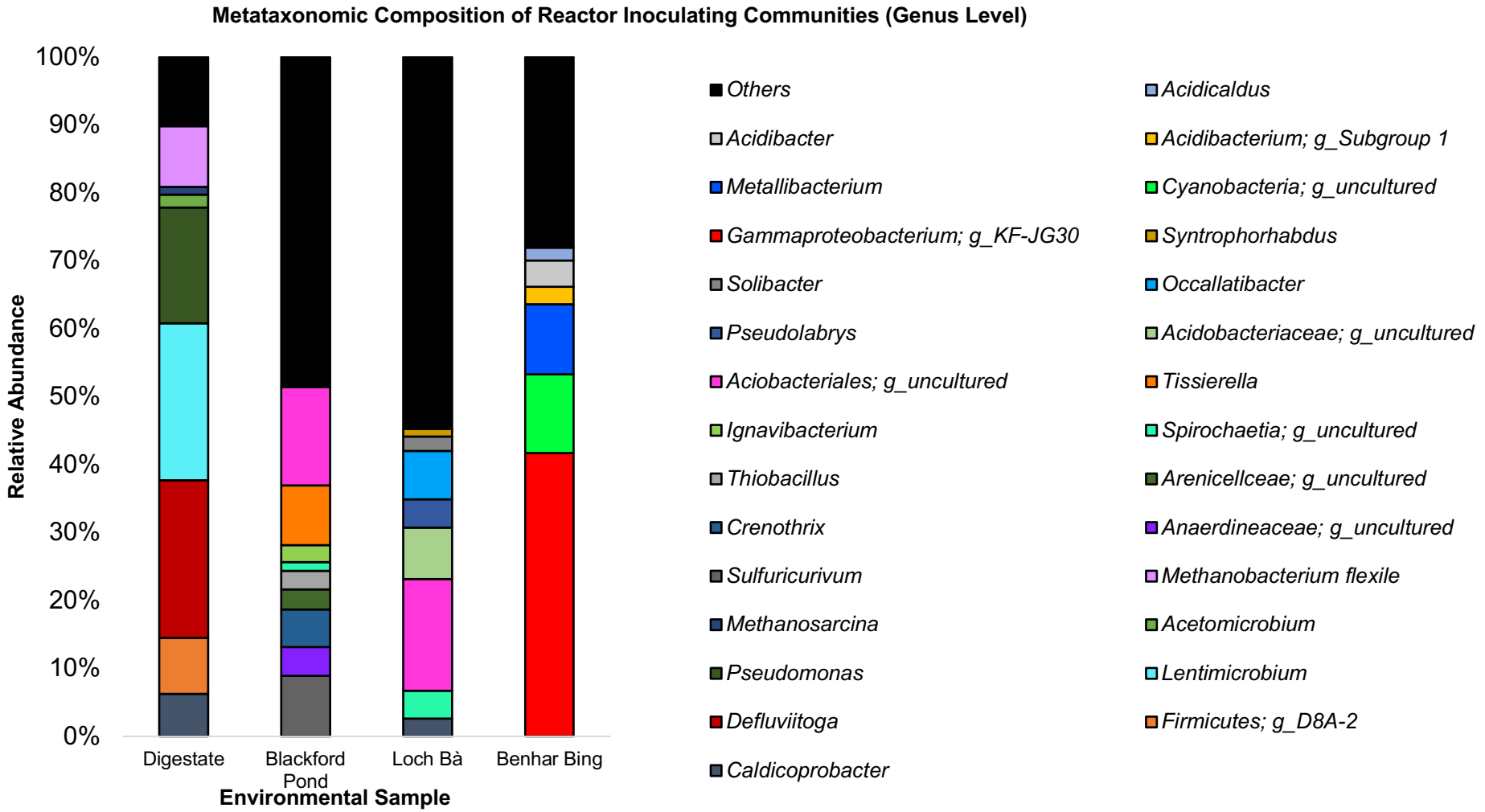

FIGURE 7.5: Microbial community structure in sediments and anaerobic digestate used as novel inoculum in bioreactors based on 16S rRNA V4 region. Taxonomy was predicted using SILVA 138 database following amplification with a515F and 806R primers. Note that taxa described as 'others' are not major contributors to the community structure and represent ≤ 1% of the total relative abundance.

7.3.7.2 Archaeal Composition of Inoculating Sediments and Digestate

As methanogenic consortia are responsible for methane generation, the archaeal contribution to the community was analysed. This was performed via pre-amplification of the entire archaeal 16S rRNA gene, followed by amplification of the V4 16S rRNA gene using the archaeal pre-amplified template.

The archaeal pre-amplification approach was successful across all sediments and the digestate which were utilised as starting inocula (the metataxonomic composition of these samples are shown in **Figure 7.6**). Dominant methanogens in active digestate were classified within *Methanobacterium, Methanosarcina* and *Methanosaeta*. Members of the Asgard superphylum were also detected in the digestate sample (Odinarchaeia contributed 22.36% to the relative abundance).

Using the archaeal pre-amplification sequencing approach, Blackford Pond appeared to be dominated by two methanogens: *Methanosaeta* and *Methanobacterium*. However, Loch Bà demonstrated an ASV termed 'RBG_16-50-25' pertaining to the Bathyarchaeia. Additionally, Crenarchaeotal sequences were detected (13.98%). Lastly, Benhar Bing was demonstrated a high relative abundance of poorly characterised Thermoplasmataceae (68.65%).

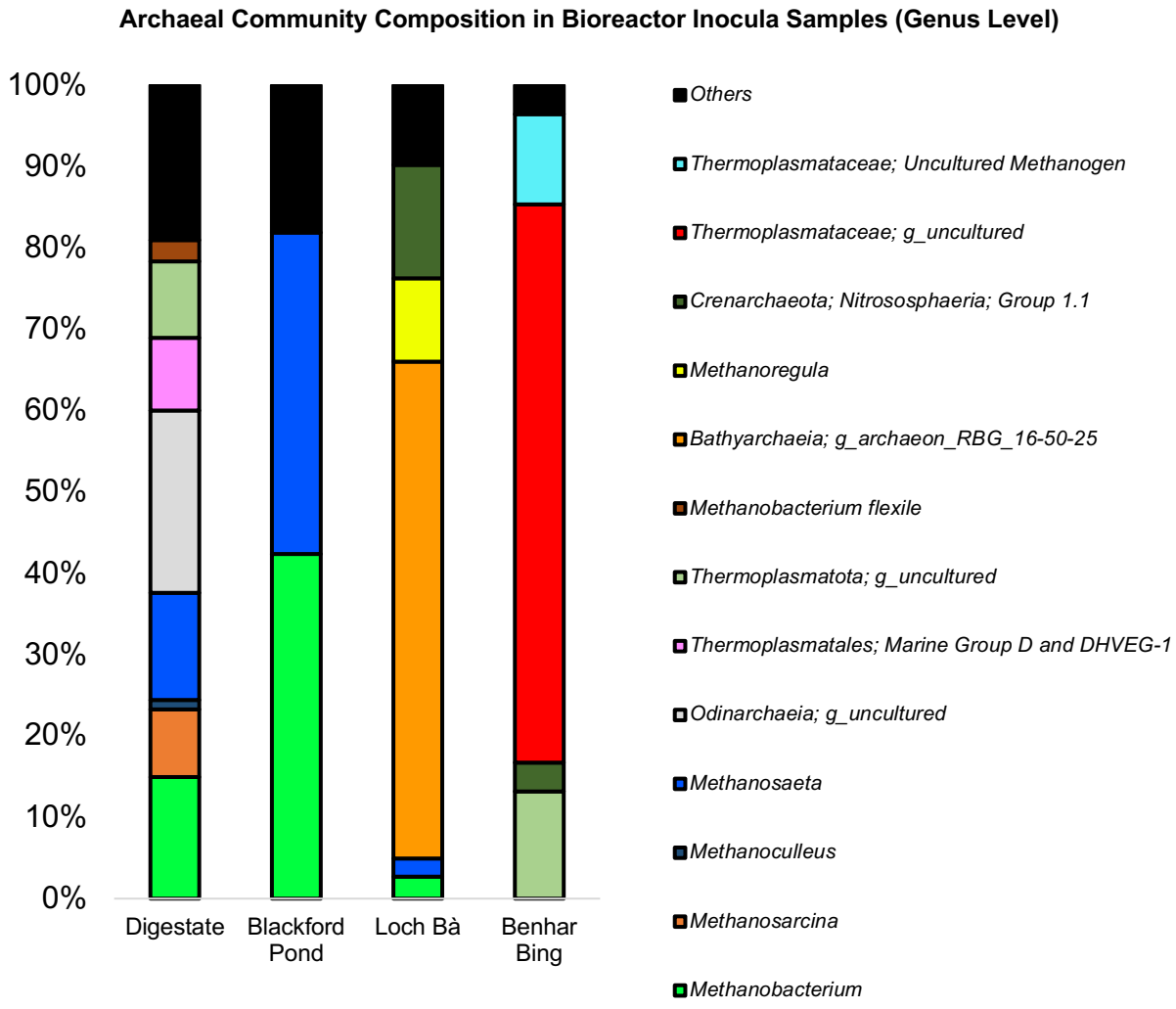

FIGURE 7.6: Results of metataxonomic composition of starting inocula based on archaeal pre-amplification and subsequent V4 region Illumina Mi-Seq sequencing. Full length archaeal 16S rRNA gene amplification was performed using the ArchF/ArchR primer set. Subsequent 16S rRNA V4 amplification and Illumina sequencing allowed detection of archaeal members by ASV clustering with SILVA 138 database. Note that taxa described as 'others' are not major contributors to the community structure and represent ≤ 1% of the total relative abundance.

7.3.7.3 Archaeal Composition Within the Final Bioreactor Samples (Collected Following Reactor Disassembly).

Following disassembly of bioreactors after 120 days, the final taxonomic archaeal composition was assessed by repeating the archaeal pre-amplification and subsequent sequencing of the V4 region as was performed previously. The final archaeal composition of each of the bioreactors is shown in **Figure 7.7**.

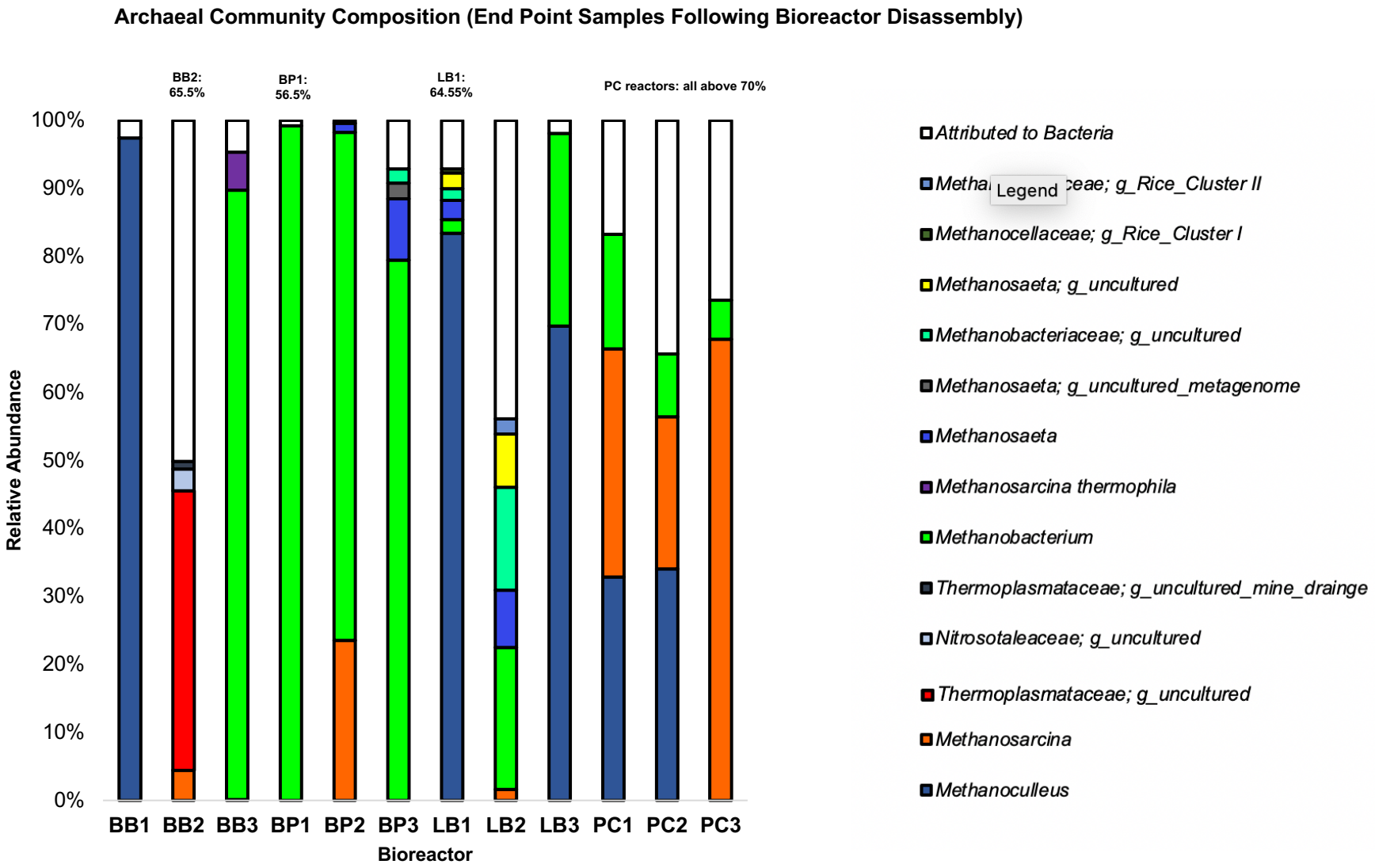

FIGURE 7.7: Results of metataxonomic composition of final bioreactor communities based on archaeal pre-amplification and subsequent V4 region Illumina Mi-Seq sequencing. Full length archaeal 16S rRNA gene amplification was performed using the ArchF/ArchR primer set. Subsequent 16S rRNA V4 amplification via a515F/806R and Illumina sequencing allowed detection of archaeal members. Taxonomic prediction performed using the SILVA 138 database. Note that taxa described as '*Attributed to Bacteria'* were bacterial sequences which amplified despite the archaeal pre-amplification stage; bacterial taxonomy has been omitted. Note that communities with active methanogenesis have the mean CH_4 % of biogas produced shown above the specific bar.

As was observed for the archaeal pre-amplification of the starting samples (**Figure 7.6)**, the nested PCR approach utilising amplification of the entire archaeal 16S rRNA gene for use as a template in subsequent V4 16S rRNA PCR allowed for detection of key archaeans present in the end point samples. Despite the second round PCR reactions amplifying bacterial reads, the amplification of archaeal taxa was observed across all bioreactor samples.

The final Benhar Bing archaeal communities varied in this composition between the three replicate reactors following the duration of the bioreactor trial. The BB2 reactor, which was the only Benhar Bing amended reactor to produce methane was the most compositionally different. As was observed in the starting Benhar Bing sediment, the reactor is dominated by a member of the Thermoplasmataceae (41.1% of the total relative abundance). A poorly taxonomically resolved member of the Nitrosolaeaceae from the Thermoproteota phyla (formally the Crenarchaea) was detected, however was rarer with just above 3% of the total relative abundance; notably the majority of sequences (over 50%) were not attributed to archaeal taxa. The remaining two Benhar Bing reactors were dominated by *Methanoculleus* (over 97% in BB1) and *Methanobacterium* (over 89% of the archaeal community in BB3).

The final archaeal community composition of the Blackford Pond reactors was consistent between the three replicates, with *Methanobacterium* being abundant in all reactors. Notably in the BP1 reactor, which proved the most active of the three, *Methanobacterium* dominated the archaeal community (> 99% of the total relative abundance). Additionally, the Blackford Pond reactors all demonstrated the least number of sequences pertaining to bacterial taxa following archaeal pre-amplification of reactor DNA samples.

The Loch Bà samples demonstrated variation between their final archaeal community compositions. Both LB1 and LB3 were dominated by *Methanoculleus* (with over 83% and 69% present of the total relative abundance, respectively). The archaeal pre-amplification approach used to boost the archaeal template DNA from the LB2 reactor appeared to perform poorly, with over 40% of sequences matching to bacterial taxa; LB2 also produced no biogas during the duration of the experiment. Additionally, the sequences observed pertaining to archaeans were more diverse, including *Methanobacterium,* and *Methanosaeta* species not observed in the other two Loch Bà sediment reactors.

Lastly, all positive control reactors were dominated by *Methanosarcina and Methanobacterium,* with PC3 demonstrating a *Methanosarcina* relative abundance of over 60 % of the total archaeal community. *Methanoculleus* also appeared in PC1 and PC2 reactors but was absent in PC3.

7.4 Discussion

7.4.1 Chemical Composition of Anaerobic Digestate

The anaerobic digestate sample collected from full scale industrial biogas reactors proved to be a dependable environmental matrix which promoted the enrichment of anaerobic consortia. However due to the recalcitrance of the previously degraded organic matter within the digestate itself, the use of additional feedstock allowed carbon degradation to occur more readily. The high organic carbon content of the digestate is reflective of the high organic load involved with wastewater treatment inflows, and the resultant production of organic-rich sludges (Yun *et al*., 2018). Anaerobic digestion promotes reduction in sludge volume and decreases the bioavailable carbon within the waste via microbial conversion to gaseous end products: CH_4 and CO_2. Despite the effective conversion of carbon-containing precursor substrates to methane rich biogas, residual recalcitrant forms of organic carbon remain; due to this, supplementation with non-digestated feedback allowed fermentative and methanogenic reactions to occur without carbon limitation. Importantly, digestate can be re-seeded back into bioreactors to promote community stability, or dewatered an applied to land, enhancing the bioavailable levels of carbon in the wider environment (Balde *et al*., 2016; Kovačić *et al*., 2022).

Additionally, the highest metals observed within the digestate (iron, calcium, and aluminium) have been noted to occur in other digestates produced from municipal sewage. The work of Dragicevic *et al*. (2018) observed that digestate containing high concentrations of metals did not impede methane generation, however, did cause detrimental issues following dewatering and land application, including aluminium leaching into soils. Importantly, in some cases, metal ions can act as microbial growth simulators in biomethane production; the addition of nickel, cobalt and copper dosing can enhance methanogenesis (Matheri *et al*., 2021). This is likely due to methanogenic *Archaea* requiring transition metals within their enzymatic co-factors, allowing an accelerated rate of methanogenesis.

The high total phosphorus levels within the digestate sample are also representative of standard anaerobic digestate conditions. High residual total phosphorus is critical in achieving a high-quality caked digestate, with phosphorus addition to land being advantageous and increasing phosphorus reserves when applied to soil, which is often noted as a limiting factor in microbial growth (Nest *et al.,* 2021). More recently, the work of Wang and Anand (2023) demonstrated that digestate is a promising valuable waste that can be utilised in electrochemical leaching and extraction of phosphorus, promoting resource recovery and a promising additional route to a more circular economy.

7.4.2 Biogas Generation and Bioreactor Performance

7.4.2.1 'Active' Digestate Positive Controls

The double autoclaved digestate and feedstock reliably acted as a matrix growth and a source of bioavailable carbon for microbial degradation of organic material and allowed methanogenic activity to be monitored in bioreactors. As expected, the most active bioreactors were the positive control reactors, as the active community was derived from a fully established anaerobic digester. This applied microbial system is designed for the derivation of robust methanogenic populations, which can generation high yields of methane.

Full scale anaerobic digesters have been noted to produce variable yields of methane depending on reactor scale, configuration, and feedstock composition (Sinsuw *et al.,* 2024). However, methane yields conventionally fall within the 50-75% range. Under standard conditions, approximately 65% methane within biogas is considered average (Usmani *et al.,* 2020). Amongst the positive control reactors, PC2 produced a mean methane content of 68.28%, however the highest noted was above 78% of methane within the headspace biogas. Due to the small scale and batch configuration of the bioreactors, it is likely that CO_2 produced during fermentative reactions was reabsorbed, and drove continual phases of hydrogenotrophic methanogenesis, achieving the elevated methane yields. Higher yields of methane (> 90% of total biogas) have been achieved in several studies, however, this often relies on chemical techniques such as 'scrubbing' using high pressure water to remove CO_2 and boost CH_4 outputs (Aswathi *et al.,* 2024). Furthermore, additives such as biochar (used to promote microbial colonisation and interspecies syntropy), nanoparticles, and hydrolytic enzymes have all been trialled improve biogas yields (Liu *et al.,* 2021).

The significant decrease in COD across all positive control reactors further demonstrated the high conversation rate of organic material to gaseous end products. Significant decreases in COD are evident within optimally functioning bioreactors, and a high residual COD indicates less effective organic waste degradation (Alibardi *et al.,* 2016). However, as the COD was measured from the soluble fraction only, the starting and end-point CODs are likely an underestimation of the total chemical oxygen demand require to oxidise all organic material present fully. Furthermore, the significant decrease in organic acids concentrations indicated that short chain organic acids were being readily converted to acetate, and subsequently to methane. The work of Grimberg *et al*. (2016) also observed a similar trend in organic acid concentrations over time, with organic acids decreasing to approximately 3 g/L. However, the authors' work utilised a dual-stage bioreactor set-up to enhance biomethane yields. The final mean pH of the positive control reactors did not demonstrate that the reactors were undergoing acid-induced stress.

7.4.2.2 Biogas Generation by Sediment Derived Communities in Bioreactors

All sediment inoculated reactors demonstrated a lag time prior to any biogas generation not observed for the positive controls. This was likely due to the environmental communities requiring time to adapt to the bioreactor conditions. It has been established in previous studies that a loss of diversity occurs within bioreactors and taxa can be lost from the community (Bagchi *et al.,* 2015; Baldwin *et al.,* 2018). Additionally, previous works have explored the use of pre-incubation of microbial consortia to overcome potential lag-periods following inoculation into applied microbial ecosystems to allow a more rapid adaptation to bioreactor conditions (*e.g.,* mesophilic temperatures). Recent work by Pastorelli *et al*. (2024) utilised a pre-incubation step during establishment of anaerobic digestate communities on biochar particles and noted a reduced lag phase when these communities were applied to soil mesocosms. However, pre-incubation of sediment communities at 37 ^{o}C prior to bioreactor set-up appeared to have no clear effect on reducing the lag time, and only the already pre-adapted digestate communities were capable of rapid biogas generation. Literature on the use of alternative inocula in anaerobic digesters is limited, however the work of Witarsa *et al*. (2016) did note a lag time in biogas generation when wetland sediment was used as cold-active inoculum, which lead to variable biogas generation.

The Blackfold Pond reactors began to overcome the lag phase the fastest (day 27) and continued to produce biogas over the longest duration compared to other environmental samples. The BP3 reactor produced the highest methane yields on average (55.65%), however did reach a yield of 71% which is comparable to methane outputs from active digestate controls. Again, the work of Witarsa *et al*. (2016) demonstrated sporadic methane outputs from wetland sediment communities, compared to the authors' methanogenic control (landfill leachate). However, the wetland sediment communities in this work did act as the most successful of the environmental samples being assessed regarding methane generation potential. The high carbon load in the Blackfold Pond sediment (see **Chapter 3**) is indicative of organic polymers which could be converted to CO_2 and CH_4 under anoxia; this copiotrophic community was the only environmental source which produced methane in all replicate bioreactors.

The degradation of complex organic polymers to biogas observed in the Blackford Pond reactors is also reflected in the bioreactors' performance more generally. Both chemical oxygen demand and organic acids levels significantly decreased, demonstrating effective carbon decomposition and production of gaseous end products over time. When performing biogeochemical cycling endogenously, freshwater sediment communities have been noted as being prolific degraders of organic acids during anoxic degradation, as has been observed in the Blackford Pond sediment amended bioreactors (Brailsford *et al*., 2019).

A single Loch Bà reactor failed to overcome the lag phase and produced no biogas. The remaining two reactors amended with Loch Bà sediment demonstrated variable responses to growth under bioreactor conditions. The Loch Bà community is oligotrophic, and exposure to carbon rich sterilised digestate and feedstock is not reflective of native substrate availability. This may have prevented establishment of a reproducibly methanogenic consortia from this sediment community. Methane emission emissions from oligotrophic sites are gaining attention due to their sensitivity to climatic fluxes, however most methane assessments are performed mimicking endogenous conditions, and do not involve providing the consortia with excess levels of organic material (McGinnis *et al*., 2015). An important consideration is the final archaeal community structure of the non-active Loch Bà reactor; native archaeans seem have been lost from the final community and this may have prevented production of biogas (this is discussed further in **Section 7.4.3.3**).

Despite the non-active Loch Bà replicate, the data presented here do demonstrate that the oligotrophic assemblage endogenous to Loch Bà was able to produce methane in some cases, however this was not observed across each replicate. Encouragingly, several complementary studies on oligotrophic lake communities state that due to the shallow depths and low carbon availability, most of the methane is oxidised by anaerobic methane oxidation and may only be produced under certain environmental conditions (Deutzmann and Schink, 2011; van Grinsven *et al*., 2022).

However, some more recent works suggest that methane generation from systems in which oligotrophy dominates may be produced via alternative precursors such as methylphosphonates under aerobic conditions, however this is poorly documented and requires further work to elucidate fully (Peoples *et al*., 2023). Importantly, the Loch Bà reactors which did produce biogas did successfully reduce the bioavailable organic acids to a significant degree. However, due to the variable methane outputs, the mean decrease in COD was not significant, likely due to the weaker establishment of methanogenic conditions, and lower methane yields resulting in residual COD remaining within the Loch Bà bioreactor contents following the end of the biogas trial.

Crucially, a single Benhar Bing sediment reactor demonstrated the production of methane-rich biogas. Despite being the most variable of the three sediment samples in terms of bioreactor performance, active methanogenesis has not been previously reported for acid mine drainage consortia. Gas release from mining waste heaps has been reported by Bortnikova *et al*. (2019), however the authors reported that the majority of mine derived gases from abandoned wastes are complex mixtures of water vapour and sulphur and selenium-containing compounds (with sulphur dioxide [SO_2] and dimethyl sulphide [C_2H_6S] being common). Exposure of metal-rich waste heaps to oxygen may impede methane release by extremophilic Mcr harbouring taxa. Yet, the methane output reported here demonstrated that methane release could occur from submerged sediments impacted by acid mine drainage and may be an overlooked source of microbially derived methane.

As stated in previous chapters, methanogenic species are poorly documented in low pH conditions, whereas their methanotrophic counterparts are more well documented (Xie *et al.,* 2011). The methane generation observed by acid mine drainage assemblage within the bioreactor system brings new attention to methane generation under extreme abiotic stress and may indicate a means of methanotrophs acquiring methane for further oxidation if acidophilic methanogens are capable of persisting under extreme conditions. The inconsistent methane generation between Benhar Bing reactor replicates suggests that any methanogens present are conditionally rare and have function has only been able to be become established once; despite producing gas the other reactors containing acidophilic inocula did not produce methane.

It should be stressed that despite not producing methane, it is likely that the gas produced in BB1 and BB3 is composed of carbon dioxide. Despite being less potent than CH_4, CO_2 remains a greenhouse gas and is to date, poorly reported as being emitted from low pH leachates. Taken together, the Benhar Bing reactors demonstrate that heavily contaminated environments can partake in carbon cycling and have the functional ability to produce methane under specific environmental conditions. This builds on work reporting on methane release from other extreme environments, not considered conventionally methanogenic such as moderately acidic hot springs and tar pits in which bioavailable carbon can be scarce and is often present in chemically recalcitrant forms (Etiope *et al.,* 2017). No other literature appears to suggest active methane generation from acid mine leachates.

Despite the variable methane outputs by members of the Benhar Bing consortia, a significant mean decrease in COD was observed across the bioreactors. Organic acid concentrations within the Benhar Bing reactors increased over the course of the bioreactor trial. This is also demonstrated in the final mean pH of the Benhar Bing reactors becoming more acidic (pH 5.53). Initially, the addition of feedstock and digestate appeared to buffer the sediment pH and cause the reactor mixture pH to rise (initial pH: 8.51). Potentially, production of acids via anoxic decomposition by community members may have led to the observed increase in organic acid concentrations. Due to the energetic challenges on low pH methanogenesis, incomplete carbon degradation may have led to this 'bottleneck' and build-up of organic acid intermediate metabolites (Hedrich and Schippers, 2021; Tong *et al.,* 2021).

7.4.3 Taxonomic Composition of Inoculating Sediments and Final Bioreactor Mixtures

7.4.3.1 Overview of Key Genera in Starting Inocula Based on V4 rRNA Sequence

The use of Illumina Sequencing to assess the metataxonomic composition of the sediment and digestate starting communities proved valuable in observing key taxa within the inoculating samples. At genus level, the active digestate was dominated by *Defluviitoga, Lemtimicrobium, Pseudomonas* and *Methanobacterium*. Members of the *Defluviitoga* have been documented routinely in full-scale anaerobic digesters treating municipal solid wastes and industrial wastes (Perman *et al*., 2024). The work of Maus *et al*. (2016) concluded that the genome of *Defluviitoga tunisiensis* L3 conferred the ability to hydrolyse a diverse range of complex polymers, including xylan, chitin, and cellulose. The authors suggested that the fermentative end products of these hydrolytic reactions (acetate, CO_2 and H_2) feed directly into methanogenic pathways. Furthermore, *Defluviitoga* is often considered thermophilic, however can proliferate at mesophilic temperatures (Maus *et al*., 2016).

Moreover, *Lentimicrobium* is also considered a key carbohydrate fermenter and producer of butyric acid for further acetogenic reactions (Zhang *et al*., 2019). However, recent evidence suggests that *Lentimicrobium* may be able to colonise biochar particles in anaerobic digesters and are capable of extracellular electron transfer (Xu *et al*., 2023). *Lentimicrobium* species may be able to form syntrophic relationships with *Methanobacterium,* however further work would be required to determine this more fully (Hu *et al*., 2022). Pseudomonads have also been repeatedly reported as being active community members in biogas reactors, whereby they are capable of degrading recalcitrant organic compounds; importantly, bioaugmentation with *Pseudomonas* species into a small-scale bioreactor appeared to lead to enhanced biogas generation and overcame the rate limited hydrolytic phase (Duran *et al*., 2006).

Finally, within the digestate, *Methanobacterium* was observed as being the predominant methanogen using the single round V4 rRNA amplification approach to metataxonomic analysis. *Methanobacterium* has been found to proliferate in bioreactors treating various organic loads and appears to tolerate both the presence of metals and acids within wastes (Li *et al*., 2018). *Methanobacterium* is considered metabolically flexible, capable of formate metabolism in some cases, as well as utilising the hydrogenotrophic methanogenic pathway.

The Blackford Pond sediment inocula demonstrated high relative abundances of *Tissierella* and *Sulfuricurvum* as well as poorly taxonomically resolved species belonging to the Actinobacteriales. There is little literature exploring the function of *Tissierella,* however has been detected in pond sediment where it is thought to be a key genus involved in organic matter decomposition (Krucon *et al*., 2021). Work by Pimenov *et al*. (2014) suggested that *Tissierella* may proliferate in conjunction with *Clostridium* species, however this did not appear to occur within the Blackford Pond community. Similarly, *Sulfuricurvum* has been only has limited metabolic characterisation performed, however is considered a sulphur oxidiser, noted to occur in ponds which undergo periods of eutrophication (Wang *et al*., 2023c).

Important genera noted in Loch Bà included *Occallatibacter, Pseudolabrys* and members of the Actinobacteria. *Pseudolabrys* appears to utilise organic acids, however, may have a more limited metabolism than has been observed in other sediment-dwelling taxa (Kämpfer *et al*., 2006). Conversely, *Occallatibacter* appears to have a broader nutritional spectrum and may be critical in driving nutrient recycling in lake and riverine sediments; disaccharides, complex polymers and proteinaceous substrates were noted to be favourable for growth of *Occallatibacter* in the work of Foesel *et al*. (2016).

The community composition of Benhar Bing has been described in detail in **Chapter 5.** The sediment sample used here as an inoculating community was collected separately from the sediment which was utilised in metagenomic analysis. Despite this, many of the key taxa remain consistent (*e.g., Metallibacterium* and 'KF-JG30' taxon pertaining to a member if the Gammaproteobacteria). It appears that due to the extreme chemical constraints of growth, community composition remains static across the dominant taxa. The function and biogeographical dispersal of these acidophiles has been described previously via analysis of assembled MAGs (**Chapter 6**). However, it is important to note differences within the relative abundances of specific taxa, due to this variation in sediment sample collection data.

Briefly, the Benhar Bing sample utilised during metagenomic analysis demonstrated higher relative abundances of both 'KF-JG30' and *Metallibacterium* compared to the sediment sample collected and used as source of microbial communities within the bioreactor tests outlined here. KF-JG30 was the most dominant community member across both samples (41.74% and 36.96% of the total relative abundances between the metagenome sediment and the bioreactor sediment, respectively). *Metallibacterium* contributed 21.12% to the total Benhar Bing community at genus level in the sediment, which was utilised for MAG assembly, however appeared less abundance, although still within the major taxa present within the bioreactor inoculating sediment (contributing 10.3% to the relative abundance at genus level).

These two key contributing taxa notwithstanding, variation between the communities between sampling was more evident when the less dominant taxa were considered. Both sediments demonstrated the presence of Acidibacteriaceae, however the sediment used as an innovative inocula contained *Cyanobacteria* unseen in the major taxa within the metagenome sample. Additionally, Gemmataceae and *Leptosprillium* were more apparent as community members within the sample utilised during long read DNA sequencing.

Despite collecting samples from the same location within Benhar Bing's constructed wetland, the samples were collected in different years which may have contributed to the changes within the taxa detected. Little work has been performed on the impacts of seasonality of acid mine drainage communities but given the apparent variation occurring in taxa other than *Metallibacterium* and KF-JG30, the potential impacts of interspaced and seasonal sampling could be a focus on future work.

Work reported by Xin *et al*. (2021) states that acid mine drainage taxa can fluctuate with season, and the authors reported that phototrophs appeared to conditionally bloom during winter, however, their growth could also be impacted by variation of concentration of mine-derived toxicants. However, making direct comparisons to this work is challenging as the acid mine drainage site being studied by Xin *et al*. (2021) was unlike in chemical composition to Benhar Bing, with noted low concentrations of iron.

Moreover, in an earlier study by Tan *et al*. (2009), the authors reported that due to the rarity of certain acidophilic taxa within mine-associated wastes, that changes in environmental conditions could lead to significant changes in the microbial composition, including the loss of taxa. Of note was the sensitivity of *Leptospirillum* to environmental fluctuations. These limited findings stress the need for future work to explore seasonal shifts in acidophilic assemblages, which may alter functionally relevant community members.

7.4.3.2 Overview of Key Genera in Starting Inocula Based on Nested PCR Archaeal Pre-amplification and V4 16S rRNA Sequencing

Due to the rarity of archaeans within most microbial consortia, amplification of the full length archaeal 16S rRNA gene prior to V4 16S rRNA amplification was performed successfully. Despite the evident skewing of the template DNA, and resulting exclusion of bacterial reads, this approach allowed archaeal ASVs to be assessed in greater detail.

Briefly, the digestate sample, plus Blackford Pond and Loch Bà all demonstrated the presence of *Methanobacterium and Methanosaeta* species; two methanogen species routinely documented as prolific members of methanogenic populations. Perhaps more unusually, non-Euryarchaeal organisms appeared dominant in Loch Bà. Bathyarchaeia 'RBG 16-50-15' appeared as a highly abundance taxon; recently, genomes of members of the Bathyarchaeia appear to include genes for methanogenesis, originally not considered to occur within these taxa (Khomyakova *et al.,* 2023). Additionally, ASVs belonging to members of the Crenarchaeota were detected in Loch Bà, which are considered globally ubiquitous in sediments, however their function remains unclear (Cai *et al.,* 2023; Kubo *et al.,* 2012).

Benhar Bing was dominated by members of the Thermoplasmatales. As discussed previously, the Thermoplasmatales and Methanoplasmatales are considered evolutionary closely related 'sister lineages' (Paul *et al.,* 2012). Further analyses and future cultivation of these archaeans would be advantageous in disentangling the relationship between these two lineages and confirming which taxa remain methanogenic, or which methanogenic metabolic routes can be exploited by these extremophiles. The potential methanogenic role of the Thermoplasmatales is discussed in **Section 7.4.3.3**.

7.4.3.3 Overview of Key Archaeal Genera in End Point Bioreactor Samples

Lastly, assessing the major archaeal contributors to each bioreactor's community at the end of the anaerobic digestion trials provided valuable insights into taxa which had persisted from the starting inocula. Most interestingly was the noted variation between BB2 and the other Benhar Bing reactors. The BB2 reactor contain archaeal taxa not observed in the final community composition of the non-methanogenic Benhar Bing syringes. Poorly taxonomically resolved members of the Thermoplasmatales were dominant, as well as a taxon predicted to belong to the Nitrosolaeaceae. Both these taxa were also detected within the initial inoculating sediment and may have caused the single methanogenic response noted amongst the acidophilic assemblages within the bioreactors.

As discussed in previous chapters (**Chapter 4 and Chapter 5),** the function of members of the Thermoplasmatales has been challenging to elucidate. Alongside their 'sister lineage', the Methanoplasmatales, they have demonstrated evolutionary divergence away from all other methanogenic lineages. Methanogenesis has been detected in members of the Methanoplasmatales, however evidence of methanogenic machinery within members of the Thermoplasmatales remains scare. Yet, the work of Poulsen *et al*. (2013) concluded that Thermoplasmatales species present within the rumen of cattle appeared to demonstrate the ability to perform methanogenesis via the methylotrophic pathway, similar to the energy conversation route performed by members of the genus *Methanomassillicoccus*. Additionally, Importantly, the work of Grettenberger and Hamilton (2021) assembled a partial MAG pertaining to a *Methanomassillicoccus*-related member of the Thermoplasmatales from a low pH acid mine drainage impacted creek, however functional annotation of the genome assembly was limited.

Additionally, a sequence pertaining to an uncultivated methanogen was attributed to the Thermoplasmataceae in the previously utilised Benhar Bing sample reported in **Chapter 5.** The biogas output detected in BB2, in conjunction with the high relative abundance of members of the Thermoplasmataceae continue to expand on current knowledge regarding this lineages' potential role in methanogenesis. future work is still required to fully determine the functional capabilities of these archaeans which appear ubiquitous in acidic leachates. Furthermore, taxa belonging to the Thermoproteota phylum have been noted to be methanogenic, however organisms from the Nitrososphaeria group native to Benhar Bing have been shown to primarily facilitate ammonia oxidation, and do not appear to perform methanogenesis (Luo *et al*., 2024).

It should be noted that the presence of conventional methanogenic taxa within the end point community composition of the additional Benhar Bing reactor (BB1 and BB3) are likely remnants of methanogenic DNA present within the sterilised digestate. The lack of methanogenic activity in these bioreactors suggests that native archaeans from Benhar Bing could not withstand the reactor conditions.

Euryarchaeal methanogens were detected in greater relative abundances in Blackford Pond, Loch Bà and the positive control reactors. As stated in **Section 7.2.3.2**, *Methanobacterium* is considered a classical methanogenic species, and appears to have persisted from the starting sediment samples through the reactor trial in the Blackford Pond reactors. The work of Vigneron *et al*. (2019) also described the high relative abundance of this taxon within littoral pond water and sediment, whereby it acted as a key member of the methanogenic population.

It is likely that the high number of bacterial reads which were detected following pre-amplification using the ArchF/ArchR primers in the Loch Bà bioreactors (reactor LB2 in particular) is largely technical. Sequence homology between the archaeal V4 and bacterial V4 16S rRNA regions, combined with the high diversity of bacterial taxa present with Loch Bà may have precluded efficient amplification of the archaeal 16S rRNA gene. Also, the most dominant archaeal member of the Loch Bà starting community, an uncultured member of the Bathyarchaeia (within the 'RBG' group) appears to have been lost from the community over the duration of the bioreactor trials. Determining function of 'RBG' members has been challenging, yet the work of Farag *et al*. (2020) suggests that these members of the Bathyarchaeia are capable of acetogenesis and potentially methane oxidation, however, do not appear to be methanogenic.

In the methanogenic Loch Bà reactors, the metataxonomic composition of the final reactor mixtures indicates that initially rarer taxa may have proliferated (*e.g., Methanobacterium*). However, this is challenging to determine fully as the Loch Bà communities performed sporadically and vary in their final community composition; LB2 which remained non-active throughout the experiment appears to have lost the majority of Loch Bà specific archaeans present in the starting sample. The high relative abundance of *Methanoculleus* present in LB1 and LB3 may have been detected from lysed methanogens present in the active digestate as they do no appear in the starting Loch Bà sediment.

Lastly, the three positive control reactor communities reflected methanogenic populations observed in fully functioning anaerobic digesters. The dominance of *Methanosarcina* across all active digestate inoculated reactors corroborates the *mcrA* sequences from *Methanosarcina* reported in **Chapter 4.** *Methanosarcina* is routinely reported as a key contributor to methane generation in biogas plants and has persisted within the positive control bioreactors due to its previous adaptation to bioreactor conditions.

Despite the positive control reactors performing most efficiently the results reported here provide new information into the use of novel and innovative methanogenic communities and their persistence within batch bioreactor systems. Going forward, the metataxonomic results pertaining to key archaeal methanogens, including those not considered 'traditional' methanogenic taxa, presented here could indicate critical taxa to target in future cultivation approaches to produce methanogenic co-cultures which could provide more resilience communities to anaerobic digesters. Most of the previous work on methanogenic community adaptation rely on whole communities (*e.g.,* cold-active methanogenic consortia), however gaps continue to remain in current knowledge regarding how best to develop more tailored consortia for industrial l uses, such as acid-tolerant methanogenic communities.

7.5 Conclusion of Chapter 7

Bioreactors proved to be a beneficial approach to studying sediment communities under controlled conditions and allowed the generation of biogas to be evaluated. Sediment communities contain methanogenic consortia capable of producing methane rich biogas, including low pH consortia, not considered conventionally methanogenic, with members of the Thermoplasmataceae appearing to perform methanogenesis. Physicochemical parameters (COD, pH, and acid levels) provided valuable insight into reactor performance over time. Future work could aim to focus on the transcriptome of active reactors to determine which genes are expressed during anoxic degradation, particularly when using extremophilic sediment as a novel and alternative inoculum.

The results presented in this final chapter highlight the exploitation of whole microbial communities which could be expanded on in the future to produce synthetic communities to enhance biogas generation via bioaugmentation, particularly in reactors which may suffer from substrate induced recalcitrance or acid stress. Additionally, and perhaps more crucially, the bioreactor trials presented above also confirm that when organic substrate availability increases in conjunction with artificial warming, methane release occurs more rapidly from endogenous communities and methanogens become metabolically active. The combination of accelerated organic leaching and global warming may cause dormant carbon cycling communities to become more active and perform methanogenesis more readily. This should be a key consideration going forward in tackling anthropogenic impacts on both conventional and extremophilic sediment communities.

CHAPTER 8 – General Discussion

8.1 Acid Mine Drainage Contaminated Environments are Unique Microbial Ecosystems

The negative environmental consequences of acid mine drainage are challenging to rectify due to the global scale of exploitative mining practices and the regenerative nature of the synthetically derived leachate (Yang *et al.,* 2023). Much of the previous research emphasis on acid mine drainage has been placed on passive wetland systems designed to prevent the wider dissemination of heavy metals. However, in these studies, little attention has been given the microbial contribution to ecosystem services and their ability to counteract the multitude of metal species prevalent in mining residues. Furthermore, the lack of literature regarding how the carbon cycle persists, and which taxa are involved in these biogeochemical reactions in heavily contaminated sites, is particularly prominent.

Previous work on iron cycling organisms, which appear less resistant to cultivation than other members of the acidophilic consortia, have dominated much of the acid mine drainage literature (Druschel *et al.,* 2004; Lu *et al.,* 2024) Due to this, current understanding of the microbial contribution to ecosystem functioning under these extreme conditions has been skewed largely to a limited number of taxa, predominantly *Acidithiobacillus* and *Leptospirillium* whereby metabolic strategies other than iron utilisation have been poorly documented (Odisi *et al.,* 2024).

Data presented in this work demonstrate how the extreme chemical composition of acid mine drainage can impact the biodiversity of prokaryotes endogenous to sites impacted by metal-laden effluents and acidic effluents present an example of a unique ecosystem dominated by specialised microbial species. Despite the extreme abiotic factors associated with acid mine effluents, this thesis aimed to characterise the previously overlooked native microbial community and elucidate the metabolic potential of key community members, thereby linking taxonomic composition to wider ecosystem function. Through multiple characterisation approaches, work presented here demonstrates that acid mine drainage consortia, despite their low diversity, harbour taxa with more diverse metabolic potential than previously documented.

To this end, the major aim of performing community characterisation was achieved.
Exploration of the extremely acidophilic consortia detected novel functions previously unreported for members of acid mine drainage populations. Importantly, comparison to more conventional microbial ecosystems, in this case, an urban pond and a highland loch, proved valuable in highlighting how chemically and biologically distinct acid mine drainage waste streams are in comparison to non-extreme systems. Given this simplistic community structure noted in the acid mine drainage consortia, the Benhar Bing assemblage provided a distinctive opportunity to determine ecological function in a community underpinned by a limited number of extremophilic taxa, which facilitated the use of novel techniques, such as long-read DNA sequencing.

8.2 Detailed Microbial Community Characterisation Relies on a Polyphasic Experimental Approach

8.2.1 Cultivation Challenges and Carbon Source Catabolism by Acidophiles

Initial chemical analysis demonstrated the high levels of metals present in Benhar Bing, and the low levels of both total and organic carbon. During the earliest stages of this work, it became evident than the unique chemistry of mine-generated wastes was impeding standard cultivation approaches and replicating acid mine conditions in culture was challenging. Due to this, focus of the work shifted away from cultivation towards a more community wide approach, with the hope of disentangling the relationships between critical acidophilic functions which promote survival in hazardous wastes, and which taxa harboured novel metabolic potential.

Metabolic profiling of microbial consortia, based upon carbon source utilisation, provided the first indication that the Benhar Bing consortium was functionally distinct from assemblages native to non-contaminated sites (Blackford Pond and Loch Bà), with utilisation of amino acids and carbohydrates generally poor compared to more conventional sediment communities. The low functional diversity observed in metabolic profiling assays corroborated the oligotrophic status of the waste stream and demonstrated that heterotrophy may not be a dominant form of energy conservation within the acidophilic community, given the low levels of organic carbon detected within the sediment and other acid mine drainage sites (She *et al*., 2023; Sajjad *et al*., 2024).

Crucially, the low biomass contained within prokaryotic assemblages from acid mine drainage may have also led to lower levels of extracellular enzyme production required to successfully catabolise the available range of substrates (Neff *et al*., 2021). A main limitation of metabolic profiling was the lack of previously published data utilising using carbon-source fingerprinting approaches on acidic mine drainage communities, which highlighted the novelty of this approach.

Following on from this, the successful cultivation of a *Thiomonas* species captured in an iChip and enriched in acidified R2A medium indicated that oligotrophic acidophiles could be grown axenically, however, may require novel cultivation strategies. The use of both more nutrient rich as well as methanogen-specific media with the aim of methanogen enrichment, proved a major limitation regarding enumeration of acidophiles. The challenges of methanogen isolation are well documented, chiefly their intolerance to trace levels of molecular oxygen, leading to enzyme inactivation (Payne *et al*., 2023). This, coupled with the complex challenges of low pH cultivation made attempts at recovering potential acidophilic methanogens unsuccessful. Nonetheless, complementing cultivation-based approaches with DNA based analysis led to greater insights into metabolic and ecological function of taxa endogenous to acidic wastes, including organisms capable of ATP conservation via methanogenesis.

8.2.2 Molecular Analysis of Acidophilic Assemblages

8.2.2.1 Analysis of Specific Functional Genes Associated with Carbon Cycling

Multiple DNA based molecular analyses proved more advantageous and less restrictive than attempting solely cultivation-based approaches. Quantification of target genes (*mcrA* and *pmoA*) and the intergenic eukaryotic ITS2 region via qPCR, proved to be a valuable starting point for further community characterisation, however, was limited to only a selection of key genes. Of note was the successful detection and quantification of the methanogenic marker gene, *mcrA*; the first time this functional gene indicative of biological methane release has been observed in pH 2.5 conditions. The presence of *mcrA* harbouring taxa in Benhar Bing expands on current understanding of methanogen dispersal and the potential for methane release from environments not traditionally considered methanogenic.

Sanger sequencing of the retrieved *mcrA* genes from the acidophilic community demonstrated that low pH Mcr dependent methanogens are taxonomically related to the order Methanoplasmatales and are likely close relatives of members of the *Methanomassillicoccus*. Only recently has the biogeographical dispersal of non-host associated *Methanomassillicoccus* species been reported, and the detection of *mcrA* genes in acidic sediment builds upon the limited work reported thus far describing environmental colonisation by members of this taxonomic family (Weil *et al*., 2023). Further to this, this provided an additional novel insight into the evolutionary relationships and potential diversification of both the Methanomassillicoccaceae, and their sister lineage, the Thermoplasmataceae, under extreme environmental pressures. Given the applicability of -omics technologies to extreme environments, evolutionary relationships between poorly represented taxa may become clearer as exploitation of extremophilic communities gathers pace to meet demand for novel consortia with unique metabolic and biotechnological potential.

Additionally, the use of both *pmoA* and the ITS2 region allowed insights into acidophilic methanotrophy, and the persistence of acid-adapted fungal species, respectively. qPCR results indicated organisms capable of facilitating reactions within the carbon cycle may be more resilient than originally thought and are capable of withstanding multiple environmental stressors. Detection of acidophilic methanotrophs corroborates the findings of multiple authors (Choi *et al.,* 2021; Hwangbo *et al.,* 2023). However, the interplay between methanogens, methanotrophs and potential syntrophic relationships with fungal species requires further work; isotopically labelled substrate studies would be a promising approach to further elucidate these relationships.

8.2.2.2 Metagenomics and Determining Metabolic Function of Key Community Members

Long read sequencing of DNA from acid mine drainage sediment by Oxford Nanopore Technology led to the most novel and informative results of this work. Unassembled DNA reads indicated a high relative abundance of genes involved in both sulphur cycling and tolerance to heavy metals when compared to a more conventional microbial ecosystem; two functional metabolic traits indicative of energy conserving strategies utilised by taxa native to acid mine drainage. However, many genes could not be annotated. To overcome this, assembly of long read DNA reads into reconstructed bacterial genomes allowed metabolic function and taxonomy of key species to be linked. This allowed previously poorly characterised taxa to have their metabolic capabilities observed fully via high-quality genomic reassemblies and assessment of their chromosomal structure. Additionally, the MAG sequences expand on current knowledge of vital biogeochemical cycles under extreme conditions.

The dominance of *Metallibacterium* within the acid mine drainage sediments collected from Benhar Bing was repeatedly confirmed using multiple approaches: taxonomic analysis of the V4 16S rRNA gene, detection within unassembled reads, and the high-quality genomic assemblies achieved pertaining to this taxon. Encouragingly, *Metallibacterium* appears to be a member of acidophilic assemblages associated with mining sites globally and has been detected in Benhar Bing previously but has been noted to vary in abundance when observed in other metataxonomic studies (Pietrzyk, 2017; Haferburg *et al.,* 2022). Variation in community composition was noted within acid mine drainage sediments collected at differing times, however, the dominating taxa, including *Metallibacterium* remained consistent.

To date, *Metallibacterium* has only had limited metabolic analyses performed (Ziegler *et al*., 2013b; Bartsch *et al*., 2017). Often the functional potential of this acid- and metal-tolerant species put forward by previous works is contradictory. The high-quality assembly of a MAG representative of a *Metallibacterium* genome presented here resolves the incongruities previously described. Genomic annotation demonstrated that despite appearing endogenous to oligotrophic, low pH niches, that the *Metallibacterium* can utilise multiple pathways involved in carbohydrate metabolism and glycolysis.

Moreover, *Metallibacterium* possesses the ability to synthesise a diverse range of enzymes to counteract heavy metal(loids) and demonstrates the ability to counteract the elevated acidity within its niche via ammonium buffering, which has now been mechanistically resolved in greater detail. *Metallibacterium* could be assessed as a candidate genus for bioremediation of pollutants *in situ*. The use of a trickling filter which promoted biofilm growth and metal detoxification by community members was trialled in the work of Evangelho *et al*. (2001) to remediate gold mining effluent and could be a potential alternative route to continual environmental reclamation. However, given the economic inputs and maintenance involved, this may not be a feasible approach in all acid mine drainage sites.

When assessed in conjunction with other assembled MAGs, principally the reconstructed chromosomes representative of *Acidiphilum* and *Mycobacterium* species, it become apparent that a diverse metabolic repertoire was harboured within several important taxa. The ability for dominant community members to perform autotrophy, hydrocarbon degradation and contribute to the wider sulphur and nitrogen cycles, as presented in this work has allowed further deduction of previously undetermined functions; many of which can be further exploited in sustainable biotechnologies, including the synthesis of extremozymes (Kuddus and Bano, 2022). Despite MAG assembly representing the more abundant species within the AMD community, the diverse repertoire of metabolic functions eluded from the highest quality genome assemblies demonstrated a significant range of ecological function.

8.2.3 Future Exploitation of Extremophilic Functions

Prior to this study, the fate of organic material in low pH systems had been poorly documented, and often had only been alluded to as an unresolved and minor biogeochemical pathway within contaminated effluents. Both qPCR and metataxonomic analysis of the acidophilic community indicated that methanogenic *Archaea,* responsible for the terminal stage of the anoxic carbon cycle, were present. Therefore, these functional groups of organisms were assessed further in reactor systems to enhance active methanogenesis. Methanogenic function was derived in a single triplicated bioreactor inoculated with acid mine drainage sediment, driven by the establishment of an active methanogenic population native to Benhar Bing. More conventional microbial consortia proved more reliable in producing methane, however the novelty of bioreactor work is stressed through methane generation by the acid mine drainage community.

Methanogenesis could not be established repeatedly in bioreactors inoculated with Benhar Bing communities However, it was apparent that Mcr-dependent methanogenesis was being facilitated, in this case, by organisms not considered amongst the more conventional methanogenic taxa. Understanding the retention of methanogenic pathways (or conversely, pathway diversification) between the divergent Methanoplasmatales and Thermoplasmates remains an area which warrants further work, particularly given the usual characteristics and biogeographical dispersal of members of these lineages within low pH effluents. Despite being present within their native sediment, persistence of methanogenic taxa derived from acid mine drainage appeared to demonstrate conditional rarity when selected in bioreactor communities. No other literature has utilised acid mine drainage communities as a bioreactor inocula, however the work of Lawson *et al*. (2015) also concluded that rare taxa involved in biological phosphorus removal in bioreactors were capable of proliferating and making metabolic contributions to the overall bioreactor performance.

Successfully bringing acidophilic methanogenesis into a cultivated state remains challenging, however an important route to pursue in future work. Given the simplistic community structure in Benhar Bing, a synthetic ecology approach could be attempted to establish methanogenic co-cultures. If acidophilic Mcr-harbouring taxa could be cultivated, they could be utilised in bioreactor systems to alleviate the loss of function caused by acid-stress due to their endogenously conferred acid-tolerance mechanisms. Anaerobic digestate is conventionally utilised for organic-rich wastes, however tailoring of the community using extremophiles that would allow the treatment of other more hazardous wastes, which to date, have limited disposal routes *e.g.,* textile wastes, and industrial effluents could lead to more sustainable waste to resource treatment options (Kumar *et al.,* 2020).

8.3 Final Conclusions

The work presented here provides a detailed characterisation of a microbial assemblage capable of proliferating under extreme acid, pollutant, and nutritional stress. Acidophilic microbial populations facilitate numerous important ecosystem functions, including, but not limited to, key metal detoxification. Results stated here also provide a clear assessment of how undoubtedly, the hazardous chemical nature of acid mine drainage influences community composition.

Moreover, the extent of damage on waterbodies impacted by mining derived leachates was alarmingly clear. The effects of mining effluent on human and environmental health warrants further investigation, particularly given the mobility of toxic metals and metalloids involved in microbially-driven redox cycles. Further chemical analysis of the sediment within Benhar Bing's constructed wetland could be performed to detect the presence of any toxic metalloids (*e.g.,* arsenic) observed in other acid mine drainage sites globally. This would also strengthen the argument for utilising the native detoxification strategies conferred by key acidophiles' genomes and assessing the potential for microbial remediation of a more diverse range of mine-derived toxicants than has been previously attempted from mining wastes.

This work presented here also stresses that moving beyond culture-based approaches is advantageous in gaining a deeper insight into microbial community characterisation. Cultivation-independent community characterisation, such as recovery and annotation of MAGs, are invaluable in inferring previously understudied function from polyextremophilic species (Grettenberger and Hamilton, 2021). Despite the prevalence of methanogens in non-extreme microbial ecosystems, potential methane emission from contaminated systems has likely been underestimated. Data presented here provide novel insights into the occurrence of taxa harbouring methanogenic molecular machinery within extremely low pH environments. Further work on methanogen dispersal is vital to fully understand the global carbon cycle and implications arising from fluxes in carbon cycling microbial populations. Greenhouse gas emissions driven by the function of previously neglected microbial consortia should be tackled with renewed focus to gain a more complete understanding of biogenic methane release and the impacts of climate.

Metagenomics proved to be the most advantageous route in inferring function from acidophilic taxa yet was complemented by both bioreactor and metabolic based approaches. Further work on acidophilic assemblages should endeavour to continue to utilise -omics techniques. An analysis of total RNA from the Benhar Bing community (via metatranscriptomics) would be valuable in assessing which genes observed within the metagenome data are expressed; the MAG sequences presented here can now act as a valuable genomic resource to facilitate this future RNA-based work. Going further, proteomics approaches could facilitate the discovery and exploitation of extremozymes synthesised by acidophiles.

Despite the detrimental consequences of metal-ore excavation, acidophiles have a key role in restoration of contaminated sites and the detoxification of mine-derived pollutants. Tighter regulations regarding the handling of metal-rich wastes, combined with improved and continual understanding of novel bioremediation strategies are vital to prevent further environmental damage. As the long-lasting effects of persistent pollutants become more pressing, emphasis must now be on implementation of the most innovative techniques to improve freshwater security. This should include exploitation of microbial function to promote resource recovery from mine wastes, which could prevent the continual overexploitation of remaining metal reserves and avert further acid mine drainage generation.

REFERENCES

Aguilar-Garrido, A., Paniagua-López, M., Sierra-Aragón, M., Martínez Garzón, F.J. and Martín-Peinado, F.J. (2023). Remediation potential of mining, agro-industrial, and urban wastes against acid mine drainage. *Scientific Reports*. **13:** 13-120.

Akacin, I., Ersoy, S., Doluca, O. and Gungormusler, M. (2022). Comparing the significance of the utilisation of next generation and third generation sequencing technologies in microbial metagenomics. *Microbiological Research*. **264:** 127-154.

Akob, D. M., Hallenbeck, M., Beulig, F., Fabisch, M., Küsel, K., Keffer, J. L., Woyke, T., Shapiro, N., Lapidus, A., Klenk, H.P and Chan, C.S. (2020), Mixotrophic iron-oxidising *Thiomonas* isolates from an acid mine drainage-affected creek. *Applied and Environmental Microbiology*. **86:** e01424-20.

Alibardi, L., Bernava, N., Cossu, R. and Spagni, A., 2016. Anaerobic dynamic membrane bioreactor for wastewater treatment at ambient temperature. *Chemical Engineering Journal*. **284**: 130-138.

Andreas, J. and Bertin, P. N. (2016). The microbial genomics of arsenic. *FEMS Microbiology Reviews*. **40:** 299-322.

Angel, R., Matthies, D. and Conrad, R. (2011). Activation of methanogenesis in arid biological soil crusts despite the presence of oxygen. *Public Library of Science ONE*. **6:** e20453.

Arias, D. E., Veluchamy, C., Dunfield, K. E., Habash, M. B. and Gilroyed, B. H. (2020). Hygienization and microbial adaptation during anaerobic co-digestion of swine manure and corn stover. *Bioresource Technology*. **306:** 123168.

Arnosti, C. (2011). Microbial extracellular enzymes and rhe marine carbon cycle. *Annual Reviews in Marine Science*. **3:** 401-425.

Ashcroft, E. and Munoz, J. (2024). A review of the principals and biotechnological applications of glycoside hydrolyses from extreme environments. *International Journal of Biological Macromolecules*. **259:** 1-12.

Awala, S.I., Gwak, J. H. and Ki, Y. M. (2021) Verrucomicrobial methanotrophs grow on diverse C3 compounds and use a homolog of particulate methane monooxygenase to oxidize acetone. *ISME Journal*. **15:** 3636–3647.

Awasthi, M.K., Rajendran, K., Vigneswaran, V.S., Kumar, V., Dregulo, A.M., Singh, V., Kumar, D., Sindhu, R. and Zhang, Z., 2024. Exploration of upgrading of biomass and its paradigmatic synthesis: Future scope for biogas exertion. *Sustainable Chemistry and Pharmacy*. **38:**.101450.

Aytar, P., Kay, C.M., Mutlu, M.B., Çabuk, A. and Johnson, D.B., 2015. Diversity of acidophilic prokaryotes at two acid mine drainage sites in Turkey. *Environmental Science and Pollution Research*, **22:** 5995-6003.

Bachmann, N. L., Salamzade, R., Manson, A. L., Whittington, R., Sintchenko, V., Earl, A. M. and Marais, B. J. (2020). Key transitions in the evolution of rapid and slow growing *Mycobacterium* identified by comparative genomics. *Frontiers in Microbiology*. **10:** 1-12.

Bagchi, S., Tellez, B.G., Rao, H.A., Lamendella, R. and Saikaly, P.E., 2015. Diversity and dynamics of dominant and rare bacterial taxa in replicate sequencing batch reactors operated under different solids retention time. *Applied Microbiology and Biotechnology*. **99:** 2361-2370.

Bailey-Watts, A. E. and Kirika, A. (1999). Poor water quality in Loch Leven (Scotland) in 1995 in spite of reduced phosphorus loadings since 1985: the influences of catchment management and inter-annual weather varation. *Hydrobiologica*. **403:** 131-151.

Baker, B. J. and Banfield, J. F. (2003). Microbial communities in acid mine drainage. *FEMS Microbiology Ecology*. **44:** 139-152.

Baker, B. J., Tyson, G. W., Webb, R. I., Flanagan, J., Hugenholtz, P., Allen, E. E. and Banfield, J. F. (2006). Lineages of acidophilic *Archaea* revealed by community genomic analysis. *Science*. **314:** 1933-1935.

Balde, H., VanderZaag, A.C., Burtt, S.D., Wagner-Riddle, C., Crolla, A., Desjardins, R.L. and MacDonald, D.J., 2016. Methane emissions from digestate at an agricultural biogas plant. *Bioresource Technology*. **216:** 914-922

Baldwin, S.A., Taylor, J.C. and Ziels, R., 2019. Genome-resolved metagenomics links microbial dynamics to failure and recovery of a bioreactor removing nitrate and selenate from mine-influenced water. *Biochemical Engineering Journal*. **151:** 107297.

Bapteste, É., Brochier, C. and Boucher, Y. (2005). Higher-level classification of the *Archaea*: evolution of methanogenesis and methanogens. *Archaea*. **1:** 353-363.

Barbosa, F., Rocha, B. A., Souza, M. C. O., Bocato, M. Z., Azevedo, L. F., Adeyemi, J. A., Santana, A. and Campiglia, A. D. (2023). Polycyclic aromatic hydrocarbons (PAHs): updated aspects of the determination, kinetics in the human body and toxicity. *Journal of Toxicology and Environmental Health*. **26:** 28-65.

Bargiela, R., Korhenkov, A. A., McIntosh, O. A., Toshchakov, S. V., Yakimov, M. M., Golyshin, P. N. and Golyshina, O. V. (2023). Evolutionary patterns of *Archaea* are predominant in acidic environments. *Environmental Microbiome*. **18:** 1-18.

Barkay, T., Miller, S. M. and Summers, A. O. (2003). Bacterial mercury resistance from atoms to ecosystems. *FEMS Microbiology Reviews*. **27:** 355-384.

Bartosiewicz, M., Venetz, J., Läubli, S., Sepúlveda, S., Bouffard, D., Zopfi, J. and Lehmann, M. F. (2023). Detritus-hosted methanogenesis sustains the methane paradox in an alpine lake. *Limnology and Oceanography*. **68:** 248-164.

Bartsch, S., Gensch, A., Stephan, S., Doetsch, A. and Gescher, J. (2017). *Metallibacterium scheffleri:* genomic data reveal a versatile metabolism. *FEMS Microbiology Ecology*. **93:** 1-11.

Basu, H., Abass, N., Dietz, R., Krummel, E., Rautino, A. and Weihe, P. (2022). The impact of mercury contamination on human health in the Arctic: a state of the science review. *Science of the Total Environment*. **831:** 154-159.

Battistuzzi, F. U., Feijao, A. and Hedges, S. B. (2004). A genomic timescale of prokaryotic evolution: insights into origin of methanogenesis, phototrophy and the colonisation of land. *BMC Evolutionary Biology*. **4:** 1-14.

Bech, P. K., Jarmusch, S. A., Rasmussen, J. A., Limborg, M. T., Gram, L. and Henriksen, N. N. S. E. (2024). Succession of microbial community composition and secondary metabolism during marine biofilm development. *ISME Journal*. **4:** 1-12.

Belova, S. E., Kulichevskaya, I. S., Bodelier, P. L. E. and Dedysh, S. N. (2013). *Methylocystis bryophila* sp. nov., a facultatively methanotrophic bacterium from acidic Sphagnum peat, and emended description of the genus *Methylocystis* '(ex Whittenbury *et al*. 1970) (Bowman *et al*. 1993)'. *International Journal of Systematic and Evolutionary Microbiology*. **63:** 1096-1104.

Ben-Fekih, I., Zhang, C., Li, Y. P., Zhao, Y., Alwathnani, H. A., Saquib, Q., Rensing, C. and Cervantes, C. (2018). Distribution of arsenic resistance genes in prokaryotes. *Frontiers in Microbiology*. **23:** 24-37.

Bender, S., Franz, C. W. and der Heijden, M. G. A. (2016). An underground revolution: biodiversity and soil ecological engineering for agricultural sustainability. *Trends in Ecology and Evolution*. **31:** 440-452.

Benov, L. (2021). Improved formazan dissolution for bacterial MTT tetrazolium assay. *Microbiology Spectrum*. **9:** e163771.

Berben, T., Bo, F. F., Zandt, M. H. I., Yang, A., Lieber, S., Welte, C. U. (2022). The Polar Fox Lagoon in Siberia harbours a community of Bathyarchaeota possessing the potential for peptide fermentation and acetogenesis. *Antonie van Leeuwenhoek*. **115:** 1229-1244.

Bergerson, J. and Lave, L. (2004). *Life Cycle Analysis of Power Generation Systems*. In: Encyclopaedia of Energy. Elsevier Inc. USA.

Berguis, B. A., Yu, F. B., Schulz, F., Blainey, P. C., Woyke, T. and Quake, S. R. (2019). Hydrogenotrophic methanogenesis in archaeal phylum Verstraetearchaeota reveals the shared ancestry of all methanogens. *Proceedings of the National Academy of Sciences*. **116:** 5037-5044.

Boase, K., Gonzalez, C., Vergara, E., Neira, G., Holmes, D. and Watkin, E. (2022). Prediction and inferred evolution of acid tolerance genes in the biotechnologically important *Acidihalobacter* genus. *Frontiers in Microbiology*. **13:** 1-16.

Bomberg, M., Mäkinen, J., Salo, M. and Kinnunen, P. (2019). High diversity in iron cycling microbial communities in acidic, iron-rich water of the Pyhäsalmi Mine, Finland. *Geofluids*. **2019:** 1-17.

Borrel, G., Adam, P. S. and Gribaldo, S. (2016). Methanogenesis and the Wood–Ljungdahl Pathway: an ancient, versatile, and fragile association. *Genome Biology and Evolution*. **8:** 1706-1711.

Borrel, G., Parisot, N., Harris, H.M., Peyretaillade, E., Gaci, N., Tottey, W., Bardot, O., Raymann, K., Gribaldo, S., Peyret, P. and O'Toole, P.W. (2014). Comparative genomics highlights the unique biology of Methanomassiliicoccales, a Thermoplasmatales-related seventh order of methanogenic archaea that encodes pyrrolysine. *BMC Genomics*. **15:** 1-24.

Bortnikova, S., Yurkevich, N., Devyatova, A., Saeva, O., Shuvaeva, O., Makas, A., Troshkov, M., Abrosimova, N., Kirillov, M., Korneeva, T. and Kremleva, T., 2019. Mechanisms of low-temperature vapor-gas streams formation from sulfide mine waste. *Science of the Total Environment*. **647:** 411-419.

Bosma, E. F., Rau, M. H., van Gijtenbeek, L. A. and Siedler, S. (2021). Regulation and distinct physiological roles of manganese in *Bacteria*. *FEMS Microbiology Reviews*. **45:** 11-28.

Bourne, D. G., McDonald, I. R. and Murrell, J. C. (2001). Comparison of *pmoA* primer sets as tools for investigating methanotroph diversity in three Danish soils. *Applied and Environmental Microbiology*. **67:** 3802-2809.

Brailsford, F.L., Glanville, H.C., Golyshin, P.N., Johnes, P.J., Yates, C.A. and Jones, D.L., 2019. Microbial uptake kinetics of dissolved organic carbon (DOC) compound groups from river water and sediments. *Scientific Reports*. **9:** 11229.

Brauer, S. L., Cadillo-Quiroz, H., Ward, R. J., Yavitt, J. B. and Zinder, S. H. (2011). *Methanoregula boonei* gen. non., sp. nov., an acidophilic methanogen isolated from peat bog. *International Journal of Systematic and Evolutionary Microbiology*. **61:** 45-52.

Brown, A.M., Bass, A.M., Skiba, U., MacDonald, J.M. and Pickard, A.E., 2023. Urban landscapes and legacy industry provide hotspots for riverine greenhouse gases: A source-to-sea study of the River Clyde. *Water Research*, **236:** 119969.

Brown, C. L., Mullet, J., Hindi, F., Stoll, J. E., Gupta, S., Choi, M., Keenum, I., Vikesland, P., Pruden, A. and Zhang, L. (2022). mobileOG-db: a manually curated database of protein families mediating the life cycle of bacterial mobile gene elements. *Applied and Environmental Microbiology*. **22:** 1-19.

Buck, D. G., Evers, D. C., Adams, E., Di Gangi, J., Beeler, B., Samanek, K., Turnquist, M. A., Speranskaya, O., Regan, K. and Johnson, S. (2019). A global-scale assessment of fish mercury concentrations and biological hotspots. *Science of the Total Environment*. **687:** 956-966.

Buessecker, S., Chadwick, G.L., Quan, M.E., Hedlund, B.P., Dodsworth, J.A. and Dekas, A.E., 2023. Mcr-dependent methanogenesis in Archaeoglobaceae enriched from a terrestrial hot spring. *The ISME Journal*. **17:** 1649-1659.

Cai, W., Yu, K., Yang, W., Mu, R., Lian, C., Xie, L., Yan, Y., Liao, S. and Wang, F., 2023. Prokaryotic Community Structure, Abundances, and Potential Ecological Functions in a Mars Analog Salt Lake. *Astrobiology*. **23:** 550-562.

Caporaso, J.G, Lauber, C.L., Walters, W.A., Berg-Lyons, D., Lozupone, C.A., Turnbaugh, P.J., Fierer, N. and Knight, R. (2011). Global patterns of 16S rRNA diversity at a depth of millions of sequences per sample. *Proceedings of the National Academy of Sciences*. **15:** 4516-22.

Catling, D. C. and Zahnle, K. J. (2020). The Archean Atmosphere. *Science Advances*. **6:** 1-16.

Chai, J., Guo, G., McSweeney, S. M., Shanklin, J. and Liu, Q. (2023). Structural basis for enzymatic terminal C-H bond functionalisation of alkanes. *Nature Structural and Molecular Biology*. **30:** 521-526.

Challacombe, J. F., Hesse, C. N., Bramer, L. M., McCue, L. A., Lipton, M., Purvine, S., Nicora, C., Gallegos-Graves, L., Porras-Alfaro, A. and Kuske, C. R. (2019). Genomes and secretomes of *Ascomycota* fungi reveal diverse functions in plant biomass decomposition and pathogenesis. *BMC Genomics*. **20:** e976.

Chandrakumar, I., Gauthier, N. P., Nelson, C., Bonsall, M. B., Locher, K., Charles, M., MacDonald, C., Krajden, M., Manges, A. R. and Chorlton, S. D. (2022). BugSplit enables genome-resolved metagenomics through highly accurate taxonomic binning of metagenomic assemblies. *Communications Biology*. **5:** 151-163.

Chen, J., Liu, Y., Diep, P. and Mahadevan, R. (2021). Genomic analysis of a newly isolated *Acidithiobacillus* JAGS strain reveals its adaptation to acid mine drainage. *Minerals*. **11:** p.74-81.

Chen, S., Zhu, M., Guo, X., Yang, B. and Zhou, R. (2023a). Coupling of the Fenton Reaction and white rot fungi for the degradation of organic pollutants. *Ecotoxicology and Environmental Safety*. **254:** 46—57.

Chen, X., Xue, D., Wang, Y., Qiu, Q., Wu, L., Wang, M., Liu, J. and Chen, H. (2023b). Variations in the archaeal community and associated methanogenesis in peat profiles of three typical peatland types in China. *Environmental Microbiome*. **18:** 1-22.

Chen, Z., Shang, J. L. Hou, S., Li, T., Li, Q., Yang, Y. W. and Qui, B. S. (2019). Genomic and transcriptomic insights into the habitat adaptation of the diazotrophic paddy-field cyanobacterium *Nostoc sphaeroides*. *Environmental Microbiology*. **23:** 5802-5822.

Cheng, L., Qiu, T. L., Yin, X. B., Wu, X. L., Hu, G. Q., Deng, Y. and Zhang, H. (2007). *Methermicoccus shengliensis* gen. nov., sp. nov., a thermophilic, methylotrophic methanogen isolated from oil-production water, and proposal of Methermicoccaceae fam. nov. *International Journal of Systematic and Evolutionary Microbiology*. **57:** 2964-2969.

Cho, J. C. and Giovannoni, S. J. (2004). Cultivation and growth characteristics of a diverse group of oligotrophic marine *Gammaproteobacteria*. *Applied and Environmental Microbiology*. **70:** 432-440.

Choi, M., Yun, T., Song, M. J., Kim, J. and Lee, B. H. (2021). Co-metabolic vinyl chloride degradation at acidic pH catalysed by acidophilic methanotrophs isolated from alpine peat bogs. *Environmental Science and Technology*. **55:** 5959-5969.

Christian, B. W. and Lind, O. T. (2006). Key issues concerning BIOLOG use for aerobic and anaerobic freshwater bacterial community level physiological profiling. *International Review of Hydrobiology*. **91:** 257-268.

City of Edinburgh Council (2011). *Hermitage of Braid and Blackford Hill Local Nature Reserve Management Plan 2011-2021*. Available from: https://www.edinburgh.gov.uk/downloads/file/22587/hermitage-of-braid-local-nature-reserve-management-plan.com. [Date accessed: 10/10/21].

Classen, A. T., Boyle, S. I., Haskins, K. E., Overby, S. T. and Hart, S. C. (2003). Community level physiological profiles of bacteria and fungi: plate type and incubation temperature on contrasting soils. *FEMS Microbiology Ecology*. **44:** 319-328.

Clemmensen, K. E., Bahr, A., Ekblad, A., Wallander, H., Stenlid, J., Finlay, R. D., Wardle, D. A. and Lindahl, B. (2013). Roots and associated fungi drive long term carbon sequestration in boreal forest. *Science*. **339:** 1615-1618.

Connon, S. A. and Giovannoni, S. J. (2002). High-throughput methods for culturing microorganisms in very-low-nutrient media yield diverse new marine isolates. *Applied and Environmental Microbiology*. **68:** 3878-3885.

Coupland, K. and Johnson, D. B. (2004). Geochemistry and microbiology of an impounded subterranean acidic water body at Mynydd Parys, Anglesey, Wales. *Geobiology*. **2:** 77-86.

Courville, P., Urbankova, E., Rensing, C., Chaloupka, R., Quick, M. Cellier, M. F. M. (2008). Solute carrier 11 cation symport requires distinct residues in transmembrane helices 1 and 6. *The Journal of Biological Chemistry*. **283:** 9651-9658.

Cozannet, M., Borrel, G., Roussel, E., Moalic, Y., Allioux, M., Sanvoisin, A., Toffin, L. and Alain, K. (2020). New insights into the ecology and physiology of Methanomassiliicoccales from terrestrial and aquatic environments. *Microorganisms*. **9:** 30-37.

Cozannet, M., Le Guellec, S. and Alain, K. (2023). A variety of substrates for methanogenesis. *Case Studies in Chemical and Environmental Engineering*. **8:** 100533.

Craddock, H. A., Motro, Y., Zilberman, B. and Khalfin, B., Bardenstein, S. and Moran-Gilad, J. (2022). Long-read sequencing and hybrid assembly for genomic analysis of clinical *Brucella melitensis* isolates. *Microorganisms*. **10:** 1-12.

Crognale, S., D'Annibale, A., Pasciaroli, L., Stazi, S. R. and Petruccioli, M. (2017). Fungal community structure and arsenic-resistant fungi in a decommissioned gold mine site. *Frontiers in Microbiology*. **9:** 1-8.

Cruz, D.R., Silva, I.A., Oliveira, R.V., Buzinaro, M.A., Costa, B.F., Cunha, G.C. and Romao, L.P., 2021. Recycling of mining waste in the synthesis of magnetic nanomaterials for removal of nitrophenol and polycyclic aromatic hydrocarbons. *Chemical Physics Letters*. **771:** 138-144.

Cunningham, L., Gruer, M.J. and Guest, J.R. (1997). Transcriptional regulation of the aconitase genes (*acnA* and *acnB*) of *Escherichia coli*. *Microbiology*. **143:** 3795-3805.

D'Andreano. S. D., Cusco, A. and Francino, O. (2020). Rapid and real-time identification of fungi up to species level with long amplicon nanopore sequencing from clinical samples. *Biology Protocols and Methods*. **1:** 1-6.

Dahl, C. (2015). Cytoplasmic sulphur trafficking in sulphur-oxidising prokaryotes. *International Union of Biochemistry and Molecular Biology – Life*. **67:** 268-274.

Daraz, U., Li, Y., Ahmad, I., Iqbal, R. and Ditta, A. (2023). Remediation technologies for acid mine drainage: recent trends and future perspectives. *Chemosphere*. **311:** 137-145.

Davenport, R. and Curtis, T. (2002). Are mycolata important in foaming? *Water Science and Technology*. **46:** 529-533.

Dean, A.P., Hartley, A., McIntosh, O.A., Smith, A., Feord, H.K., Holmberg, N.H., King, T., Yardley, E., White, K.N. and Pittman, J.K. (2019). Metabolic adaptation of a *Chlamydomonas acidophila* strain isolated from acid mine drainage ponds with low eukaryotic diversity. *Science of the Total Environment*. **647:** 75-87.

Denkmann, K., Grien, F., Zigann, R., Siemen, A., Bergmann, J., van Helmont, S., Nicolai, A., Pereira, I. A. C. and Dahl, C. (2012). Thiosulphate dehydrogenase: a widespread acidophilic *c*-type cytochrome. *Environmental Microbiology*. **14:** 2673-2688.

Deutzmann, J.S. and Schink, B., 2011. Anaerobic oxidation of methane in sediments of Lake Constance, an oligotrophic freshwater lake. *Applied and Environmental Microbiology*. **77***:* 4429-4436.

Ding, Z, Wu, J., You, A., Huang, B. and Cao, C. (2017). Effects of heavy metals on soil microbial community structure and diversity of rice (*Oryza sativa* L. subsp. *japonica)*. *Soil Science and Plant Nutrition*. **63:** 75-83.

Distaso, M.A., Bargiela, R., Brailsford, F.L., Williams, G.B., Wright, S., Lunev, E.A., Toshchakov, S.V., Yakimov, M.M., Jones, D.L., Golyshin, P.N. and Golyshina, O.V., 2020. High representation of archaea across all depths in oxic and low-pH sediment layers underlying an acidic stream. *Frontiers in Microbiology*. **11:** 576520.

Dlugokencky, E. J., Nisbet, E. G., Fisher, R. and Lowry D. (2011). Global atmospheric methane: budget, changes and dangers. *Philosophical Transactions of the Royal Society A: Mathematical, Physical and Engineering Sciences*. **369:** 2058-2072.

Dobranic, J. K. and Zak, J. C. (1999). A microtitre plate procedure for evaluating fungal functional diversity. *Mycologia*. **91:** 756-765.

Dong, J., Fischer, R. A., Stixrude, L. P. and Lithgow-Bertelloni, C. R. (2021). Constraining the volume of Earth's early oceans with a temperature-dependent mantle water storage capacity model. *AGU Advances*. **2:** 1-24.

Dong, X., Yu, Y., Liu, J., Cao, D., Xiang, Y., Bi, K., Yuan, X., Li, S., Wu, T. and Zhang, Y. (2023).Whole-genome sequencing provides insights into a novel species: *Providencia hangzhouensis* associated with urinary tract infections. *Microbiology Spectrum*. **11:** e01227-23.

Dos Santos, J.D.N., João, S.A., Martín, J., Vicente, F., Reyes, F. and Lage, O.M., 2022. iChip-inspired isolation, bioactivities, and dereplication of *Actinomycetota* from Portuguese Beach sediments. *Microorganisms*. **10:** 1471-1478.

Douglas, G. M., Maffei, V. J., Zaneveld, J. R., Yurgel, S. N., Brown, J. R., Taylor, C. M., Huttenhower, C. and Langille, M. G. (2020). PICRUSt2 for prediction of metagenome functions. *Nature Biotechnology*. **38:** 685-688.

Dragicevic, I., Eich-Greatorex, S., Sogn, T. A., Horn, S. J. and Krogstad, T. (2018). Use of high metal containing biogas digestates in cereal production: mobility of chromium and aluminium. *Journal of Environmental Management*. **207:** 12-22.

Drake, H., Ivarsson, M., Heim, C., Snoeyenbos-West, O., Bengtson, S., Belivanova, V. and Whitehouse, M. (2021). Fossilised anaerobic and possibly methanogenesis-fuelling fungi identified deep within the Siljan impact structure, Sweden. *Nature Communications: Earth and Environment*. **2:** 1-10.

Dridi, B., Fardeau, M.L., Ollivier, B., Raoult, D. and Drancourt, M. (2012). *Methanomassiliicoccus luminyensis* gen. nov., sp. nov., a methanogenic archaeon isolated from human faeces. *International Journal of Systematic and Evolutionary Microbiology*. **62:** 1902-1907.

Druschel, G.K., Baker, B.J., Gihring, T.M. and Banfield, J.F., 2004. Acid mine drainage biogeochemistry at Iron Mountain, California. *Geochemical Transactions*. **5:** 1-20.

DSMZ (2022a). *120: Methanosarcina Medium*. Available from: https://www.dsmz.de/microorganisms/medium/pdf/DSMZ_Medium120.com. [Date accessed: 12/07/18].

DSMZ (2022b). *1190: Ferrous Sulphate/Yeast Extract Medium*. Available from: https://bacmedia.dsmz.de/medium/1190 [Date accessed: 17/08/18].

Du, R., Chai, F., Zhu, R., Yan, Y., Li, S. and Niu, Y. (2023). Achieving efficient biodegradation of hydrophobic toluene via the enhancement of b-cyclodextrin and atomisation. *Process Safety and Environmental Protection*. **170:** 1151-1160.

Ducret, V., Gonzalez, D. and Perron, K. (2023). Zinc homeostasis in *Pseudomonas*. *Biometals*. **36:** 729-744.

Duin, E. C. (2013). *Methyl-coenzyme M reductase*. In: Encyclopaedia of Metalloproteins. Springer, New York.

Duquesne, K., Lieutaudm A., Ratouchniak, J., Muller, D. and Lett, M. C. (2008). Arsenite oxidation by a chemoautoptrophic moderately acidophilic *Thiomonas* species: from the strain isolation to the gene study. *Environmental Microbiology*. **10:** 228-237.

Duran, M., Tepe, N., Yurtsever, D., Punzi, V.L., Bruno, C. and Mehta, R.J., 2006. Bioaugmenting anaerobic digestion of biosolids with selected strains of Bacillus, Pseudomonas, and Actinomycetes species for increased methanogenesis and odor control. *Applied Microbiology and Biotechnology*. **73***:* 960-966.

Dutta S, Gorain B, Choudhury H, Roychoudhury S and Sengupta P. (2022). Environmental and occupational exposure of metals and female reproductive health. *Environmental Science and Pollution* **41:** 62067-62092.

Duzs, A., Miklovics, N., Paradgi, G., Rakhely, G. and Toth, A. (2021). Inishgts into the catalytic mechanism of type IV sulphide:quinone oxidoreductases. *Biochimica et Biophysica Acta – Bioenergetics*. **1862:** 1-12.

Dyksma, S., Jansen, L. and Gallert, C. (2020). Syntrophic acetate oxidation replaces acetoclastic methanogenesis during thermophilic digestion of biowaste. *Microbiome*. **8:** 1-14.

Dziewit, L., Pyzik, A., Romaniuk, K., Sobczak, A., Paewl Szczesny, Lipinski, L., Bartosik, D. and Drewniak, L. (2015). Novel molecular markers and phylogenetic analysis of methanogenic communities. *Frontiers in Microbiology*. **6:** 694-701.

Dziewit, L., Pyzik, A., Romaniuk, K., Sobczak, A., Paewl Szczesny, Lipinski, L., Bartosik, D. and Drewniak, L. (2015). Novel molecular markers and phylogenetic analysis of methanogenic communities. *Frontiers in Microbiology*. **6:** 694-701.

Echavarri-Bravo, V., Paterson, L., Aspray, T., Porter, J. S., Winson, M. K., Thorton, B. and Hartl, M. G. J. (2015). Shifts in the metabolic function of a benthic estuarine microbial community following a single pulse exposure to silver nanoparticles. *Environmental Pollution*. **201:** 91-99.

Eckley, C. S., Luxton, T. P., Stanfield, B., Baldwin, A., Holloway, J., McKernan, J. and Johnson, M. G. (2021). Effect of organic matter concentration and characteristics on mercury mobilisation and methylmercury production at abandoned mine sites. *Environmental Pollution*. **271:** 116-123.

Elghali, A., Benzaazoua, M., Taha, Y., Amar, H., Ait-khouia, Y., Bouzahzah, H. and Hakkou, R. (2023). Prediction of acid mine drainage: Where are we? *Earth-Science Reviews* **10:**, e104-116.

Emerson, D., Roden, E. and Twining, B. S. (2012). The microbial ferrous wheel: iron cycling in terrestrial, freshwater and marine environments. *Frontiers in Microbiology*. **3:** 383-403.

Ermler, U., Grabarse, W., Shima, S., Goubeaud, M. and Thauer, R. K. (1997). Crystal structure of methyl-coenzyme M reductase: the key enzyme of biological methane formation. *Science*. **21:** 1457-1462.

Etiope, G., Doezema, L.A. and Pacheco, C., 2017. Emission of methane and heavier alkanes from the La Brea Tar Pits seepage area, Los Angeles. *Journal of Geophysical Research: Atmospheres*. **121:** 12-008.

European Environmental Agency. (2019). *Annual European Union Greenhouse Gas Inventory (1990–2017) and Inventory Report*. Available from: https://www.eea.europa.eu/publications/european-union-greenhouse-gas-inventory-2019. [Date accessed: 04/01/2023].

Evangelho, M.R., Gonçalves, M.M.M., Sant'Anna Jr, G.L. and Boas, R.V. (2001). A trickling filter application for the treatment of a gold milling effluent. *International Journal of Mineral Processing*. **62:** 279-292.

Falkinham, J. O. (2021). Ecology of non-tuberulous *Mycobacterium*. *Microorganisms*. **9:** 1-10.

Fenchel, T., King, G. M. and Blackburn, T. H. (2006). Bacterial Biogeochemistry: The Ecophysiology of Mineral Cycling. 2nd Ed. Elsevier Academic Press: USA.

Fenibo, E.O., Selvarajan, R., Wang, H., Wang, Y. and Abia, A.L.K., 2023. Untapped talents: insight into the ecological significance of methanotrophs and its prospects. *Science of The Total Environment*. **903:** 1-20.

Fernandez-Caliani, J. C., Giraldez, M. I. and Barba-Brioso, C. (2019). Oral bioaccessibility and human health risk of trace elements in agricultural soils impacted by acid mine drainage. *Chemosphere*. **237:** 124441.

Ferry, J. G. (2010). CO in methanogenesis. *Annuals of Microbiology*. **60:** 1-12.

Ferry, J. G. (2020). *Methansarcina acetivorans:* a model for mechanistic understanding of acetoclastic and reverse methanogenesis. *Frontiers in Microbiology*. **28:** e1806.

Flower, R. J., Battarbee, R. W., Natkanski, J., Rippey, B. and Appleby, P. G. (1988). The recent acidification of a large Scottish loch within a national nature reserve and site of special scientific interest. *Journal of Applied Ecology*. **25:** 715-724.

Foesel BU, Mayer S, Luckner M, Wanner G, Rohde M, Overmann J. (2016). *Occallatibacter riparius* gen. nov., sp. nov. and Occallatibacter savannae sp. nov., acidobacteria isolated from Namibian soils, and emended description of the family Acidobacteriaceae. *Int J Syst Evol Microbiol*. **66:** 219-229.

Fontecilla-Camps, J. C. (2022). Nickel and the origin and early evolution of life. *Metallomics*. **14:** 1-8.

Fordyce, F., Everett, P., Bearcock, J., & Lister, T. (2017). Soil metal/metalloid concentrations in the Clyde Basin, Scotland, UK: Implications for land quality. *Earth and Environmental Science Transactions of The Royal Society of Edinburgh*. **108**: 191-216.

Fournier, G. P. and Gogarten, J. P. (2008). Evolution of acetoclastic methanogenesis in *Methanosarcina* via horizontal gene transfer from cellulolytic *Clostridia*. *Journal of Bacteriology*. **190:** 1124-1127.

Free, A., McDonald, M. A, and Pagaling E. (2018). *Diversity-function relationships in natural, applied, and engineered microbial ecosystems*. In: Advances in Applied Microbiology. Vol. 105. Academic Press.

Freel, K. C., Krueger, M. C., Farasin, J. Bouchier-Armanet, C., Barbe, V., Andres, J., Cholley, P. E., Dillies, M. A., Jagla, B., Koechler, S. and Leva, Y. (2015). Adaptation in toxic environments: arsenic genomic islands in the bacterial genus *Thiomonas*. *PloS One*. **10:** e0139011.

Galazka, A., Grzadziel, J., Galazka, R., Ukalska-Jarunga, A., Stzelecka, J. and Smreczak, B. (2018). Genetic and functional diversity of bacterial microbiome in soils with long term impacts of petroleum hydrocarbons. *Frontiers in Microbiology*. **9:** 1-11.

Garber, A. I., Nealson, K. H., Okamoto, A., McAllister, S. M., Chan, C. S., Barco, R. A. and Merico, N. (2020). FeGenie: a comprehensive tool for the identification of iron genes and iron gene neighbourhoods in genome and metagenome assemblies. *Frontiers in Microbiology*. **31:** 1-13.

Garbinski, L. D., Rosen, B. P. and Chen, J. (2019). Pathways of arsenic uptake and efflux. *Environment International*. **126:** 585-597.

Garcia-Maldonado, J. Q., Latisnere-Barragán, H., Escobar-Zepeda, A., Cadena, S., Ramirez-Arenas, P. J., Vazquez-Juarez, R., Rojas-Contreras, M. and López-Juárez, R. (2023). Revisiting microbial diversity on hypersaline microbial mats from Guerroro Negro for a better understanding of methanogenic archaeal communities. *Microorganisms*. **11:** 1-18.

Garland, J. L. and Mills, A. L. (1991). Classification and characterisation of heterotrophic microbial communities on the basis of patterns of community-level sole carbon source utilisation. *Applied and Environmental Microbiology*. **57:** 2351-2359.

Garland, R. M. (2012). Acid mine drainage: can it effect human health? *Academy of Science of South Africa*. **7:** 46-47.

Geets, J., Borremans, B., Diels, L., Springael, D., Vangronsveld, J., van der Lelie, D. and Vanbroekhoven. (2016). *DsrB* gene-based DGGE for community and diversity surveys of sulfate-reducing bacteria. *Journal of Microbiological Methods*. **66:** 194-206.

Geller, W., Klapper, H. and Salomons, W. (2012). *Acidic mining lakes: acid mine drainage, limnology, and reclamation*. 2nd Ed. Springer Science: Germany.

Gendron, A. and Allen, K. D. (2022). Overview of diverse methyl/alkyl-coenzyme M reductases and considerations for their potential heterologous expression. *Frontiers in Microbiology*. **13**: 1-18.

Ghosh, S., N. R. Mahapatra, and P. C. Banerjee. (1997). Metal resistance in *Acidocella* strains and plasmid-mediated transfer of this characteristic to *Acidiphilium multivorum* and *Escherichia coli*. *Applied and Environmental Microbiology*. **63:** 4523-4527.

Gios, E., Mosley, O. E., Weaver, L., Close, M., Daughtey, C. and Handley, K. M. (2023). Ultra-small bacteria and archaea exhibit genetic flexibility towards groundwater oxygen content, and adapatations for attached or planktonic lifestyles. *ISME Journal*. **13:** 1-14.

Gomes, P., Valente, T., Geraldo, D. and Ribeiro, C. (2020). Photosynthetic pigments in acid mine drainage: seasonal patterns and associations with stressful abiotic characteristics. *Chemosphere*. **239:** 124-135.

Grabarse, W., Mahlert, F., Shima, S., Thauer, R. K. and Ermler, U. (2000). Comparison of three methyl-coenzyme M reductases from phylogenetically distant organisms: unusual amino acid modification, conservation, and adaptation. *Journal of Molecular Biology*. **303:** 329-344.

Grettenberger, C. L., McCauley, R. L., Gruen, D. S., Mills, D. B., Carney, C., Brainard, J., Hamasaki, H., Ramirez, R., Watanabe, Y., Amaral-Zettler, L. A., Ohmoto, H. and McCalady, J. L. (2020). Mocrobial population structure in a stratified aicd pit lake. *Geomicrobiology Journal*. **37:** 623-634.

Grettenberger, C.L. and Hamilton, T.L. (2021). Metagenome-assembled genomes of novel taxa from an acid mine drainage environment. Applied and Environmental Microbiology. **87:** 1-21.

Grimberg, S.J., Hilderbrandt, D., Kinnunen, M. and Rogers, S., 2015. Anaerobic digestion of food waste through the operation of a mesophilic two-phase pilot scale digester–assessment of variable loadings on system performance. *Bioresource technology*, *178*, pp.226-229.

Grossart, H. P., Frindte, K., Dziallas, C., Eckert, W. and Tang, K. W. Microbial methane production in oxygenated water column of an oligotrophic lake. (2011). *Proceedings of the National Academy of Sciences*. **108:** 19657-19661.

Grossart, H. P., Massana, R., McMahon, K. D. and Walsh, D. A. (2020). Linking metagenomes to aquatic microbial ecology and biogeochemical cycles. *Limnology and Oceanography*. **65:** 2-20.

Groves, J. T., Feng, L. and Austin, R. N. (2023). Structure and function of alkane monooxygenase (AlkB). *Accounts of Chemical Research*. **30:** 2180-2188.

Gryta, A., Frac, M. and Oszurt, K. (2014). The application of the BIOLOG EcoPate approach in ecotoxicological evaluation of dairy sewage sludge. *Applied Biochemistry and Biotechnology*. **174:** 1434-1443.

Guggenheim, C., Brand, A., Burgmann, H., Sigg, L. and Wehrli, B. (2019). Aerobic methane oxidation under copper scarcity in a stratified lake. *Scientific Reports*. **9:** 1-11.

Guo, S., Toth, C. R., Luo, F., Chen, X., Xiao, J. and Edwards, E. A. (2022). Transient oxygen exposure causes profound and lasting changes to a benzene-degrading methanogenic community. *Environmental Science and Technology*. **56:** 13036-13045.

Gupta, A., Saha, A. and Sar, P. (2021). Thermoplasmata and Nitrososphaeria as dominant archaeal members in acid mine drainage sediment of Malanjkhand Copper Project, India. *Archives of Microbiology*. **203:** 1833-1841.

Hach Lange (2019a). *LCK365 Chemical Oxygen Demand (COD) Working Procedure*. Available from: https://uk.hach.com/cod-cuvette-test-100-2000-mg-l-o-25-tests/product-downloads?id=26370291495. [Date accessed: 12/01/20].

Hach Lange (2019b) *Sulphate Working Procedure*. Available at: https://uk.hach.com/sulphate-cuvette-test-40-150-mg-l-so-25-tests/product-downloads?id=26370268945. [Date accessed: 19/01/21].

Hach Lange (2019c). *Sulphate Dissolved Working Solution*. Available from: https://uk.hach.com/sulphide-cuvette-test-0-1-2-0-mg-l-s2-25-tests/product-downloads?id=26370291516. [Date accessed: 23/02/22].

Hach Lange (2019d). *Ammonium Working Procedure*. Available from: https://uk.hach.com/ammonium-cuvette-test-2-0-47-0-mg-l-nh-sub-4-sub-n/. [Date accessed: 13/01/23].

Hach Lange (2020). *LCK 365 Organic Acid / Butanoic Acid Working Procedure*. Available at: https://uk.hach.com/organic-acids-cuvette-test-50-2500-mg-l-25-tests/product-downloads?id=26370291461/. [Date accessed: 10/01/21].

Haferberg, G., Krichler, T. and Hedrich, S. (2022). Prokaryotic communities in the historic silver mine, Reiche Zeche. *Extremophiles*. **2:** 1-17.

Hakemian, A. S., Kondapalli, K. C., Telser, J., Hoffmann, B. M., Stemmler, T. L. and Rosenzweig, A. C. (2008). The metal centres of particulate methane monooxygenase from *Methylosinus trichosporium* OB3b. *Biochemistry*. **47:** 6793-6801.

Hakobyan, A. and Liesack, W. (2020). Unexpected metabolic versatility among type II methanotrophs in the Alphaproteobacteria. *Biological Chemistry*. **401:** 469-1477.

Hall, B.G. (2013). Building phylogenetic trees from molecular data with MEGA. *Molecular Biology and Evolution*. **30:** 1229-1235.

Hama, H., Kayahara, T., Ogawa, W., Tsuda, M. and Tsuchiya, T. (1994). Enhancement of serine-sensitivity by a gene encoding rhodanese-like protein in *Escherichia coli*. *The Journal of Biochemistry*. **115:** 135-1140.

Hao, C., Wang, L., Gao, Y., Zhang, L. and Dong, H. (2010). Microbial diversity in acid mine drainage of Xiang Mountain sulfide mine, Anhui Province, China. *Extremophiles*. **14:** 465-474.

Harada, M., Yoshida, T., Kuwahara, H., Shimamura, S., Takaki, Y., Kato, C., Miwa, T., Miyake, H. and Maruyama, T. (2009). Expression of genes for sulphur oxidation in the intracellular chemoautotrophic symbiont of the deep-sea bivalve *Calyptogena okutanii*. *Extremophiles*. **13:** 895-903.

Hatzios, S. K. and Bertozzi, C. R. (2011). The regulation of sulphur metabolism in *Mycobacterium tuberculosis*. *PloS Pathogens*. **7:** e10002036.

Hausmann, B., Pelikan, C., Herbold, C.W., Köstlbacher, S., Albertsen, M., Eichorst, S.A., Glavina del Rio, T., Huemer, M., Nielsen, P.H., Rattei, T. and Stingl, U. (2018). Peatland Acidobacteria with a dissimilatory sulfur metabolism. *The ISME Journal*. **12:** 1729-1742.

Havig, J. R., Grettenberger, C. and Hamilton, T. L. (2017). Geochemistry and microbial community composition across a range of acid mine drainage impacted and implications for the Neoarchean-Paleoproterozic transition. *Journal of Geophysical Research: Biogeosciences*. **122:** 1404-1422.

Heal, K. V. and Salt, C. A. (1999). Treatment of acidic metal-rich drainage from reclaimed ironstone mine spoil. *Water Science and Technology*. **39:** 141-148.

Hedrich, S. and Schippers, A. (2021). Distribution of acidophilic microorganisms in natural and man-made acidic environments. *Current Issues in Molecular Biology*. **40:** 25-48.

Hernández, M., Klose, M., Claus, P., Bastviken, D., Marotta, H., Figueiredo, V., Enrich-Prast, A. and Conrad, R. (2019). Structure, function, and resilience to desiccation of methanogenic microbial communities in temporarily inundated soils of the Amazon rainforest (Cunia Reserve, Rondonia). *Environmental Microbiology*. **21:** 1702-1717.

Herrero-Ortega, S., Gonzalez-Quiljano, R., Casper, R., Singer, G. A. and Gessner, M. O. (2019). Methane emissions from contrasting urban freshwaters: rates, drivers and a whole-city footprint. *Global Change Biology*. **25:** 4234-5243.

Hoegenauer C, Hammer HF, Mahnert A, Moissl-Eichinger C. (2022). Methanogenic archaea in the human gastrointestinal tract. *Nature Reviews Gastroenterology & Hepatology*. **19:** 805-813.Hoellein, T. J., Tank, J. L., Kelly, J. J. and Rosi-Marshall, E. J. (2010). Seasonal variation in nutrient limitation of microbial biofilms colonising organic and inorganic substrata in streams. *Hydrobiologica*. **649:** 331-345.

Hou, J., Wang, Y., Zhu, P., Yang, N., Liang, L., Yu, T., Niu, M., Konhauser, K., Woodcroft, B.J. and Wang, F., (2023). Taxonomic and carbon metabolic diversification of Bathyarchaera during its coevolution history with early Earth surface environment. *Science Advances*. **9:** 50-69.

Huang, L. N., Chen, Y. Q., Zhou, H., Luo, S., Lan, C. Y. and Qu, L. H. (2003). Characterisation of methanogen *Archaea* in the leachate of a closed municipal solid waste landfill. *FEMS Microbial Ecology*. **46:** 171-177.

Huang, Q., Huang, Y., Li, B., Li., X., Guo, Y., Jiang, Z., Liu, X., Yang, Z., Ning, Z., Xiao, T., Jiang, C. and Hao, L. (2023). Metagenomic analysis characterised resistomes of an acidic, multimetal(loid)-enriched coal source mine drainage treatment system. *Journal of Hazardous Materials*. **448:** 130898.

Huang, Y., Li, X. T., Jiang, Z. L. and Wang, P. (2021). Key factors governing microbial community in extremely acidic mine drainage (pH < 3). *Frontiers in Microbiology*. **12:** 761-795.

Hughes, M. (2002). Arsenic toxicity and potential mechanisms of action. *Toxicology Letters*. **133:** 1–16.

Hwangbo, M., Shao, Y., Hatzinger, P. B. and Chu, K. H. (2023). Acidophilic methanotrophs: occurrence, diversity, and possible bioremediation applications. *Environmental Microbiology Reports*. **15:** 265-281.

Ikeda, H., Tokonami, A., Nishii, S., Shan, X., Yamamoto, Y., Sadanaga, Y., Chen, Z. and Shiigi, H. (2023). Evalution of bacterial activity based on the electrochemical properties of tetrazolium salts. *Analytical Chemistry*. **95:** 12358-12364.

Invitrogen (2006). *Quant-iT Assays for high-throughput quantitation of DNA, RNA, and oligos*. Available at: https://www.thermofisher.com/document-connect/document-connect.html?url=https://assets.thermofisher.com/TFS-Assets%2FLSG%2Fbrochures%2FF-065432%20quantit%20htp_FLR.pdf. [Date accessed: 13/01/22].

Invitrogen (2014). *TA Cloning Kit: Cloning of Taq Polymerase Amplified PCR Products*. Available from: https://tools.thermofisher.com/content/sfs/manuals/topota_man.pdf. [Date accessed: 13/01/23].

Ishikita, H. and Knapp, E. W. (2007). Protonation states of ammonia/ammonium in the hydrophobic pore of the ammonia transporter protein AmtB. *Journal of the American Chemical Society*. **129:** 1210-1215.

Jaarsma, A.H., Sipes, K., Zervas, A., Jiménez, F.C., Ellegaard-Jensen, L., Thøgersen, M.S., Stougaard, P., Benning, L.G., Tranter, M. and Anesio, A.M. (2023). Exploring microbial diversity in Greenland Ice Sheet supraglacial habitats through culturing-dependent and-independent approaches. *FEMS Microbiology Ecology*. **99:** 101-119.

Jamy, M., Foster, R., Barbera, P., Czech, L., Kozlov, A., Stamatakis, A., Bending, G., Hilton, S., Bass, D. and Burki, F. (2020). Long read metabarcoding of the eukaryotic rDNA operon to resolve environmental diversity phylogenetically and taxonomically. *Molecular Ecology Resources*. **20:** 429-443.

Jensen, L.J., Julien, P., Kuhn, M., von Mering, C., Muller, J., Doerks, T. and Bork, P., 2007. eggNOG: automated construction and annotation of orthologous groups of genes. *Nucleic Acids Research*. **36:** 250-254.

Jesenska, A., Pavlova, M., Strouhal, M., Chaloupkova, R., Tesinska, I., Monincova, M., Prokop, Z., Bartos, M., Pavlik, I., Rychik, I. and Mobius, P. (2005). Cloning, biochemical properties and distribution of mycobacterial haloalkane dehalogenases. *Applied and Environmental Microbiology*. **71:** 6736-6745.

Ji, M., Smith, A. F., Rattray, J. E., England, W. E. and Hubert, C. R. (2023). Potential for natural attenuation of crude oil hydrocarbons in benthic microbiomes near coastal communities in Kivalliq, Nunavut, Canada. *Marine Pollution Bulletin*. **196:** 115557

Jiang, X. T., Guo, F. and Zhang, T. (2016). Population dynamics of bulking and foaming bacteria in a full-scale wastewater plant over five years. *Scientific Reports*. **6:** 24180.

Jiang, X., Ha, C., Lee, S., Kwon, J., Cho, H., Gorham, T. and Lee, J. (2019). Characterisation of cyanophages in Lake Erie: interaction mechanisms and structural damage of toxic cyanobacteria. *Toxins*. **11:** 444-458.

Jin, Q. and Kirk, M. F. (2018). pH as a primary control in environmental microbiology: thermodynamic perspective. *Frontiers in Environmental Science*. **21:** 1-15.

Johnson, D. B. and Hallberg, K. B. (2003). The microbiology of acidic mine waters. *Research in Microbiology*. **154:** 466-473.

Johnson, D. B. and Hallberg, K. B. (2007) *Techniques for detecting and identifying acidophilic mineral-oxidizing microorganisms*. In: Biomining. Springer: Berlin Heidelberg.

Jones, D. S., Schaperdoth, I. and MaCalady, J. L. (2013). Metagenomc evidence for sulphide oxidation in extremely acidic cave biofilms. *Geomicrobiology Journal*. **31:** 194-294.

Jones, S. and Santini, J. M. (2023). Mechanisms of bioleaching: iron and sulphur oxidation by acidophilic microorganisms. *Essays in Biochemistry*. **67:** 685-699.

Jones, S. E. and Lennon, J. T. (2010). Dormancy contributes to the maintenance of microbial diversity. *Proceedings of the National Academy of Sciences*. **107:** 5881-5886.

Josts, I., Veith, K., Normant, V., Schalk, I. J. and Todow, H. (2021). Structural insights into a novel family of integral membrane siderophore reductases. *Proceedings of the National Academy of Sciences*. **118:** e1210195.

Kabiraj, A., Biswas, R., Halder, U. and Bandopadhyay, R. (2022). Bacterial arsenic metabolism and its role in arsenic bioremediation. *Current Microbiology*. **79:** e131.

Kallistova, A. Y., Koval, D. D., Kadnikov, V. V., Toshchakov, S. V., Yusupov, S. K., Izotova, A. O., Vinogradova, E. N., Zekker, I. and Pimeniv, N. V. (2023). Methane cycle in a littoral site of a temperate freshwater lake. *Microbiology*. **92:** 153-170.

Kämpfer, P., Young, C.C., Arun, A.B., Shen, F.T., Jäckel, U., Rosselló-Mora, R., Lai, W.A. and Rekha, P.D., 2006. *Pseudolabrys taiwanensis* gen. nov., sp. nov., an alphaproteobacterium isolated from soil. *International Journal of Systematic and Evolutionary Microbiology*. **56:** 2469-2472.

Kang, N.K., Chau, T.H.T. and Lee, E.Y. (2024). Engineered methane biocatalysis: strategies to assimilate methane for chemical production. *Current Opinion in Biotechnology*. **85:** 1-8.

Karthikeyan, O. P., Smith, T. J., Dandare, S. U., Parwin, K. S., Singh, H., Loh, H. X., Cunningham, M. R., Williams, P. N., Nichol, T., Subramanian, A., Ramasamy, K. and Kumaresan, D. (2021). Metalloid speciation and transformation by aerobic methanotrophs. *Microbiome*. **9:** 1-18.

Kasting, J. F. and Siefert, J. L. (2002). Life and the evolution of Earth's atmosphere. *Science*. **296:** 1066-1068.

Katayama, T., Yoshioka, H., Kaneko, M., Amo, M., Fujii, T., Takahashi, H. A., Yoshida, S. and Sakata, S. (2022). Cultivation and biogeochemical analyses revels insights into methanogenesis in deep sea sediment at a biogenic hydrate site. *ISME Journal*. **16:** 1464-1472.

Kauserud, H. (2023). ITS alchemy: on the use of ITS as a DNA marker in fungal ecology. *Fungal Ecology*. **65:** 1-11.

Kenarova, A., Encheva, M., Chipeva, V., Chipev, N., Hristova, P. and Moncheva, M. (2013). Physiological diversity of bacterial communities from different soil locations on Livingston Island, South Shetland Archipelago, Antarctica. *Polar Biology*. **36:** 223-233.

Khachatryan, A., Vardanyan, N., Willscher, S., Sevoyan, G., Zhang, R. and Vardanyan, A., 2023. Bioleaching of Chalcopyrite by a New Strain *Leptospirillum ferrodiazotrophum* Ksh-L Isolated from a Dump-Bioleaching System of Kashen Copper-Molybdenum Mine. *Minerals*. **14:** p.26-36.

Khan, A. and Sarkar, D. (2012). Nitrate reduction pathways in mycobacteria and their implications during latency. *Microbiology*. **158:** 301-307.

Khelaifia S., Raoult, D. and Drancourt, M. (2013). A versatile medium for cultivating methanogenic *Archaea*. *Public Library of Science ONE*. **8:** e61563.

Khelaifia, S., Raoult, D. and Drancourt, M. (2013). A versatile medium for cultivating methanogenic *Archaea*. *Public Library of Science ONE*. **8:** e61563.

Khelaifia, S., Raoult, D. and Drancourt, M. (2013). A versatlile medium for cultivating methanogenic Archaea. *PLoS One*. **8:** e61563.

Khomich, M., Davey, M. L., Kauserud, H., Rasconi, S. and Andersen, T. (2018). Fungal communities in Scandinavian lakes along a longitudinal gradient. *Fungal Ecology*. **27:** 36-46.

Khomyakova, M.A., Merkel, A.Y., Mamiy, D.D., Klyukina, A.A. and Slobodkin, A.I., 2023. Phenotypic and genomic characterization of Bathyarchaeum tardum gen. nov., sp. nov., a cultivated representative of the archaeal class Bathyarchaeia. *Frontiers in Microbiology*. **14:** 1214631.

Khudur, L. S., Gleeson, D. B., Ryan, M. H., Shahsavari, E., Haleyur, N., Nugegoda, D. and Ball, A. S. (2018). Implications of co-contamination with aged heavy metals and total petroleum hydrocarbons on natural attenuation and ecotoxicology in Australian soils. *Environmental Pollution*. **243:** 94-102.

Kim, I.T., Lee, Y.E., Jeong, Y. and Yoo, Y. S. (2020). A novel method to remove nitrogen from reject water in wastewater treatment plants using a methane-and methanol-dependent bacterial consortium. *Water Research*. **172:** 115-133.

Kirschner, R. A., Parker, B. C. and Falkinham, J. O. (1992). Epidemiology of infection by non-tuberculous mycobacteria: *Mycobacterium avium, Mycobacterium intracellulare,* and *Mycobacterium scrofulaceum* in acid, brown-water swamps of south-eastern United States and their association with environmental variables. *The American Review of Respiratory Disease*. **145:** 271-275.

Knapp, A., Voget, S., Gao, R., Zaburannyi, N., Krysciak, D., Breuer, M., Hauer, B., Streit, W. R., Muller, R., Daniel, R. and Jaeger, K. E. (2016). Mutations improving production and secretion of extracellular lipase by *Burkholderia glumae* PG1. *Applied Microbiology and Biotechnology*. **100:** 1265-1273.

Knight, M. E. (2023). Anthropogenic and natural factors influencing the prevalence and persistence of antimicrobial resistance genes in the Scottish environment. PhD Thesis. The University of Edinburgh.

Koechler, S., Arsene-Ploteze, F., Brochier-Armanet, C., Goulhen-Chollet, F., Heinrich-Salmeron, A., Jost, B., Lievremont, D., Philipps, M., Plewniak, F., Bertin, P. N. and Lett, M. C. (2015). Constitutive arsenite oxidase expression in arsenic-hypertolerant *Pseudomonas xanthomarina* S11. *Research in Microbiology*. **166:** 205-214.

Koner, S., Chen, J. S., Hsu, B. M., Rathod, J., Haung, S. W., Chien, H. Y., Hussain, B. and Chan, M. W. Y. (2022). Depth-resolved microbial diversity and functional profiles of trichloroethylene contaminated souls for Biolog EcoPlate based biostimulation strategy. *Journal of Hazardous Materials*. **424:** 127266.

Kong, X., Wei, Y., Xu, S., Liu, J., Li, H., Liu, Y. and Yu, S. (2016). Inhibiting excessive acidification using zero-valent iron in anaerobic digestion of food waste at high organic loading rates. *Bioresource Technology*. **211:** 65-71.

Kormi, T., Ali, N. B. H., Abichou, T. and Green, R. (2017). Estimation of landfill methane emissions using stochastic search methods. *Atmospheric Pollution Research*. **8:** 597-605.

Korzhenkov, A. A., Toshchakov, S. V., Bargiela, R., Gibbard, H., Ferrer, M., Teplyuk, A. V., Jones, D. L., Kublaniv, I. V., Golyshin, P. N. and Golyshina, O. V. (2019). Archaea dominate the microbial community in an ecosystem with low to moderate temperature and extreme acidity. *Microbiome*. **7:** 1-12.

Kouzuma, A., Kato, S. and Watanabe, K. (2015). Microbial interspecies interactions: recent findings in syntrophic consortia. *Frontiers in Microbiology*. **6:** 1-8.

Kovačić, Đ., Lončarić, Z., Jović, J., Samac, D., Popović, B. and Tišma, M. (2022). Digestate management and processing practices: a review. *Applied Sciences*. **12:** e9216.

Krucon, T., Dziewit, L. and Drewniak, L. (2021). Insight Into Ecology, Metabolic Potential, and the Taxonomic Composition of Bacterial Communities in the Periodic Water Pond on King George Island (Antarctica). *Frontiers in Microbiology*. **12***:* 708607.

Kubo, K., Lloyd, K.G., F Biddle, J., Amann, R., Teske, A. and Knittel, K. (2012). Archaea of the Miscellaneous Crenarchaeotal Group are abundant, diverse and widespread in marine sediments. *The ISME Journal*. **7***:*1949-1965.

Kuddus, M. and Bano, N. (2022). *Microbial screening for extremozymes*. In: Microbial Extremozymes. **1:** 1-7.

Kumar, M., Srivastava, M.K., Kishor, K. and Singh, A.K. (2023). An assessment of the environmental impact of coal mining through acid mine drainage and soil degradation from Makum Coalfields, Upper Assam, India. *Journal of the Geological Society of India*. **99:** 1113-1120.

Kumar, P., Samuchiwal, S. and Malik, A. (2020). Anaerobic digestion of textile industries wastes for biogas production. *Biomass Conversion and Biorefinery*. **10***:* 715-724.

Kumar, S., Chiemhaisri, C. and Mudhoo, A. (2011). Bioreactor landfill technology in municipal solid waste treatment: an ovieeview. *Criticial Reviews in Biotechnology*. **31:** 77-97.

Kurth, J. M., Brito, J. A., Reuter, J., Flegler, A., Koch, T., Franke, T., Klein, E. M., Rowe, S. F., Butt, J. N., Denkmann, K., Pereira, I. A. C., Archer, M. and Dahl, C. (2016). Electron accepting units of the diheme cytochrome *c* TsdA, a bifunctional thiosulphate dehydrogenase/tetrathionate reductase. *Journal of Biological Chemistry*. **291:** 24804-24818.

Kurth, J. M., Op den Camp, H. J., and Welte, C. U. (2020). Several ways one goal—methanogenesis from unconventional substrates. *Applied Microbiology and Biotechnology*. **104:** 6839-6854.

Kurth, J.M., Nobu, M.K., Tamaki, H., de Jonge, N., Berger, S., Jetten, M.S., Yamamoto, K., Mayumi, D., Sakata, S., Bai, L. and Cheng, L. (2021). Methanogenic *Archaea* use a bacteria-like methyltransferase system to demethoxylate aromatic compounds. *The International Society Microbial Ecology Journal*. **15:** 3549-3565.

Kuziminov, A. (2014). The precarious prokaryotic chromosome. *Journal of Bacteriology*. **196:** 1793-1806.

Laroche, E., Joulian, C., Duee, C., Casiot, C., Hery, M. and Battaglia-Brunet, F. (2023). Bio-precipitation of arsenic and antimony in a sulphate-reducing bioreactor treating real acid mine drainage water. *FEMS Microbiology Ecology*. **99:** 1-11.

Lascols, C., Cherney, B., Conley, A.B., Rishishwar, L., Crawford, M.A., Morse, S.A., Fisher, D.J., Anderson, K., Hodge, D.R., Pillai, S.P. and Hughes, M.A. (2023). Investigation of multidrug-resistant plasmids from carbapenemase-producing *Klebsiella pneumoniae* clinical isolates from Pakistan. *Frontiers in Microbiology*. **14:** 1-15.

Lawson, C.E., Strachan, B.J., Hanson, N.W., Hahn, A.S., Hall, E.R., Rabinowitz, B., Mavinic, D.S., Ramey, W.D. and Hallam, S.J. (2015). Rare taxa have potential to make metabolic contributions in enhanced biological phosphorus removal ecosystems. *Environmental Microbiology*. **17:** 4979-4993.

Leang, C., Coppi, M. V. and Lovley, D. R. (2003). OmcB, a *c*-type polyheme cytochrome, involved in Fe(III) reduction in *Geobacter sulfurreducens*. *Journal of Bacteriology*. **185:** 2096-2103.

Lei, L. and Watkins, R. (2005). Acid drainage reassessment of mining tailings, Black Swan nickel mine, Kalgoorlie, Western Australia. *Applied Geochemistry*. **20:** 661-667.

Lemke, M. J., Lienau, E. K., Rothe, J., Pagioro, T. A., Rosenfeld, J. and DeSalle, R. (2009). Description of freshwater bacterial assemblages from the upper Paraná river floodpulse system, Brazil. *Microbial Ecology*. **57:** 94-103.

Lever, M. A. and Teske, A. P. (2015). Diversity of methane-cycling *Archaea* in hydrothermal sediment investigated by general and group-specific PCR primers. *Applied and Environmental Microbiology*. **81:** 1426-1441.

Lewis, A. and Swartbooi, A. (2006). Factors affecting metal removal in mixed sulphide precipitation. *Chemical Engineering and Technology*. **29:** 277-280.

Li Y, Ye Z, Yu Y, Li Y, Jiang J, Wang L, Wang G, Zhang H, Li N, Xie X, Cheng X. (2023). A combined method for human health risk area identification of heavy metals in urban environments. *Journal of Hazardous Materials*. **449:**131-149.

Li, L., Liu, Z., Zhang, M., Meng, D., Liu, X., Wang, P., Li, X., Jiang, Z., Zhong, S., Jiang, C. and Yin, H. (2020a). Insights into the metabolism and evolution of the genus *Acidiphilium*, a typical acidophile in acid mine drainage. *mSystems*. **5:** 00867-20.

Li, Y. T., Li, D., Lai, L. J., Li, Y. H. (2020b). Remediation of petroleum hydrocarbon contaminated soil by using activated persulphate with ultrasound and ultrasound/Fe. *Chemosphere*. **238:** 124657.

Li, Y., Yang, G., Li, L. and Sun, Y., 2018. Bioaugmentation for overloaded anaerobic digestion recovery with acid-tolerant methanogenic enrichment. *Waste Management*. **79,** 744-751.

Li, Y.F, Chen, P.H., and Yu, Z. (2014). Spatial and temporal variations of microbial community in a mixed plug-flow loop reactor fed with dairy manure. *Microbial Biotechnology*. **7:** 332-346.

Lin, Y. F., Walmsley, A. R. and Rosen, B. P. (2006). An arsenic metallochaperone for an arsenic detoxification pump. *Proceedings of the National Academy of Sciences*. **103**: 15616-15622.

Ling, L. L., Schneider, T., Peoples, A. J., Spoering, A. L., Engels, I., Conlon, B. P., Mueller, A., Schaberle, T. F., Hughes, D. E., Epstein, S. and Jones, M. (2015). A new antibiotic kills pathogens without detectable resistance. *Nature*. **517:** 455-459.

Liu, L. Y., Xie., G. J., Ding, J., Lui, B. F., Xing., D. F., Ren, N. Q. and Wang, Q. (2022). Microbial methane emissions from non-methanogenesis processes: a critical review. *Science of the Total Environment*. **806:** e151362.

Liu, M., Wei, Y. and Leng, X. (2021). Improving biogas production using additives in anaerobic digestion. *Journal of Cleaner Production*. **297:** 126-143.

Liu, S., Moon, C. D., Zheng, N., Huws, S., Zhao, S. and Wang, J. (2022). Opportunities and challenges of using metagenomic data to bring uncultured microbes into cultivation. *Microbiome*. **10:** 1-14.

Liu, S., Zeng, J., Yu, H., Wang, C., Yang, Y., Wang, J., He, Z. and Yan, Q. (2023). Antimony efflux underpins phosphorus cycling and resistance of phosphate-solubilising bacteria in mining soils. *ISME Journal*. **17:** 1278-1289.

Lodhi, A.F., Zhang, Y., Adil, M. and Deng, Y. (2023). Design and application of a novel culturing chip (cChip) for culturing the uncultured aquatic microorganisms. *Archives of Microbiology*. **205:** 285-301.

Lofrano, G. and Brown, J. (2012). Wastewater management through the ages: a history of mankind. *Science of the Total Environment*. **408:** 5254-5264.

Lu, L., Luo, Z., Yu, X., Li, Y., Cui, H., Khan, S., Lei, M. and Du, H. (2024). Oxidative weathering of neutral mine drainage from gold mine tailings impoundment: tracking formation and transformation of biogenic iron minerals and associated arsenic. *ACS Earth and Space Chemistry*. **8:** 335-347.

Lu, Z. and Imlay, J. A. (2021). When anaerobes encounter oxygen: mechanisms of oxygen toxicity, tolerance and defence. *Nature Reviews Microbiology*. **19:** 774-785.

Lucking, R., Aime, M. C., Robbertse, B., Miller, A. N., Aoki, T., Ariyawansa, H. A., Cardinali, G., Crous, P. W., Druzhinina, I. S., Geiser, D. M. and Hawksworth, D. L. (2021). Fungal taxonomy and sequence-based nomenclature. *Nature Microbiology*. **6:** 540-548.

Lugli, G. A., Milani, C., Duranti, S., Alessandri, G., Turroni, F., Mancabelli, L., Tatoni, D., Ossiprandi, M. C., van Sinderen, D. and Ventura, M. (2019). Isolation of novel gut *Bifidobacteria* using a combination of metagenomic and cultivation approaches. *Genome Biology*. **20:** 1-6.

Lund, P. A., Biase, D. D., Liran, O., Scheler, O., Mira, N. P., Cetecipglu, Z., Fernandez, E. N., Bover-Cid, S., Hall, R., Sauer, M. and O'Byrne (2020). Understanding how microorganisms respond to acid pH is central to their control and successful exploitation. *Frontiers in Microbiology*. **11**: 1-19.

Luo Z., H, Li, Q, Xie, Y. G, Lv, A.P., Qi, Y., L, Li, M. M, Qu, Y, N., Liu, Z.T., Li Y., X, Rao, Y. Z., Jiao, J.Y., Liu, L., Narsing, R., Rao, M. P., Hedlund, B.P., Evans, P.N., Fang, Y., Shu, W.S., Huang, L.N,. Li, W.J. and Hua Z, S. (2024). Temperature, pH, and oxygen availability contributed to the functional differentiation of ancient Nitrososphaeria. *ISME Journal*. **18:** 31-45.

Luton, P. E., Wayne, J. M., Sharp, R. J. and Riley, P. W. (2002). The *mcrA* gene as an alternative to 16S rRNA in the phylogenetic analysis of methanogen populations in landfill. *Microbiology*. **148:** 3521-3530.

Ly, T., Wright, J.R., Rummel, S. and Lamendella, R. (2019). Microbial communities associated with passive acidic abandoned coal mine remediation. *Frontiers in Microbiology*. **10:** 410022.

Lyautey, E., Billard, E., Tissot, N., Jacquet, S. and Domaizon, I. (2021). Seasonal dynamics of abundance, structure, and diversity of methanogens and methanotrophs in lake sediments. *Microbial Ecology*. **82:** 559-571.

Lynes, M. M., Krukenberg, V., Jay, Z.J., Kohtz, A.J., Gobrogge, C.A., Spietz, R.L. and Hatzenpichler, R., (2023). Diversity and function of methyl-coenzyme M reductase-encoding archaea in Yellowstone hot springs revealed by metagenomics and mesocosm experiments. *ISME Communications*. **3:** 22-31.

Ma, K., Kim, J., Hatzenpichler, R., Karymov, M. A., Hubert, N., Hanan, I. M., Cheng, E. B. and Ismagilov, R. F. (2014). Gene-targeted microfluidic cultivation validated by isolation of a gut bacterium listed in Human Microbiome Project's Most Wanted taxa. *Proceedings of the National Academy of Sciences*. **111:** 9768-9773.

MacGregor, K., MacKinnon, G., Farmer, J. G. and Graham, M. C. (2015). Mobility of antimony, arsenic, and lead at a former antimony mine, Glendinning, Scotland. *Science of the Total Environment*. **529:** 213-222.

Maderia, F., Pearce, M., Tivey, A. R., Basutkar, P., Lee, J., Edbali, O., Madusoodanan, N., Kolesnikov, A. and Lopez, R. (2022). Search and sequence analysis tools services from EMBL-EBI in 2022. *Nucleic Acids Research*. **240:** 276-279.

Maeder, D. L., Anderson, I., Brettin, T. S., Bruce, D. C., Gilna, P., Han, C. S., Lapidus, A., Metcalf, W. W., Saunders, E., Tapia, R. and Sowers, K. R. (2006). The *Methanosarcina barkeri* genome: comparative analysis with *Methanosarcina acetivorans* and *Methanosarcina mazei* reveals extensive rearrangement within Methanosarcinal genomes. *Journal of Bacteriology*. **188:** 7922-7931.

Manceau, A., Merkulova, M., Murdzek, M., Batanova, V., Baran, R., Glatzel, P., Saikia, B. K., Paktunc, D. and Lefticariu, L. (2018). Chemical forms of mercury in pyrite: implications for predicting mercury releases in acid mine drainage. *Environmental Science and Technology*. **52:** 10286-10296.

Marić, J., Križanović, K., Riondet, S., Nagarajan, N. and Šikić, M. (2024). Comparative analysis of metagenomic classifiers for long-read sequencing datasets. *BMC Bioinformatics*. **25:** 15-25.

Marín-Paredes, R., Bolívar-Torres, H.H., Coronel-Gaytán, A., Martínez-Romero, E. and Servín-Garcidueñas, L.E. (2023). A metagenome from a steam vent in Los Azufres Geothermal Field shows an abundance of Thermoplasmatales archaea and bacteria from the phyla Actinomycetota and Pseudomonadota. *Current Issues in Molecular Biology*. **45:** 5849-5864.

Markert, S., Arndt, C., Felbeck, H., Becher, D., Sievert, S. M., Hugler, M., Albrecht, D., Rovidart, J., Bench, S., Feldman, R. A., Hecker, M. and Schweder, T. (2007). Physiological proteomics of the uncultured endosymbiont of *Riftia pachyptila*. *Science*. **315:** 247-250.

Marques, E., Martins, J. V., Santos, P., Ribeiro, J., Mansilha, C., Melo, A., Rocha, F. and Flores, D. (2021). Changes induced by self-burning technosols from a coal mine waste pile: a hydropedological approach. *Geosciences*. **195:** 1150-1159.

Martínez-Pérez, C., Greening, C., Bay, S.K., Lappan, R.J., Zhao, Z., De Corte, D., Hulbe, C., Ohneiser, C., Stevens, C., Thomson, B. and Stepanauskas, R. (2022). Phylogenetically and functionally diverse microorganisms reside under the Ross Ice Shelf. *Nature Communications*. **13:** 117-128.

Martinez, V. D., Vucic, E. A., Becker-Santos, D. D., Gil, L. and Lam, W. L. (2011). Arsenic exposure and the induction of human cancers. *Journal of Toxicology*. **2011:** 1-13

Martins, A. C., Ke, T., Bowman, A. B. and Aschner, M. (2021). New insights on mechanisms underlying methylmercury-induced and manganese-induced neurotoxicity. *Current Option in Toxicology*. **25:** 30-35.

Mateos, L. M., Ordonez, E., Letek, M. and Gil, J. A. (2006). *Corynebacterium glutamicum* as a model bacterium for the bioremediation of arsenic. *International Microbiology*. **9:** 207-215.

Mateos, L., M., Almudena, F., Villadangos, A. G., de la Rubia, A. M., Marcos-Pascual, L., Letek, M., Pedre, B., Messens, J. and Gil, J. A. (2017). *The arsenic detoxification system in cornyebacteria: basis and application for bioremediation and redox control*. In: Advances in Microbiology. Vol. 99. 103-137.

Matsubara, A. and Hurtado, J. E. (2013). Isolation and characterisation of actinomycetes from acidic cultures of ores and concentrates. *Advanced Materials Research*. **825:** 406-409.

Matsuzawa, Y., Kanabe, T., Suzuki, J. and Hiraishi, A. (2000). Ultrastructure of the acidophilic aerobic photosynthetic bacterium *Acidiphilum rubrum*. *Current Microbiology*. **40:** 398-401.

Maus, I., Cibis, K. G., Bremges, A., Stozle, Y., Wibberg, D., Tomazetto, G., Blom, J., Sczyra, A., Konig, H., Puhler, A. and Schluter, A. (2016). Genomic characterization of *Defluviitoga tunisiensis* L3, a key hydrolytic bacterium in a thermophilic biogas plant and its abundance as determined by metagenome fragment recruitment. *Journal of Biotechnology*. **232:** 50-60.

Mayr, M. J., Zimmermann, M., Dey, J., Brand, A., Wehrli, B. and Burgmann, H. (2020). Growth and rapid succession of methanotrophs effectively limit methane release during lake overturn. *Communications Biology*. **6:** 1-9.

Mayumi, D., Mochimaru, H., Tamaki, H., Yamamoto, K., Yoshioka, H., Suzuki, Y., Kamagata, Y. and Sakata, S. (2016). Methane production from coal by a single methanogen. *Science*. **1354:** 222-225.

Mazhar, S. H., Li, X., Rashid, A., Su, J., Xu, J., Brejnrod, A. D., Su, J. Q., Qu, Y., Zhu, G., Zhou, S. G. and Feng, R. (2021). Co-selection of antibiotic resistance genes, and mobile genetic elements in the presence of heavy metals in poultry farm environments. *Science of the Total Environment*. **755:** 124702.

McGinnis, D.F., Kirillin, G., Tang, K.W., Flury, S., Bodmer, P., Engelhardt, C., Casper, P. and Grossart, H.P., 2015. Enhancing surface methane fluxes from an oligotrophic lake: exploring the microbubble hypothesis. *Environmental Science & Technology*. **49:** 873-880.

Meng, Y., Lei, Y., Gao, J., Liu, Y., Ma, E., Ding, Y., Bian, Y., Zu, H., Dong, Y. and Zhu, X. (2022). Genome sequence assembly algorithms and misassembly identification methods. *Molecular Biology Reports*. **49:** 11133-11148.

Menzel, P., Ng, K.L. and Krogh, A., 2016. Fast and sensitive taxonomic classification for metagenomics with Kaiju. *Nature Communications*. **7:** 11257-11268.

Meong, K. (2019). Community perceptions on the health risks of acid mine drainage: the environmental justice struggles of communities near mining fields. *Environment, Development and Sustainability*. **21:** 629-636.

Mesa, V., Gallego, J.L., González-Gil, R., Lauga, B., Sánchez, J., Méndez-García, C. and Peláez, A.I., 2017. Bacterial, archaeal, and eukaryotic diversity across distinct microhabitats in an acid mine drainage. *Frontiers in Microbiology*. **8:** 1-17.

Metziti, A., Rodriguez, L. M., Hatt, K., Pena-Gonzalez, A., Levy, K. and Konstantinidis, K. T. (2021). The reliability of metagenome assembled genomes (MAGs) in representing natural populations: insights from comparing MAGs against isolate genomes derived from the same faecal sample. *Applied and Environmental Microbiology*. **87:** 1-15.

Meyer, J. S., Lloyd, E. H., Bevers, S. and Ranville, J. F. (2022). Physical-chemical recovery of a montane stream after remediation of acid mine drainage: timing and extent after turning off the tao. *Environmental Toxicology and Chemistry*. **42:** 495-511.

Mišić, I.D.R., Mitić, S.S., Kostić, D.A., Tošić, S.B., Pecev-Marinković, E.T. and Miletić, A.S. (2021). Kinetic-spectrophotometric approach to the modified Berthelot procedure for serum urea determination. *Chemical Papers*. **75:** 565-574.

MoBio (2014). *PowerSoil DNA Isolation Kit Handbook*. Available from: https://www.qiagen.com/gb/resources/resourcedetail?id=5c00f8e4-c9f5-4544-94fa-653a5b2a6373&lang=en. [Date accessed: 13/01/22].

Moore, E. K., Jelen, B. I., Giovannelli, D., Raanan, H. and Falkowski, P. G. (2017). Metal availability and the expanding network of microbial metabolisms in the Archaean Eon. *Nature Geoscience*. **10:** 629-636.

Moore, E.K., Jelen, B. I., Giovannelli, D., Raanan, H. and Falkowski, P. G. (2017). Metal availability and the expanding network of microbial metabolisms in the Archaean Eon. *Nature Geoscience*. **10:** 629-636.

Moran, J. J., House, C. H., Freeman, K. H. and Ferry, J. G. (2005). Trace methane oxidation in several Euryarchaeota under diverse conditions. *Archaea*. **1:** 303-309.

Moreira, D. and Amils, S. (1997). Phylogeny of *Thiomonas cuprinis* and other mixotrophic thiobacilli: a proposal for *Thiomonas* gen. nov. *International Journal of Systematic Bacteriology*. **47:** 522-528.

Mori, K., Yamamoto, H., Kamagata, Y., Hatsu, M. and Takamizawa, K. (2000). *Methanocalculus pumilus* sp. nov., a heavy metal tolerant methanogen isolated from a waste-disposal site. *International Journal of Systematic and Evolutionary Microbiology*. **50:** 1723-1729.

Moriya, Y., Itoh, M., Okuda, S., Yoshizawa, A.C. and Kanehisa, M. (2007). KAAS: an automatic genome annotation and pathway reconstruction server. Nucleic Acids Research, **35:** 182-185.

Mosier, A. C., Miller, C. S., Frischkorn, K. R., Ohm, R. A., Li, Z., LaButti, K., Lapidus, A., Lipzen, A., Chen, C., Johnson, J., Lindquist, E. A., Pan, C., Hettich, R. L., Grigoriev, I. V., Singer, S. W. and Banfield, J. F. (2016). Fungi contribute critical but spatially varying roles in nitrogen and carbon cycling in acid-mine drainage. *Frontiers in Microbiology*. **7:** 1-18.

Muniz, S., Lacarta, J., Pata, M. P., Jimenez, J. J. and Navarro, E. (2014). Analysis and diversity of substrate utilisation of soil bacteria exposed to Cd and earthworm activity using generalised additive models. *PloS One*. **9:** e85057.

Munyai, R., Ogola, H. J. O. and Mxolisi, D. (2021). Microbial community diversity dynamics in acid mine drainage and acid mine drainage polluted soils: implication on mining water irrigation agricultural sustainability. *Frontiers in Sustainable Food Systems*. **5:** 1-19.

Murray, J. and Pullar, L. (1910). *Bathymetrical survey of the freshwater lochs of Scotland Volume Three: Loch Ba, Lochan na h-Achlaise, Lochan na Stainge and Loch Buidhe*. Available from: https://maps.nls.uk/bathymetric/chart/2075. [Date accessed: 13/12/21].

Muyzer, G., de Waal, E. C. and Uitterlinder, A. G. (1993). Profiling of complex microbial populations by DGGE analysis of PCR amplified genes coding for 16S rRNA. *Applied and Environmental Microbiology*. **59:** 695-700.

Myers, T. (2016). Acid mine drainage risks: a modelling approach to siting mine facilities in northern Minnesota, USA. *Journal of Hydrology*. **533:** 277-290.

Nancucheo, I., Rowe, O. F., Hedrich, S. and Johnson, D. B. (2016). Solid and liquid media for isolating and cultivating acidophilic and acid-tolerant sulphate-reducing bacteria. *Federation of European Microbiology Society Microbiology Letters*. **363:** 1-18.

Nankonieczna, A. S., Pytlak, A., Grzadziel, J., Kubazynski, A., Banach, A., Gorski, A., Goraj, W., Kuzniar, A., Galazka, A. and Stepniewska, Z. (2019). Changes in the substrate source reveal novel interactions in the sediment-derived methanogenic microbial community. *International Journal of Molecular Science*. **20:** 1-20.

National Record of the Historic Environment (2006). *Benhar Colliery: 19th and 20th Century*. Available at: https://canmore.org.uk/site/79674/benhar-colliery. [Date accessed: 18/03/24].

Neff, A. M., DeNicola, D. M. and Maltman, C. (2021). Passive treatment for acid mine drainage partially restores microbial community structure in different stream habitats. *Water*. **13:** 1-10.

Neira, G., Vergara, E. and Holmes, D. S. (2022). Genome-guided prediction of acid resistance mechanisms in acidophilic methanotrophs of phylogenetically deep-rooted Verrucomicrobia isolated from geothermal environments. *Frontiers in Microbiology*. **13:** 900531.

Nelson, W.C., Tully, B.J. and Mobberley, J.M. (2020). Biases in genome reconstruction from metagenomic data. *PeerJ*. **8:** e10119.

Nest, T.V., Amery, F., Fryda, L., Boogaerts, C., Bilbao, J. and Vandecasteele, B., 2021. Renewable P sources: P use efficiency of digestate, processed animal manure, compost, biochar, and struvite. *Science of the Total Environment*. **750:** 41699-41707.

Newman, J., Peat, T. S., Richard, R., Kan, L., Swanson, P. E., Affholter, J. A., Holmes, I. H., Schindler, J. F., Unkefer, C. J. and Terwilliger, T. C. (1999). Haloalkane dehydrogenases: structure of a *Rhodococcous* enzyme. **38:** 16105-16114.

Nichols, D., Cahoon, N., Trakhtenberg, E. M., Pham, L., Mehta, A., Belanger, A., Kanigan, T., Lewis, K. and Epstein, S. (2010). Use of iChip for high throughput *in situ* cultivation of 'uncultivable' microbial species. *Applied and Environmental Microbiology*. **76:** 2445-2450.

Nijman, T. P., Davidson, T. A., Weideveld, S. T. Audet, J., Esposito, C., Levi, E. E., Ho, A., Lamers, L. P., Jeppesen, E and Veraat, A. J. (2021). Warming and eutrophication interactively drive changes in the methane-oxidising community in shallow lakes. *ISME Communications*. **1:** 1-13.

Nilsson, R. H., Larsson, K. H., Taylor, A. F. S., Bengtsson-Palme, J., Jeppensen, T. S., Schigel, D., Kennedy, P., Picard, K., Glockner, F. O., Tedersoo, L., Saar, I., Kolialg, U. and Abarenkov, K. (2018). The UNITE database for molecular identification of fungi: handling dark taxa and parallel taxonomic classification. *Nucleic Acids Research*. **47:** 259-264.

Niu, J., Deng, J., Xiao, Y., He, Z., Zhang, Z., van Nostrand, J. D., Liang, Y., Deng, Y., Liu, X. and Yin, H. (2016). The shift in microbial communities and their roles in sulphur and iron cycling in a copper ore bioleaching system. *Scientific Reports*. **6:** 1-18.

Noguiera, E. W., de Godoi, L. A. G., Yabuki, L. N. M., Brucha, G. and Damianovic, M. H. R. Z. (2021). Sulphate and metal removal from acid mine drainage using sugarcane vinasse as electron donor: performance and microbial community of the down-flow structured-bed bioreactor. *Bioresource Technology*. **330:** 124968.

Novak, H. R., Sayer, C., Isupov, M. N., Gotz, D., Spragg, A. M. and Littlechild, J. A. (2014). Biochemical and structural characterisation of a haloalkane dehalogenase from a marine *Rhodobacteraceae*. *Federation of European Biochemical Societies Letters*. **588:** 1616-1622.

Odisi, E. J., de Freitas, R. C., do Amaral, da Silva, S. B., da Silva, M. A. C., de Oliveria Sant Ana, W., de Souza Lima, A. O. and Rörig, L. R. (2024). Metataxonomy of acid mine drainage microbiomes from the Santa Catarina Carboniferous Basin (Southern Brazil). *Extremophiles*. **28:** 1-16.

Oest, A., Alsaffar, A., Fenner, M., Azzopardi, D. and Tiquia-Arashiro, S. M. (2018). Patterns of change in metabolic capabilities of sediment microbial communities in river and lake ecosystems. *International Journal of Microbiology*. **27:** 1-16.

Offre, P., Kerou, M., Spang, A. and Schleper, C. (2014). Variability of the transporter gene complement in ammonia-oxidising archaea. *Trends in Microbiology*. **22:** 665-675.

Olsvik, P. A, Ulvund, J.B., Teien, H. C., Urke, H.A., Lie, K.K. and Kristensen T. (2016). Transcriptional effects of metal-rich acid drainage water from the abandoned Løkken Mine on Atlantic salmon (*Salmo salar)* smolt. *Journal of Toxicology and Environmental Health*. **79:** 612-632.

Op De Beeck, M., Lievens, B., Busschaert, P., Declerck, S., Vangronsveld, J. and Colpaert, J. V. (2014). Comparison and validation of some ITS primer pairs useful for fungal metabarcoding studies. *Public Library of Science ONE*. **9:** e97629.

Overholt, W. A., Holzer, M., Geesink, P., Diezel, C., Marz, M. and Kusel, K. (2020). Inclusion of Oxford Nanopore long reads improves all microbial and viral metagenome-assembled genomes from a complex aquifer system. *Environmental Microbiology*. **9:** 4000-4013.

Oxford Nanopore (2022). *Ligation Sequencing gDNA (SQK-LSK109)*. Available at: https://store.nanoporetech.com/uk/ligation-sequencing-kit.html [Date accessed: 12/01/23].

Páez-Espino, A. D., Nikel, P. I., Chavarría, M. and de Lorenzo, V. (2020). ArsH protects *Pseudomonas putida* from oxidative damage caused by exposure to arsenic. *Environmental Microbiology*. **22:** 2230-2242.

Pagaling, E., Strathdee, F., Spears, B. M., Cates, M. E., Allen, R. J. and Free, A. (2014). Community history affects the predictability of microbial ecosystem development. *ISME Journal*. **8:** 19-30.

Palù, M., Peprah, M., Tsapekos, P., Kougais, P., Campanaro, S., Angelidaki, I. and Treu, L. (2022). In-situ biogas upgrading assisted by bioaugmentation with hydrogenotrophic methanogens during mesophilic and thermophilic co-digestion. *Bioresource Technology*. **348:** 27-39.

Pan, Y., Yu, S.S., Xiao, Z.C., Min, Y., Tian, T., Zheng, Y.M., Zhao, Q.B., Yuan, Z.H. and Yu, H.Q. (2023). Re-evaluation and modification of dehydrogenase activity tests in assessing microbial activity for wastewater treatment plant operation. *Water Research*. **246:** 120737.

Panova, I. A., Ikkert, O., Avakyan, M. R., Kopitsyn, D. S., Mardanov, A. V., Pimenov, N. V., Scherbakova, V. A., Ravin, N. V. and Karnachuk, O. V. (2021). *Desulfosporosinus metallidurans* sp. nov., an acidophilic, metal-resistant sulphate-reducing bacterium from acid mine drainage. *International Journal of Systematic and Evolutionary Microbiology*. **71:** 004876.

Panyushkina, A., Bulaev, A. and Belyi, A. V. (2021). Unravelling the central role of sulphur-oxidising *Acidiphilium multivorum* LMS in industrial bioprocessing of gold-bearing sulphide concentrates. *Microorganisms*. **9:** 984-990.

Parmar., A., Iyer, A., Prior, S. H., Lloyd, D. G., Goh, E. T. L., Vincent, C. S., Palmai-Pallag, T., Bachrati, C. Z., Breukink, E., Madder, A. and Lakshuminarayanan, R. (2017). Teixobactin analoues reveal enduracididine to be non-essential for highly potent antibacterial activity and lipid II binding. *Chemical Science*. **8:** 8183-8192.

Pastorelli, R., Casagli, A., Rocchi, F., Tampio, E., Laaksonen, I., Becagli, C. and Lagomarsino, A. (2024). Effects of anaerobic digestates and biochar amendments on soil health, greenhouse gas emissions, and microbial communities: a mesocosm study. *Applied Sciences*. **14:** 1917-1922.

Paul, K., Nonoh, J. O., Mikulski, L. and Brune, A. (2012). 'Methanoplasmatales,' Thermoplasmatales-related *Archaea* in termite guts and other environments, are the seventh order of methanogens. *Applied and Environmental Microbiology*. **78:** 8245-53.

Payne, D., Spietz, R. L. and Boyd, E. S. (2021). Reductive dissolution of pyrite by methanogenic *Archaea*. *The International Society of Microbial Ecology Journal*. **15:** 3498-3507.

Payne, D., Spietz, R. L., Newell, D. L., Dijkstra, P. and Boyd, E. S. (2023). Influence of sulphide on diazotrophic growth of the methanogen *Methanococcus maripaludis* and its implications for the origin of nitrogenase. *Nature Communications*. **6:** 1-13.

Peoples, L.M., Dore, J.E., Bilbrey, E.M., Vick-Majors, T.J., Ranieri, J.R., Evans, K.A., Ross, A.M., Devlin, S.P. and Church, M.J., 2023. Oxic methane production from methylphosphonate in a large oligotrophic lake: limitation by substrate and organic carbon supply. *Applied and Environmental Microbiology*. **89:** 01097-23.

Perman, E., Westerholm, M., Liu, T. and Schnürer, A., 2024. Comparative study of high-solid anaerobic digestion at laboratory and industrial scale–Process performance and microbial community structure. *Energy Conversion and Management*. **300:** 117978.

Pickles, B., Wilhelm, R., Asay, A. K., Hahn, A. S., Simard, S. W. and Mohn, W. W. Transfer of ^{13}C between paired Douglas-fir seedlings reveals plant kinship effects and uptake of exudates by ectomycorrhizas. *New Phytologist*. **214:** 400-411.

Piddock, L. J. V. (2015). Teixobactin, the first of a new class of antibiotics discovered by iChip technology? *Journal of Antimicrobial Chemotherapy*. **70:** 2679-2680.

Pietrzyk, J. D. (2017). Use of microbial consortia for conversion of biomass pyrolysis liquids into value added products. PhD Thesis. The University of Edinburgh.

Pimenov, N.V., Zakharova, E.E., Bryukhanov, A.L., Korneeva, V.A., Kuznetsov, B.B., Tourova, T.P., Pogodaeva, T.V., Kalmychkov, G.V. and Zemskaya, T.I., 2014. Activity and structure of the sulfate-reducing bacterial community in the sediments of the southern part of Lake Baikal. *Microbiology*. **83:** 47-55.

Pollard, P., Devlin, M. and Holloway, D. (2001). Managing a complex river catchment: a case study on the River Almond. *Science of the Total Environment*. **265:** 343-357.

Poulsen, M., Schwab, C., Borg Jensen, B., Engberg, R.M., Spang, A., Canibe, N., Højberg, O., Milinovich, G., Fragner, L., Schleper, C. and Weckwerth, W. (2013). Methylotrophic methanogenic Thermoplasmata implicated in reduced methane emissions from bovine rumen. Nature Communications. **4:** 1428-1438.

Prakash, D., Chauhan, S. S. and Ferry, J. G. (2019). Life on the thermodynamic edge: respiratory growth of an acetotrophic methanogen. *Science Advances*. **5:** 1-7.

Priyadarshanee, M., Chatterjee, S., Rath, S., Dash, H. R. and Das, S. (2022). Cellular and genetic mechanism of bacterial mercury resistance and their role in biogeochemistry and bioremediation. *Journal of Hazardous Materials*. **423:** 126985.

Promega (2009). *Wizard SV Gel and PCR Clean Up System – Quick Protocol*. https://www.promega.co.uk/products/nucleic-acid-extraction/clean-up-and-concentration/wizard-sv-gel-and-pcr-clean-up-system/?catNum=A9281. [Date accessed: 12/01/23].

Promega (2018). *ProNex Size-Selective Purification System: Technical Bulletin*. https://www.promega.co.uk/products/sequencing/ngs-library-prep/pronex-size-selective-purification-system/?catNum=NG2001#protocols. [Date accessed: 12/01/23].

Prosser, J.I., Bohannan, B.J., Curtis, T.P., Ellis, R.J., Firestone, M.K., Freckleton, R.P., Green, J.L., Green, L.E., Killham, K., Lennon, J.J. and Osborn, A. M. (2007). The role of ecological theory in microbial ecology. *Nature Reviews Microbiology*. **5:** 384-392.

Pugh, J. (2023). *The current state of nanopore sequencing*. In: Methods in Molecular Biology. Humana Publishing: New York.

Pyzik, A., Ciezkowska, M., Krawczyk, P. A., Sobczak, A., Drewniak, L., Dziembowski, A. and Lipinski, L. (2018). Comparative analysis of deep sequences methanogenic communities: identification of microorganisms responsible for methane production. *Microbial Cell Factories*. **17:** 1-6.

Qiagen (2017). *DNeasy PowerSoil Kit Handbook*. Available from: https://www.qiagen.com/gb/resources/resourcedetail?id=5a0517a7-711d-4085-8a28-2bb25fab828a&lang=en. [Date accessed: 13/01/23].

Qiagen (2022). *DNeasy PowerSoil Pro Kit Handbook*. Available from: https://www.qiagen.com/gb/resources/resourcedetail?id=9bb59b74-e493-4aeb-b6c1-f660852e8d97&lang=en. [Date accessed: 12/01/23].

Quast, C., Pruesse, E.,Yilmaz, P., Gerken, J., Schweer, T., Yarza, P., Peplies, J. and Glöckner, F. O. (2013). The SILVA ribosomal RNA gene database project: improved data processing and web-based tools, *Nucleic Acids Research*. **41:** 590–596.

Radomski, N., Roguet, A., Lucas, F. S., Veyrier, F. J., Cambau, E., Accrombessi, H., Moilleron, R., Behr, M. A. and Moulin, L. (2013). *atpE* gene as a new useful specific molecular target to quantify *Mycobacterium* in environmental samples. *BMC Microbiology*. **13:** 1-13.

Raffa, C. M., Chaimpo, F. and Shanthakumar, S. (2021). Remediation of metal/metalloid polluted soils: a short review. *Applied Sciences*. **11:** 4134-4138.

Ramanathan, B., Boddicker, A. M., Roane, T. M. and Mosier, A. C. (2017). Nitrifier gene abudance and diversity in sediments impacted by acid mine drainage. *Frontiers in Microbiology*. **8:** 2136-2144.

Reddington, K., Eccles, D., O'Grady, J., Drown, D. M., Hansen, L. H., Nielsen, T. K., Ducluzeau, A. L., Leggett, R. M., Heavens, D., Peel, N., Snutch, T. P., Bayega, A., Oikonomopoulos, S., Ragoussis, J., Barry, T., van der Helm, E., Jolic, D., Richardson, H., Jansen, H., Tyson, J. R., Jain, M. and Brown, B. L. (2020). Metagenomic analysis of planktonic riverine microbial consortia using nanopore sequencing reveals insight into river microbe taxonomy and function. *Gigascience*. **9:** 1-15.

Regnier, P., Resplandy, L., Naijar, R. G. and Cais, P. (2022). The land-to-ocean loops of the global carbon cycle. *Nature*. **603:** 401-410.

Reis, A., C. and Cunha, M. V. (2021). Genome-wide estimation of recombination, mutation and positive selection enlightens diversification drivers of *Mycobacterium bovis*. *Scientific Reports*. **11**: 18789.

Ren, Z., Wang, F., Qu, X., Elser, J. J., Liu, Y. and Chu, L. (2017). Taxonomic and functional differences between microbial communities in Qinghai Lake and its input streams. *Frontiers in Microbiology*. **8:** 1-14.

Robichaux M, Howell M, Boopathy R. (2003). Growth and activities of sulphate-reducing and methanogenic bacteria in human oral cavity. *Current Microbiology*. **47:** 00126.

Rojo, F. (2005). Specificity at the end of the tunnel: understanding substrate length discrimination by the AlkB alkane hydroxylase. *Journal of Bacteriology*. **187:** 19-22.

Rosa, L. H., da Silva, T. H., Ogaki, M. B., Pinto, O. H. B., Stech, M., Convey, P., Carvalho-Silva, M., Rosa, C. A. and Camara, P. E. A. S. (2020). DNA metabarcoding uncovers fungal diversity in soils of protected and non-protected areas on Deception Island, Antarctica. *Scientific Reports*. **10:** 1-9.

Rosienski, M.D., Lee, M.K., Yu, J.H., Kaspar, C.W. and Gibbons, J.G. (2018). Genome sequence of the extremely acidophilic fungus *Acidomyces richmondensis* FRIK2901. *Microbiology Resource Announcements*. **7:** 1028-1128.

Ross, D. E., Lipus, D. and Gulliver, D. (2022). Predominance of Methanomicrobiales and diverse hydrocarbon-degrading taxa in the Appalachian coalbed biosphere revealed through metagenomics and genome-resolved metabolisms. *Environmental Microbiology*. **24:** 5984-5997.

Rossello-Mora, R. and Amann, R. (2015). Past and future species definitions for *Bacteria* and *Archaea*. *Systematic and Applied Microbiology*. **38:** 209-216.

Rotaru, A. E., Shrestha, P. M., Liu, F., Shrestha, M., Shrestha, D., Embree, M., Zengler, K., Wardman, C., Nevin, K. P. and Lovley, D. R. (2014). A new model for electron flow during anaerobic digestion: direct interspecies electron transfer to *Methanosaeta* for the reduction of carbon dioxide to methane. *Energy and Environmental Science*. **7:** 408-415.

Rothman, D. H., G. P. Fournier, G. P., French, K. L., Alm, E. J., Boyle, E. A., Cao, C. and Summons, R. E. (2014). Methanogenic burst in the end-Permian carbon cycle. *Proceedings of the National Academy of Sciences*.**111:** 5462–5467.

Rubin-Blum, M., Dubilier, N. and Kleiner, M. (2019). Genetic evidence for two carbon fixation pathways (the Calvin-Benson-Bassham Cycle and the reverse tricarboxylic acid cycle) in symbiotic and free-living bacteria. *mSphere*. **4:** 4-18.

Ruiz-Gonzalez, C., Nino-Garcia, J. P., Lapierre, J. F. and del Giorgio, P. A. (2015). The quality of organic matter shapes the functional biogeography of bacterioplankton across boral freshwater ecosystems. *Global Ecology and Biogeography*. **24:** 1487-1498.

Rutgers, M., Wouterse, M., Drost, S. M., Breure, A. M., Mulder, C., Stone, D., Creamer, R. E., Winding, A. and Bloem, J. (2016). Monitoring soil bacteria with community level physiological profiles using BIOLOG EcoPlates in the Netherlands, Europe. *Applied Soil Ecology*. **97:** 23-35.

Saha, S., Badhe, N., De Vrieze, J., Biswas, R. and Nandy, T. (2015). Methanol induces low temperature resilient methanogens and improves methane generation from domestic wastewater at low to moderate temperatures. *Bioresource Technology*. **189:** 370-378.

Saito, M. A., Sigman, D. M. and Morel, F. M. M. (2003). The bioinorganic chemistry of the ancient ocean: the co-evolution of cyanobacterial metal requirements and biogeochemical cycles at the Archean-Proterozoic boundary? *Inorganic Chimica Acta*. **356:** 308-318.

Sajjad, W., Ilahi, N., Kang, S. and Bahadur, A. (2024). Microbial diversity and community structure dynamics in acid mine drainage: acidic fire with dissolved heavy metals. *Science of the Total Environment*. **909:** 1-13.

Sala, M. M., Ruiz-Gonzalez, C., Bourill, E., Azua, I., Bana, Z., Ayo, B., Alvarez-Salgado, X. A., Gasol, J. M. and Duarte, C. M. (2020). Prokaryotic capability to use organic substrates across the global tropical and subtropical ocean. *Frontiers in Microbiology*. **11:** 1-21.

Sanchez-Andrea, I., Sanz, J. L., Bijmans, M. F. M. and Stams, A. J. M. (2014). Sulphate reduction at low pH to remediate acid mine drainage. *Journal of Hazardous Materials*. **269:** 98-109.

Sandhu, M., Paul, A. T. and Jha, P. N. (2022). Metagenomic analysis for taxonomic and functional potential of polyaromatic hydrocarbons (PAHs) and polychlorinated biphenyl (PCB) degrading bacterial communities in steel industrial soil. *PloS ONE*. **17:** e0266808.

Sarfo, M. K., Gyasi, S. F., Kabo-Bah, A. T., Adu, B., Mohktar, Q., Appiah, A. S. and Serfor-Armah, Y. (2023). Isolation and characterisation of crude-oil dependent bacteria from the coast of Ghana using Oxford Nanopore sequencing. *Heliyon*. **9:** 1-12.

Sauterey, B., Charnay, B., Affholder, A., Mazevet, S. and Ferriere, R. (2020). Co-evolution of primitive methane-cycling ecosystems and early Earth's atmosphere and climate. *Nature Communications*. **11:** 1-12.

Savinova, E., Evans, C., Lèbre, É., Stringer, M., Azadi, M. and Valenta, R. K. (2023). Will global cobalt supply meet demand? The geological, mineral processing, production, and geographic risk profile of cobalt. *Resources, Conservation and Recycling*. **190:**106855.

Schmitz, R. A., Peeters, S. H., Versantvoort, W., Picone, N., Pol, A., Jetten, M. S. and Op den Camp, H. J. (2021). Verrucomicrobial methanotrophs: ecophysiology of metabolically versatile acidophiles. *FEMS Microbiology Reviews*. **45:** 7-17.

Schreiber, M. E. and Cozzarelli, I. M. (2021). Arsenic release to the environment from hydrocarbon production: storage, transportation, use and waste management. *Journal of Hazardous Materials*. **411:** 125013.

Scottish Water (2023). *Seafield WWTP*. Available from: https://www.scottishwater.co.uk/in-your-area/investments-in-your-area/seafield. [Date accessed: 23/03/23].

Shade A, Jones, S.E., Caporaso, J. G., Handelsman, J., Knight, R., Fierer, N. and Gilbert, J. A. (2014). Conditionally rare taxa disproportionately contribute to temporal changes in microbial diversity. *mBio*. **29:** 101-128.

Shade, A., Peter, H., Allison, S. D., Baho, D. L., Berga, M., Burgmann, H., Huber, D. H., Langerheder, S., Lennon, J. T., Martiney, J. B. H., Matulich, K. L., Schmidt, T. M and Handelsman, J. (2012). Fundaments of microbial community resistance and resilence. *Frontiers in Microbiology*. **3:** 1-19

Shaji, E., Santosh, M., Sarath, K. V., Prakash., Deppchand, V. and Divya, B. V. (2021). Arsenic contamination of groundwater: a global synopsis with focus on the Indian Peninsula. *Geoscience Frontiers*. **12:** 101079.

Sharp, C.E., Smirnova, A.V., Graham, J.M., Stott, M.B., Khadka, R., Moore, T.R., Grasby, S.E., Strack, M. and Dunfield, P.F. (2014). Distribution and diversity of Verrucomicrobia methanotrophs in geothermal and acidic environments. Environmental Microbiology. **16:** 1867-1878.

She, Z., Wang, J., He, C., Jiang, Z., Pan, X., Wang, M., Ma, D., Shi, Q. and Yue, Z. (2023). Molecular insights into the impacts of acid mine drainage on dissolved organic matter in pit lakes. *Science of the Total Environment*. **888:** 1-13.

Shima, S. and Thauer, R. K. (2005). Methyl-coenzyme M reductase and the anaerobic oxidation of methane in methanotrophic *Archaea*. *Current Opinion in Microbiology*. **8:** 643-648.

Shima, S., Krueger, M., Ureinert, T., Demmer, U., Kahnt, J., Thauer, R. K. and Ermler, U. (2012). Structure of a methyl co-enzyme M reductase from Black Sea mats that oxidise methane anaerobically. *Nature*. **481:** 98-101.

Shukla, R., Lavore, F., Maity, S., Derks, M.G., Jones, C.R., Vermeulen, B.J., Melcrová, A., Morris, M.A., Becker, L.M., Wang, X. and Kumar, R. (2022). Teixobactin kills bacteria by a two-pronged attack on the cell envelope. *Nature*. **608:** 390-396.

Siegel, D. I., Glaser, P. H., So, J. and Janecjy, D. R. (2006). The dynamic balance between organic acids and circumneutral groundwater in a large boreal peat basin. *Journal of Hydrology*. **320:** 421-431.

Siliakus, M. F., van der Oost J. and Kengen, S. W. M. (2017). Adaptations of archaeal and bacterial membranes to variations in temperature, pH and pressure. *Extremophiles*. **21:** 651-670.

Sims, L. P., Lockwood, C. W. J., Crombie, A. T., Bradley, J. A., Le Brun, N. E. and Murrell, J. C. (2022). Purification and characterisation of the isoprene monooxygenase from *Rhodococcus* strain AD45. *Applied and Environmental Microbiology*. **88:** 1-23.

Sinsuw, A.A.E., Chen, T.H., Dokmaingam, P., Suriandjo, H.S. and Chu, C.Y., 2024. Life cycle assessment of environmental impacts for two-stage anaerobic biogas plant between commercial and pilot scales. *International Journal of Hydrogen Energy*. **52:** 58-70

Smolders, A. J. P., Lock, R. A. C., van der Velde, G., Medina-Hoyos, R. I. and Roelofs, J. G. M. (2003). Effects of mining acrivities on heavy metal concentrations in water, sediment and macroinvertebrates in different reaches of the Pilcomayo River, South America. *Achieves of Environmental Contamination and Toxicology*. **44:** 314-323.

Sogin, E. M., Putnam, H. M., Nelson, C. E., Anderson, O. and Gates, R. D. (2017). Correspondence of coral holobiont metabolome with symbiotic bacteria, archaea and *Symbiodinium* communuities. *Environmental Microbiology Reports*. **9:** 310-315.

Sollinger, A. and Urich, T. (2019). Methylotrophic methanogens everywhere: physiology and ecology of novel players in global methane cycling. *Biochemical Society Transactions*. **47:** 1895-1907.

Spietz, R. L., Devon, P., Gargi, K., Metcalf, W. W., Roden, E. E. and Boyd, E. S. (2022a). Investigating abiotic and biotic mechanisms of pyrite reduction. *Frontiers in Microbiology*. **13:** 1-17.

Spietz, R. L., Payne, D., Szilagyi, R. and Boyd, E. S. (2022b). Reductive biomining of pyrite by methanogens. *Trends in Microbiology*. **30:** 1-16.

Spietz, R.L., Payne, D. and Boyd, E.S. (2023). Methanogens acquire and bioaccumulate nickel during reductive dissolution of nickelian pyrite. *Applied and Environmental Microbiology*. **89:** 17-23.

Staley, J. T. and Konopka, A. (1985). Measurements of *in situ* activities of non-photosynthetic microorganisms in aquatic and terrestrial habitats. *Annual Reviews in Microbiology*. **39:** 321-346.

Stassen, M. J. M., Preeker, N. L., Ragas, A. M. J., ven de Ven, M. W. P. M., Smolders, A. J. P. and Roeleveld, N. (2012). Metal exposure and reproductive disorders in indigenous communities living along the Pilcomayo River, Bolivia. Science of the Total Environment. **15:** 26-34.

Steinberg, L. M and Regan, J. M. (2008). Phylogenetic comparison of the methanogenic communities from an acid, oligotrophic fen and an anaerobic digester treating municipal wastewater sludge. *Applied and Environmental Microbiology*. **74:** 6663-6671.

Sun, W., Xiao, E., Dong, Y., Li, B., Deng, J., Wang, Q., Xiao, T. and Liu, J. (2019). Comparitive analyses of the microbial communities inhabiting coal mining waste dump and an adjacent acid mine drainage creek. *Microbial Ecology*. **78:** 651-664.

Sutcliffe, B., Hose, G. C., Harford, A. J., Midgley, D. J., Greenfield, P., Paulsen, I. T. and Chariton, A. A. (2019). Microbial communities are sensitive indicators for freshwater sediment copper contamination. *Environmental Pollution*. **247:** 1028-1038.

Suzuki, K., Wakao, N., Kimura, T., Sakka K., and Ohmiya, K. (1998). Expression and regulation of the arsenic resistance operon of *Acidiphilium multivorum* AIU 301 plasmid pKW301 in *Escherichia coli*. *Applied and Environmental Microbiology*. **64:** 411-418.

Tan, G.L., Shu, W.S., Zhou, W.H., Li, X.L., Lan, C.Y. and Huang, L.N. (2009). Seasonal and spatial variations in microbial community structure and diversity in the acid stream draining across an ongoing surface mining site. *FEMS Microbiology Ecology*. **70:** 277-285.

Tanabe, T. S., Leimkuhler, S. and Dahl, C. (2019). *The functional diversity of the prokaryotic sulphur carrier protein* TusA. In: Advances in Microbial Physiology. Vol 75. 233-277. Academic Press: United Kingdom.

Tanaka, Y., Tamaki, H., Tanaka, K., Tozawa, E., Matsuzawa, H., Toyama, T., Kamagata, Y. and Mori, K. (2018). 'Duckweed-microbe co-cultivation method' for isolating a wide variety of microbes including taxonomically novel microbes. *Microbes and Environments*. **33:** 402-406.

Thermo Fisher (2015). *Qubit dsDNA HS Assay*. Available from: https://tools.thermofisher.com/content/sfs/manuals/Qubit_dsDNA_HS_Assay_UG.pdf [Date accessed: 13/01/22].

Thermo Fisher (2022). *Product Description – R2A Agar Dehydrated*. Available from: https://www.thermofisher.com/document-connect/document-connect.html?url=https://assets.thermofisher.com/TFS-Assets%2FMBD%2FSpecification-Sheets%2FPS-CM0906-V3.pdf. [Date accessed: 15/01/23].

Tian, J., Zhu, D., Wang, J., Wu, B., Hussian, M. and Liu, X. (2018). Environmental factors driving fungal distrubition in freshwater lake sediments across the Headwater Region of the Yellow River, China. *Scientific Reports*. **8:** 2-18.

Tikhonova, E. N., Grouzdev, D. S., Avtukh, A. N. and Kravchenko, I. K. (2021). *Methylocystis silviterre* sp. nov., a high affinity methanotrophic bacterium isolated from the boreal forest soil. *International Journal of Systematic and Evolutionary Microbiology*. **71:** 1-11.

Tomiyama, S. and Igarashi, T. (2022). The potential threat of mine drainage to groundwater resources. *Current Opinion in Environmental Science and Health*. **27:** 100347.

Tong, L., Fan, R., Yang, S. and Li, C., 2021. Development and status of the treatment technology for acid mine drainage. *Mining, Metallurgy & Exploration*, *38*, pp.315-327.

Tripathi, C., Mishra, H., Khurana, H., Dwivedi, V., Karma, K., Negi, R. K. and Lal, R. (2017). Complete genome analysis of *Thermus parvatiensis* and comparative genomics of *Thermus* species provide insights into genomic variability and evolution of natural competence as strategic survival attributes. *Frontiers in Microbiology*. **8:** 1-23.

Tsola, S.L., Zhu, Y., Chen, Y., Sanders, I.A., Economou, C.K., Brüchert, V. and Eyice, Ö. (2024). *Methanolobus* use unspecific methyltransferases to produce methane from dimethylsulphide in Baltic Sea sediments. *Microbiome*. **12:** 1-9.

Tung, H. C., Prince, P. B., Bramall, N. E. and Vrdolijak, G. (2006). Microorganisms metabolising on clay grains in 3 km deep Greenland basal ice. *Astrobiology*. **1:** 69-86.

Tutu, H., McCarthy, T. S. and Cukrowska, E. (2008). The chemical characteristics of acid mine drainage with reference to sources, distribution and remediation: the Witwatersrand Basin, South Africa as a case study. *Applied Geochemistry*. **23:** 3666-3684.

Tyson, G.W., Chapman, J., Hugenholtz, P., Allen, E.E., Ram, R.J., Richardson, P.M., Solovyev, V.V., Rubin, E.M., Rokhsar, D.S. and Banfield, J.F. (2004). Community structure and metabolism through reconstruction of microbial genomes from the environment. *Nature*. **428:** 37-43.

Uddin, M. J., Haque, F., Jabeen, I. and Shuvo, S. R. (2022). Characterisation and whole genome sequencing of an extreme arsenic tolerant *Citrobacter freundii* SRS1 strain isolated from the Savar area in Bangladesh. *Canadian Journal of Microbiology*. **69:** 44-52.

United Nations (2023). *Ramsar Convention on Wetlands*. Available at: https://www.ramsar.org. [Date accessed: 19/12/23].

Uno, U. A., Ekpo, B. O., Etuk, V. E., Etuk, H. S. and Ibok, U. J. (2012). Comparitive study of levels of trace metals in airborne particulates in some cities of the Niger Delta Region of Nigeria. *Environmental Pollution*. **2:** 1-12.

Usmani, Z., Sharma, M., Karpichev, Y., Pandey, A., Kuhad, R.C., Bhat, R., Punia, R., Aghbashlo, M., Tabatabaei, M. and Gupta, V.K., 2020. Advancement in valorization technologies to improve utilization of bio-based waste in bioeconomy context. *Renewable and Sustainable Energy*. **16:** 1-19.

Van der Graaf, C.M., Sánchez-España, J., Yusta, I., Ilin, A., Shetty, S.A., Bale, N.J., Villanueva, L., Stams, A.J. and Sánchez-Andrea, I. (2020). Biosulfidogenesis mediates natural attenuation in acidic mine pit lakes. *Microorganisms*. **8:** 1275-1279.

Van der Walt, A. J., Van Goethem, M. W., Ramond, J. B., Makhalanyane, T. P., Reva, O. and Cowan, D. A. (2017). Assembling metagenomes, one community at a time. *BMC Genomics*. **521:** 1-13.

Van Grinsven, S., Meier, D.V., Michel, A., Han, X., Schubert, C.J. and Lever, M.A., 2022. Redox zone and trophic state as drivers of methane-oxidizing bacterial abundance and community structure in lake sediments. *Frontiers in Environmental Science*. **10:** 857358.

Van Ooteghem, S. A., Suelle, A., Jones, A., van der Lelie, D., Dong, B. and Mahajan, D. (2004). H2 production and carbon source utilisation by *Thermotoga neapolitana* under anaerobic and microaerobic growth conditions. *Biotechnology Letters*. **26:** 1223-1232.

Vanwonterghem, I., Evans, P. N., Parks, D. H., Jensen, P. D., Woodcroft, B. J., Hugenholtz, P. and Tyson, G. W. (2016). Methylotrophic methanogenesis discovered in the archaeal phylum Verstraetearchaeota. *Nature Microbiology*. **1:** 16170.

Varjani, S.J., 2017. Microbial degradation of petroleum hydrocarbons. Bioresource Technology. **223:** 277-286.

Veitch, T., Bleicker, T., Eschbach-Bludau, M., Brunink, S., Muhlemann, B., Schneider, J., Beheim-Schwarzbach, J., Rakotondranary, S. J., Ratovonamana, Y. R., Tsagnangara, C., Ernest, R., Randraintafika, F., Sommer, S., Stetter, N., Jones, T. C., Drosten, C., Ganzhorn, J. U. and Corman, V. M. (2023). Non-structural genes of novel lemur adenoviruses reveal codivergence of virus and host. *Virus Evolution*. **9:** 1-14.

Venton, D. (2017). Highlight: Applying the biological species concept across all of life. *Genome Biology and Evolution*. **9:** 502-503

Venturini, A. M., Gontijo, J. B., Mandro, J. A., Paula, F. S., Yoshira, C. A., da Franca, A. G. and Tsai, S. M. (2022). Genome-resolved metagenomics reveals novel archaeal and bacterial genomes from Amazonian Forest and pasture soils. *Microbial Genomics*. **8:** 1-11.

Vidal, P., Martínez-Martínez, M., Fernandez-Lopez, L., Roda, S., Méndez-García, C., Golyshina, O. V. and Ferrer, M. (2022). Metagenomic mining for esterases in the microbial community of Los Rueldos acid mine drainage formation. *Frontiers in Microbiology*. **13:** 868839.

Vigneron, A., Cruaud, P., Bhiry, N., Lovejoy, C. and Vincent, W.F., 2019. Microbial community structure and methane cycling potential along a thermokarst pond-peatland continuum. *Microorganisms*. **7:** e486.

Vincenten, J. A., Zastenskaya, I., Schroder-Back, P., and Jarosinska, D. I. (2020). Priorities for improving chemical management in the WHO European Region: stakeholders' views. *European Journal of Public Health*. **30:** 812-817.

Vissers, E. W. (2012). *Spatial and temporal dynamics of Thaumarchaeota in deep European lakes*. In: Netherlands Institute of Ecology Report. [Date accessed: 20/01/24].

Vogel, C. F. A., van Winkle, L. S., Esser, C. and Haarmann-Stemmann, T. (2020). The aryl hydrocarbon receptor as a target of environmental stressors: implications for pollution mediated stress and inflammatory responses. *Redox Biology*. **34:** 101530.

Wagner-Dobler, I. (2003). Pilot plant for bioremediation of mercury-containing industrial wastewater. *Applied Microbiology and Biotechnology*. **62:** 124-133.

Wagner, T., Wegner, C. E., Kahnt, J., Ermler, U. and Shima, S. (2017). Phylogenetic and structural comparisons of the three types of methyl coenzyme M reductase from *Methanococcales* and *Methanobacteriales*. *Journal of Bacteriology*. **199:** e00197.

Walker, M. J. C. and Lowe, J. J. (1977). Postglacial environmental history of Rannoch Moor, Scotland. *Journal of Biogeography*. **4:** 333-351.

Wang, Y., Wegener, G., Williams, T. A., Xie, R., Hou, J., Tian, C., Zhang, Y., Wang, F. and Xiao, X. (2021a). A methylotrophic origin of methanogenesis and early divergence of anaerobic multicarbon alkane metabolism. *Science Advances*. **7:** 1-12.

Wang, Y., Zhao, Y., Bollas, A., Wang, Y. and Au, K. F. (2021b). Nanopore sequencing technology, bioinformatics, and applications. *Nature Biotechnology*. **39:** 1348-1365.

Wang, S., Cui, L., Alain, K., Xie, S. and Shao, Z. (2023a). Transcriptome analysis of cyclooctasulphur oxidation and reduction by the neutrophilic chemolithotrophic *Sulfurovum indicum* from deep-sea hydrothermal ecosystems. *Antioxidants*. **12:** e627.

Wang, J., Wei, Z.P., Chu, Y.X., Tian, G. and He, R. (2023b). Eutrophication levels increase sulfur biotransformation and emissions from sediments of Lake Taihu. *Science of The Total Environment*. **887:** 164054.

Wang, J., Qu, Y.N., Evans, P.N., Guo, Q., Zhou, F., Nie, M., Jin, Q., Zhang, Y., Zhai, X., Zhou, M. and Yu, Z., (2023c). Evidence for non-traditional *mcr*-containing archaea contributing to biological methanogenesis in geothermal springs. *Science Advances*. **9:** 60-64.

Wang, Z. and Anand, D. (2023). Phosphorus recovery from whole digestate through electrochemical leaching and precipitation. *Environmental Science and Technology*. **57:** 10107-10116.

Weber, K. P. and Legge, R. L. (2009). One-dimensional metric for tracking bacterial community divergence using soil carbon source utilisation patterns. *Journal of Microbiological Methods*. **79:** 55-61.

Weber, P.A., Skinner, W.M., Hughes, J.B., Lindsay, P. and Moore, T.A. (2006). Source of Ni in coal mine acid rock drainage, West Coast, New Zealand. *International Journal of Coal Geology*, **67:** 214-220.

Wegner, C.E., Gorniak, L., Riedel, S., Westermann, M. and Küsel, K. (2019) Lanthanide-dependent methylotrophs of the family Beijerinckiaceae: physiological and genomic insights. *Applied and Environmental Microbiology*. **86:** e01839.

Weil, M., Wang, H., Zak, D. and Urich, T. (2023). Spatial and temporal niche separation of Methanomassiliicoccales phylotypes in temperate fens. *FEMS Microbiology Ecology*. **99:** 49-54.

Williams, C., Macalady, J. and Grettenberger, C. (2023). Metagenome assembled genomes from Appalachian acid mine drainage sites. *Microbiology Resource Announcements*. **12:** e10280-22.

Willms, I. M., Rudolph, A. Y., Goschel, I., Bolz, S. H., Schneider, D., Penone, C., Poehlein, A., Schoning, I. and Nacke, H. (2020). Globally abundant '*Candidatus Udaeobacter'* benefits from release of antibiotics in soil and potentially performs trace gas oxidation. *mSphere*. **5:** 1-17.

Woese, C. R and Fox, G. E. (1977). Phylogenetic structure of the prokaryotic domain: the primary kingdoms. *Proceedings of the National Academy of Sciences*. **74:** 5088-5090.

Wolfe, J. M. and Fournier, G. P. (2018). Horizontal gene transfer constrains the timing of methanogen evolution. *Nature Ecology and Evolution*. **2**: 897–903.

Wongnate, T. and Ragsdale, S. W. (2015). The reaction mechanism of methyl co-enzyme reductase: how an enzyme enforces strict bonding order. *Journal of Biological Chemistry*. **290:** 9322-9334.

Wood, D.E. and Salzberg, S.L. (2014). Kraken: ultrafast metagenomic sequence classification using exact alignments. *Genome Biology*. **15:** 1-12.

Woolway, R.I., Jennings, E., Shatwell, T., Golub, M., Pierson, D.C. and Maberly, S. C. (2021). Lake heatwaves under climate change. *Nature*. **589:** 402-407.

Woolway, R.I., Kraemer, B.M., Lenters, J.D., Merchant, C.J., O'Reilly, C.M. and Sharma, S. (2020). Global-lake responses to climate change. *Nature Reviews Earth and Environment*. **8:** 388-403.

World Health Organisation. (2022). *Toxicological Profile for Arsenic*. Available from: www.who.int/news-room/fact-sheets/detail/arsenic. [Date accessed: 01/11/23].

Wu, J. and Chen, S. L. (2022). Key piece in the Wolfe cycle of methanogenesis: the S-S bond dissociation conducted by noncubane [Fe_4S_4] cluster-dependent heterodisulphide reductase. *Catalysis*. **12:** 2606-2622.

Wu, J., Xie, W., Tan, J. and Liu, L. (2023). Understanding the sources of mercury release from coal: a combined experimental and molecular simulation study. *Journal of Hazardous Materials*. **460:** 132429.

Wullenbucher, K., Wibberg, D., Huang, L., Conrady, M., Ramm, O., Gatcke, J., Busche, T., Brandt, C., Szewzyk, I., Schluter, A., Canosa, J. B. and Maus, I. (2022). Phage genome diversity in a biogas producing microbiome analysed by Illumina and Nanopore gridION sequencing. *Microorganisms*. **10:** 1-19.

Xiao, E., Ning, Z., Sun, W., Jiang, S., Fan, W., Ma, L. and Xiao, T., 2021. Thallium shifts the bacterial and fungal community structures in thallium mine waste rocks. *Environmental Pollution*. **268:** p.115-135.

Xie, J., He, Z., Liu, X., Liu, X., Van Nostrand, J.D., Deng, Y., Wu, L., Zhou, J. and Qiu, G., 2011. GeoChip-based analysis of the functional gene diversity and metabolic potential of microbial communities in acid mine drainage. *Applied and Environmental Microbiology*. **77:** 991-999.

Xin, R., Banda, J.F., Hao, C., Dong, H., Pei, L., Guo, D., Wei, P., Du, Z., Zhang, Y. and Dong, H., 2021. Contrasting seasonal variations of geochemistry and microbial community in two adjacent acid mine drainage lakes in Anhui Province, China. *Environmental Pollution*. **268:** 115826.

Xiu, W., Wu, M., Nixon, S. L., Lloyd, J. R., Bassil, N. M., Gai, R., Zhang, T., Su, Z. and Guo, H. (2022). Genome-resolved metagenomic analysis of groundwater: insights into arsenic mobilisation in biogeochemical interaction networks. *Environmental Science and Technology*. **56:** 10105-10119.

Yan, W., Yan, Y., Chen, M., Qian, B., Li, M., He, X., Lin, C. and Mao, Z. (2024). High arsenic pollution of the eutrophic Lake Taihu and its relationship with iron, manganese, and dissolved organic matter: high-resolution synchronous analysis. *Journal of Hazardous Materials*. **467**: 1-12.

Yang, Y., Li, N., Wang, W., Li, B., Xie, S. and Liu, Y. (2017). Vertical profiles of sediment methanogenic potential and communities in two plateau freshwater lakes. *Biogeosciences*. **14:** 341-352.

Yang, Y., Chen, J., Tong, T., Xie, S. and Liu, Y., (2020a). Influences of eutrophication on methanogenesis pathways and methanogenic microbial community structures in freshwater lakes. *Environmental Pollution*. **260:** 114-124.

Yang, L., Zhang, Y., Wang, F., Luo, Z., Gou, S. and Strahle, U. (2020b). Toxicity of mercury: molecular evidence. *Chemosphere*. **245:** e125586.

Yang, Y., Li, B., Li, T., Zheng, B. and Che, L. (2023). A review of treatment technologies for acid mine drainage and sustainability assessment. *Journal of Water Process Engineering*. **55:** 1-23.

Yerulker, G., Patel, P., Chafale, A., Rathod, V., Das, S., Pandey, P., Khan, N.A., Devi, A., Munshi, N.S., Dhodapkar, R. and Kapley, A. (2023). Comparative assessment of soil microbial community in crude oil contaminated sites. *Environmental Pollution*. **328:** 121-131

Yu, R. Q. and Barkay, T. (2022). *Microbial mercury transformations: molecules, functions, and organisms*. In: Advances in Applied Microbiology. Vol 118. 31-90.

Yu, X., Zhou, J. Song, W., Xu, M., He, Q., Peng, Y., Tain, Y., Wang, C., Shu, L., Wang, S., Yan, Q., Liu, J., Tu, Q. and He, Z. (2020). SCycDB: a curated functional gene database for metagenomic profiling of sulphur cycling pathways. *Molecular Ecology Resources*. **21:** 924-940.

Yu, Y., Yang, J., Zheng, L. Y., Sheng, Q., Li, C. Y., Wang, M. and Zhang, X. Y. (2020). Diversity of D-amino acid utilising bacteria from the Kongsfjorden Arctic and the metabolic pathways for seven D-amino acids. *Frontiers in Microbiology*. **10:** 1-18.

Yuan, Y., Conrad, R. and Lu, Y. (2009). Responses of methanogenic archaeal community to oxygen exposure in rice field soil. *Environmental Microbiology Reports*. **1:** 347-354.

Yun, S., Fang, W., Du, T., Hu, X., Huang, X., Li, X., Zhang, C. and Lund, P. D. (2018). Use of biobased carbon materials for improving biogas yield and digestate stability. *Energy*. **14:** 898-909.

Zamkovaya, T., Foster, J. S., de Crecy-Lagard, V. and Conesa, A. (2021). A network approach to elucidate and prioritise microbial dark matter in microbial communities. *The International Society of Microbial Ecology Journal*. **15:** 228-244.

Zeng, K., Huang, X., Dai, C., He, C., Chen, H., Guo, J. and Xin, G. (2024). Bacterial community regulation of soil organic matter molecular structure in heavy metal-rich mangrove sediments. *Journal of Hazardous Materials*. **465:** 1-13.

Zhang, F., Wang, H., Ye, Y., Liu, Y., Deng, Y. and Lyu, D. (2022). Did high temperature rather than low O2 hinder the evolution of eukaryotes in the Precambrian? *Precambrian Research*. **378:** 106755.

Zhang, F., Zhang, W., Qian, D.K., Dai, K., van Loosdrecht, M.C. and Zeng, R.J., 2019. Synergetic alginate conversion by a microbial consortium of hydrolytic bacteria and methanogens. *Water Research*. **163**: 114892.

Zhang, R., Neu, T. R., Li, Q., Blanchard, V., Zhang, Y., Schippers, A. and Sand, W. (2019). Insight into interactions of thermoacidophilic archaea with elemental sulfur: biofilm dynamics and EPS analysis. *Frontiers in Microbiology*. **10:** 896-911.

Zhang, X., Li, D., Liu, Y., Li, J. and Hu, H. (2023). Soil organic matter contents modulate the effects of bacterial diversity on the carbon cycling processes. *Journal of Soils and Sediments*. **23:** 911-922.

Zhao, Z., Zhang, Y., Wang, L. and Quan, X. (2015). Potential for direct interspecies electron transfer in an electric-anaerobic system to increase methane production from sludge digestion. *Scientific Reports*. **5:** 11094.

Zhao, D., Yang, J., Liu, T., Lu, D., Zhang, S., Yan, L. and Ni, Y. (2021). Complete genome sequence analysis of *Acidithiobacillus ferrivorans* XKFY6S-08 reveals environmental adaptation to alpine acid mine drainage. *Current Microbiology*. **78:** 1488-1498.

Zhou, Z., Pan, J., Wang, F., Gu, J. D. and Li, M. (2018). Bathyarchaeota: globally distributed metabolic generalists in anoxic environments. *FEMS Microbial Ecology Reviews*. **42:** 639-655.

Zhou, J., Yu, X., Liu, J., Qin, W., He, Z., Stahl, D., Jiao, N., Zhou, J. and Tu, Q. (2021). Vitamine B_{12} pathway for accurate metagenomic profiling of microbially driven cobalamin synthesis pathways. *Microbial Ecology*. **6:** e00497

Ziegler, S., Ackermann, S., Majzlan, J. and Gescher, J. (2009). Matrix composition and community structure analysis of a novel bacterial pyrite leaching community. *Environmental Microbiology*. **11:** 2329-2338.

Ziegler, S., Dolch, K., Geiger, K., Krause, S., Asskamp, M., Eusterhues, K., Kriews, M., Wilhelms-Dick, D., Goettlicher, J., Majzlan, J. and Gescher, J. (2013a). Oxygen-dependent niche formation of a pyrite-dependent acidophilic consortium built by archaea and bacteria. *The ISME Journal*. **7:** 1725-1737.

Ziegler, S., Waidner, B., Itoh, T., Schumann, P., Spring, S. and Gescher, J. (2013b). *Metallibacterium scheffleri* gen. nov., sp. nov., an alkalinising gammaproteobacterium isolated from an acidic biofilm. *International Journal of Systematic and Evolutionary Microbiology*. **63:** 1499-1504.

SUPPLEMENTARY DATA

SUPPLEMENTARY TABLE S1: Summary of taxonomic bins containing assembled reads < 100,000 bp in length produced from nanopore sequencing and assembly of DNA from Benhar Bing. Contig length/number, protein prediction, repeat regions and RNAs detected via Proksee and Prokka annotation.

Taxonomic bin	Size (bp)	Number of contigs	Hypothetical/total proteins	Sequence annotation: non-coding RNAs and repeat regions
Ktedonobacterales	98,128	4	101/177	1 tRNA
Planctomycetia	89,891	6	117/150	1 5S rRNA, 1 23S rRNA, 1 tRNA
Steriodobacter	88,693	5	52/133	2 tRNAs
Xanthomonadales	88,183	5	52/97	1 tRNA
Reticulibacter	83,243	5	86/157	N/A
Silvibacterium	82,880	10	83/126	N/A
Ktedonobacteria	76,615	3	89/132	1 tRNA
Leptospirillum	72,127	3	77/144	4 tRNAs
Rhodanobacter	49,062	3	57/75	N/A
Actinomadura	48,099	7	25/56	N/A
Bradyrhizobium	45,992	6	53/64	N/A
Acidisarcina	46,033	3	29/61	N/A
Sphaerobacter	42,338	4	29/44	N/A
Paludisphaera	40,606	4	70/71	N/A
Roseomonas	37,677	3	42/50	N/A
Dyella	36,546	3	29/38	1 tRNA
Acidobacterium	35,414	6	24/58	N/A
Mycolicibacterium	34,609	3	17/36	N/A
Terriglobus	32,384	8	42/48	N/A
Occallatibacter	31,527	2	29/50	N/A
Dictyobacter	25,765	3	33/41	N/A
Acidocella	25,363	3	24/36	N/A
Isosphaeraceae	24,598	2	35/41	N/A
Pseudoacidobacterium	24,014	3	43/43	N/A
Steriodobacteraceae	23,669	1	15/30	N/A
Streptomyces	23,203	4	19/28	N/A
Inmairania	22,743	1	5/25	N/A
Nevskiales	22,258	1	13/31	N/A
Azospirillium	22,097	3	21/31	N/A
Fimbriiglobus	20,900	1	35/37	N/A
Acidithrix	20,666	4	16/26	2 tRNAs
Nocardiodes	20,358	5	20/21	N/A
Pseudoamionobacter	19,447	1	30/41	N/A
Legionella	19,287	2	25/25	N/A
Inhella	18,708	1	16/17	N/A
Nitrobacteraceae	18,389	1	23/25	N/A

Desertimonas	18,382	3	22/25	N/A
Prosthecomicrobium	17,811	2	23/29	N/A
Singulisphaera	16,631	1	25/33	N/A
Rhabdothermicola	16,445	1	6/24	N/A
Nonomuraea	16,192	4	15/19	N/A
Acidithiobacillus	16,074	2	19/19	N/A
Solimonas	16,052	1	4/16	N/A
Aquihabitans	15,849	3	7/18	N/A
Planctomyces	15,671	2	20/21	N/A
Elioraea	15,225	1	13/17	N/A
Kitasatosporales	14,531	1	10//12	N/A
Mumia	14,402	1	19/24	N/A
Mycobacterium bohemicum	13,411	1	22/27	N/A
Pelomoprha	13,140	1	10/13	N/A
Lysobacter	13,054	2	10/11	N/A
Ktedonosporobacter	12,927	1	14/21	1 tRNA
Cellulomonas	12,769	1	10/12	N/A
Mesorhizobium	12,498	2	19/22	N/A
Frateuria	12,409	1	15/21	N/A
Thiohalobacter	12,325	1	16/25	N/A
Iamia	12,051	2	14/17	N/A
Xanthomonadaceae	11,967	1	4//14	N/A
Afipia	11,955	1	17/17	N/A
Acidisphaera	11,948	1	3//11	N/A
Acidmicrobiaceae	11,911	1	8/17	N/A
Tautonia	11,816	1	23/23	N/A
Micromonospora	11,793	1	21/21	N/A
Rhodopsuedomonas	11,645	2	15/17	**1 repeat region**
Myxococcus	11,201	1	14/16	N/A
Marmoricola	11,170	1	12/17	N/A
Acrinomarinicola	10,937	3	15/18	N/A
Isopshaera	10,815	1	19/19	N/A
Frankia	10,682	1	9/13	N/A
Acidithrix ferrooxidans	10,441	1	15/17	N/A
Methylobrevis	10,155	1	19/20	N/A
Kribbella	10,075	1	16/16	N/A
Rhodocyclales	9686	1	5/17	N/A
Thermobispora	9162	1	3/10	N/A
Ralstonia	8911	2	16/16	N/A
Betaproteobacteria	8816	1	12/13	N/A
Arthrobacter	8700	2	8/13	N/A
Zeimonas	8255	1	7/14	N/A
Arhodomonas	7669	1	5/10	N/A
Planosporagium	7491	1	6/9	N/A
Saccharopolyspora	6465	1	4/7	N/A
Martelella	6087	1	3/3	**1 repeat region**
Conexibacter	5732	1	8/8	N/A
Thauera	5704	1	12/12	N/A
Thermomonospora	5520	1	1/5	N/A
Mizugakiibacter	5498	1	5/9	N/A
Pseudocardia	5479	1	7/9	N/A

Bacteriodota	5322	2	7/8	N/A
Miltoncostaceae	4508	1	5/5	N/A
Pseudoroseomonas	4436	1	4/7	N/A
Acidimicrobium	4266	1	9//9	N/A
Neoroseomonas	4176	1	5/5	N/A
Paraburkholderia	3913	1	0/4	N/A
Methylocapsa	3861	1	9/9	N/A
Segnochrobactrum	3790	1	8/9	N/A
Zavarzinella	3790	1	6/9	N/A
Rhodoglobus	3777	1	4/4	N/A
Pseudomonadaceae	3487	1	7/7	N/A
Thermopolyspora	3478	1	4/5	N/A
Xanthomonas	3408	1	1/1	**1 repeat region**
Polaromonas	3040	1	1/2	N/A
Actinoplanes	2931	1	3/3	N/A
Jatrophihabitans	2931	1	3/3	N/A
Pseudomonas	2916	1	0/2	N/A
Nakaseomyces	2841	1	0/3	N/A
Fulvimonas	2724	1	4/4	N/A
Blechomonas	2710	1	0/1	N/A
Hymenobacter	2694	1	2/3	N/A
Streptosporangium	2626	1	3/4	N/A
Sporsorium	2619	1	0/2	N/A
Lichenicola	2576	1	0/2	N/A
Phytophthora	2422	1	0/2	N/A
Aquaspirillum	2410	1	1/3	N/A
Limimonas	2318	1	4/4	N/A
Opitutus	2309	1	2//3	N/A
Babesia	2277	1	0/2	N/A
Acidiferrobacter	2245	1	3/3	N/A
Specibacter	2068	1	2/2	N/A
Methylococcus	2048	1	2/2	N/A
Leekyejoonella	1970	1	3/3	N/A
Burkholderia	1892	1	4/4	N/A
Spongiactinospora	1822	1	1/3	N/A
Maribius	1702	1	1/3	N/A
Thermus	1613	1	0/2	N/A
Geodermatophilius	1441	1	2/2	N/A
Roseococcus	1347	1	0/1	N/A
Cryobacterium	1133	1	0/1	N/A

EcoPlate™

A1 Water	A2 β-Methyl-D-Glucoside	A3 D-Galactonic Acid γ-Lactone	A4 L-Arginine	A5 Water	A6 β-Methyl-D-Glucoside	A7 D-Galactonic Acid γ-Lactone	A8 L-Arginine	A9 Water	A10 β-Methyl-D-Glucoside	A11 D-Galactonic Acid γ-Lactone	A12 L-Arginine
B1 Pyruvic Acid Methyl Ester	B2 D-Xylose	B3 D-Galacturonic Acid	B4 L-Asparagine	B5 Pyruvic Acid Methyl Ester	B6 D-Xylose	B7 D-Galacturonic Acid	B8 L-Asparagine	B9 Pyruvic Acid Methyl Ester	B10 D-Xylose	B11 D-Galacturonic Acid	B12 L-Asparagine
C1 Tween 40	C2 i-Erythritol	C3 2-Hydroxy Benzoic Acid	C4 L-Phenylalanine	C5 Tween 40	C6 i-Erythritol	C7 2-Hydroxy Benzoic Acid	C8 L-Phenylalanine	C9 Tween 40	C10 i-Erythritol	C11 2-Hydroxy Benzoic Acid	C12 L-Phenylalanine
D1 Tween 80	D2 D-Mannitol	D3 4-Hydroxy Benzoic Acid	D4 L-Serine	D5 Tween 80	D6 D-Mannitol	D7 4-Hydroxy Benzoic Acid	D8 L-Serine	D9 Tween 80	D10 D-Mannitol	D11 4-Hydroxy Benzoic Acid	D12 L-Serine
E1 α-Cyclodextrin	E2 N-Acetyl-D-Glucosamine	E3 γ-Amino Butyric Acid	E4 L-Threonine	E5 α-Cyclodextrin	E6 N-Acetyl-D-Glucosamine	E7 γ-Amino Butyric Acid	E8 L-Threonine	E9 α-Cyclodextrin	E10 N-Acetyl-D-Glucosamine	E11 γ-Amino Butyric Acid	E12 L-Threonine
F1 Glycogen	F2 D-Glucosaminic Acid	F3 Itaconic Acid	F4 Glycyl-L-Glutamic Acid	F5 Glycogen	F6 D-Glucosaminic Acid	F7 Itaconic Acid	F8 Glycyl-L-Glutamic Acid	F9 Glycogen	F10 D-Glucosaminic Acid	F11 Itaconic Acid	F12 Glycyl-L-Glutamic Acid
G1 D-Cellobiose	G2 Glucose-1-Phosphate	G3 α-Keto Butyric Acid	G4 Phenylethyl-amine	G5 D-Cellobiose	G6 Glucose-1-Phosphate	G7 α-Keto Butyric Acid	G8 Phenylethyl-amine	G9 D-Cellobiose	G10 Glucose-1-Phosphate	G11 α-Keto Butyric Acid	G12 Phenylethyl-amine
H1 α-D-Lactose	H2 D,L-α-Glycerol Phosphate	H3 D-Malic Acid	H4 Putrescine	H5 α-D-Lactose	H6 D,L-α-Glycerol Phosphate	H7 D-Malic Acid	H8 Putrescine	H9 α-D-Lactose	H10 D,L-α-Glycerol Phosphate	H11 D-Malic Acid	H12 Putrescine

AN MicroPlate™

A1 Water	A2 N-Acetyl-D-Galactosamine	A3 N-Acetyl-D-Glucosamine	A4 N-Acetyl-D-Mannosamine	A5 Adonitol	A6 Amygdalin	A7 D-Arabitol	A8 Arbutin	A9 D-Cellobiose	A10 α-Cyclodextrin	A11 β-Cyclodextrin	A12 Dextrin
B1 Dulcitol	B2 i-Erythritol	B3 D-Fructose	B4 L-Fucose	B5 D-Galactose	B6 D-Galacturonic Acid	B7 Gentiobiose	B8 D-Gluconic Acid	B9 D-Glucosaminic Acid	B10 α-D-Glucose	B11 Glucose-1-Phosphate	B12 Glucose-6-Phosphate
C1 Glycerol	C2 D,L-α-Glycerol Phosphate	C3 m-Inositol	C4 α-D-Lactose	C5 Lactulose	C6 Maltose	C7 Maltotriose	C8 D-Mannitol	C9 D-Mannose	C10 D-Melezitose	C11 D-Melibiose	C12 3-Methyl-D-Glucose
D1 α-Methyl-D-Galactoside	D2 β-Methyl-D-Galactoside	D3 α-Methyl-D-Glucoside	D4 β-Methyl-D-Glucoside	D5 Palatinose	D6 D-Raffinose	D7 L-Rhamnose	D8 Salicin	D9 D-Sorbitol	D10 Stachyose	D11 Sucrose	D12 D-Trehalose
E1 Turanose	E2 Acetic Acid	E3 Formic acid	E4 Fumaric Acid	E5 Glyoxylic Acid	E6 α-Hydroxy-butyric Acid	E7 β-Hydroxy-butyric Acid	E8 Itaconic Acid	E9 α-Ketobutyric Acid	E10 α-Ketovaleric Acid	E11 D,L-Lactic Acid	E12 L-Lactic Acid
F1 D-Lactic Acid Methyl Ester	F2 D-Malic Acid	F3 L-Malic Acid	F4 Propionic Acid	F5 Pyruvic Acid	F6 Pyruvic Acid Methyl Ester	F7 D-Saccharic Acid	F8 Succinamic Acid	F9 Succinic Acid	F10 Succinic Acid Mono-Methyl Ester	F11 M-Tartaric Acid	F12 Urocanic Acid
G1 Alaninamide	G2 L-Alanine	G3 L-Alanyl-L-Glutamine	G4 L-Alanyl-L-Histidine	G5 L-Alanyl-L-Threonine	G6 L-Asparagine	G7 L-Glutamic Acid	G8 L-Glutamine	G9 Glycyl-L-Aspartic Acid	G10 Glycyl-L-Glutamine	G11 Glycyl-L-Methionine	G12 Glycyl-L-Proline
H1 L-Methionine	H2 L-Phenylalanine	H3 L-Serine	H4 L-Threonine	H5 L-Valine	H6 L-Valine plus L-Aspartic Acid	H7 2'-Deoxy Adenosine	H8 Inosine	H9 Thymidine	H10 Uridine	H11 Thymidine-5'-Mono-phosphate	H12 Uridine-5'-Mono-phosphate

SUPPLEMENTARY FIGURE S1: EcoPlate and anaerobic BIOLOG plate layouts. EcoPlates contain 31 substrates in triplicate. Anaerobic microplates contain 95 substrates. Water is utilised as a control well in both 96 well plate assays.

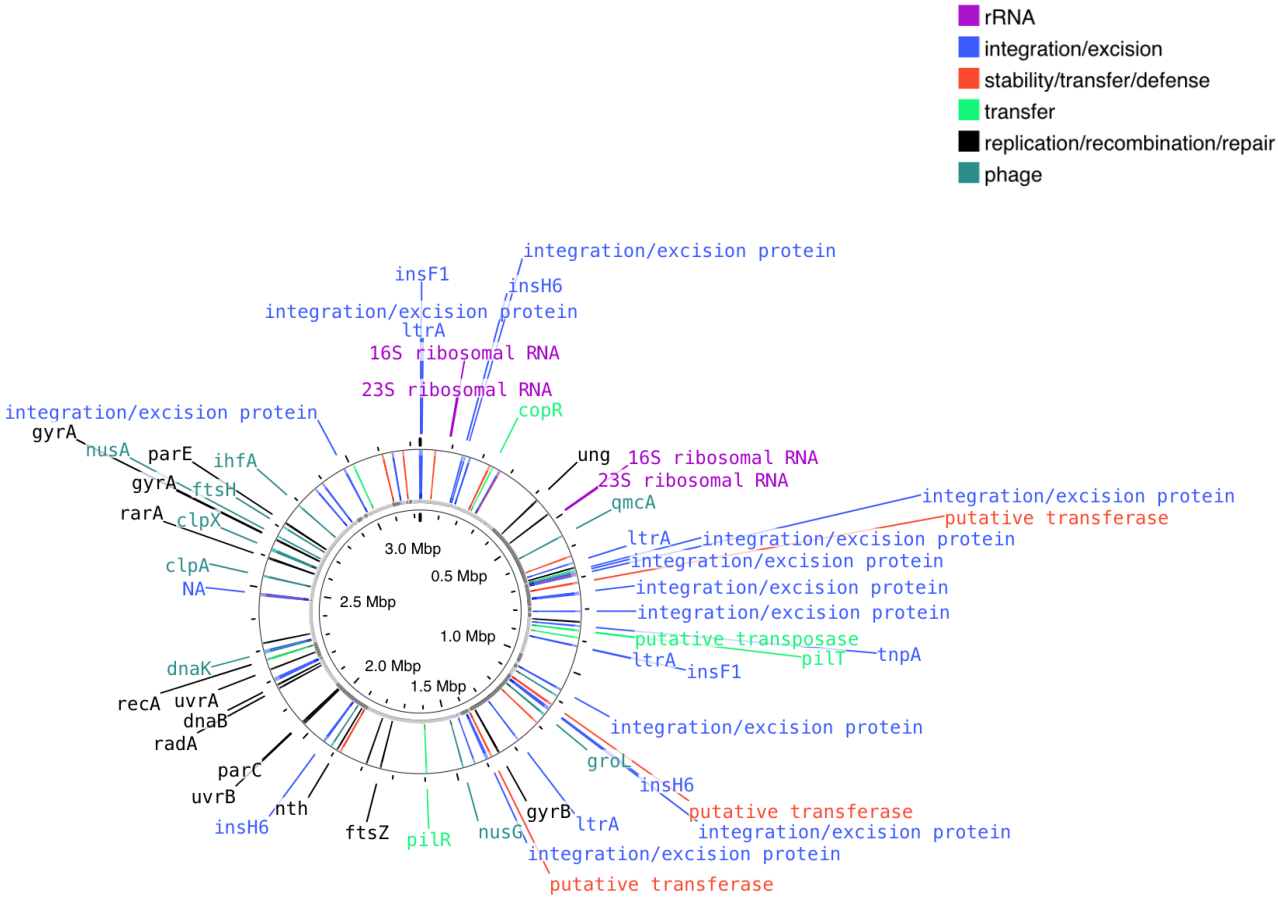

SUPPLEMENTARY FIGURE S2: Locations of predicted mobile genetic elements (MGEs) within the *Metallibacterium* MAG. Gene sequences allocated to MGE function determined by *mobileOG-db tool (v.1.1.3).* Note the genes within the rRNA operon are not classed MGEs but are retained to allow identification of the MAG. **(Total MGE features = 115. Integration/excision proteins = 49; replication/recombination/repair = 23; Bacteriophage derived sequences = 15; Genomic stability/transfer/defence proteins = 20; Transfer mechanisms = 8).**